

# **Development of an equation based on physicochemical properties of plastic and polycyclic aromatic hydrocarbons (PAH) to predict plastic-water partition coefficients ( $\log K_{p-w}$ ) for PAHs**



**IWAR**

vom Fachbereich Bau- und Umweltingenieurwissenschaften  
der Technischen Universität Darmstadt

zur Erlangung des akademischen Grades eines  
Doktor-Ingenieurs (Dr.-Ing.)

genehmigte Dissertation  
von Michael Gottschling, M.Sc. aus Heidelberg

Erstgutachterin: Prof. Dr. rer. nat. Liselotte Schebek  
Zweitgutachter: Prof. Dr.-Ing. Andreas Eichhorn

Darmstadt 2023

Development of an equation based on physicochemical properties of plastic and polycyclic aromatic hydrocarbons (PAH) to predict plastic-water partition coefficients ( $\log K_{p-w}$ ) for PAHs

Entwicklung einer Gleichung auf der Grundlage der physikalisch-chemischen Eigenschaften von Kunststoffen und polyzyklischen aromatischen Kohlenwasserstoffen (PAK) zur Vorhersage von Kunststoff-Wasser-Verteilungskoeffizienten ( $\log K_{p-w}$ ) für PAK

Gottschling, Michael: Development of an equation based on physicochemical properties of plastic and polycyclic aromatic hydrocarbons (PAH) to predict plastic-water partition coefficients ( $\log K_{p-w}$ ) for PAHs

Darmstadt. Technische Universität Darmstadt.

Jahr der Veröffentlichung der Dissertation auf TUPrints: 2024

URN: urn:nbn:de:tuda-tuprints-280334

Tag der Einreichung: 21.06.2023

Tag der mündlichen Prüfung: 12.12.2023

Veröffentlichung unter CC BY 4.0 International

<https://creativecommons.org/licenses/>

„Kunststoff herzustellen ist keine Kunst mehr  
aber diesen Stoff zu beseitigen, ist eine Kunst,  
denn Kunststoff ist nicht von Pappe.“  
- Gerhard Uhlenbruck

---

## Acknowledgements (Danksagung)

---

An dieser Stelle möchte ich mich bei den folgenden Personen bedanken, nur durch ihre Unterstützung ist diese vorliegende Doktorarbeit zustande gekommen:

Mein Dank gilt zunächst meiner Professorin und Erstgutachterin Frau Schebek, für ihre hilfsbereite und wissenschaftliche Unterstützung während der gesamten Bearbeitungsphase meiner Dissertation.

Herrn Eichhorn danke ich sehr für die kurzfristige Zusage als Zweitgutachter, sein großes Interesse an meiner Arbeit, die guten Fragen zum Themenbereich und den wertvollen Input.

Besonders möchte ich mich bei Kaori bedanken, für die zahlreichen und unermüdlichen fachlichen Gespräche, Ratschläge und Anmerkungen, ihre herzliche und hilfsbereite Betreuung in den letzten sieben Jahren. Sie war stets meine treue Beraterin, egal zu welcher Uhrzeit und zu welchem Wochentag. Auch die vielen nichtwissenschaftlichen und motivierenden Gespräche haben meine Arbeit unterstützt.

Ich danke Arijan und Dario für den wissenschaftlichen Austausch und für eures unermüdlichen Engagement. Es war mir eine Ehre eure Masterarbeiten betreuen zu dürfen.

Meinen Kollegen Lili und Dominik danke ich für die vielen Gespräche auf intellektueller und persönlicher Ebene. Sie werden mir immer als bereichernder und konstruktiver Austausch in Erinnerung bleiben. Ich habe unsere Dialoge stets als motivierend und ermutigend empfunden.

Hajo und Luisa danke ich für die zuverlässige Unterstützung bei der Messung der Kunststoffeigenschaften.

Frau Regine Peter vom Fraunhofer IWKS und Frau Claudia Fasel aus dem Fachgebiet Strukturforschung der Technischen Universität Darmstadt danke ich sehr für die zuverlässige Unterstützung bei der Bestimmung der Kunststoffeigenschaften.

Des Weiteren möchte ich mich bei Andrea für das Korrekturlesen dieser Doktorarbeit bedanken.

Mein ganz besonderer Dank aber gilt meinen Eltern, Erich und Theresia, für die Unterstützung in jeglicher Hinsicht. Ich danke dir Mutti, dass du mich stets mit Essen versorgt hast ;-) und vor allem danke ich meiner Frau Kristin und meiner Tochter Liara, für eure Liebe und euer Glauben an mich.

## Summary (Zusammenfassung)

Das Verständnis des Sorptionsverhaltens von Schadstoffen an der Oberfläche von Kunststoffpartikeln ist entscheidend für die Bewertung der ökotoxikologischen Auswirkungen von Mikroplastik in der Umwelt. Insbesondere im aquatischen Milieu ist der Kunststoff-Wasser-Verteilungskoeffizient ( $\log K_{p-w}$ ) einer der wichtigsten Parameter zur Quantifizierung und dient zum Vergleich der Adsorption von Schadstoffen an verschiedenen Kunststoffmaterialien. Die  $\log K_{p-w}$ -Werte wurden für eine Vielzahl von Schadstoffen im Labor oder in Feldversuchen bestimmt. Log  $K_{p-w}$ -Werte für Schadstoffe mit geringer Wasserlöslichkeit sind jedoch oft nicht verfügbar oder werden mit Hilfe einer mathematischen Gleichung geschätzt, die auf chemisch-physikalischen Eigenschaften der Sorbate, wie der molaren Masse (MW), dem Ocatnol-Wasser-Verteilungskoeffizienten ( $\log K_{ow}$ ) oder der Wasserlöslichkeit ( $\log C_w^{sat}$ ), beruhen. Solche Gleichungen werden meist nur für Polyethylen (PE) entwickelt.

In dieser Dissertation wurde eine Gleichung zur Vorhersage von  $\log K_{p-w}$ -Werten für drei weit verbreitete Kunststoffe aufgestellt, nämlich Polyethylen niedriger Dichte (LDPE), Polypropylen (PP) und Polyethylenterephthalat (PET) sowie ein allgemein bekanntes biologisch abbaubares Polybutylensuccinat (PBS).

Zunächst wurden die  $\log K_{p-w}$ -Werte von Naphthalin, Fluoren und Phenanthren anhand einer Reihe von kleinen Laborversuchen mit diesen vier Kunststoffen und der Freundlich-Isotherme abgeleitet. Darüber hinaus wurden die Kunststoffeigenschaften im Labor bestimmt und mit den PAK-Eigenschaften kombiniert, um Gleichungen für die Vorhersage von  $\log K_{p-w}$  aufzustellen. Aus diesen Gleichungen wurde die am besten geeignete und robusteste Gleichung mit Hilfe statistischer Instrumente ausgewählt, einschließlich des zweidimensionalen Korrelationskoeffizienten und des mittleren quadratischen Fehlers (eng. root mean square error = RMSE). Schließlich wurde die Gültigkeit dieser Gleichung durch den Vergleich der mit dieser Gleichung vorhergesagten  $\log K_{p-w}$ -Werte mit den in der Literatur verfügbaren  $\log K_{p-w}$ -Werten bewertet.

Bei der Entwicklung einer Gleichung bestätigte sich, dass zwei Kunststoffeigenschaften (Kristallinität =  $X_c$ , Dichte =  $\rho$ ) und eine PAK-Eigenschaft (Wasserlöslichkeit =  $\log C_w^{sat}$ ) wichtige Variablen für das Verständnis des Sorptionsverhaltens von PAK an Kunststoffen in der wässrigen Umgebung sind. Das wichtigste Ergebnis dieser Arbeit ist die Entwicklung einer universellen Gleichung für vier wichtige Polymere zur Vorhersage von  $\log K_{p-w}$  für PAK auf der Grundlage dieser Kunststoff- und PAK-Eigenschaften:

$$\log K_{p-w} \text{ von PAK} = (-1,85 * \log C_w^{sat} + 1,00) * X_c * \rho + 2,50.$$

Es wurde eine Übertragung dieser Gleichung auf zuvor veröffentlichte  $\log K_{p-w}$ -Werte durchgeführt. Das Ergebnis zeigte, dass 93,0 % (93 von 100 veröffentlichten Werten), 91,7 % (11 von 12 veröffentlichten Werten), 100 % (2 von 2 veröffentlichten Werten) und 50 % (2 von 4 veröffentlichten Werten) der  $\log K_{p-w}$  von LDPE, PP, PBS bzw. PET innerhalb der Grenzen dieser Gleichung lagen.

Das Verfahren zur Entwicklung der Gleichung in dieser Arbeit sowie die Gleichung selbst können als Grundlage für i) die weitere Optimierung der Gleichung auf der Grundlage von tatsächlich im Labor und im Feld ermittelten  $\log K_{p-w}$ -Werten, ii) die Vorhersage von  $\log K_{p-w}$  für nicht in dieser Arbeit getestete Kombinationen eines Schadstoffs und eines Polymers und iii) die Vorhersage von ökotoxikologischen Wirkungen durch Mikroplastik im aquatischen Milieu verwendet werden.

---

## Abstract

---

Understanding the sorption behaviour of pollutants onto the surface of plastic particles is crucial to evaluate the ecotoxicological impact of microplastics in the environment. Especially in the aquatic milieu, plastic-water partition coefficients ( $\log K_{p-w}$ ) is one of the important parameters to quantify and compare the adsorption of pollutants on different plastic materials.  $\log K_{p-w}$  for a variety of pollutants have been determined in the laboratory or in the field experiments.  $\log K_{p-w}$  values for pollutants with low water solubility are, however, often not available or estimated using a mathematical equation based on physicochemical properties of sorbates such as molar mass (MW), octanol-water partition coefficient ( $\log K_{ow}$ ) or water solubility ( $\log C_w^{sat}$ ). Such equations are developed mostly only for polyethylene (PE).

In this dissertation, an equation was established to predict  $\log K_{p-w}$  values for three widely used plastics, namely, low density polyethylene (LDPE), polypropylene (PP) and polyethylene terephthalate (PET) as well as a commonly known biodegradable polybutylene succinate (PBS).

First,  $\log K_{p-w}$  values of naphthalene, fluorene and phenanthrene were derived on a set of small laboratory scale experiments using four plastics and the Freundlich isotherm. In addition, plastic properties were determined in the laboratory, which were combined with PAH properties to establish a number of equations for the prediction of  $\log K_{p-w}$ . From these equations, the most appropriate and robust equation was selected using statistical tools, including two-dimensional correlation coefficient and root mean square error (RMSE). Finally, the validity of this equation was evaluated by comparing predicted  $\log K_{p-w}$  values using the equation with the  $\log K_{p-w}$  values that are available in the literature.

In the process of the development of an equation, it was confirmed that two plastic properties (crystallinity =  $X_c$ , density =  $\rho$ ) and one PAH property (aqueous solubility =  $\log C_w^{sat}$ ) are significant variables to understand the sorption behavior of PAHs on plastics in the aqueous environment. The major outcome of this work is the development of a universal equation for four important polymers to predict  $\log K_{p-w}$  for PAHs based on these plastic and PAH properties:

$$\log K_{p-w} \text{ of PAH} = (-1.85 * \log C_w^{sat} + 1.00) * X_c * \rho + 2.50.$$

A transferability of this equation to previously published  $\log K_{p-w}$  was performed. The result showed that 93.0 % (93 out of 100 published values), 91.7% (11 out of 12 published values), 100 % (2 out of 2 published values) and 50% (2 out of 4 published values) of the  $\log K_{p-w}$  of LDPE, PP, PBS, and PET, respectively, were found to be within the limits of this equation.

The procedure for the development of the equation in this work as well as the equation itself can be utilized as a basis for i) the further optimization of the equation based on  $\log K_{p-w}$  values actually determined in the laboratory and in the field, ii) the prediction of  $\log K_{p-w}$  for untested combinations of a pollutant and a polymer and iii) prediction of ecotoxicological effects of microplastics in the aquatic milieu.

---

## Table of Contents

---

Acknowledgements (Danksagung) .....	II
Summary (Zusammenfassung).....	III
Abstract .....	IV
Table of Contents .....	V
List of Figures .....	VII
List of Tables .....	IX
List of Abbreviations .....	X
1....Introduction.....	12
2....Basic information.....	14
2.1.    Plastic .....	14
2.1.1.    Basic information Polyethylene (PE) .....	16
2.1.2.    Basic information Polypropylene (PP) .....	16
2.1.3.    Basic information Polyethylene terephthalate (PET) .....	17
2.1.4.    Basic information Polybutylene succinate (PBS).....	17
2.2.    General information of plastic production .....	17
2.3.    Plastic waste in the marine environment .....	18
2.4.    Persistent organic pollutants / polycyclic aromatic hydrocarbons .....	19
2.5.    Sorption/Sorption isotherm.....	21
2.6.    Prediction of plastic-water partition coefficients.....	22
2.7.    Theory .....	23
3....Method and Material .....	23
3.1.    Sorption Experiment.....	23
3.1.1.    Preparation of stock solutions and PAH aqueous solutions for the experiments .....	23
3.1.2.    Experimental setup.....	24
3.1.3.    Determination of PAH concentrations .....	24
3.1.4.    Kinetic models .....	25
3.2.    Method determination of regression model .....	26
4....Determination of plastic-water partition coefficients .....	27
4.1.    Sorption isotherm experiments.....	28
4.1.1.    Linear vs Freundlich isotherm models .....	28
4.2.    Comparison of log $K_{p-w}$ from this thesis versus published studies .....	29
4.2.1.    Log $K_{LDPE-w}$ of PAHs from this thesis versus published studies.....	29
4.2.2.    Log $K_{p-w}$ of PAHs for PP, PET and PBS from this thesis versus published studies .....	30

---

5.....Correlations of PAH properties and log K <sub>p-w</sub> .....	32
5.1.    Correlation of log K <sub>p-w</sub> and log K <sub>ow</sub> of this thesis .....	32
5.2.    Correlation of log K <sub>p-w</sub> and MW of this thesis .....	38
5.2.1.  Correlation between log K <sub>LDPE-w</sub> and MW from this thesis versus published studies .....	39
5.2.2.  Correlation between log K <sub>p-w</sub> and MW for PP and PET .....	40
5.3.    Correlation of log K <sub>p-w</sub> and log C <sub>w<sup>sat</sup></sub> of this thesis .....	43
5.3.1.  Correlation between log K <sub>LDPE-w</sub> and log C <sub>w<sup>sat</sup></sub> from this thesis versus published studies.....	44
5.4.    Correlation of log K <sub>p-w</sub> and log K <sub>hdw</sub> of this thesis.....	45
5.4.1.  Correlation between log K <sub>LDPE-w</sub> and log K <sub>hdw</sub> from this thesis versus published studies .....	46
6.....Correlations of plastic properties and log K <sub>p-w</sub> .....	49
6.1.    Characterization of the microplastics.....	49
6.1.1.  Literature values of plastic properties.....	49
6.1.2.  Measured plastic properties of this thesis compared with literature plastic properties .....	50
6.2.    Correlation of film thickness of sorbent materials on log K <sub>p-w</sub> of selected PAHs.....	53
6.3.    Correlation of log K <sub>p-w</sub> and thermal plastic properties .....	56
6.3.1.  Influence of glass transition temperature (T <sub>g</sub> ) of the tested plastics on log K <sub>p-w</sub> .....	56
6.3.2.  Influence of crystallinity (X <sub>c</sub> ) of the tested plastics on log K <sub>p-w</sub> .....	57
6.3.3.  Influence of melting temperature (T <sub>m</sub> ) of the tested plastics on log K <sub>p-w</sub> .....	58
6.4.    Correlation of log K <sub>p-w</sub> and physical polymer properties .....	60
7.....Development of an equation to predict log K <sub>p-w</sub> .....	62
7.1.    Polymer properties and PAH properties versus values of this thesis – method 1.....	62
7.1.1.  Calculation of the equations of method 1 .....	64
7.1.2.  Selection of equations from method 1 .....	66
7.2.    Polymer properties and PAH properties versus values of this thesis – method 2.....	68
7.3.    Evaluating the final equation from method 1 and 2 .....	69
7.4.    Proof of concept: comparison of modelled values versus published data.....	70
7.4.1.  Proof of concept for LDPE.....	71
7.4.2.  Proof of concept for PP .....	72
7.4.3.  Proof of concept for PBS .....	74
7.4.4.  Proof of concept for PET .....	75
8.....Conclusion and outlook.....	77
9.....References .....	79
10...List of posters (June 2023) .....	A-I
11...Appendices .....	A-II

---

## List of Figures

---

<b>Figure 1:</b> Different polymer phases (Camarda et al., 2021) .....	16
<b>Figure 2:</b> Development of global plastic production (Geyer et al., 2017) and the worldwide population (United Nations, 2019) .....	18
<b>Figure 3:</b> Five largest ocean garbage gyres .....	19
<b>Figure 4:</b> Comparison of $t_{95}$ of the sorption experiments of naphthalene (white circle), fluorene (gray circle) and phenanthrene (black circle) on LDPE, PBS, PP and PET; $t_{95}$ calculated by PFO model (top); $t_{95}$ calculated by PSO model (bottom). .....	27
<b>Figure 5:</b> Comparison of Log $K_D$ (left) and log $K_{Fr}$ (right) of naphthalene, fluorene and phenanthrene on LDPE, PP, PBS and PET. ....	29
<b>Figure 6:</b> Comparison of Log $K_{LDPE-W}$ values of naphthalene, fluorene and phenanthrene: this thesis versus other studies.....	30
<b>Figure 7:</b> log $K_{p-w}$ regression with log $K_{ow}$ : results from the experiment (left) and log $K_{p-w}$ modelled from the derived equations (right).....	33
<b>Figure 8:</b> Correlation of log $K_{LDPE-W}$ and log $K_{ow}$ from this thesis versus published studies .....	34
<b>Figure 9:</b> Correlation of log $K_{PP-W}$ and log $K_{ow}$ from this thesis versus published studies .....	36
<b>Figure 10:</b> Correlation of log $K_{PET-W}$ and log $K_{ow}$ from this thesis versus Lončarski et al. (2021) .....	37
<b>Figure 11:</b> log $K_{p-w}$ regression with MW: results from the experiment (left) and log $K_{p-w}$ modelled from the derived equations (right) .....	38
<b>Figure 12:</b> Correlation of log $K_{LDPE-W}$ and MW from this thesis versus published studies .....	39
<b>Figure 13:</b> Correlation of log $K_{PP-W}$ and MW from this thesis versus published studies.....	41
<b>Figure 14:</b> Correlation of log $K_{PET-W}$ and MW from this thesis versus Lončarski et al. (2021).....	42
<b>Figure 15:</b> log $K_{p-w}$ regression with log $C_w^{sat}$ : results from the experiment (left) and log $K_{p-w}$ modelled from the derived equations (right) .....	43
<b>Figure 16:</b> Correlation of log $K_{PE-W}$ and log $C_w^{sat}$ from this study versus Lohmann (2012). ....	45
<b>Figure 17:</b> log $K_{p-w}$ regression with log $K_{hdw}$ : results from the experiment (left) and log $K_{p-w}$ modelled from the derived equations (right).....	46
<b>Figure 18:</b> Correlation of log $K_{PE-W}$ and log $K_{hdw}$ from this study versus Lohmann (2012). ....	47
<b>Figure 19:</b> drip image capture of a) distilled water b) diiodomethane and c) ethylene glycol on LDPE, PP, PBS and PET .....	53
<b>Figure 20:</b> correlation between log $K_{p-w}$ of selected PAHs and glass transition temperature ( $T_g$ ) of the tested polymer materials .....	56
<b>Figure 21:</b> correlation of log $K_{p-w}$ and crystallinity ( $X_c$ ) .....	57
<b>Figure 22:</b> correlation between log $K_{p-w}$ and melting temperature ( $T_m$ ) of the tested polymer materials .....	58
<b>Figure 23:</b> correlation of plastic properties $T_m$ and $X_c$ .....	59

<b>Figure 24:</b> Correlation of density and $\log K_{p-w}$ .....	60
<b>Figure 25:</b> Linear regression of SA a), V <sub>p</sub> b), disperse SFE c), polar SFE d) and sum of SFE e) .....	61
<b>Figure 26:</b> Results of literature LDPE-water partition coefficients within upper and lower limits of equation 75 .....	71
<b>Figure 27:</b> Results of literature PP-water partition coefficients $\log K_{PP-w}$ within upper and lower limits of equation 75 .....	73
<b>Figure 28:</b> Results of literature PBS-water partition coefficients $\log K_{PBS-w}$ within upper and lower limits of equation 75 .....	74
<b>Figure 29:</b> Results of literature PET-water partition coefficients $\log K_{PET-w}$ within upper and lower limits of equation 75 .....	75

---

## List of Tables

---

<b>Table 1:</b> Constants of Linear and Freundlich sorption isotherm models for tested sorbates.....	28
<b>Table 2:</b> Comparison of literature $\log K_{p-w}$ and $\log K_{p-w}$ of this thesis .....	29
<b>Table 3:</b> Comparison of polyethylene-water partition coefficient ( $\log K_{LDPE-w}$ ): this thesis versus published data.....	29
<b>Table 4:</b> Comparison of $\log K_{p-w}$ values of naphthalene, fluorene and phenanthrene for PP, PET and PBS: this thesis versus published data .....	31
<b>Table 5:</b> SPSS analysis of $\log K_{LDPE-w} - \log K_{ow}$ regression of this study and literature models .....	35
<b>Table 6:</b> SPSS analysis of $\log K_{PP-w} - \log K_{ow}$ regression models of this thesis and models on the basis of $\log K_{PP-w}$ from the literature.....	36
<b>Table 7:</b> SPSS analysis of $\log K_{PET-w} - \log K_{ow}$ regression model of this thesis and modelled equation on the basis of $\log K_{PET-w}$ by Lončarski et al. (2021) .....	37
<b>Table 8:</b> SPSS analysis of $\log K_{LDPE-w} - MW$ regression of this thesis and literature regression models .....	40
<b>Table 9:</b> SPSS analysis of $\log \log K_{PP-w} - MW$ regression models of this thesis and models on the basis of $\log K_{PP-w}$ from the literature.....	41
<b>Table 10:</b> SPSS analysis of $\log K_{PET-w} - MW$ regression models of this thesis and modelled equation on the basis of $\log K_{PET-w}$ by Lončarski et al. (2021) .....	42
<b>Table 11:</b> SPSS analysis of $\log K_{PE-w} - \log C_w^{sat}$ regression models of this thesis and Lohmann (2012) .....	44
<b>Table 12:</b> SPSS analysis of $\log K_{PE-w} - \log K_{hdw}$ regression models of this thesis and Lohmann (2012) .....	46
<b>Table 13:</b> Physical and thermal properties of polymers used for the sorption experiments and literature values .....	51
<b>Table 14:</b> Comparison of polyethylene-water partition coefficient .....	54
<b>Table 15:</b> Comparison of polypropylene-water partition coefficient .....	55
<b>Table 16:</b> Matrix (A) of polymer density and $\log K_{ow}$ of PAHs .....	62
<b>Table 17:</b> Matrix (B) of $\log K_{p-w}$ from chapter 4.....	62
<b>Table 18:</b> $R_v^2$ and $R_h^2$ calculation of the matrix of one PAH and one plastic properties with the $\log K_{p-w}$ matrix.....	64
<b>Table 19:</b> $R_v^2$ and $R_h^2$ calculation of the matrix of one PAH and two plastic properties ( $\rho$ as fixed parameter) with the $\log K_{p-w}$ matrix .....	65
<b>Table 20:</b> $R_v^2$ and $R_h^2$ calculation of the matrix of one/two PAH and three plastic properties ( $X_c * \rho$ as fixed parameters) with the $\log K_{p-w}$ matrix .....	65
<b>Table 21:</b> Equations derived through method 2.....	68
<b>Table 22:</b> RMSE calculation of the selected equations of method 1 and 2 .....	70

---

---

## List of Abbreviations

---

$\Delta H_c$	enthalpy of crystallisation
$\Delta H_m$	enthalpy of fusion
$\Delta H_{m0}$	heat of fusion of the completely crystalline materials at the equilibrium melting temperature
$\Sigma SFE$	sum of disperse and polar surface free energy
$\mu g\ g^{-1}$	microgram per gram
$\mu L$	microliter
$\mu m$	micrometre
$C_{i,s}$	concentration of the solid phase
$C_{i,w}$	concentration of the liquid phase
$C_{S,eq}$	concentration in the polymer sorbent at equilibrium
$C_{W,eq}$	equilibrium concentrations in the aqueous phase
$d_{50}$	median diameter
DDT	dichlorodiphenyl-trichloroethane
DSC	differential scanning calorimetry
EPA	Environmental Protection Agency
EPS	expandable polystyrene
FLN	fluorene
GC/MS	gas-chromatography-mass spectrometry
HCH	hexachlorocyclohexane
HDPE	high-density polyethylene
DSC	High Performance Liquide Chromatography
IPW	International Pellet Watch
$K_D$	distribution coefficient
$K_{i,d}$	partition coefficient
$K_{P-sw}$	plastic-water distribution coefficient in salt water
LDPE	low density polyethylene
$\log C_w^{sat}$	water solubility
$\log K_{Fr}$	Freundlich partition coefficient
$\log K_{hdw}$	hexadecane-water partitioning
$\log K_{LDPE-w}$	low density polyethylene-water partition coefficient
$\log K_{ow}$	ocatnol-water partition coefficient
$\log K_{PBS-w}$	polybutylene succinate-water partition coefficient
$\log K_{PET-w}$	polyethylene terephthalate-water partition coefficient
$\log K_{PE-w}$	polyethylene-water partition coefficient
$\log K_{PP-w}$	polypropylene-water partition coefficient
$\log K_{p-w}$	plastic-water partition coefficients
$m/z$	mass-to-charge ratio
mg	milligram
ml	millilitre
mm	millimetre

---

mN	mega Newton
MP	microplastic
MT	million tonnes
MW	molecular weight
NAPH	naphthalene
NF	not found
ng g-pellet <sup>-1</sup>	nano gram per g plastic pellet
nm	nano meter
PAH	polycyclic aromatic hydrocarbons
PBS	polybutylene succinate
PCB	polychlorinated biphenyls
PE	polyethylene
PET	polyethylene terephthalate
PFO	pseudo-first-order
PHEN	phenanthrene
POP	Persistent organic pollutants
PP	polypropylene
PS	polystyrene
PSO	pseudo-second-order
PVC	polyvinyl chloride
q <sub>e</sub>	amount of sorbate adsorbed at equilibrium
q <sub>t</sub>	amount of sorbate adsorbed on the sorbent at time t
R <sup>2</sup>	coefficient of determination
r <sub>h</sub>	horizontal correlation coefficient
RMSE	root mean square error
rpm	revolutions per minute
r <sub>v</sub>	vertical correlation coefficient
SA	surface area
SD	standard deviation
SFE	surface free energy
SIM	selected ion mode
SSA	specific surface area
T <sub>g</sub>	glass transition temperature
T <sub>m</sub>	melting temperature
USEPA	United States Environmental Protection Agency
vol.-%	percent by volume
Vp	pore volume
X <sub>c</sub>	crystallinity
μS	microsiemens
ρ	density

## 1. Introduction

---

Plastics, especially microplastics (MPs) in the environment, are becoming a subject of increasing concern. According to Jambeck et al. (2015), out of 275 million tonnes plastic waste generated by 93 % of the global population living in 192 coastal countries in 2010, 4.8 to 12.7 million metric tonnes were assumed to end up in the ocean, while the global plastic production in 2010 was determined to be 270 million tonnes. In other words, approximately 1.8 to 2.7 % of the globally produced plastic products in 2010 entered the ocean. Meanwhile, the annual report “Plastics – the Facts 2020” by PlasticsEurope found that global plastic production increased to 368 million tonnes in 2019. In addition, production of biodegradable plastic increased from 1.1 million tonnes in 2018 to 1.2 million tonnes in 2019 (European Bioplastics, 2020). Whether conventional or biodegradable, plastic waste leaking into the ocean becomes a greater concern as more plastic and plastic waste are generated globally.

Not only plastic waste, but also a variety of hydrophobic organic pollutants are found in the environment. In aquatic milieus, nonpolar hydrophobic pollutants tend to adsorb on the non-polar surface of many plastic materials. Plastic waste can, thus, become a carrier of toxic pollutants and endanger the health of marine organisms. The organization International Pellet Watch (IPW), for instance, analysed a large number of plastic pellets (size < 5 mm) collected on beaches worldwide to investigate the accumulation of hydrophobic pollutants on polymer materials. They have shown that pollutants like polycyclic aromatic hydrocarbons (PAH), polychlorinated biphenyls (PCB), hexachlorocyclohexane (HCH) and dichlorodiphenyl-trichloroethane (DDT) can accumulate on polyethylene (PE) and other polymers weathered in the marine environment (Mato et al., 2001, Endo et al., 2005; Rios et al., 2007; Ogata et al., 2009; Hirai et al., 2011; Haskett et al., 2012; Van et al., 2012; Yamashita et al., 2018; Rodrigues et al., 2019; Camacho et al., 2019). Among hydrophobic organic pollutants, PAHs are the major pollutant group with the highest sorption mass of up to  $24.4 \times 10^3$  ng/g-pellet (Yeo et al., 2017). The question arises then whether every polymer type accumulates the same amount of pollutants?

Rochman et al. (2013) investigated the accumulation of PAHs and PCBs on five different types of plastic resin pellets, i.e. high-density polyethylene (HDPE), low-density polyethylene (LDPE), polypropylene (PP), polyvinyl chloride (PVC) and polyethylene terephthalate (PET) in the marine ecosystem and found that sorption behaviour largely varied depending on polymer types. The accumulation of 15 PAHs, for instance, decreased in the order of HDPE ( $797 \text{ ng g-pellet}^{-1}$ ) > LDPE ( $722 \text{ ng g-pellet}^{-1}$ ) > PP ( $122 \text{ ng g-pellet}^{-1}$ ) > PVC ( $27 \text{ ng g-pellet}^{-1}$ ) > PET ( $17 \text{ ng g-pellet}^{-1}$ ). Their results are useful to compare the sorption behaviour of bulk PAHs which were available in the system with different polymers deployed in a certain period of time in the same environment. However, the sorption masses of other plastic types cannot be compared with the available data, since it is not possible to repeat the experiment under the exact same conditions.

For a fair comparison of the accumulation degree of a pollutant on plastic materials, plastic-water partition coefficients ( $\log K_{p-w}$ ) are to be determined in laboratory experiments under controlled conditions. In general,  $\log K_{p-w}$  values are determined through a series of laboratory experiments in distilled water using isotherm models. To compare the degree of sorption of a particular substance (sorbate) on a polymer material (sorbent) in aquatic milieu, plastic-water partition coefficient ( $\log K_{p-w}$ ) is an important parameter. A number of researchers conducted laboratory experiments to calculate  $\log K_{p-w}$  of PAHs, mainly using LDPE as a sorbent material (Booij et al., 2003; Adams et al., 2007; Cornelissen et al., 2008; Fernandez et al., 2009; Smedes et al., 2009; Hale et al., 2010; Choi

et al., 2013; Zhu et al., 2015; J. Wang et al., 2019). These researchers observed that sorbate properties, such as octanol-water partition coefficient ( $\log K_{ow}$ ), molecular weight (MW), and solubility in water clearly influence its sorption behaviour on LDPE. As investigated by Adams et al. (2007), Smedes et al. (2009), Choi et al. (2013), and Hüffer and Hofmann, (2016), a linear correlation was found between  $\log K_{p-w}$  and  $\log K_{ow}$  of PAHs on LDPE, indicating that  $\log K_{p-w}$  of a new PAH can be estimated if its  $\log K_{ow}$  is known.

In addition to LDPE, which accounted for 17 % of the global plastic production in 2015, other major polymers for example PP and PET were also examined in some studies and determined to account for 23 % and 7 % of the global plastic production (Plastics Europe, 2015). A handful of studies determined partition coefficients of PP ( $\log K_{PP-w}$ ) in the laboratory (Teuten et al., 2007; Karapanagioti and Klontza, 2008; Lee et al., 2014; and J. Wang et al., 2019). With regard to the biodegradable polymers and PET, two studies have been recently published: i) investigation of the sorption of four PAHs (phenanthrene, pyrene, 1-nitronaphthalene and 1-naphthylamine) on a biodegradable polymer polybutylene succinate (PBS) by Zhao et al. (2020) ii) sorption experiments of naphthalene, fluorene, fluoranthene and pyrene on three non-degradable types of polymers including PET were carried out by Lončarski et al. (2021). Plastic-water partition coefficients of the above mentioned studies for PE are summarized in Table A1.1 (Appendix) and for PP, PET and PBS in Table A1.2.

It is not easy to conduct sorption isotherm experiments on hydrophobic pollutants with low water solubility (Zhu et al., 2015), especially on polymers that accumulate hydrophobic pollutants well in the water phase because of their hydrophobicity. Thus, researchers attempted to estimate  $\log K_{p-w}$  using linear regression models. Typically, physicochemical properties of sorbates, like octanol-water partitioning ( $\log K_{ow}$ ) (Adams et al., 2007; Smedes et al., 2009; Lohmann, 2012; Choi et al., 2013; Hüffer and Hofmann, 2016), hexadecane-water partitioning ( $\log K_{hdw}$ ) (Choi et al., 2013; Hüffer and Hofmann, 2016), aqueous solubility (Lohmann, 2012) and molecular weight (Smedes et al., 2009; Choi et al., 2013) were used to estimate  $\log K_{p-w}$  values of organic hydrophobic compounds. For PAHs on PE, correlations between  $\log K_{PE-w}$  and  $\log K_{ow}$  were determined with coefficients of determinations ( $R^2$ ) in the range of 0.89-0.97 (Adams et al., 2007; Smedes et al., 2009; Lohmann, 2012; Choi et al., 2013; Hüffer and Hofmann, 2016), whereas  $\log K_{PE-w}$  correlates with  $\log K_{hdw}$  with an  $R^2$  of 0.94 - 0.97 (Choi et al., 2013; Hüffer and Hofmann, 2016). According to Lohmann (2012),  $\log K_{PE-w}$  correlates better with aqueous solubility of PAHs ( $R^2 = 0.94$ ) than with  $\log K_{ow}$  ( $R^2 = 0.92$ ) in a log linear model. For PAHs, another parameter that correlates well with  $\log K_{PE-w}$  is molecular weight:  $R^2 = 0.970$  and 0.99, according to Smedes et al. (2009) and Choi et al (2013), respectively. The experimental data of these studies resulted in correlations between 0.89 and 0.99 for PE, however, they only took into consideration the physicochemical properties of the sorptive; properties of the sorbent were not taken into account.

In this regard, J. Wang et al. (2019) determined plastic-water partition coefficient of naphthalene and phenanthrene on five different polymers (HDPE, LDPE, PP, PVC, PS) of two different size classes. In the case of the smaller plastic size class, J. Wang et al. (2019) obtained different  $\log K_{p-w}$ -orders for naphthalene (PP > PVC > LDPE > PS > HDPE) and phenanthrene (HDPE > PVC > PP > LDPE > PS). Therefore, Zuo et al. (2019), J. Wang et al. (2019), as well as and Praveena and Aris (2020) assumed that polymer properties could affect sorption affinity of organic sorbates on plastics. A mathematical correlation of  $\log K_{p-w}$  and polymer properties could not be derived.

In this dissertation, the correlation between  $\log K_{p-w}$  and the sorbent, as well as sorbate properties of selected PAHs for three conventional polymers and one biodegradable polymer, were investigated. First, a series of sorption isotherm experiments were conducted in the laboratory to determine  $\log$

$K_{p-w}$  of three PAHs, i.e. naphthalene (molecular weight = 128.16 g mol<sup>-1</sup>; log  $K_{ow}$  = 3.37), fluorene (molecular weight = 166.21 g mol<sup>-1</sup>; log  $K_{ow}$  = 4.18) and phenanthrene (molecular weight = 178.22 g mol<sup>-1</sup>; log  $K_{ow}$  = 4.46), for three conventional polymers (LDPE, PP and PET) and one biodegradable polymer (PBS). This study has three focus points.

Firstly, the correlation between log  $K_{p-w}$  and sorbate properties for LDPE derived in this work was compared to the correlations in published studies to verify the feasibility of this experimental settings. Then, correlations between log  $K_{p-w}$  and log  $K_{ow}$ , MW, log  $C_w^{sat}$  and log  $K_{hdw}$  of PAHs for PP, PET and PBS were determined. To the best of knowledge, the models to determine log  $K_{p-w}$  of PAHs for PP, PET and PBS from log  $K_{ow}$  are reported for the first time.

Secondly, the influence of thermodynamic and surface polymer properties on log  $K_{p-w}$  of three investigated PAHs (naphthalene, fluorene, phenanthrene) using three conventional polymers, LDPE, PP and PET and one biodegradable polymer PBS was analysed. These account for approximately 40 % of global primary polymer production (Ritchie and Roser, 2018). Their crystallinity ( $X_c$ ), melting temperature ( $T_m$ ) and glass transition temperature ( $T_g$ ) were measured using differential scanning calorimetry (DSC) and correlated with log  $K_{p-w}$ .

Finally, physicochemical properties of sorbate and sorbent from the previous two focus points are combined in equations to predict partition coefficients in the water phase. The partition coefficients calculated from the equations are compared with the partition coefficients obtained from the laboratory experiments. If the partition coefficients determined from the equations exceed a specified agreement with the partition coefficients determined from the laboratory experiments, these equations are compared with previously published equations. The expected result from the literature comparison is an equation that has a higher accuracy than the previously published equations.

---

## 2. Basic information

---

The following chapter will explain the basics of polymers and organic pollutants like polycyclic aromatic hydrocarbons (PAH). When plastics are released in the environment, they interact not only with the environment, but also the substances associated with it. For example, plastics can be fragmented due to the climate conditions and weathering as well as desorb and adsorb chemicals, metals or other solid particles. In an aquatic milieu, organic chemicals like PAHs tend to adsorb on polymer particles, so the sorption process in an aqueous phase is described in detail. Since many different plastic types exist, each with their unique physicochemical properties, the main goal is to identify which of these physicochemical properties has the biggest effect on the sorption process. Therefore, a selected number of PAHs and different polymer types were tested in order to represent a variety of different physicochemical properties of PAHs and plastics.

### 2.1. Plastic

The basic elements of plastic are monomers consisting of organic chemicals. Couplings of the monomers create polymers, that have a high molecular weight. Plastics are omnipresent due to simple processing and a high variety of applications. Since the early 20<sup>th</sup> century, plastics have been produced from crude oil, and the possible uses have multiplied. Plastic production has increased every year since its beginning and reached 381 million tonnes in 2015 (Ritchie and Roser, 2018). The most

common polymers are polypropylene (PP), low density polyethylene (LDPE), high density polyethylene HDPE), polyethylene terephthalate (PET), and polyvinyl chloride (PVC) (Geyer et al., 2017). In the first step of plastic production, crude oil is separated into fractions made up of hydrocarbon chains, which differ in size and composition. Three different processes are used to produce synthetic plastic: polymerization, polyaddition and polycondensation.

In polymerization, monomers are connected by splitting multiple compounds through chain reactions. During this process, the chemical composition of the reactant is not changed and no by-products are separated. Temperature and pressure can affect the seamless polymerization process. Polycondensation, on the other hand, takes place in stages and requires different raw materials. During polycondensation by-products are separated into two functional groups. The structure of the bond can be chain-like or cross-linked. Similar to polycondensation, polyaddition takes places in stages, but no by-products are separated. In polyaddition, monomers bind together due to the intermolecular migration processes of hydrogen atoms (Baur et al., 2010).

Depending on the process conditions, synthetic polymers can turn into thermoplastics, elastomers or thermosets. Thermoplastics are characterized by their malleability during heating and shows linear or branched structures. Increasing the temperature affects chemical and mechanical properties and can result in reversible deformation. Polypropylene and polyethylene, for example, are such thermoplastics. Thermosets, on the other hand, are more heat-resistant and do not deform. They are characterized as highly cross-linked plastics and therefore no longer change shape after hardening. The consistency of thermosets can be influenced depending on the additives used. The reason thermosets do not melt is that their glass transition temperature is higher than the decomposition temperature. Phenolic and epoxy resins belong to this group. Finally, there are elastomers with their high molecular weight, wide-meshed cross-linked polymers and elastic properties. They will deform when stress is applied in the form of tension or pressure, but then return to their original shape once it passes. Elastomers are favoured in the production of tires and rubber tubes. (Bonnet, 2016)

Depending on polymer type and molecular structure, polymers differ in their properties. In general, synthetic plastics have a low electrical and thermal conductivity and density. Polymer properties can be influenced by monomers, polymerization, shape and length of polymer chains, branching of polymer chains, additives and interactions of polymer chains between each other. Furthermore, conformation as well as configuration affect polymer properties. Confirmation is defined as the spatial arrangement of rotatable bonds on carbon atoms, whereas configuration is defined as the distribution of atoms in the molecule. Polarity and mobility of macromolecules influence the confirmation, while the degree of branching and linearity of the polymer chain structures influence the configuration. In addition, the properties of polymers are influenced by atomic and intermolecular bonds, which are in turn affected by the distance between polymer chains.

Furthermore, polymers in their solid state can exist in different phases: amorphous, semi-crystalline and crystalline (see Figure 1). Crystalline phase macromolecules form an even chemical structure and a regular arrangement of substituents, whereas the macromolecules in the amorphous phase have an irregular form and no ordered structure due to its chain structures and available side groups. The semi-crystalline phase is a mixture of the crystalline and amorphous phases. There will be both irregular and ordered structures within one macromolecule. The quantitative proportion of crystalline phase is determined by the crystallinity, which has an effect on polymer properties. The more crystalline a polymer is, the greater its dimensional stability and higher the melting point due to more uniformly arranged macromolecules and the associated intermolecular binding force. Li et al. (2019)

also observed a correlation between crystallinity and density. (Domminghaus, 2012; Klotzenburg et al., 2014; Bonnet, 2016)

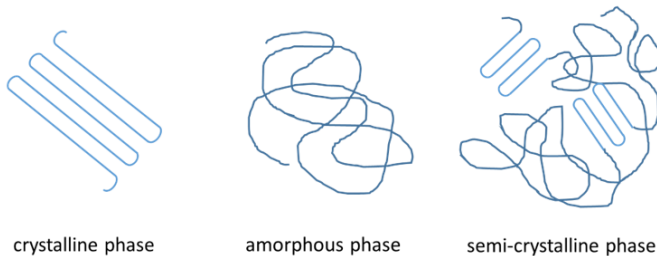


**Figure 1:** Different polymer phases (Camarda et al., 2021)

For this study, four different polymer types were chosen: polyethylene, polypropylene, polyethylene terephthalate and polybutylene succinate. The following paragraphs will analyse their characteristics according to the basic properties detailed above/in the previous chapter.

### 2.1.1. Basic information Polyethylene (PE)

Polyethylene (PE) is a semi-crystalline thermoplastic polymer made from ethylene through a polymerisation process. The basic components of polyethylene are hydrogen and carbon atoms. Depending on the manufacturing process, the properties of polyethylene can vary despite similar structures. Changes in pressure, temperature and catalysts used during the production due to chain length, degree of branching and molecular weight distribution affect polyethylene properties. However, polyethylene is always highly hydrophobic. Low-pressure and high-pressure processes are primarily used to produce polyethylene with different properties. For example, the harder and more heat-resistant HDPE is formed through a low-pressure process. The molecular strands form linearly and are closely bound by Van-der-Waals forces. High-pressure process, on the other hand, result in strong molecular branching, which prevent molecules from binding tightly and result in lower density. Therefore, LDPE is manufactured in a high-pressure process. In addition, density correlates well with crystallinity for polyethylene. Due to low degree of branching of HDPE, crystallinities of 80 % can be achieved and the melting temperature is set at 128 to 136 °C. LDPE has a higher degree of branching compared to HDPE, which results in a lower crystallinity of 40 to 50 % and a lower melting temperature at 105 to 115 °C.

### 2.1.2. Basic information Polypropylene (PP)

Polypropylene (PP) is a semi-crystalline thermoplastic based on propene produced through polymerisation. The particularity of polypropylene is the methyl group, which can be located laterally isotactically, syndiotactically or atactically placed on the main chain. Generally, the structure of polypropylene is isotactic, which creates an even structure with high crystallinity. This also leads to high stiffness and high melting temperatures. Isotactic and syndiotactic polypropylene are both semi-crystalline, while atactic polypropylene is amorphous. The crystallinity of isotactic polypropylene can reach up to 50 percent. However, the methyl side groups of isotactic polypropylene inhibit a close aggregation of the monomers, resulting in low densities ranging from 0.89 to 0.92 g cm<sup>-3</sup>, and a glass transition temperature between -10 and 0 °C. Due to the semi-crystalline structure of isotactic and

syndiotactic polypropylene, its properties can be influenced by temperature changes during manufacturing processes. In addition, polypropylene is non-polar and therefore resistant to polar fluids and water repellent. These characteristics make polypropylene popular in the fibre, automotive and packaging industry because it is very flexible and can withstand dynamic loads.

### **2.1.3. Basic information Polyethylene terephthalate (PET)**

Polyethylene terephthalate (PET) is a thermoplastic polymer made through polycondensation. It was originally used as fibre material and is now used in the packaging industry. Around 25 percent of packaging materials are made from PET by now. The structure of PET is formed by splitting methanol from dimethyl terephthalate and glycol. Depending on the manufacturing process, the structure of PET can either be amorphous-transparent or semi-crystalline. Furthermore, PET properties are significantly correlated to the crystallinity, which can reach up to 40 percent. Crystalline PET, for example, has low dynamic friction, high stiffness, electric insulating properties, and low water adsorption. Meanwhile, amorphous PET has good barrier properties. The density of PET is between 1.38 and 1.52 g cm<sup>-3</sup> and the glass transition temperature is at 80 °C. Due to the polar chemical structure of PET, it is resistant to non-polar solvents such as oil, grease, alcohol and hydrocarbon compounds. However, PET is not resistant to strong acids, bases and carbon acids.

### **2.1.4. Basic information Polybutylene succinate (PBS)**

Polybutylene succinate (PBS) belongs to the group of biodegradable bio-polymers and is a linear aliphatic polyester. It is obtained through a reaction of succinic acid with 1,4-butanediol. Both educts can be of petrochemical or biological origin. Depending on the basis of the educts, PBS can be made up to 100 percent bio-based. Succinic acid serves as a dicarboxylic acid for the thermoplastic polyester, while 1,4-butanediol is a dihydric alcohol from butane. The bio-based production of succinic acid results from the fermentation metabolism of the bacterium *Basfia succiniproducens* (DD1). The bacterium metabolizes substrates in the form of glucose, fructose, xylose and crude glucose to sustain the fermentation process. PBS has a modulus of elasticity between 300 and 950 MPa. The melting point of PBS is 84 °C and the glass transition temperature ranges from -45 to -30 °C. PBS is one of the heavier bio-polymers with a density of 1.24 to 1.28 g cm<sup>-3</sup>. The area of application of PBS is mainly in the packaging industry and as mulch film. Due to the semi-crystalline structure of PBS, some properties are comparable with the physicochemical properties of LDPE. (Türk, 2014)

## **2.2. General information of plastic production**

The first plastic product was manufactured in 1907 and was called "Bakelite". In 1950, plastic production reached 0.35 million metric tonnes (Verla et al., 2019), and ever since it has continually increased together with the world population (Figure 2). Plastic offered a lot of benefits because of its resilience, light weight and diverse applicability, for example in the packaging (40 %), building (20 %) and automotive (8 %) sectors (Ibrahim et al., 2021). Furthermore, its cheap manufacturing process contributed to globalization, so that the worldwide plastic production finally reached 381 million tonnes in 2015 (Verla et al., 2019).

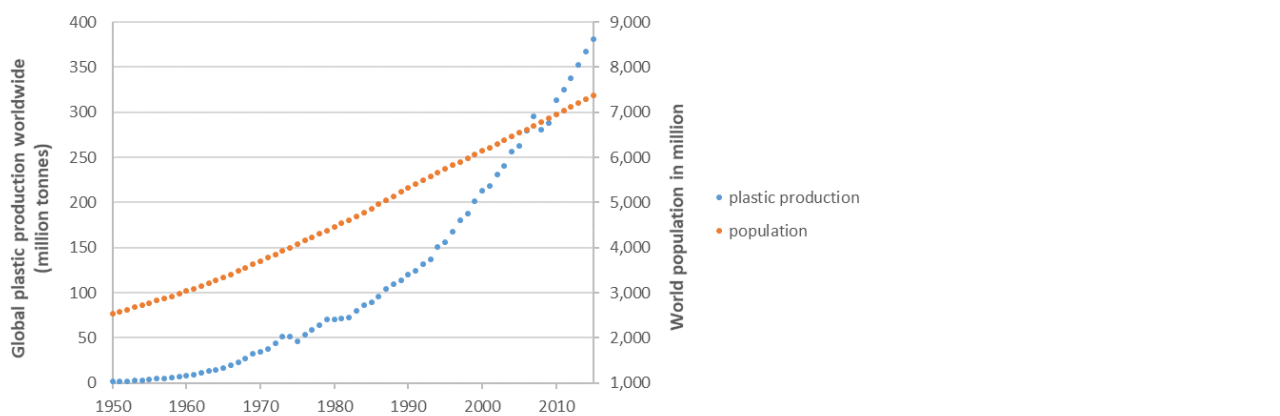


**Figure 2:** Development of global plastic production (Geyer et al., 2017) and the worldwide population (United Nations, 2019)

Unfortunately, a vast majority of synthetic plastics are not biodegradable, recyclable or usable for thermal energy generation after usage, causing an environmental problem with increasing amounts of solid plastic waste. To overcome the environmental problem of plastics, research was conducted to develop biodegradable plastics, such as bioplastic. Bioplastics are defined as materials that are either bio-based, biodegradable or both. While bio-based means that plastic materials are derived from biomass, biodegradable describes a chemical degradation process through microorganisms, which are present in the environment and convert biological material into natural substances (water, carbon dioxide, compost). Compared to traditional plastic materials, bioplastics represent less than one percent of the annual plastic production, but have a higher growth rate. According to data published by European Bioplastics (2019), the global production of bioplastic increased from 2.09 million tonnes in 2020 to 2.42 million tonnes in 2021, and has substituted some traditional plastics in the packaging, automotive, and consumer electronics markets, among others. In addition, the use cases and product variety of bioplastics continue to diversify.

### 2.3. Plastic waste in the marine environment

Between 1950 and 2015, around 8300 million tonnes of polymers, synthetic fibres and additives were produced globally. Nearly 30 % (2500 million tonnes) of the earliest plastics were still in use in 2015. Out of the remaining 5800 million tonnes that were used once, 4600 million tonnes went directly to landfills or were otherwise discarded, 700 million tonnes were incinerated, and 500 million tonnes were recycled (Geyer et al., 2017). Of these 500 million tonnes recycled plastics, 100 million tonnes were reused until 2015, while 100 million tonnes were later incinerated and 300 million tonnes were discarded after recycling. Recycling and incineration of plastic increased since 1980, and Geyer et al. (2017) estimated that by 2010, 62 percent of the global plastic waste had been discarded, 22 percent had been incinerated and 16 percent had been recycled. However, plastic waste is also released into the environment through improper disposal.

In 2010, 275 million tonnes of plastic waste were produced. This includes one-time use plastic waste as well as waste from plastic produced in previous years. From those 275 million tonnes, 99,5 million tonnes were used within 50 km of the coastline, which represents the plastic that is most likely to end up entering the marine environment, with 31.9 million tonnes having a particularly high probability of leaking into the oceans, as they were stored in open and unsecured landfills. In total, it is estimated

that 4.8 to 12.7 million tonnes of the annual global plastic waste entered the oceans through other channels such as rivers (Jambeck et al., 2015) and 150 million tonnes were already present (Rujnić-Sokole, 2015). When plastic ends up in the ocean, it is moved and distributed by wind and ocean surface currents. In the oceans, the surface currents create large circulating systems called gyres. Overall, there are five large gyres distributed across the oceans and once plastic finally ends up in a gyre, it stays there (Figure 3). “The 5 gyre Institute” is the first organisation to research plastic pollution in all five gyres and has estimated the number of plastic particles floating on the surface of the oceans to be 270,000 metric tonnes, which corresponds to about 5.25 trillion particles (Eriksen et al., 2014). However, not only plastics are present in the marine environment, but also dissolved substances including environmental pollutants like persistent organic pollutants.



Figure 3: Five largest ocean garbage gyres

## 2.4. Persistent organic pollutants / polycyclic aromatic hydrocarbons

Persistent organic pollutants (POP) are ubiquitous and present in the atmosphere, soil and water. Because of their chemical structure, POPs linger in the environment for a long time and are bio-accumulative. The hydrophilic properties of the POPs can lead to an accumulation in the fatty tissues of organisms when ingested. In the marine environment, this affects mainly fish and birds (Gray, 2002; Cheung et al., 2007; Corsolini and Sarà, 2017; Mwakalapa, et al., 2018; Sonne et al., 2020). Due to the polarity of POPs, they tend to accumulate on plastic particles. Because POPs are a global environmental problem, the Stockholm convention was passed in 2001 to protect human health, wildlife and the environment from chemicals that remain intact in the ecosystem for a long time. The group of POPs includes polycyclic aromatic hydrocarbons.

Polycyclic aromatic hydrocarbons (PAH) belong to a group of hydrocarbon compounds, with over 200 different organic compounds consisting of at least two benzene rings. These benzene rings are connected to one another via at least two ring members of the benzene ring (condensation). Furthermore, PAHs are assigned in two categories, “light PAHs” and “heavy PAHs”. While light PAHs have between two and four benzene rings, heavy PAHs consist of more than four benzene rings. In addition to the fused ring systems, the hydrocarbons can have additional substituents (methyl groups, or oxygen and nitrogen), resulting in many individual variants (Harvey, 1997). PAH can arise through

natural or anthropogenic processes. In both cases, PAHs are formed as a result of incomplete combustion processes of organic substances in the environment. PAHs from natural sources occur for example through volcanic eruptions or fires, while anthropogenic sources of PAHs are emitted through small combustion plants and industrial processes like fossil combustion engines. PAHs released in the atmosphere either remain in a gaseous state or bind to aerosols. Meanwhile, the hydrophobic properties of PAHs ensure accumulation on sediments, soils and adsorb on lipophilic surfaces. Light PAHs are biologically degradable through photochemical processes, while heavy PAHs are only partially degradable. PAHs rarely occur as individual components and some are highly toxic, carcinogenic, mutagenic, teratogenic and bio-accumulating (ATSDR 1995). Naphthalene, fluorene and phenanthrene as well as 13 other PAHs are on the United States Environmental Protection Agency's (USEPA) list of priority pollutants (Yan and Wang, 2004). The molecular weight of these 16 priority PAH pollutants is between 128 and 278 g mol<sup>-1</sup>, and in their purest form they are colourless crystalline solids. The boiling point of most PAHs is 300 to 500 °C. Due to the lacking hydrophilic functional groups, PAHs are hydrophobic and only slightly soluble in water, but dissolve well in organic solvents. As the number of benzene rings increases, so does the hydrophobicity and also the lipophilicity. In the fluid state, PAHs are transported according to their solubility. For example, the 16 priority pollutants have very different water solubilities. Thus, as the number of benzene rings increases, water solubility and mobility in an aqueous phase decrease. The accumulation of PAHs in a solid state is driven by retardation and diffusion. In the fluid state, the substance transport mainly takes place via advection, diffusion, dispersion and sorption. These four transport processes determine the partition in a gaseous, fluid and solid phase. The distribution of the different phases is given by the partition coefficient.

In this thesis, four widely considered predictors of partition coefficients are examined, namely log K<sub>ow</sub>, MW, water solubility (log C<sub>w</sub><sup>sat</sup>) by Ma et al. (2010) ( $\log C_w^{sat} = -0.032 \text{ MW} + 4.09$ ) and hexadecane-water partition coefficient (log K<sub>hdw</sub>) by Schwarzenbach et al. (2003) ( $\log K_{hdw} = 1.21 \log K_{ow} - 0.43$ ). Where, log C<sub>w</sub><sup>sat</sup> describes the logarithmic water solubility of subcooled liquid and the log K<sub>hdw</sub>, which is the ratio of a molar concentration of a dissolved substance in the n-hexadecane phase to the molar concentration of the solute in the water phase. In Table A2.1 are the values of the log K<sub>ow</sub>, MW, log C<sub>w</sub><sup>sat</sup> and log K<sub>hdw</sub> for the 16 EPA-PAHs listed.

## 2.5. Sorption/Sorption isotherm

Sorption describes the process of a molecule passing from one state into another. In this thesis one state is solid, which is represented by plastics particles and the other state is liquid, which is represented by distilled water. The sorptive is the unbound compound in the gaseous or liquid phase and the sorbate is the compound bound to a solid phase (sorbent). The accumulation of a compound in a solid phase can take place through adsorption or absorption and can be followed by desorption. When the compound only interacts with the surface of the solid phase, it is called adsorption. However, when the compound moves into the solid phase, it is called absorption. Desorption is the reversal of adsorption or absorption: the bound compounds are removed from the solid phase during the desorption process and released in a gaseous or liquid phase. Adsorption, absorption and desorption are together referred to as sorption.

The distribution of a compound (*i*) in a two-phase system is determined by the partition coefficient ( $K_{D,i}$ ). The sorbate concentration of the solid phase ( $C_{s,i}$ ) is set in relation to the sorptive concentration of the liquid phase ( $C_{w,i}$ ) at a constant temperature. The following equation applies for the equilibrium state:

$$K_{D,i} = \frac{C_{s,i}}{C_{w,i}} \quad \text{equation 1}$$

### Sorption isotherm

Linear and Freundlich isotherm models were applied to calculate plastic-water partition coefficients like in J. Wang et al. (2019), Zuo et al. (2019) and Zhao et al. (2020) who confirmed the suitability of these models with high R<sup>2</sup>-values for a PAH-plastic-water system. PAH equilibrium concentrations in the aqueous phase  $C_{w,eq}$  ( $\mu\text{g L}^{-1}$ ) were determined by analysing aliquots taken from the vials of the sorption isotherm experiments. The PAH concentration in the polymer sorbent at equilibrium  $C_{s,eq}$  ( $\mu\text{g g}^{-1}$ ) was then calculated from the  $C_{w,eq}$  ( $\mu\text{g L}^{-1}$ ) through mass balance.

The partition coefficient of Linear isotherm model assumes a linear correlation of the concentration of the sorbate in the aqueous phase and the solid phase (equation 2). This represents the simplest approach

$$K_D = \frac{C_{s,eq}}{C_{w,eq}} \quad \text{equation 2}$$

where  $K_D$  (L/kg) is the distribution coefficient.

In contrast, the Freundlich isotherm model presumes sorbate distributes heterogeneously on the surface of a sorbent (Yang, 1998). The Freundlich equation is as follows:

$$C_{s,eq} = K_{Fr} * C_{w,eq}^n \quad \text{equation 3}$$

The log-linear equation of the Freundlich model is as follows:

$$\log C_{s,eq} = \log K_{Fr} + n * \log C_{w,eq} \quad \text{equation 4}$$

with  $\log K_{Fr}$  (L kg<sup>-1</sup>) being the Freundlich partition coefficient, while  $n$  (-) is the Freundlich exponential coefficient.

## 2.6. Prediction of plastic-water partition coefficients

### PAH properties including $\log K_{ow}$ , MW, $\log C_w^{sat}$ , $\log K_{hdw}$

For hydrophobic pollutants with low water solubility, it is not easy to conduct sorption isotherm experiments (Zhu et al., 2015), especially for polymers that accumulate hydrophobic pollutants well in the water phase. Thus, researchers attempted to estimate  $\log K_{p-w}$  using linear regression models. Typically, physicochemical properties of sorbates, like octanol-water partitioning ( $\log K_{ow}$ ) (Adams et al., 2007; Smedes et al., 2009; Lohmann, 2012; Choi et al., 2013; Hüffer and Hofmann, 2016), hexadecane-water partitioning ( $\log K_{hdw}$ ) (Choi et al., 2013; Hüffer and Hofmann, 2016), aqueous solubility (Lohmann, 2012) and molecular weight (Smedes et al., 2009; Choi et al., 2013), were used to estimate  $\log K_{p-w}$  values of organic hydrophobic compounds. For PAHs on PE, correlations between  $\log K_{PE-w}$  and  $\log K_{ow}$  were determined with a coefficient of determinations ( $R^2$ ) in the range of 0.89 - 0.97 (Adams et al., 2007; Smedes et al., 2009; Lohmann, 2012; Choi et al., 2013; Hüffer and Hofmann, 2016), whereas  $\log K_{PE-w}$  correlates with  $\log K_{hdw}$  with an  $R^2$  of 0.94 - 0.97 (Choi et al., 2013; Hüffer and Hofmann, 2016). According to Lohmann (2012),  $\log K_{PE-w}$  correlates better with aqueous solubility of PAHs ( $R^2 = 0.94$ ) than with  $\log K_{ow}$  ( $R^2 = 0.92$ ) in a log linear model. For PAHs, another parameter that correlates well with  $\log K_{PE-w}$  is molecular weight:  $R^2 = 0.97$  and 0.99, according to Choi et al (2013) and Smedes et al. (2009), respectively.

### Polymer properties

Only a few studies are available to determine PAH accumulation on other polymers like PP, PET and PBS. J. Wang et al. (2019) conducted sorption experiments with selected PAHs (naphthalene and phenanthrene) on five different polymer types, i.e. HDPE, LDPE, PP, PVC and polystyrene (PS) as meso- and microplastic in order to determine plastic-water partition coefficient according to the Freundlich isotherm model ( $\log K_{Fr}$ ). For microplastics,  $\log K_{Fr}$  of naphthalene followed the order of PP (4.06) > PVC (2.85) > LDPE (2.84) > PS (2.71) > HDPE (2.61), whereas the  $\log K_{Fr}$  of phenanthrene decreased from HDPE (4.2) > PVC (4.19) > PP (4.18) > LPDE (4.08) > PS (2.64). Partition coefficients determined by J. Wang et al. (2019) showed that This indicates that the sorption behaviour of a sorbate is influenced by the properties of a sorbent material.

Indeed, different polymer materials possess different properties like density, glass transition temperature, melting point or crystallinity. Many sorption experiments were conducted using a variety of polymer materials to determine the influence of polymer properties on sorption behaviour of hydrophobic organic compounds. However, the results are inconsistent. For example, J. Wang et al. (2019) found that the specific surface area (SSA) of plastic particles strongly influences sorption affinity. The higher the SSA of a certain polymer type, the higher plastic-water partition coefficient ( $\log K_{p-w}$ ), though with some exceptions: phenanthrene on PS for microplastics and on expandable PS (EPS) for mesoplastics; naphthalene on PVC for both micro- and mesoplastics. EPS mesoplastics and PVC mesoplastics showed higher sorption ability than PS/PVC microplastics, despite their lower SSA. J. Wang et al. (2019) assumed the higher sorption affinity may have resulted from the availability of certain functional groups on the surface of EPS and PVC, due to polymer additives like lubricants, stabilizers or flame retardants in EPS and PVC. Furthermore, temperature-sensitive polymer properties like polymer phase, crystallinity and melting point were found to affect the sorption affinity (Endo and Koelmans, 2016; Li et al., 2018; Über et al., 2019; J. Wang et al., 2019; Wang et al., 2020). Although the impact of sorbent properties on sorption affinity is often discussed, a correlation of  $\log K_{p-w}$  and thermodynamic polymer properties has not yet been proven.

## 2.7. Theory

Published studies have shown that the plastic-water partition coefficient of PAHs can be correlated with different PAH properties. Most common correlations of PAH properties could be found for a linear correlation of octanol-water partition coefficient and MW of PAHs and LDPE-water partition coefficient (Booij et al., 2003; Adams et al., 2007; Smedes et al., 2009; Lohmann, 2012; Choi et al., 2013; Zhu et al., 2015), which is defined as

$$\log K_{p-w} = m_1 * \text{properties}_{PAH} + b_1 \quad \text{equation 5}$$

where  $\log K_{p-w}$  is the plastic-water partition coefficient ( $L \text{ kg}^{-1}$ ), PAH properties represents  $\log K_{ow}$  and MW, and  $m_1$  and  $b_1$  are the parameters of the slope and intercept of the linear regressions. Furthermore, this work could identify polymer properties that correlate with plastic-water partition coefficients and result in equation 6

$$\log K_{p-w} = m_2 * \text{properties}_{plastic} + b_2 \quad \text{equation 6}$$

where the slope and intercept of the equations are determined as  $m_2$  and  $b_2$  respectively.

In this work, modelled plastic-water partition coefficients are determined by a combination of physicochemical properties of polymers and PAHs, resulting in equations that were compared to published equations based on PAH properties and regressed against previously reported  $\log K_{p-w}$  values. This comparison with previously published equations is used to evaluate the equations obtained in this work.

## 3. Method and Material

### 3.1. Sorption Experiment

A series of sorption isotherm experiments were conducted in the laboratory to determine the  $K_{p-w}$  of three PAHs, i.e. naphthalene (molecular weight = 128.16 g mol<sup>-1</sup>;  $\log K_{ow}$  = 3.37), fluorene (molecular weight = 166.21 g mol<sup>-1</sup>;  $\log K_{ow}$  = 4.18) and phenanthrene (molecular weight = 178.22 g mol<sup>-1</sup>;  $\log K_{ow}$  = 4.46), for three conventional polymers (LDPE, PP and PET) and one biodegradable polymer (PBS).

#### 3.1.1. Preparation of stock solutions and PAH aqueous solutions for the experiments

Naphthalene (> 99 %) and phenanthrene (> 97 %) were purchased from Fluka (Switzerland), and fluorene (> 98 %) from Sigma Aldrich (USA). Ethanol (HPLC grade) was obtained from Fisher Scientific (Germany). For each PAH, a 5 mg L<sup>-1</sup> stock solution was prepared by dissolving the solid standard compound in ethanol. These stock solutions were then further diluted with the same ethanol. All original and diluted stock solutions were kept in a dark refrigerator until ready to use. PAH aqueous solutions were prepared by adding a given PAH stock solution to Milli-Q water (conductivity < 0.056  $\mu\text{S cm}^{-1}$  at 25 °C) to achieve certain initial concentrations. The volume of ethanol in the PAH solutions was kept at less than 0.25 vol.-% to avoid co-solvent effects. Solutions containing a single PAH with different concentrations were filled in individual glass bottles and placed on a horizontal shaker at 150 rpm for 48 hours to ensure homogeneity.

### 3.1.2. Experimental setup

All sorption experiments were conducted in 20 mL crimp top glass vials at ambient temperature (21 °C). Each vial was filled with 16 mL of well-mixed PAH aqueous solution and carefully weighed plastic particles and sealed with a Teflon-faced butyl rubber septum and aluminium crimp top cap. A couple of references were prepared under the same conditions without polymers to document the glass adsorption behaviour of a given PAH. All vials were shaken gently on a horizontal shaker at 150 rpm during the sorption experiments.

A total of twelve series of sorption experiments were conducted in the laboratory to determine twelve  $\log K_{p-w}$ . Each series consisted of a combination of single PAH (naphthalene, fluorene or phenanthrene) and single polymer (LDPE, PET, PP or PBS). To determine a  $\log K_{p-w}$ , at least six different final concentrations were generated at the sorption equilibrium. The final concentrations for naphthalene, fluorene and phenanthrene were designed to be in the range of 25 - 3,500  $\mu\text{g L}^{-1}$ , 30 - 500  $\mu\text{g L}^{-1}$  and 20 - 250  $\mu\text{g L}^{-1}$ , respectively. Thus, for each sorption experiment series, at least six different polymer-to-PAH mass ratios were prepared.

For a given polymer-to-PAH mass ratio, several vials were prepared in the same manner: one vial was designated for kinetic experimentation and the rest were used for isotherm experiments. From the vial for the kinetic experiment, 0.5 mL of PAH aqueous solution were taken at certain intervals and analysed through High Performance Liquide Chromatography (HPLC) to investigate the evolution of the PAH concentration in the aqueous phase. The sampling interval for kinetic samples were 1, 2, 3, 7, 14 and 28 days for all four polymers. Additional samples were taken after 1 h and 3 h for PBS, and after 3 h and 5 h for LDPE. Based on the outcome of the kinetic experiment, the time required to reach 95 %-equilibrium was estimated using pseudo-first-order (PFO) and pseudo-second-order (PSO) models. Accordingly, the minimum duration of the sorption experiment was set to be 36 days to ensure equilibrium.

Regarding the sorption isotherm experiments, 0.5 mL of the PAH aqueous solution was taken from the designated vials. These vials had been prepared and initiated analogue to the vial for kinetic experiment. An aliquot was taken only once to determine PAH concentration of the aqueous phase at equilibrium.

### 3.1.3. Determination of PAH concentrations

At each sampling event, 0.5 mL of the aqueous samples was taken for the HPLC analysis. A stainless steel/glass syringe was used for the sampling. Every sampling was executed through the Teflon/butyl rubber septum, i.e. the crimp top cap was kept closed to minimize the loss of PAHs in the headspace of the vial as well as to prevent the loss of polymer particles, which lightly adhered to the outside of the syringe needle during the sampling. After every sampling event, the syringe was thoroughly cleaned using ethanol (HPLC grade) and Milli-Q water.

The concentrations of the PAH stock solutions, aqueous solutions for experiments, and aliquots taken from the vials were analysed with the DIONEX/Thermo Fisher Scientific UHPLC with a Diode Array Detector (UltiMate 3000, Germany). The separation of PAHs was performed on a "HYPERSIL Green PAH" column (4.6 x 150 mm, HV-01889-92 Thermo Scientific, Germany) in isocratic mode using acetonitrile-water (80 % - 20 %, v v<sup>-1</sup>) as mobile phase at a flow rate of 1 mL min<sup>-1</sup>. Naphthalene, fluorene and phenanthrene were measured at wavelengths of 220, 206 and 250 nm, respectively.

In general, hydrophobic organic substances may adsorb not only on the surface of plastic particles in the vial but also on the inner glass surface of the vial to some extent. Thus, to determine the PAHs adsorption on the inner surface of the vials, the vials that had been used for the isotherm experiment were further investigated. They were emptied and lightly rinsed with Milli-Q water to remove all polymer particles. A volume of 4 mL of n-hexane and 10  $\mu$ L of an internal standard, i.e. a mixture of five deuterated PAHs (10  $\mu$ g mL $^{-1}$  in cyclohexane, NEOCHEMA GmbH, Germany) were added to the empty vial and placed on a horizontal shaker at 150 rpm for 144 h.

The extract with the internal standard was analysed via gas-chromatography-mass spectrometry (GC-MS). GC-MS analysis was carried out using the gas chromatograph TRACE 1310 coupled to a quadrupole mass spectrometer ISQ 7000 (Thermo Fisher Scientific, Germany). To separate the PAHs, a capillary column TG-5MS (5 % Diphenyl, 95 % Dimethyl-Polysiloxan, 30 m, inner diameter 0.25 mm, film thickness 0.25  $\mu$ m) (Thermo Fisher Scientific, Germany) was applied. A volume of 1  $\mu$ L of an aliquot was taken from the extract and deposited into the injector heated at 270 °C. The GC oven temperature started at 70 °C and was kept for 1 min. The column was then heated up to 120 °C (holding time 1 min.) at a rate of 20 °C min $^{-1}$ , then to 190 °C (holding time: 6 min) at 15 °C min $^{-1}$ , until the final temperature of 320 °C (holding time: 9 min) at a rate of 35 °C min $^{-1}$ . No memory effect was detected.

For the MS analysis, selected ion mode (SIM) was applied to determine peak areas of selected mass-to-charge ratio ( $m\ z^{-1}$ ) for naphthalene ( $m\ z^{-1} = 127, 128, 129$ ), fluorene ( $m\ z^{-1} = 165, 166, 167$ ), phenanthrene ( $m\ z^{-1} = 176, 178, 179$ ) as well as two deuterated PAHs, i.e. naphthalene-d<sub>8</sub> ( $m\ z^{-1} = 134, 136, 137$ ) and phenanthren-d<sub>10</sub> ( $m\ z^{-1} = 184, 188, 189$ ).

### 3.1.4. Kinetic models

Both PFO and PSO models are commonly used to describe adsorption data for non-equilibrium conditions (Lin and Wang, 2009; Rochman et al., 2013; Wang and Wang, 2018). The pseudo-first-order model for adsorption was developed by Lagergren (1898) and is described as follows:

$$\frac{dq_t}{dt} = k_1(q_e - q_t) \quad \text{equation 7}$$

where  $k_1$  (d $^{-1}$ ) is the rate constant for adsorption,  $q_t$  ( $\mu$ g g $^{-1}$ ) is the amount of sorbate adsorbed on the sorbent at time  $t$  and  $q_e$  ( $\mu$ g g $^{-1}$ ) is the amount of sorbate adsorbed at equilibrium.

The non-linear equation of PFO was applied for further calculation and is expressed as follows:

$$q_t = q_e(1 - e^{-k_1 t}) \quad \text{equation 8}$$

The PSO model for adsorption was developed by Ho (1995) as:

$$\frac{dq_t}{dt} = k_2(q_e - q_t)^2 \quad \text{equation 9}$$

where  $k_2$  (g ( $\mu$ g d) $^{-1}$ ) is the rate constant for adsorption.

The non-linear equation of PSO was utilized for further calculation and can be described using the following equation:

$$q_t = \frac{k_2 q_e^2 t}{1 + k_2 q_e t} \quad \text{equation 10}$$

### 3.2. Method determination of regression model

Partition coefficients were calculated using Linear and Freundlich isothermal models after equilibrium was reached. The isothermal model with the highest accuracy is used to compare the resulting partition coefficients with individual PAH properties ( $\log K_{ow}$ , MW,  $\log C_w^{sat}$ ,  $\log K_{hdw}$ ) and individual plastic properties (density, crystallinity, melting temperature, glass transition temperature, pore volume, median diameter of the particles, surface free energy), and to test for a linear relationship.

Furthermore, combinations of the PAH and plastic properties were created and also compared to the partition coefficients. Each combination resulted in a matrix with rows representing the plastics and columns representing the PAH properties. This property matrix was compared with the matrix containing the partition coefficients according to Dikbaş' (2017) method, that were similar enough, to be valid in the purpose of this thesis. According to the method of Dikbaş (2017), two-dimensional correlation coefficients were determined. On the one hand, the horizontal results of two matrices are compared with each other and are combined to a horizontal correlation coefficient ( $r_h$ ), and on the other hand, the vertical results are combined to a vertical correlation coefficient ( $r_v$ ) which represent the two-dimensional correlation coefficient. The following formula is used for this purpose:

$$r = \frac{\sum_m \sum_n (A_{mn} - \bar{A})(B_{mn} - \bar{B})}{\sqrt{[\sum_m \sum_n (A_{mn} - \bar{A})][\sum_m \sum_n (B_{mn} - \bar{B})]}} \quad \text{equation 11}$$

where  $r$  is the correlation coefficient of two matrices A and B, while the matrices A and B have the same size. The overall average of the matrices were  $\bar{A}$  and  $\bar{B}$ , while the index m represents the horizontal rows of the matrices and the index n represents the vertical columns. Equation 11 represented the basis to calculate both the  $r_h$  (equation 12) and the  $r_v$  (equation 13).

$$r_h = \frac{\sum_m \sum_n (A_{mn} - \bar{A}_m)(B_{mn} - \bar{B}_m)}{\sqrt{[\sum_m \sum_n (A_{mn} - \bar{A}_m)][\sum_m \sum_n (B_{mn} - \bar{B}_m)]}} \quad \text{equation 12}$$

$$r_v = \frac{\sum_m \sum_n (A_{mn} - \bar{A}_n)(B_{mn} - \bar{B}_n)}{\sqrt{[\sum_m \sum_n (A_{mn} - \bar{A}_n)][\sum_m \sum_n (B_{mn} - \bar{B}_n)]}} \quad \text{equation 13}$$

where  $\bar{A}_m$  was the average of the m<sup>th</sup> row of matrix A, and  $\bar{B}_m$  was the average of the m<sup>th</sup> row of matrix B for equation 12. While  $\bar{A}_n$  was the average of the n<sup>th</sup> row of matrix A, and  $\bar{B}_n$  was the average of the n<sup>th</sup> row of matrix B for equation 13.

The correlation coefficients ( $r_h$  and  $r_v$ ) can take values between -1 and 1, therefore, for better comparability, the correlation coefficients are converted into coefficients of determination ( $R_h^2$  and  $R_v^2$ ), which can take values between 0 and 1.

#### 4. Determination of plastic-water partition coefficients

The results of three PAH kinetic adsorption experiments on the four polymers are presented in Table A4.1. The  $R^2$  values of PFO (0.669 to 1.00) and PSO (0.718 to 1.00) indicate a good fit for both models. Hence, samples for sorption isotherm experiments were taken between  $t_{95}$  (day) of PFO and PSO, where  $t_{95}$  represents the duration to the 95 % sorption equilibrium.

Figure 4 illustrates the comparison of the  $t_{95}$  determined by PFO and PSO for the sorption experiments of PAHs on LDPE, PBS, PP and PET. It should be noted that only a general trend among polymers or PAHs is discussed with Figure 4, since the main objective of these kinetic experiments was to estimate the sampling time for sorption isotherm experiments, and therefore the amount of polymers and the initial concentrations in each batch is different.

One of two significant tendencies from Figure 4 is the duration to the 95 % equilibrium, generally estimated to be much longer when applying PSO compared to the  $t_{95}$  determined by PFO. Therefore, samples for sorption isotherm experiments were taken between the  $t_{95}$  values by PFO and PSO. Further, the minimum duration was set to be 36 days for this thesis. The other tendency is the duration to the 95% equilibrium, which was determined to be significantly longer when the “rubbery” PET was used as sorbent, compared to the other “glassy” polymers, indicating that the polymer state may have a certain influence on sorption kinetics.

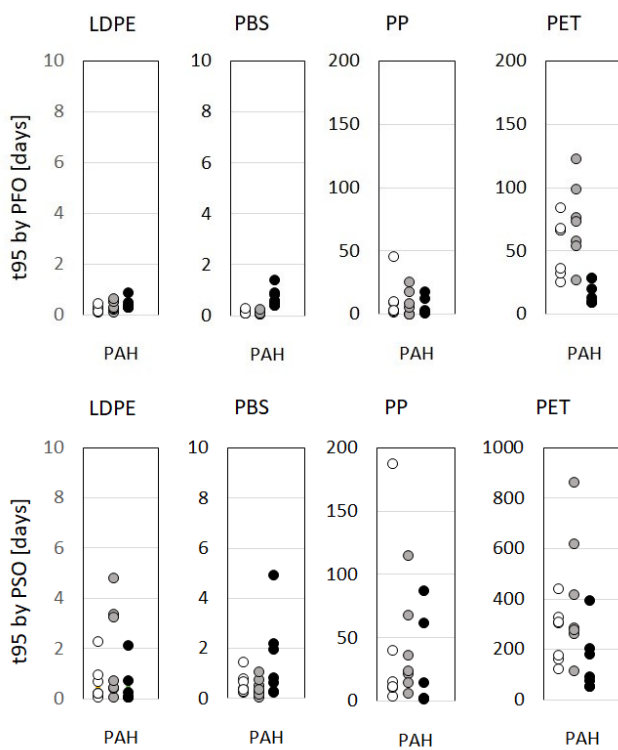


**Figure 4:** Comparison of  $t_{95}$  of the sorption experiments of naphthalene (white circle), fluorene (gray circle) and phenanthrene (black circle) on LDPE, PBS, PP and PET;  $t_{95}$  calculated by PFO model (top);  $t_{95}$  calculated by PSO model (bottom).

For the glass adsorption study, one representative sample from each concentration series and each series of experiments was analysed with a duplicate determination in the GC/MS. No glass adsorption was detected for any of the samples examined and was not considered further (Table A4.2 - A4.4).

## 4.1. Sorption isotherm experiments

### 4.1.1. Linear vs Freundlich isotherm models

Sorption isotherm experiments were implemented to determine the  $\log K_{p-w}$  of naphthalene, fluorene and phenanthrene on LDPE, PP, PBS and PET using two models: Linear and Freundlich isotherm models. The  $\log K_{p-w}$  values determined by Linear and Freundlich isotherm models are referred to as  $\log K_D$  and  $\log K_{Fr}$ , respectively. The constants calculated based on both models are summarized in Table 1 and Figure 5.

Figure 5 illustrates that both the  $\log K_D$  and  $\log K_{Fr}$  values increased in order of naphthalene < fluorene < phenanthrene for all four polymers, with the exception of LDPE for  $\log K_D$ . This tendency is remarkable when the Freundlich sorption isotherm model was applied. Furthermore, the  $\log K_{Fr}$  values clearly increased in order of PET < PP < LDPE < PBS, while the tendency is less significant when the Linear model was applied.

As seen in Table 1,  $R^2$  values are in the range of  $0.911 \pm 0.080$  for Linear and  $0.878 \pm 0.101$  for Freundlich isotherm models, indicating a good performance of both models. A paired t-test resulted in no significant difference between the mean  $R^2$  values of Linear and Freundlich isotherm models ( $p$ -value  $> 0.05$ ). Similarly, no significant difference was found between  $\log K_D$  and  $\log K_{Fr}$  values ( $p$ -value  $> 0.05$ ) calculated using Linear and Freundlich isotherm models, respectively.

With regard to the reproducibility of the experiments, the standard deviation (SD) by the Freundlich isotherm model was significantly smaller than the SD determined through Linear isotherm model, indicating that the reproducibility in calculating  $\log K_{Fr}$  is significantly better when applying the Freundlich isotherm model. Lower SD values of  $\log K_{Fr}$  are clearly observed in Figure 5 as well. Thus, the  $\log K_{Fr}$  values derived by the Freundlich isotherm model was used for the investigation of correlations between  $\log K_{Fr}$  and PAH and plastic physicochemical properties. In the following chapters, the  $\log K_{Fr}$  values of the Freundlich isotherm are referred to as  $\log K_{p-w}$  or as  $\log K_{LDPE-w}$ ,  $\log K_{PP-w}$ ,  $\log K_{PBS-w}$  and  $\log K_{PET-w}$  when referring specifically to the partition coefficient for LDPE, PP, PBS and PET.

**Table 1:** Constants of Linear and Freundlich sorption isotherm models for tested sorbates

plastic	Linear isotherm model			Freundlich isotherm model			
	$K_d$ (L kg $^{-1}$ )	SD (L kg $^{-1}$ )	$R^2$	$\log K_{Fr}$ (L kg $^{-1}$ )	SD (L kg $^{-1}$ )	n (-)	$R^2$
<i>halene</i>							
LDPE	13,726	434	0.983	2.93	0.33	1.33	0.854
PP	13,982	413	0.985	2.88	0.32	1.34	0.859
PBS	9,937	977	0.859	3.35	0.22	1.17	0.916
PET	224	9	0.967	2.68	0.13	0.90	0.942
<i>ne</i>							
LDPE	31,021	3.224	0.845	3.88	0.28	1.21	0.844
PP	36,716	4.154	0.821	3.64	0.35	1.34	0.798
PBS	31,797	1.784	0.946	4.24	0.17	1.08	0.912
PET	3,061	181	0.940	2.81	0.24	1.26	0.884
<i>nthrene</i>							
LDPE	25,559	2.906	0.928	4.33	0.10	0.93	0.981
PP	37,121	4.037	0.944	3.83	0.20	1.29	0.968
PBS	74,087	4.402	0.983	5.16	0.10	0.81	0.965
PET	5,918	1.471	0.730	2.82	1.06	1.31	0.612

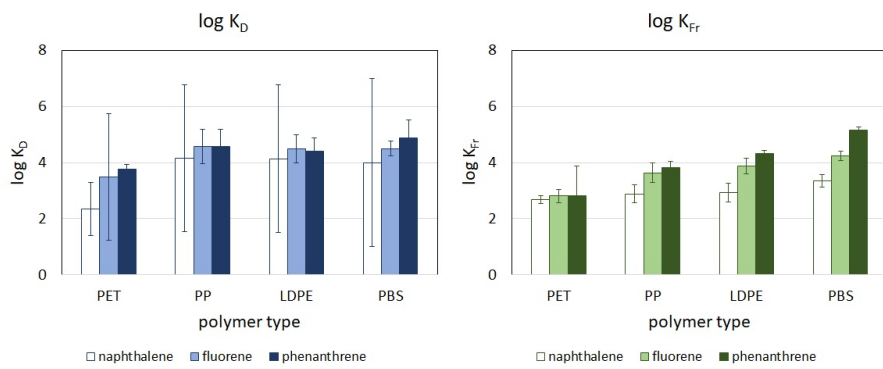


**Figure 5:** Comparison of Log  $K_D$  (left) and  $\log K_{Fr}$  (right) of naphthalene, fluorene and phenanthrene on LDPE, PP, PBS and PET.

#### 4.2. Comparison of $\log K_{p-w}$ from this thesis versus published studies

In the following subchapters the  $\log K_{p-w}$  values of this thesis are compared with already published results. An overview of published  $\log K_{p-w}$  and  $\log K_{p-w}$  of this thesis are shown in the following table:

**Table 2:** Comparison of literature  $\log K_{p-w}$  and  $\log K_{p-w}$  of this thesis

	NAPH		FLN		PHEN	
	literature	this thesis	literature	this thesis	literature	this thesis
LDPE	2.81 - 3.23	$2.93 \pm 0.33$	3.67 - 4.14	$3.88 \pm 0.28$	4.04 - 4.41 <sup>a</sup>	$4.33 \pm 0.10$
PP	2.72 - 4.18	$2.88 \pm 0.32$	4.16	$3.64 \pm 0.35$	2.43 - 4.18	$3.83 \pm 0.20$
PBS		$3.35 \pm 0.22$		$4.24 \pm 0.17$	4.92	$5.16 \pm 0.10$
PET	4.39	$2.68 \pm 0.13$	4.55	$2.81 \pm 0.24$		$2.82 \pm 1.06$

<sup>a</sup>  $\log K_{LDPE-w}$  value was determined by Booij et al. (2003) at 13 °C

##### 4.2.1. Log $K_{LDPE-w}$ of PAHs from this thesis versus published studies

The plausibility of the experimental and analytical settings is to be discussed by comparing the  $\log K_{LDPE-w}$  values of LDPE derived in this thesis and in other studies.

In Table 3,  $\log K_{LDPE-w}$  values of naphthalene, fluorene and phenanthrene in this study and in other studies are summarized.

**Table 3:** Comparison of polyethylene-water partition coefficient ( $\log K_{LDPE-w}$ ): this thesis versus published data

	This thesis	A	B	C	D	E	F	G	H	I
Polyethylene	LDPE	LDPE	LDPE	LDPE	LDPE	LDPE	PE	LDPE	LDPE	LDPE
Film thickness ( $\mu\text{m}$ )	455 <sup>a</sup>	70	51	100	25	70	51	51	76	12 $\mu\text{m}$
$\rho$ ( $\text{g cm}^{-3}$ )	0.92			0.92				0.92		0.92
SA ( $\text{m}^2 \text{ g}^{-1}$ )	3.16									1.58
temperature (°C)	21	13, 30	$24 \pm 1$	$20 \pm 1$	21	20	20	20	25	25
$\log K_{LDPE-w/PE-w}$ ( $\text{L kg}^{-1}$ )										
naphthalene	$2.93 \pm 0.33$			$3.04 \pm 0.14$		$2.81 \pm 0.14$		$3.23 \pm 0.06$	$2.94 \pm 0.04$	$2.84 \pm 1.85$
fluorene	$3.88 \pm 0.28$			$3.78 \pm 0.04$		$3.77 \pm 0.11$		$3.67 \pm 0.04$	$4.14 \pm 0.07$	
phenanthrene	$4.33 \pm 0.10$	$4.41 \pm 0.01$ (13 °C)	$4.30 \pm 0.1$	$4.14 \pm 0.02$	$4.30 \pm 0.10$	$4.22 \pm 0.11$	$4.13 \pm 0.03$	$4.04 \pm 0.03$	$4.22 \pm 0.07$	$4.08 \pm 3.70$

References: A (Booij et al., 2003), B (Adams et al., 2007), C (Cornelissen et al., 2008), D (Fernandez et al., 2009), E (Smedes et al., 2009), F (Hale et al., 2010), G (Choi et al., 2013), H (Zhu et al., 2015), I (J. Wang et al, 2019)

<sup>a</sup> median diameter ( $d_{50}$ ); Abbreviations:  $\rho$  = density; SA = surface area

As seen in Figure 6, the log  $K_{LDPE-w}$  values determined by the Freundlich isotherm model in this study falls in the range of available studies for all three selected PAHs, although the film thickness 455  $\mu\text{m}$  ( $d_{50}$ ) of LDPE particles in this study is significantly greater than the film thickness in the other studies (12-100  $\mu\text{m}$ ), confirming the results from Lohmann (2012) about how the log  $K_{LDPE-w}$  of hydrophobic organic compounds does not change significantly with the thickness of the LDPE material.

Regarding log  $K_{LDPE-w}$  of naphthalene, the result (as log  $K_{LDPE-w} = 2.93 \pm 0.33$ ) of this thesis was in the range of the log  $K_{LDPE-w}$  2.81 to 3.23 by Cornelissen et al. (2008), Smedes et al. (2009), Choi et al. (2013), Zhu et al. (2015) and J. Wang et al. (2019). Similarly, the log  $K_{LDPE-w}$  value of this thesis of fluorene was determined to be  $3.88 \pm 0.28$  using the Freundlich isotherm model, which lay between 3.67 and 4.14 by these researchers (Cornelissen et al., 2008; Smedes et al., 2009; Choi et al., 2013; Zhu et al., 2015). For phenanthrene, log  $K_{LDPE-w}$  of this thesis was calculated to be  $4.33 \pm 0.10$ , which is slightly higher than the data of log  $K_{LDPE-w}$  and log  $K_{PE-w}$  in the literature (Booij et al., 2003; Adams et al., 2007; Cornelissen et al., 2008; Karapanagioti and Klontza, 2008; Smedes et al., 2009; Hale et al., 2010; Choi et al., 2013; Zhu et al., 2015; J. Wang et al., 2019), however, the difference is not statistically significant.

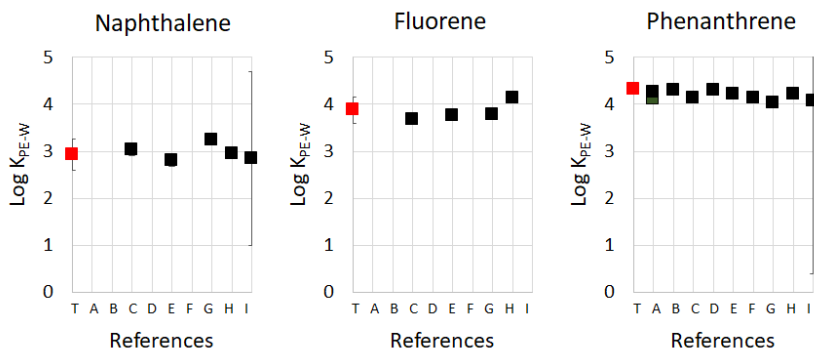


**Figure 6:** Comparison of Log  $K_{LDPE-w}$  values of naphthalene, fluorene and phenanthrene: this thesis versus other studies

References: T This thesis (red square); A (Booij et al., 2003; log  $K_{LDPE-w}$  for phenanthrene at 13 and 30 °C), B (Adams et al., 2007), C (Cornelissen et al., 2008), D (Fernandez et al., 2009), E (Smedes et al., 2009), F (Hale et al., 2010), G (Choi et al., 2013), H (Zhu et al., 2015), I (Wang et al., 2019)

Hence, the results showed that i) the experimental settings of this thesis are plausible to derive reasonable log  $K_{p-w}$  values and ii) since the size and shape of LDPE sorbent materials had little influence on log  $K_{LDPE-w}$  of the selected PAHs.

#### 4.2.2. Log $K_{p-w}$ of PAHs for PP, PET and PBS from this thesis versus published studies

In terms of log  $K_{p-w}$  of PAHs for other polymers, only few values are available in the literature that can be compare to the results of this thesis. Table 4 illustrates the log  $K_{p-w}$  values of naphthalene, fluorene and phenanthrene for PP, PET and PBS calculated in this study based on the Freundlich isotherm model and log  $K_{p-w}$  determined by other researchers using these polymers as sorbent materials. For comparison purposes, the log  $K_{p-w}$  calculated according to Freundlich's isotherm model was selected for Table 4, if log  $K_{p-w}$  values were calculated by multiple models by the same study. It should be noted that the log  $K_{Fr}$  values for PP, PET and PBS determined in this study are referred to as log  $K_{PP-w}$ , log  $K_{PET-w}$  and log  $K_{PBS-w}$ , respectively.

**Table 4:** Comparison of log  $K_{p-w}$  values of naphthalene, fluorene and phenanthrene for PP, PET and PBS: this thesis versus published data

Polymer	This thesis	A	B	C	D	E	This thesis	F	This thesis	E
	PP	PP	PP	PP	PP	PP	PBS	PBS	PET	PET
Film thickness ( $\mu\text{m}$ )	536 <sup>a</sup>	200-250	< 2000		59	12.5	3000	535 <sup>a</sup>	150-200	658 <sup>a</sup>
$\rho$ (g $\text{cm}^{-3}$ )	0.91				0.91	0.92		1.24		1.34
SA ( $\text{m}^2 \text{ g}^{-1}$ )	11.44	1.56			3.327	0.207		2.77	0.04	4.24
log $K_{p-w}$ ( $\text{L kg}^{-1}$ )										
naphthalene	2.88 ± 0.32				4.06 ± 2.03	2.72 ± 1.70	4.18 <sup>c</sup>	3.35 ± 0.22		2.68 ± 0.13
fluorene	3.64 ± 0.35						4.16 <sup>c</sup>	4.24 ± 0.17		2.81 ± 0.24
phenanthrene	3.83 ± 0.20	3.06 <sup>b</sup>	2.43 ± 1.90	3.73 <sup>b</sup>	4.18 ± 3.28	3.75 ± 2.68		5.16 ± 0.10	4.92	2.82 ± 1.06

References: A: (Teuten et al., 2007), B: (Karapanagioti and Klontza 2008), C: (Lee et al., 2014), D: (J. Wang et al., 2019), E: (Lončarski et al., 2021), F: (Zhao et al., 2020)

<sup>a</sup> median diameter ( $d_{50}$ ); <sup>b</sup> seawater log  $K_{PP-sw}$  values were converted to freshwater log  $K_{PP-w}$  using the Setschenow constant by Jonker and Muijs (2010) and the ionic strength of seawater by González-Dávila et al. (2009); <sup>c</sup> log  $K_{p-w}$  values were determined in synthetic water enriched with a mixture of salts; values are not converted to fresh water log  $K_{p-w}$

Concerning the plastic PP, five other studies are available (Teuten et al., 2007; Karapanagioti and Klontza, 2008; Lee et al., 2014; J. Wang et al., 2019; Lončarski et al., 2021) to compare log  $K_{PP-w}$  values with the results of this thesis. It must be brought to attention that the sorption isotherm experiments in some studies were conducted in seawater (Teuten et al., 2007; Lee et al., 2014) or synthetic water enriched with a mixture of salts (Lončarski et al., 2021), thus the results of the log  $K_{PP-w}$  values in salt-rich water cannot be compared directly to the log  $K_{PP-w}$  values in Milli-Q water. In general, hydrophobic organic compounds dissolve less in seawater than in fresh water, and thus adsorb more on solid surfaces (Jonker and Muijs, 2010). This results in a greater plastic-water partition coefficient than the counterpart in fresh water. For the log  $K_{PP-w}$ , values determined in seawater can, however, be converted to log  $K_{PP-w}$  in fresh water by the following equation of Jonker and Muijs (2010) with Setschenow constant:

$$K_{p-sw} = K_{p-w} * 10^{k_s * I} \quad \text{equation 14}$$

where  $K_{p-sw}$  is the plastic-water distribution coefficient in salt water ( $\text{L kg}^{-1}$ ), log  $K_{p-w}$  is the plastic-water distribution coefficient in salt-free water ( $\text{L kg}^{-1}$ ),  $k_s$  is the salting-out Setschenow constant ( $\text{L mol}^{-1}$ ) and  $I$  is the ionic strength ( $\text{mol L}^{-1}$ ).

The original log  $K_{PP-w}$  of phenanthrene 3.33 by Teuten et al. (2007) and 4.00 by Lee et al. (2014) can be converted to 3.06 and 3.73, respectively, when the Setschenow constant of phenanthrene 0.38 ( $\text{L mol}^{-1}$ ) by Jonker and Muijs (2010) and ionic strength of the seawater 0.7 ( $\text{mol L}^{-1}$ ) by González-Dávila et al. (2009) are applied.

The log  $K_{PP-w}$  of naphthalene ( $2.88 \pm 0.32$ ) and phenanthrene ( $3.83 \pm 0.20$ ) determined in this thesis fell within the range of the published values of naphthalene (2.79 to 4.06) and phenanthrene (3.06 to 4.18) in fresh water. The log  $K_{PP-w}$  values of naphthalene and phenanthrene that are the closest to the results of this thesis are the ones by J. Wang et al. (2019), although the physical properties of the PP are significantly different. Whereas the log  $K_{PP-w}$  of fluorene ( $3.64 \pm 0.35$ ) in this study is the only published value that has been derived by the sorption isotherm experiment in salt-free water. The log  $K_{PP-w}$  value of fluorene of 4.16 by Lončarski et al. (2021) in salt-rich synthetic water is slightly higher than the upper value of this thesis. Because the log  $K_{PP-w}$  by Lončarski et al. (2021) were determined in salt-enriched synthetic water, it is reasonable that their value is larger than the fresh water value of this thesis.

Regarding PET,  $\log K_{PET-w}$  of naphthalene ( $2.68 \pm 0.13$ ), fluorene ( $2.81 \pm 0.24$ ) and phenanthrene ( $2.82 \pm 1.06$ ) determined by the Freundlich isotherm experiments in this thesis, to the best of knowledge, are the first published values in salt-free water. Lončarski et al. (2021) investigated the sorption of four different PAHs (naphthalene, fluorene, fluoranthene and pyrene) on standard granulated PET in a salt-enriched synthetic water matrix (conductivity at  $25^\circ\text{C}$   $226 \pm 23 \mu\text{S cm}^{-1}$ ) similar to Danube River. The  $\log K_{PET-w}$  values of naphthalene and fluorene by Lončarski et al. (2021) were 4.39 and 4.55, respectively. Both values are significantly greater than the counterparts in this thesis in salt-free water. Besides the difference in sorption water matrix, the study by Lončarski et al. (2021) resulted in greater  $\log K_{PET-w}$  than  $\log K_{PP-w}$  for both naphthalene and fluorene, unlike the results of this thesis.

Similar to this study, sorption capacity of PP was greater than PET in the field investigation by Rochman et al. (2013), who conducted sorption experiments in seawater in San Diego Bay using commercial HDPE, LDPE, PP, PVC and PET pellets. Rochman et al. (2013) explained the smaller sorption capacity of PET with its glassy polymer structure. The glass transition temperature ( $T_g$ ) of the PET used in this work is higher than that of PP, while the  $T_g$  of PP is lower than room temperature. Thus the state of amorphous region of the PP in this thesis is “glassy” while the counterpart of PET is “rubbery”, which agrees with the statement by Rochman et al. (2013).

The highest sorption capacity of the three selected PAHs in this thesis was achieved by PBS, a biodegradable polymer, as shown in Figure 5. The  $\log K_{PBS-w}$  of naphthalene, fluorene and phenanthrene were determined to be  $3.35 \pm 0.22$ ,  $4.24 \pm 0.17$  and  $5.16 \pm 0.10$ , respectively. Currently, only one study is available to compare the  $\log K_{PBS-w}$  values with the results of this thesis. Zhao et al. (2020) conducted sorption experiments of five organic chemicals including phenanthrene on three polar polymer materials, i.e. PBS, polycaprolactone and polyurethane as well as a nonpolar material polystyrene. From the results by Zhao et al. (2020), the only value that can be compared to the result of this thesis is the  $\log K_{PBS-w}$  of phenanthrene at 4.92, which is slightly smaller than the  $\log K_{PBS-w}$  ( $5.16 \pm 0.10$ ) of this study, although the difference in physical properties like film thickness and specific surface area of PBS materials in these two studies are significant.

## 5. Correlations of PAH properties and $\log K_{p-w}$

In the following chapter, linear correlations of  $\log K_{p-w}$  of this work and PAH properties were determined and compared with published data.

### 5.1. Correlation of $\log K_{p-w}$ and $\log K_{ow}$ of this thesis

The  $\log K_{p-w}$  values determined based on the Freundlich isotherm model from chapter 4 were selected as  $\log K_{p-w}$  for the investigation of the correlation between  $\log K_{p-w}$  and  $\log K_{ow}$  (listed in Table A2.1). Log  $K_{ow}$  values of naphthalene (NAPH), fluorene (FLN) and phenanthrene (PHEN) were 3.37, 4.18 and 4.46, respectively (Mackay et al., 1992).

The correlations between  $\log K_{p-w}$  (i.e.  $\log K_{LDPE-w}$ ,  $\log K_{PP-w}$ ,  $\log K_{PBS-w}$  and  $\log K_{PET-w}$ ) determined from the sorption experiments in this thesis and the  $\log K_{ow}$  of PAHs for LDPE, PP, PBS and PET are presented in Figure 7 (left) and expressed in equations 15 (a) - (d):

$\log K_{LDPE-w} = 1.26 * \log K_{ow} - 1.32$	( $R^2 = 0.995$ )	equation 15 (a)
$\log K_{PP-w} = 0.88 * \log K_{ow} - 0.09$	( $R^2 = 0.997$ )	equation 15 (b)
$\log K_{PBS-w} = 1.54 * \log K_{ow} - 1.92$	( $R^2 = 0.924$ )	equation 15 (c)
$\log K_{PET-w} = 0.14 * \log K_{ow} + 2.22$	( $R^2 = 0.964$ )	equation 15 (d)

The log  $K_{p-w}$  values were then modelled based on the derived equations 15 (a) - (d) with the log  $K_{ow}$  values in the range of 0 to 6.5 and presented in Figure 7 (right).

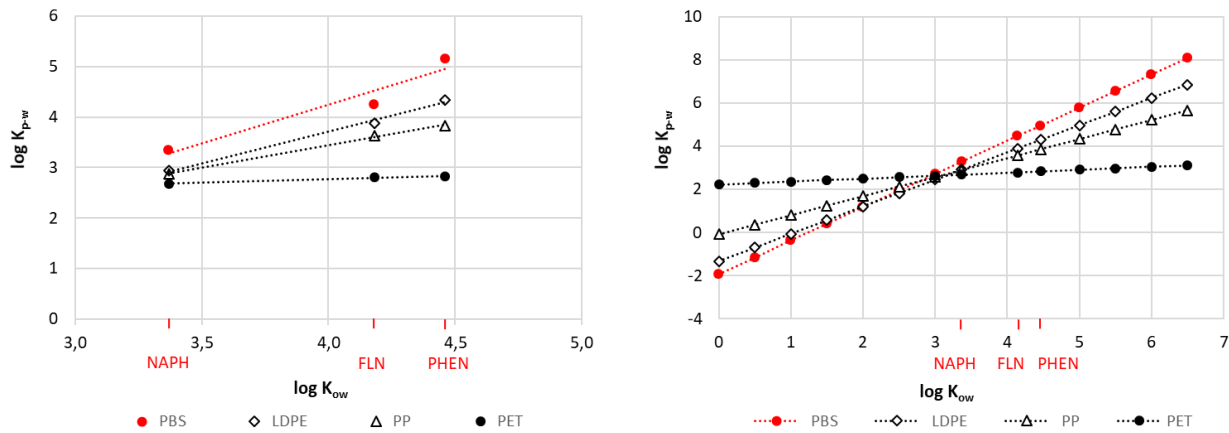


**Figure 7:**  $\log K_{p-w}$  regression with  $\log K_{ow}$ : results from the experiment (left) and  $\log K_{p-w}$  modelled from the derived equations (right).

The  $\log K_{p-w}$  determined from the experiments on the four tested polymers correlated positively with  $\log K_{ow}$ , similar to other studies by Booij et al. (2003), Adams et al. (2007), Smedes et al. (2009), Lohmann (2012), Choi et al. (2013), Lee et al. (2014) and Hüffer and Hofmann (2016). The range of  $R^2$  values in this thesis were between 0.924 to 0.997, which is also similar or greater than in other studies. The regressions shown on the right in Figure 7 are extrapolated regressions that also show values outside the empirical fitting range ( $\log K_{ow}$  3.37 - 4.46). The error of the regressions increases sharply with increasing distance from the fitting area to the edges.

Equations 15 (a) - (d) show that the slope increased in order of PET (0.14) < PP (0.88) < LDPE (1.26) < PBS (1.54). This result shows that the increase of hydrophobicity of pollutants influences the sorption capacity in order of PET < PP < LDPE < PBS. Meanwhile, the intercept decreases in order of PET (2.22) > PP (-0.09) > LDPE (-1.32) > PBS (-1.92). These results lead to the conclusion that the linear correlation of  $\log K_{p-w}$  and  $\log K_{ow}$  is unique to the polymer type. Further, as illustrated in Figure 7 (right), the  $\log K_{p-w}$  values among these polymers become nearly identical when  $\log K_{ow}$  is 3. The order of  $\log K_{p-w}$  PET < PP < LDPE < PBS at  $\log K_{ow}$  of 4 completely reverses to PBS < LDPE < PP < PET when  $\log K_{ow}$  value becomes smaller than 1.5, suggesting the possibility that the glassy PET adsorbs more PAHs with lower hydrophobicity. However, the equations 15 (a) - (d) were limited by the range of tested PAHs represented by their  $\log K_{ow}$ , but within this  $\log K_{ow}$  range all equations resulted in accuracies > 0.92.

### Correlation between log K<sub>LDPE-W</sub> and log K<sub>ow</sub> from this thesis versus published studies

A handful of regression models for the correlation between log K<sub>LDPE-W</sub> and log K<sub>ow</sub> were published (Booij et al., 2003; Adams et al., 2007; Smedes et al., 2009; Lohmann, 2012; Choi et al., 2013; Zhu et al., 2015) (Table A5.1). The log K<sub>LDPE-W</sub> - log K<sub>ow</sub> correlation of this thesis and other researchers are presented in Figure 8. The modelled log K<sub>LDPE-W</sub> values using equation 15 (a) are within the range of reported values (Booij et al., 2003; Adams et al., 2007; Smedes et al., 2009; Choi et al., 2013; Zhu et al., 2015).

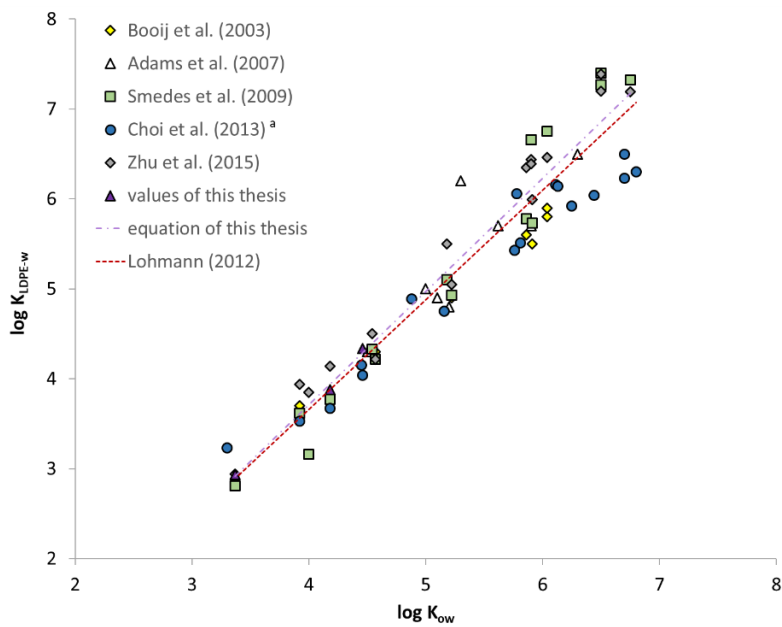


**Figure 8:** Correlation of log K<sub>LDPE-W</sub> and log K<sub>ow</sub> from this thesis versus published studies

<sup>a</sup> log K<sub>LDPE-W</sub> of 17 parent PAHs were presented

Table 5 shows the regression models by Booij et al. (2003), Adams et al. (2007), Smedes et al. (2009), Lohmann (2012), Choi et al. (2013) and Zhu et al. (2015) as well as the model derived from this study. A positive slope and negative intercept for each linear regression model with at least R<sup>2</sup> > 0.92 show that log K<sub>ow</sub> in general is a good predictor for log K<sub>LDPE-W</sub>. In addition, the p-values for slopes and intercepts were determined using statistical software SPSS to compare reported linear regression models and the model from this study (Table 5). The p-value showed no significant difference between the results from this study and Booij et al. (2003), Adams et al. (2007), Smedes et al. (2009), Lohmann (2012), Choi et al. (2013) as well as Zhu et al. (2015) having p-values higher than 0.05. The influence of the differing experimental settings of Booij et al. (2003), Adams et al. (2007) and Zhu et al. (2015) as well as a co-solvent model (Smedes et al., 2009) and a regression model based on 17 parent PAHs (Choi et al., 2013) seem to be negligible. Furthermore, the regression by Lohmann (2012), which can be used as a reference regression since it contains n = 65 log K<sub>LDPE-W</sub> - log K<sub>ow</sub> values of PAHs of different authors, also showed no significant difference to the log K<sub>LDPE-W</sub> - K<sub>ow</sub> regression of this study.

In summary, the log K<sub>LDPE-W</sub> value of selected PAHs determined from these Freundlich isotherm experiments and the log K<sub>LDPE-W</sub> - log K<sub>ow</sub> regression model moderately relate to the reported log K<sub>LDPE-W</sub> values as well as the regression models for LDPE by other authors, indicating that the validity of this experimental setting was adequate.

**Table 5:** SPSS analysis of log K<sub>LDPE-w</sub> – log K<sub>ow</sub> regression of this study and literature models

Reference	log K <sub>ow</sub> regression models		SPSS
	equations	R <sup>2</sup>	
This thesis	log K <sub>LDPE-w</sub> = 1.26 log K <sub>ow</sub> - 1.32	0.995	
Zhu et al. (2015) <sup>b</sup>	log K <sub>LDPE-w</sub> = 1.31 log K <sub>ow</sub> - 1.45	0.98	0.840
Choi et al. (2013) <sup>c</sup>	log K <sub>LDPE-w</sub> = 1.00 log K <sub>ow</sub> - 0.26	0.96	0.389
Lohmann (2012)	log K <sub>LDPE-w</sub> = 1.22 ( $\pm$ 0.046) log K <sub>ow</sub> - 1.22 ( $\pm$ 0.24)	0.92	0.880
Smedes et al. (2009)	log K <sub>LDPE-w</sub> = 1.48 log K <sub>ow</sub> - 2.45	0.97	0.609
Adams et al. (2007)	log K <sub>LDPE-w</sub> = 1.2 log K <sub>ow</sub> - 0.97	0.95	0.853
Booji et al. (2003)	log K <sub>LDPE-w</sub> = 0.972 log K <sub>ow</sub> - 0.13	0.95	0.095

<sup>a</sup> Calculated p-value by SPSS; p > 0.05 no significant difference; p < 0.05 significant difference between log K<sub>LDPE-w</sub> - log K<sub>ow</sub> of individual study from the literature and log K<sub>LDPE-w</sub> - log K<sub>ow</sub> of this thesis; <sup>b</sup> Calculated log K<sub>LDPE-w</sub> - log K<sub>ow</sub> regression of 16 EPA-PAHs determined by Zhu et al. (2015); <sup>c</sup> 16 parent PAHs were selected and evaluated

### Correlation between log K<sub>p-w</sub> and log K<sub>ow</sub> for PP and PET

Only few studies are available to compare the correlation between log K<sub>p-w</sub> and log K<sub>ow</sub> for PP and PET, mainly due to the lack of log K<sub>p-w</sub> of PAHs for these polymers.

For PP, only Lee et al. (2014) in seawater and Lončarski et al. (2021) in synthetic water, i.e. distilled water enriched with a mixture of salts determined log K<sub>PP-w</sub> for three or more PAHs. The experimental data from Lee et al. (2014) in seawater was converted into log K<sub>PP-w</sub> in distilled water using the Setschenow constant by Jonker and Muijs (2010) and the ionic strength of seawater 0.7 mol L<sup>-1</sup> by González-Dávila et al. (2009). For the conversion of log K<sub>PP-w</sub> for the synthetic water by Lončarski et al. (2021), the ionic strength of the water matrix was estimated to be 5.28 x 10-3 mol L<sup>-1</sup>, based on the concentration of chlorides, sulfates and bicarbonates provided by the authors (Lončarski et al., 2021). The Setschenow constants of naphthalene, fluorene, fluoranthene and pyrene used for the conversion are respectively 0.32 (Burant et al., 2016), 0.362 (Burant et al., 2016), 0.364 (Jonker and Muijs, 2010) and 0.354 L mol<sup>-1</sup> (Jonker and Muijs, 2010). The results are presented in Figure 9 with the log K<sub>PP-w</sub> from this thesis.

Furthermore, a compilation of regression models of log K<sub>PP-w</sub> - log K<sub>ow</sub> in this thesis, Lee et al. (2014) and Lončarski et al. (2021) are presented in Table 6 with the p-values determined using SPSS. Basic data are listed in the Table A5.2. For coefficients of determination with a small number of data points, it is formally true that these are generally high.

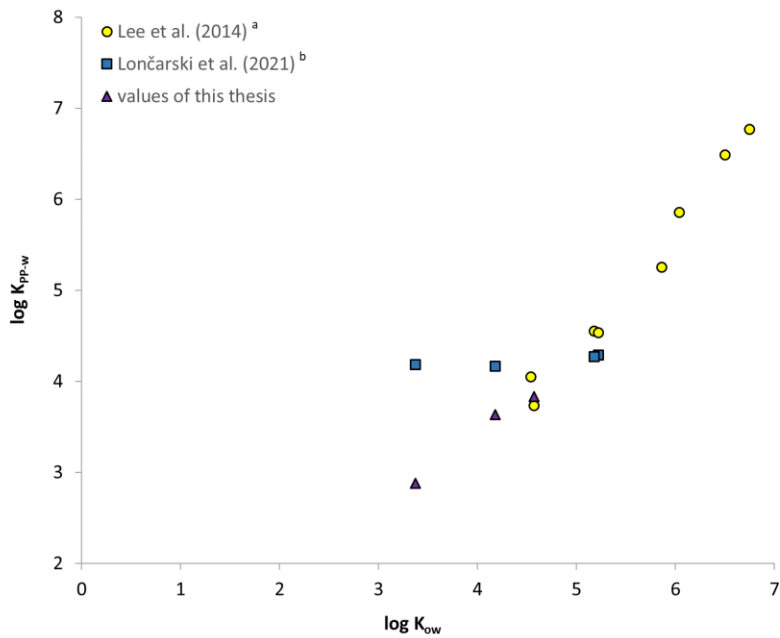


**Figure 9:** Correlation of log K<sub>PP-w</sub> and log K<sub>ow</sub> from this thesis versus published studies

<sup>a</sup> converted to log K<sub>PP-w</sub> in fresh water based on the Setschenow constant from Jonker and Muijs (2010); <sup>b</sup> converted to log K<sub>PP-w</sub> in fresh water based on the Setschenow constant from Burant et al. (2016) and Jonker and Muijs (2010)

**Table 6:** SPSS analysis of log K<sub>PP-w</sub> - log K<sub>ow</sub> regression models of this thesis and models on the basis of log K<sub>PP-w</sub> from the literature

Reference	log K <sub>ow</sub> <sup>a</sup> regression models		SPSS
	equation	R <sup>2</sup>	
This thesis	log K <sub>PP-w</sub> = 0.88 log K <sub>ow</sub> - 0.09	0.997	
Lee et al. (2014) <sup>c</sup>	log K <sub>PP-w</sub> = 1.33 log K <sub>ow</sub> - 2.27	0.977	0.103
Lončarski et al. (2021) <sup>d</sup>	log K <sub>PP-w</sub> = 0.06 log K <sub>ow</sub> + 3.95	0.754	0.001

<sup>a</sup> log K<sub>ow</sub> values from Mackay et al. (1992); <sup>b</sup> Calculated p-value by SPSS; p > 0.05 no significant difference; p < 0.05 significant difference between log K<sub>PP-w</sub> - log K<sub>ow</sub> of individual study from the literature and log K<sub>PP-w</sub> - log K<sub>ow</sub> of this thesis; <sup>c</sup> Seawater log K<sub>PP-sw</sub> by Lee et al. (2014) were converted to freshwater log K<sub>PP-w</sub> based on the Setschenow constant by Jonker and Muijs (2010); <sup>d</sup> log K<sub>p-w</sub> of PAHs for PP in the synthetic water by Lončarski et al. (2021) were converted to freshwater log K<sub>PP-w</sub> based on the Setschenow constant by Burant et al. (2016) and Jonker and Muijs (2010)

As shown in both Figure 9 and Table 6, the regression model of this thesis is comparable to the regression model based on log K<sub>PP-w</sub> by Lee et al. (2014) ( $p > 0.05$ ). The log K<sub>PP-w</sub> - log K<sub>ow</sub> regression model based on data from Lončarski et al. (2021), however, is significantly different from the model in this thesis ( $p < 0.05$ ). It is remarkable that log K<sub>PP-w</sub> values of all four PAHs (naphthalene, fluorene, pyrene and fluoranthene) are similar (4.16 - 4.29) for the PP material tested by Lončarski et al. (2021). In particular, the extremely high log K<sub>PP-w</sub> of naphthalene for the PP material makes the slope of the regression model by Lončarski et al. (2021) significantly smaller compared to the slope in this thesis and Lee et al. (2014). The physicochemical properties of the PP are not provided by Lončarski et al. (2021), except for the size of the PP (3 mm). Thus, it is difficult to explain the reason for the high log K<sub>PP-w</sub> value of naphthalene in their study.

For PET, log K<sub>PET-w</sub> determined in Milli-Q water, distilled water or fresh water are not available for comparison or verification of the results using equation 15 (d) in this thesis. The only study that is somewhat relevant to this thesis is the one by Lončarski et al. (2021), where they determined PET-

$\log K_{\text{Fr}}$  values in sorption experiments using synthetic water enriched with salts and Danube River water, as they did for PP. Using the estimated ionic strength of  $5.28 \times 10^{-3} \text{ mol L}^{-1}$  of the synthetic water and the Setschenow constants of naphthalene 0.32 (Burant et al., 2016), fluorene 0.362 (Burant et al., 2016), pyrene 0.354 (Jonker and Muijs, 2010) and fluoranthene 0.364  $\text{L mol}^{-1}$  (Jonker and Muijs, 2010), the  $\log K_{\text{PET-w}}$  values of these PAHs in synthetic water with salts were converted to  $\log K_{\text{PET-w}}$  in fresh, distilled water.

The converted  $\log K_{\text{PET-w}}$  by Lončarski et al. (2021) and the  $\log K_{\text{PET-w}}$  of this thesis are plotted against  $\log K_{\text{ow}}$  and shown in Figure 10. Basic data are shown in the Table A5.3.

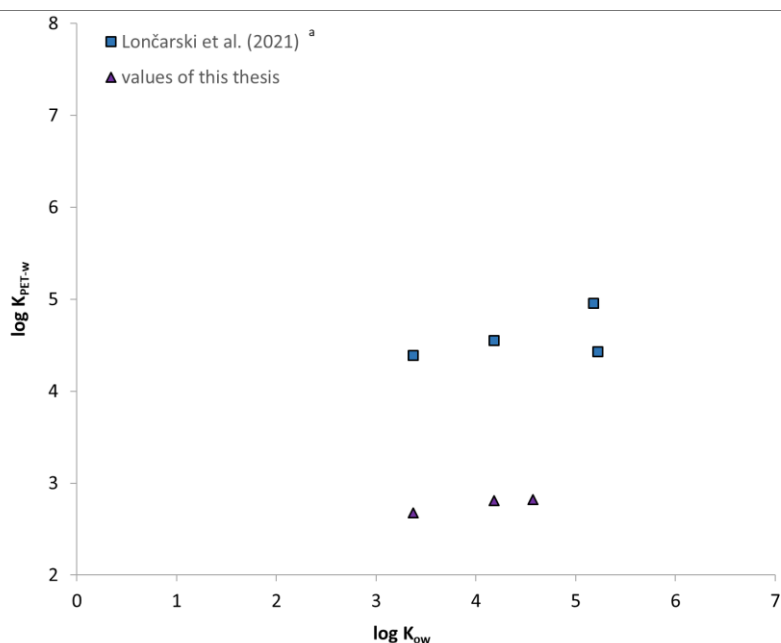


**Figure 10:** Correlation of  $\log K_{\text{PET-w}}$  and  $\log K_{\text{ow}}$  from this thesis versus Lončarski et al. (2021)

<sup>a</sup>  $\log K_{\text{PET-w}}$  values of four PAHs in synthetic water by Lončarski 2021 were converted to  $\log K_{\text{PET-w}}$  in fresh water, based on the Setschenow constant from Burant et al. (2016) and Jonker and Muijs (2010)

From the  $\log K_{\text{PET-w}} - \log K_{\text{ow}}$  plot in Figure 10, the regression models of this study and Lončarski et al. (2021) are compared with the p-values generated using SPSS (Table 7).

**Table 7:** SPSS analysis of  $\log K_{\text{PET-w}} - \log K_{\text{ow}}$  regression model of this thesis and modelled equation on the basis of  $\log K_{\text{PET-w}}$  by Lončarski et al. (2021)

Reference	$\log K_{\text{ow}}$ <sup>a</sup> regression models		SPSS
	equation	R <sup>2</sup>	
This thesis	$\log K_{\text{PET-w}} = 0.14 \log K_{\text{ow}} + 2.22$	0.964	
Lončarski et al. (2021) <sup>c</sup>	$\log K_{\text{PET-w}} = 0.16 \log K_{\text{ow}} + 3.87$	0.293	0.232

<sup>a</sup>  $\log K_{\text{ow}}$  values from Mackay et al. (1992); <sup>b</sup> Calculated p-value by SPSS;  $p > 0.05$  no significant difference;  $p < 0.05$  significant difference between  $\log K_{\text{PET-w}} - \log K_{\text{ow}}$  of individual study from the literature and  $\log K_{\text{PET-w}} - \log K_{\text{ow}}$  of this thesis; <sup>c</sup>  $\log K_{\text{Fr}}$  of PAHs for PET in the synthetic water by Lončarski et al. (2021) were converted to freshwater  $\log K_{\text{PET-w}}$  based on the Setschenow constant by Burant et al. (2016) and Jonker and Muijs (2010)

The regression models in this thesis and Lončarski et al. (2021) show a similarity in slope (0.14 and 0.16, respectively) and a difference in intercept (2.22 and 3.87, respectively). This indicates a similar increase in sorption capacity on PET according to PAH hydrophobicity increase, regardless of the PET type.

## 5.2. Correlation of log K<sub>p-w</sub> and MW of this thesis

The correlation of the plastic-water partition coefficient based on the partition coefficient of the Freundlich isotherm model from chapter 4 and the molar weight of naphthalene (128.16 g mol<sup>-1</sup>), fluorene (166.21 g mol<sup>-1</sup>) and phenanthrene (178.22 g mol<sup>-1</sup>) by Mackay et al. (1992) is described in this chapter.

The linear regressions between log K<sub>p-w</sub> (i.e. log K<sub>LDPE-w</sub>, log K<sub>PP-w</sub>, log K<sub>PBS-w</sub> and log K<sub>PET-w</sub>) and the MW of PAHs for LDPE, PP, PBS and PET are presented in Figure 11 (left) and shown in equations 16 (a) - (d):

$$\log K_{LDPE-w} = 0.027 * MW - 0.572 \quad (R^2 = 0.992) \quad \text{equations 16 (a)}$$

$$\log K_{PP-w} = 0.019 * MW + 0.430 \quad (R^2 = 0.999) \quad \text{equations 16 (b)}$$

$$\log K_{PBS-w} = 0.033 * MW - 0.982 \quad (R^2 = 0.914) \quad \text{equations 16 (c)}$$

$$\log K_{PET-w} = 0.003 * MW + 2.302 \quad (R^2 = 0.970) \quad \text{equations 16 (d)}$$

The log K<sub>p-w</sub> values were then modelled based on the derived equations 16 (a) - (d) with the MW values in the range of 0 to 300 g mol<sup>-1</sup> shown in Figure 11 (right).

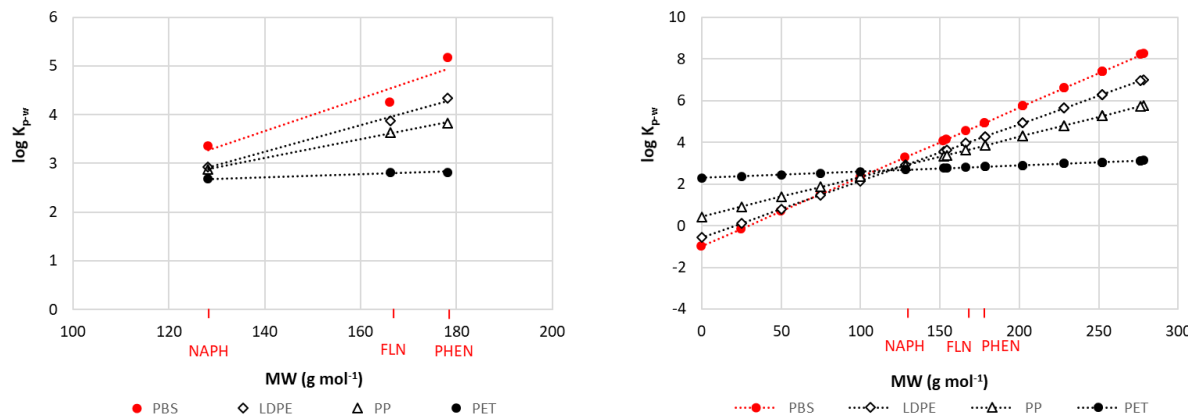


**Figure 11:** log K<sub>p-w</sub> regression with MW: results from the experiment (left) and log K<sub>p-w</sub> modelled from the derived equations (right)

The log K<sub>p-w</sub> determined from the experiments on the four tested polymers correlated positively with MW, similar to other studies by Smedes et al. (2009), Lohmann (2012) and Choi et al. (2013). The range of R<sup>2</sup> values in this thesis was determined at 0.914 to 0.999, which is also similar or greater than other studies. The regressions shown on the right in Figure 11 are extrapolated regressions that also show values outside the empirical fitting range (MW 128.16 – 178.22 g mol<sup>-1</sup>). The error of the regressions increases sharply with increasing distance from the fitting area to the edges.

Equations 16 (a) - (d) show an increasing slope in order of PET (0.003) < PP (0.019) < LDPE (0.027) < PBS (0.033). However, the intercept of the equation 16 (a) - (d) follows the order of PBS (-0.982) < LDPE (-0.572) < PP (0.430) < PET (2.303), showing a contrary tendency compared to the slope. As a result, the equations 16 (a) - (d) lead to the assumption that the linear correlation of  $\log K_{p-w}$  and MW depends on the polymer type. In addition, Figure 11 (right) shows that all linear correlations became nearly identical when MW is  $115 \text{ g mol}^{-1}$ . For an MW higher than  $115 \text{ g mol}^{-1}$ , PET has the lowest sorption affinity and increases in order of PP > LDPE > PBS, but for an MW smaller than  $115 \text{ g mol}^{-1}$ , PET has a higher sorption affinity for PAHs in order of PP > LDPE > PBS, suggesting the possibility that the glassy PET adsorbs more PAHs with lower hydrophobicity. However, the equations 16 (a) - (d) were limited by the range of the tested PAHs represented by their MW, but within this MW range all equations had a coefficient of determination ( $R^2$ ) higher than 0.914.

### 5.2.1. Correlation between $\log K_{LDPE-w}$ and MW from this thesis versus published studies

Some regression models for the correlation between  $\log K_{LDPE-w}$  and MW were published by Smedes et al. (2009), Lohmann (2012) and Choi et al. (2013). The  $\log K_{LDPE-w}$  - MW correlation of this dissertation and other researchers are presented in Figure 12 and the basic data in Table A5.4. The modelled  $\log K_{LDPE-w}$  values using equation 16 (a) are in the range of reported values (Smedes et al., 2009; Lohmann, 2012; Choi et al., 2013).

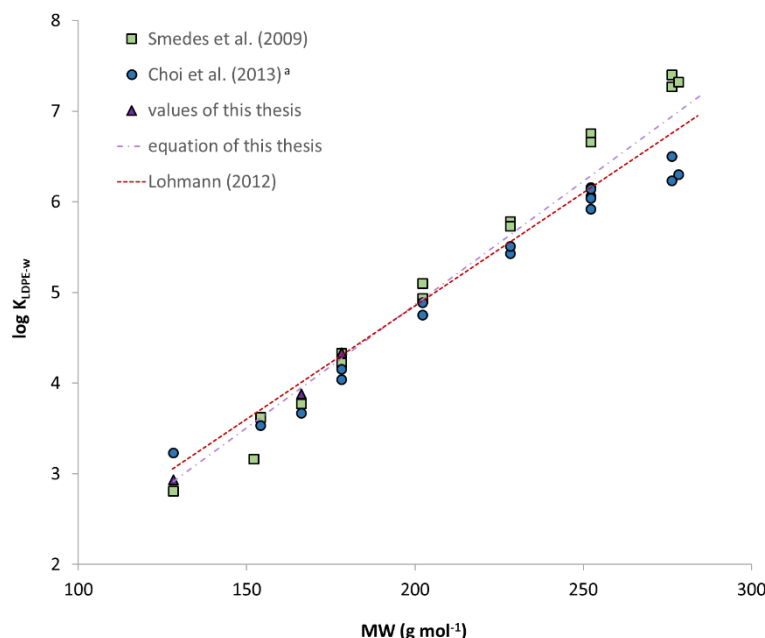


Figure 12: Correlation of  $\log K_{LDPE-w}$  and MW from this thesis versus published studies

<sup>a</sup>  $\log K_{LDPE-w}$  of 17 parent PAHs were presented

In Table 8 the regression models by Smedes et al. (2009), Lohmann (2012), Choi et al. (2013) and the model derived from this thesis are presented. All regression models have a positive slope and an intersection between -1.19 to 0.109 with an  $R^2 > 0.90$ , indicating that MW is a property to estimate  $\log K_{LDPE-w}$ . Furthermore, the statistical software SPSS was used to determine p-values for slopes and intersections by comparing reported linear regression models and the model from this thesis (Table

8). The p-value showed no significant difference between the results from this thesis and Smedes et al. (2009), Lohmann (2012) and Choi et al. (2013). All p-values from Table 8 reached a higher value than 0.05. Furthermore, the influence of different experimental setups of a co-solvent model (Smedes et al., 2009), a regression model based on 17 parent PAHs (Choi et al., 2013), as well as the regression model by Lohmann (2012) based on  $n = 65$   $\log K_{LDPE-w}$  MW values of different authors seems to be negligible.

Finally, the  $\log K_{LDPE-w}$  - MW regression model from this thesis relates moderately to the reported  $\log K_{LDPE-w}$  - MW regression model by other authors, suggesting that the experimental setup was adequate for PAHs with an MW ranging from 128.18 to 178.24 g mol<sup>-1</sup>.

**Table 8:** SPSS analysis of  $\log K_{LDPE-w}$  - MW regression of this thesis and literature regression models

Reference	MW regression models		SPSS p-value <sup>a</sup>
	equation	R <sup>2</sup>	
present study	$\log K_{LDPE-w} = 0.027 \text{ MW} - 0.573$	0.992	
Choi et al. (2013) <sup>b</sup>	$\log K_{LDPE-w} = 0.0235 \text{ MW} + 0.109$	0.97	0.424
Lohmann (2012)	$\log K_{LDPE-w} = 0.025 (\pm 0.001) \text{ MW} - 0.149 (\pm 0.217)$	0.90	0.997
Smedes et al. (2009)	$\log K_{LDPE-w} = 0.031 \text{ MW} - 1.19$	0.99	0.202

<sup>a</sup> Calculated p-value by SPSS; p > 0.05 no significant difference; p < 0.05 significant difference between  $\log K_{LDPE-w}$  - MW of individual study from the literature and  $\log K_{LDPE-w}$  - MW of this thesis; <sup>b</sup> 17 parent PAHs were selected and evaluated

### 5.2.2. Correlation between $\log K_{p-w}$ and MW for PP and PET

Only few studies are available to compare the correlation between  $\log K_{p-w}$  and MW for PP and PET, mainly due to the lack of  $\log K_{p-w}$  of PAHs for these polymers.

However, there are two data sets for PP from Lee et al. (2014) in seawater and Lončarski et al. (2021) in distilled water enriched with a mixture of salts that determined  $\log K_{PP-w}$  for three or more PAHs (Table A5.5). Both data sets were transformed into  $\log K_{PP-w}$  in distilled water using the Setschenow constant by Jonker and Muijs (2010) and the ionic strength of seawater 0.7 mol L<sup>-1</sup> (González-Dávila et al., 2009) for Lee et al. (2014), and the ionic strength of the water matrix of 5.28\*10<sup>-3</sup> mol L<sup>-1</sup> for Lončarski et al. (2021). Setschenow constants of naphthalene, fluorene, fluoranthene and pyrene used for the conversion are presented in the previous chapter 4. The results of the transformed  $\log K_{PP-w}$  values are presented in Figure 13.

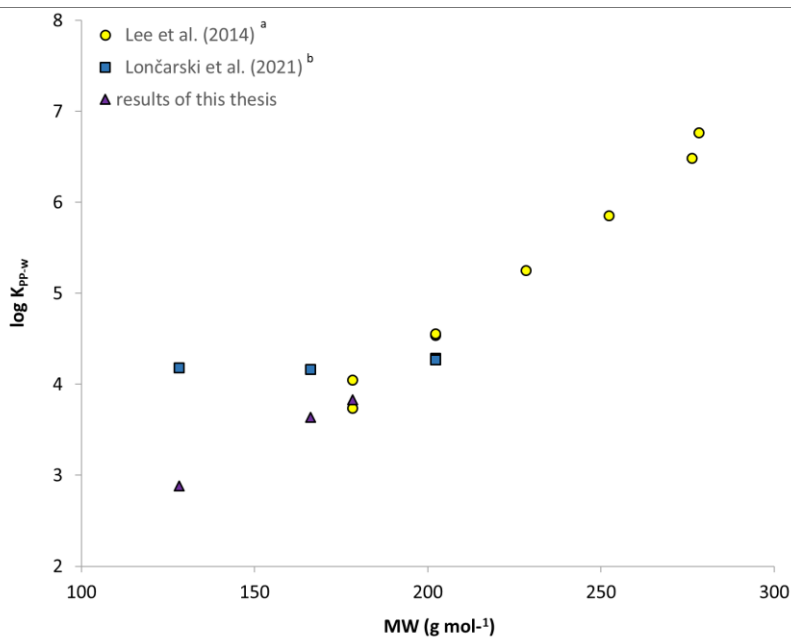


**Figure 13:** Correlation of log K<sub>PP-w</sub> and MW from this thesis versus published studies

<sup>a</sup> converted to log K<sub>PP-w</sub> in fresh water based on the Setschenow constant from Jonker and Muijs (2010); <sup>b</sup> converted to log K<sub>PP-w</sub> in fresh water based on the Setschenow constant from Burant et al. (2016) and Jonker and Muijs (2010)

**Table 9:** SPSS analysis of log log K<sub>PP-w</sub> - MW regression models of this thesis and models on the basis of log K<sub>PP-w</sub> from the literature

Reference	MW regression models		SPSS p-value <sup>a</sup>
	equation	R <sup>2</sup>	
This thesis	log K <sub>PP-w</sub> = 0.019 MW + 0.430	0.997	
Lee et al. (2014) <sup>b</sup>	log K <sub>PP-w</sub> = 0.027 MW - 1.010	0.991	0.030
Lončarski et al. (2021) <sup>c</sup>	log K <sub>PP-w</sub> = 0.001 MW + 3.972	0.687	0.004

<sup>a</sup> Calculated p-value by SPSS; p > 0.05 no significant difference; p < 0.05 significant difference between log K<sub>PP-w</sub> - MW of individual study from the literature and log K<sub>PP-w</sub> - MW of this thesis; <sup>b</sup> Seawater log K<sub>PP-sw</sub> by Lee were converted to freshwater log K<sub>PP-w</sub> based on the Setschenow constant by Jonker and Muijs (2010); <sup>c</sup> K<sub>Fr</sub> of PAHs for PP in the synthetic water by Lončarski et al. (2021) were converted to freshwater log K<sub>PP-w</sub> based on the Setschenow constant by Burant et al. (2016) and Jonker and Muijs (2010)

As shown in Figure 13 and Table 9, the log K<sub>PP-w</sub> - MW regression model of this thesis and the regression model based on data by Lee et al. (2014) and Lončarski et al. (2021) resulted in p-values < 0.05, indicating significant differences of slope and intercept. The log K<sub>PP-w</sub> values of Lončarski et al. (2021) for naphthalene, fluorene, pyrene and fluoranthene are within a 0.13 order of magnitude. Since the log K<sub>PP-w</sub> of naphthalene is so high, the slope of the regression model by Lončarski et al. (2021) is significantly smaller compared to the slope in this thesis and Lee et al. (2014). Apart from the size of PP (3 mm), no other polymer properties were specified by Lončarski et al. (2021). Therefore, it is difficult to explain the reason for the high log K<sub>PP-w</sub> value of naphthalene. A comparison with Lee et al. (2014) shows that both density and particle distribution of the PP particles are in the same order of magnitude as this thesis, but are not specified further. Therefore, an influence of PP properties and the experimental setting in seawater, which could have led to a significant difference, cannot be excluded for the log K<sub>PP-w</sub> - MW regression model.

In the case of log K<sub>PET-w</sub> for distilled water or fresh water, there is no data available to confirm the results from equation 16 (d) in this thesis. However, Lončarski et al. (2021) was the only study that

could be relevant to the determined PET-log  $K_{p\text{-}w}$  values of this thesis, although the experimental setting was performed in synthetic water that has been enriched with salts, as they did for PP. An ionic strength  $5.28 \times 10^{-3}$  mol L<sup>-1</sup> and the Setschenow constants of naphthalene 0.32 (Burant et al., 2016), fluorene 0.362 (Burant et al., 2016), pyrene 0.354 (Jonker and Muijs, 2010) and fluoranthene 0.364 L mol<sup>-1</sup> (Jonker and Muijs, 2010) were estimated for the conversion from the log  $K_{\text{PET-sw}}$  in synthetic water to log  $K_{\text{PET-w}}$  in fresh water and distilled water.

In Figure 14, the converted log  $K_{\text{PET-w}}$  by Lončarski et al. (2021) and the log  $K_{\text{PET-w}}$  of this thesis are plotted against MW (basic data are listed in Table A5.6).

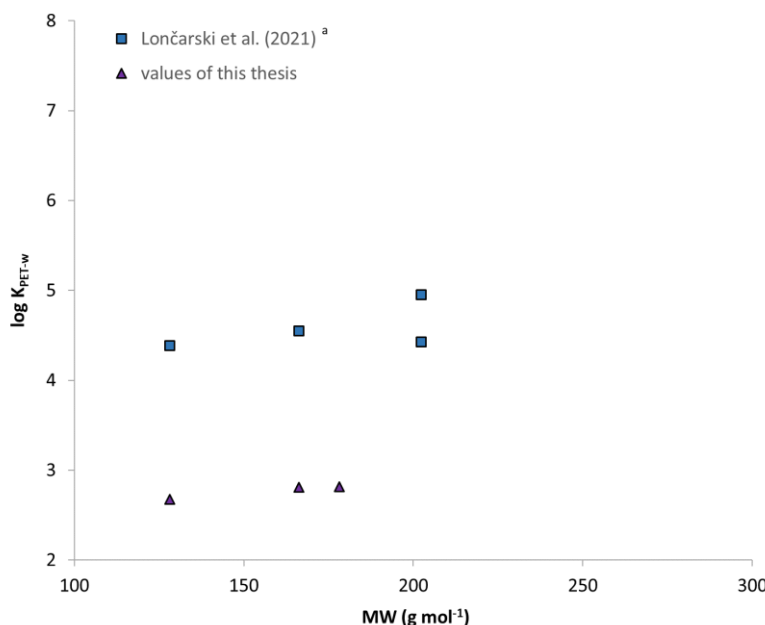


**Figure 14:** Correlation of log  $K_{\text{PET-w}}$  and MW from this thesis versus Lončarski et al. (2021)

<sup>a</sup> Log  $K_{\text{PET-w}}$  values of four PAHs in synthetic water by Lončarski et al. 2021 were converted to log  $K_{\text{PET-w}}$  in fresh water, based on the Setschenow constant from Burant et al. (2016) and Jonker and Muijs (2010)

**Table 10:** SPSS analysis of log  $K_{\text{PET-w}}$  - MW regression models of this thesis and modelled equation on the basis of log  $K_{\text{PET-w}}$  by Lončarski et al. (2021)

Reference	MW regression models		SPSS p-value <sup>a</sup>
	equation	R <sup>2</sup>	
This thesis	log $K_{\text{PET-w}} = 0.003 \text{ MW} + 2.302$	0.970	
Lončarski et al. (2021) <sup>b</sup>	log $K_{\text{PET-w}} = 0.004 \text{ MW} + 3.865$	0.312	0.252

<sup>a</sup> Calculated p-value by SPSS; p > 0.05 no significant difference; p < 0.05 significant difference between log  $K_{\text{PET-w}}$  - MW of individual study from the literature and log  $K_{\text{PET-w}}$  - MW of this thesis; <sup>b</sup> log  $K_{\text{Fr}}$  of PAHs for PET in the synthetic water by Lončarski et al. (2021) were converted to freshwater log  $K_{\text{PET-w}}$  based on the Setschenow constant by Burant et al. (2016) and Jonker and Muijs (2010)

The regression models in the present thesis and Lončarski et al. (2021) show a similarity in intercept (2.302 and 2.063, respectively) and difference in slopes (0.003 and 0.015, respectively), but a p-value of > 0.05. This indicates a good comparability for PAHs with MW < 202.23 g mol<sup>-1</sup>.

### 5.3. Correlation of $\log K_{p-w}$ and $\log C_w^{sat}$ of this thesis

Furthermore, Lohmann (2012) correlated the logarithmic aqueous solubility ( $\log C_w^{sat}$ ) of 19 different PAHs with  $n = 65$  partition coefficients of published literature values, resulting in the best correlation in his study. Although Lohmann (2012) represented the only study case of pairing  $\log C_w^{sat}$  and polyethylene partition coefficients, this approach is also being examined for further polymers in the scope of this thesis. The  $\log C_w^{sat}$ -values for PAHs mentioned here based on linear correlation of MW and  $\log C_w^{sat}$  developed by Ma et al. (2010). The linear correlation of plastic-water partition coefficient  $\log K_{p-w}$  from chapter 4 and the logarithmic aqueous solubility ( $\log C_w^{sat}$ ) of naphthalene (-0.01 mol m<sup>-3</sup>), fluorene (-1.23 mol m<sup>-3</sup>) and phenanthrene (-1.61 mol m<sup>-3</sup>) will be investigated in this section.

The following equation by Ma et al. (2010) was used to calculate  $\log C_w^{sat}$ :

$$\log C_w^{sat} (\text{mol m}^{-3}) = -0.032 * \text{MW} (\text{g mol}^{-1}) + 4.09 \quad \text{equation 17}$$

The linear regressions between  $\log K_{p-w}$  (i.e.  $\log K_{LDPE-w}$ ,  $\log K_{PP-w}$ ,  $\log K_{PBS-w}$  and  $\log K_{PET-w}$ ) and  $\log C_w^{sat}$  of PAHs for LDPE, PP, PBS and PET are presented in Figure 15 (left) and shown in equations 18 (a) - (d):

$$\log K_{LDPE-w} = -0.851 * \log C_w^{sat} + 2.907 \quad (R^2 = 0.992) \quad \text{equations 18 (a)}$$

$$\log K_{PP-w} = -0.599 * \log C_w^{sat} + 2.880 \quad (R^2 = 0.999) \quad \text{equations 18 (b)}$$

$$\log K_{PBS-w} = -1.038 * \log C_w^{sat} + 3.263 \quad (R^2 = 0.914) \quad \text{equations 18 (c)}$$

$$\log K_{PET-w} = -0.092 * \log C_w^{sat} + 2.681 \quad (R^2 = 0.970) \quad \text{equations 18 (d)}$$

The  $\log K_{p-w}$  values were then modelled based on the derived equations 18 (a) - (d) with the  $\log C_w^{sat}$  values in the range of 0 to -5.5 mol m<sup>-3</sup>, as shown in Figure 15 (right).

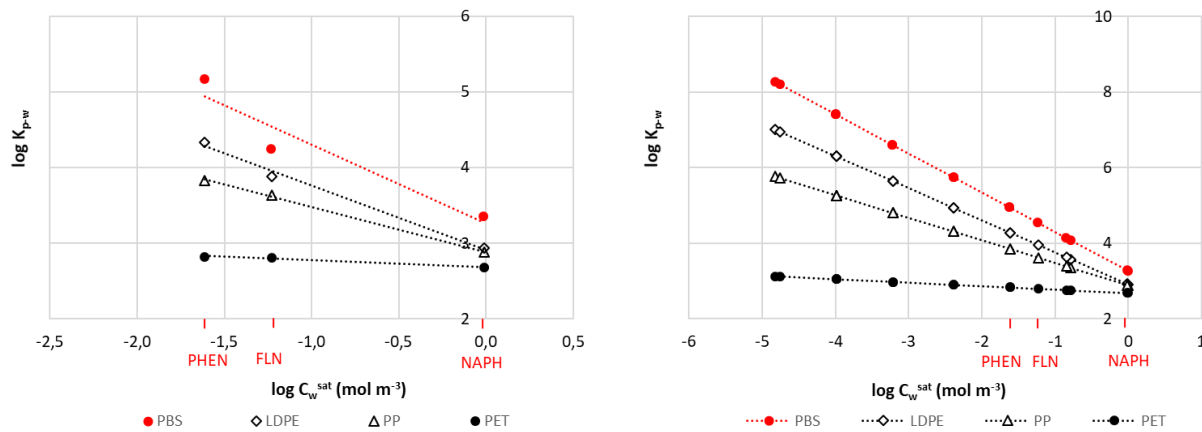


**Figure 15:**  $\log K_{p-w}$  regression with  $\log C_w^{sat}$ : results from the experiment (left) and  $\log K_{p-w}$  modelled from the derived equations (right)

The  $\log K_{p-w}$  determined from the experiments on the four tested polymers correlated negatively with  $\log C_w^{sat}$ , similar to Lohmann (2012). The range of  $R^2$  values in this thesis was determined from 0.914 to 0.999, which are also similar or greater than the  $R^2$  of the published study. The regressions shown on the right in Figure 15 are extrapolated regressions that also show values outside the empirical

fitting range ( $\log \log C_w^{\text{sat}}$  -1.61 to -0.01 mol m<sup>-3</sup>). The error of the regressions increases sharply with increasing distance from the fitting area to the edges.

The slopes of equations 18 (a) - (d) illustrate that the negative slope decreases with increasing sorption capacity of the plastics from -1.038 (PBS) < -0.851 (LDPE) < -0.599 (PP) < -0.092 (PET), while the intercept decreased from PBS (3.263) > LDPE (2.907) > PP (2.880) > PET (2.681). In Figure 15 b), the  $\log K_{\text{p-w}}$ 's for the 16 EPA PAHs were extrapolated using equations 18 (a) - (d) and  $\log C_w^{\text{sat}}$  according to Ma et al. (2010). However, the equations 18 (a) - (d) were limited by the range of the tested PAHs represented by their  $\log C_w^{\text{sat}}$ , but within this  $\log C_w^{\text{sat}}$  range all equations resulted in a good accuracy.

### 5.3.1. Correlation between $\log K_{\text{LDPE-w}}$ and $\log C_w^{\text{sat}}$ from this thesis versus published studies

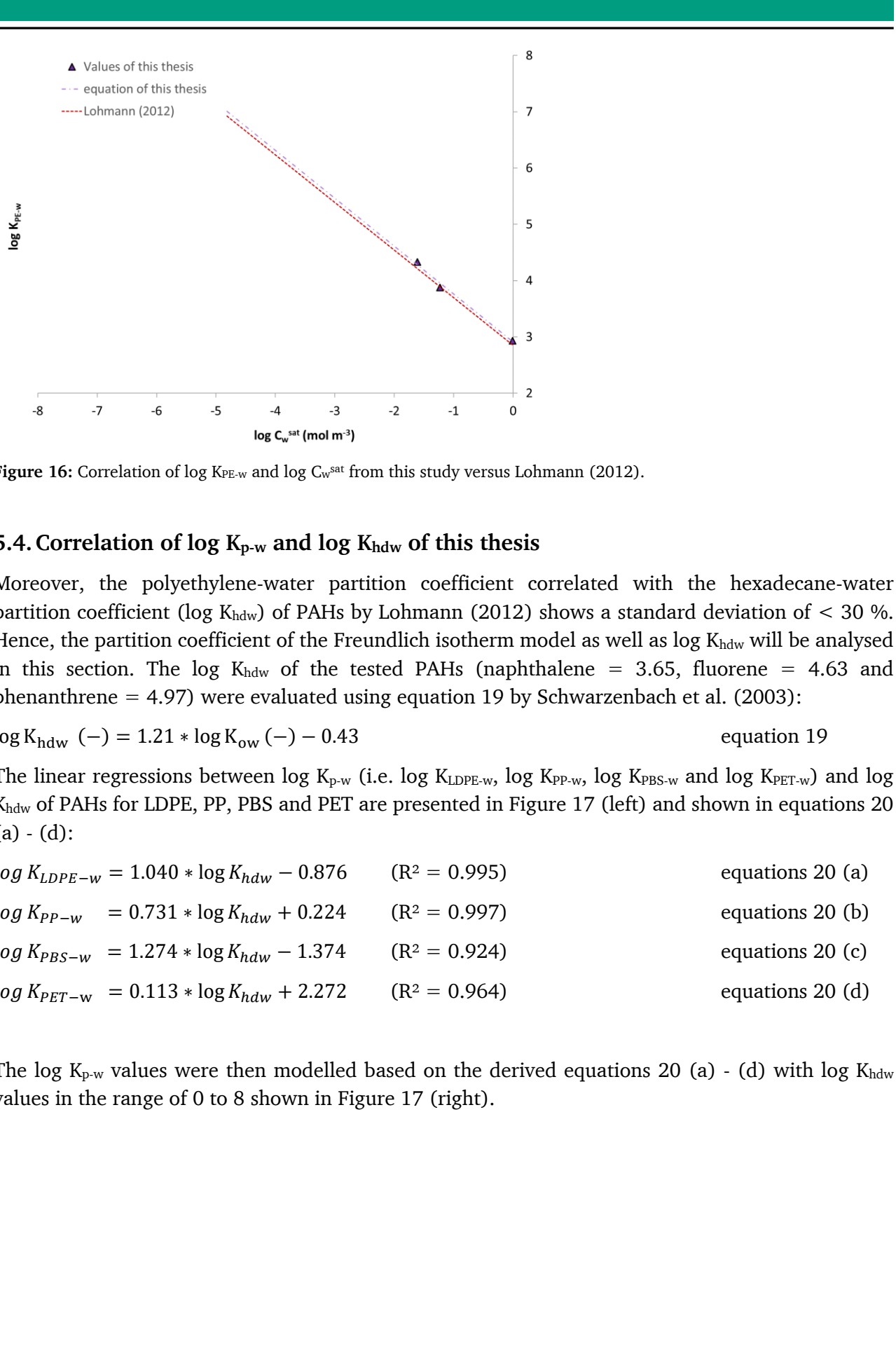
Since there is just one other study that correlated  $\log C_w^{\text{sat}}$  and plastic-water partition coefficient for polyethylene (Lohmann, 2012), no further comparisons of the remaining polymers can be made. Lohmann (2012) has used a data set of  $n = 65 \log K_{\text{PE-w}}$  to derive the linear regression model shown in Table 11. According to the SPSS-value of value (0.796), there is no significant difference between the regression model of this thesis and Lohmann (2012).

**Table 11:** SPSS analysis of  $\log K_{\text{PE-w}} - \log C_w^{\text{sat}}$  regression models of this thesis and Lohmann (2012)

Reference	$\log C_w^{\text{sat}}$ regression models		SPSS
	equation	R <sup>2</sup>	
This thesis	$\log K_{\text{LDPE-w}} = -0.851 \log C_w^{\text{sat}} + 2.907$	0.992	
Lohmann (2012)	$\log K_{\text{PE-w}} = -0.845 (\pm 0.027) \log C_w^{\text{sat}} + 2.851 (\pm 0.071)$	0.94	0.796

<sup>a</sup> Calculated p-value by SPSS; p > 0.05 no significant difference; p < 0.05 significant difference between  $\log K_{\text{PET-w}}$  - MW of individual study from the literature and  $\log K_{\text{PET-w}}$  - MW of this study

Both models from Table 11 are visualized in Figure 16 and affirm that there is no significant difference between the existing linear regressions. However, references were missing for equations 18 (b) - (d) in order to make a comparison.



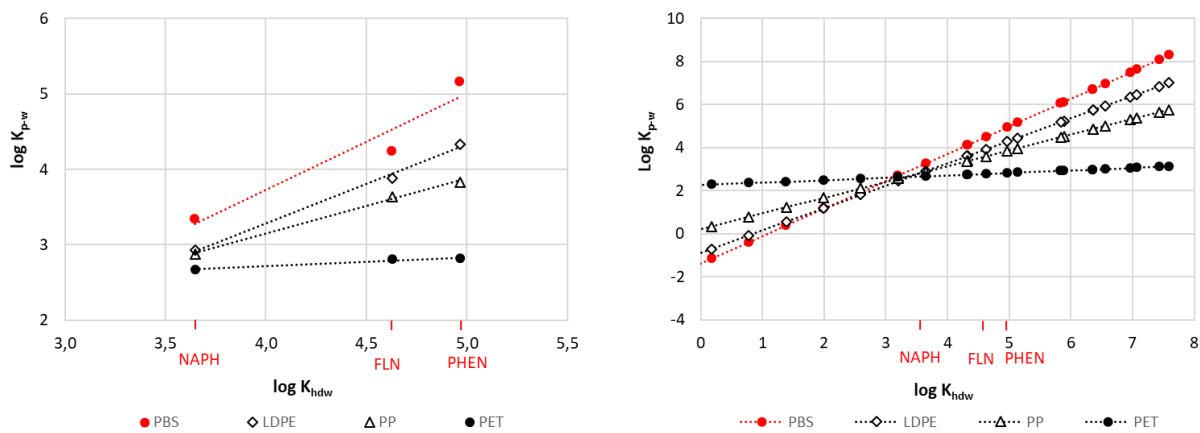


**Figure 17:**  $\log K_{p\text{-}w}$  regression with  $\log K_{\text{hdw}}$ : results from the experiment (left) and  $\log K_{p\text{-}w}$  modelled from the derived equations (right).

The  $\log K_{p\text{-}w}$  determined from the experiments on the four tested polymers showed positive correlations with  $\log K_{\text{hdw}}$ , similar to Lohmann (2012). In this thesis, the coefficient of determination was within a range from 0.924 to 0.997. The regressions shown on the right in Figure 17 are extrapolated regressions that also show values outside the empirical fitting range ( $\log K_{\text{hdw}}$  3.65 - 4.97). The error of the regressions increases sharply with increasing distance from the fitting area to the edges.

Equations 20 (a) - (d) illustrated an increase in slope with increasing sorption capacity for the tested plastics (1.274 (PBS) > 1.040 (LDPE) > 0.731 (PP) > 0.113 (PET)), while the intersection decreased from PET (2.272) > PP (0.224) > LDPE (-0.876) > PBS (-1.374). In Figure 17 on the right, the  $\log K_{p\text{-}w}$ s for the 16 EPA PAHs were extrapolated using equations 20 (a) - (d) and  $\log K_{\text{hdw}}$  according to Schwarzenbach et al. (2003). Furthermore, an intersection point of all four linear regressions showed up around  $\log K_{\text{hdw}}$  3.20, which is the lowest PAH, naphthalene. However, the equations 20 (a) - (d) were limited by the range of the tested PAHs represented by their  $\log K_{\text{hdw}}$ , but within this  $\log K_{\text{hdw}}$  range, all equations resulted in a good accuracy.

#### 5.4.1. Correlation between $\log K_{\text{LDPE}\text{-}w}$ and $\log K_{\text{hdw}}$ from this thesis versus published studies

Since there is just one other study that correlated  $\log C_w^{\text{sat}}$  and plastic-water partition coefficient for polyethylene (Lohmann, 2012), no further comparisons of the remaining polymers can be made. Lohmann (2012) has used a data set of  $n = 65 \log K_{\text{PE}\text{-}w}$  to derive the linear regression model shown in Table 12. According to the SPSS-value (0.118), there is no significant difference between the regression model of this thesis and Lohmann (2012).

**Table 12:** SPSS analysis of  $\log K_{\text{PE}\text{-}w}$  –  $\log K_{\text{hdw}}$  regression models of this thesis and Lohmann (2012)

Reference	$\log K_{\text{hdw}}$ regression models		SPSS
	equation	$R^2$	
This thesis	$\log K_{\text{LDPE}\text{-}w} = 1.040 \log K_{\text{hdw}} - 0.851$	0.995	
Lohmann (2012)	$\log K_{\text{PE}\text{-}w} = 1.007 (\pm 0.038) \log K_{\text{hdw}} - 0.790 (\pm 0.220)$	0.92	0.118

<sup>a</sup> Calculated p-value by SPSS;  $p > 0.05$  no significant difference;  $p < 0.05$  significant difference between  $\log K_{\text{PET}\text{-}w}$  - MW of individual study from the literature and  $\log K_{\text{PET}\text{-}w}$  - MW of this study

Both models from Table 12 are visualized in Figure 18, which confirms that there is no significant difference between the existing linear regressions. However, references were missing for equations 20 (b) - (d) in order to make a comparison.

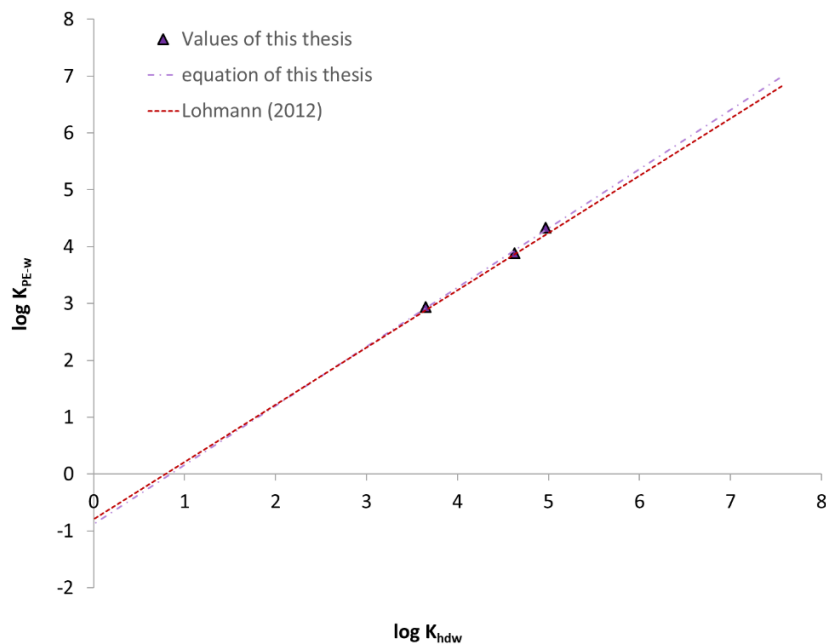


Figure 18: Correlation of  $\log K_{\text{PE-w}}$  and  $\log K_{\text{hdw}}$  from this study versus Lohmann (2012).

### Summary

In this research, sorption isotherm experiments were conducted and  $\log K_{\text{p-w}}$  of three PAHs, naphthalene, fluorene and phenanthrene, on three conventional polymers (LDPE, PP, PET) and one biodegradable polymer PBS with the size of approx.  $500 \mu\text{m}$  in  $d_{50}$  were determined. To the best of knowledge, this is the first study that calculated  $\log K_{\text{p-w}}$  values of naphthalene and fluorene for PBS as well as  $\log K_{\text{p-w}}$  of naphthalene, fluorene and phenanthrene for PET in salt-free water.

Both the Freundlich and linear models fit the experimental data well, with  $R^2 > 0.80$  and  $R^2 > 0.82$ , respectively, except for phenanthrene on PET. In this thesis, the reproducibility in calculating  $\log K_{\text{p-w}}$  was significantly better when applying the Freundlich isotherm model. The  $\log K_{\text{p-w}}$  using the Freundlich model increased in order of PET < PP < LDPE < PBS for all tested PAHs. The results of this thesis show that physicochemical properties of the polymer materials must have influenced the sorption of these PAHs in the water phase.

Furthermore, a correlation between  $\log K_{\text{p-w}}$ , MW,  $\log C_{\text{w}}^{\text{sat}}$ ,  $\log K_{\text{hdw}}$  and the partition coefficient of the Freundlich model for the selected PAHs and four polymers was investigated. Significant linear correlations were observed between  $\log K_{\text{p-w}}$  and  $\log K_{\text{ow}}$  of the tested PAHs for LDPE, PP, PBS and PET, with  $R^2$ 's of 0.995, 0.997, 0.924 and 0.964, respectively. All regression models showed a unique correlation depending on the polymer type. In terms of LDPE, the  $\log K_{\text{LDPE-w}} - \log K_{\text{ow}}$  regression model in this thesis showed no significant difference compared to published ones, which shows that the validity of this experimental settings were adequate. For PP, PBS and PET,  $\log K_{\text{p-w}} - \log K_{\text{ow}}$  regression models were developed for the first time. These models can be applied to estimate  $\log K_{\text{p-w}}$  values of other PAHs with an adequate accuracy, especially three-ring PAHs with  $\log K_{\text{ow}}$  values between 3.35 and 4.45 for LDPE, PBS, PP and PET.

The correlation of MW and the LDPE Freundlich partition coefficient showed a good accuracy and had no significant difference with published data. However, for PP, PET and PBS, there are a few publications available showing no significant difference for PET, but for PP. In the case of PBS, there is no comparable data set available for further investigation. For PP, PBS and PET, log  $K_{p-w}$  - MW regression models were developed for the first time. These models can be applied to estimate log  $K_{p-w}$  values of other PAHs with good accuracy, especially three-ring PAHs with log MW values between 128.16 and 178.22 g mol<sup>-1</sup> for LDPE, PBS, PP and PET.

Since MW and log  $K_{ow}$  showed good correlation with partition coefficient, especially for LDPE, aqueous solubility based on MW-values as well as log  $K_{hdw}$ -values, which are based on log  $K_{ow}$ , showed a similar accuracy. Published data for PP, PET, as well as PBS were not available for log  $C_w^{sat}$  and log  $K_{hdw}$ . Therefore, a comparison with literature data for PP, PET and PBS cannot be made. However, one data set each for log  $C_w^{sat}$  and log  $K_{hdw}$  can be compared with the results of this thesis and shows no significant difference.

## 6. Correlations of plastic properties and log K<sub>p-w</sub>

In chapter 6, linear correlations of plastic-water partition coefficients in this thesis and plastic properties were determined and compared with published data.

### 6.1. Characterization of the microplastics

The thermal properties (crystallinity = X<sub>c</sub>, glass transition temperature = T<sub>g</sub>, melting temperature T<sub>m</sub>), surface structures (surface area = SA, pore volume = V<sub>p</sub>), density ( $\rho$ ) and median diameter of the plastic particles (d<sub>50</sub>) were analysed to identify differences between the plastic materials used. In Table 13, all results of LDPE, PP, PBS and PET are listed with the same sizes used for the determination of log K<sub>p-w</sub> in the laboratory. In order to determine the surface free energy (SFE) including the dispersive and polar proportions, plates of the selected plastic type were used.

#### 6.1.1. Literature values of plastic properties

The following plastic properties were taken from the relevant sorption studies on the one hand and from further literature on the other. Density, thermoplastic properties and surface free energy are specific plastic properties. As only a few details of these plastic properties are available in the sorption studies, values and value ranges from the general literature are used, as these are generally valid.

In the literature, the density range is between 0.91 and 0.93 g cm<sup>-3</sup> for LDPE (Lambert and Wagner, 2018), while for PBS the range is between 1.24 and 1.26 g cm<sup>-3</sup> (Lin et al., 2020), for PP between 0.85 and 0.93 g cm<sup>-3</sup> (Andrady, 2011), and for PET between 1.34 and 1.41 g cm<sup>-3</sup> (Lambert and Wagner, 2018; Brignac et al., 2019), respectively.

Materials used for sorption test varied in their thickness between 12 and 100  $\mu\text{m}$  for LDPE (J. Wang et al., 2019; Cornelissen et al., 2008), 150 and 200  $\mu\text{m}$  for PBS (Zhao et al., 2020), and 12.5 and 3000  $\mu\text{m}$  for PP (J. Wang et al., 2019; Lončarski et al., 2021). The material thickness of the only relevant PET sorption test is 3000  $\mu\text{m}$  (Lončarski et al., 2021).

Furthermore, the surface area in relevant sorption studies is 1.58 m<sup>2</sup> g<sup>-1</sup> for LDPE (J. Wang et al., 2019), 0.04 m<sup>2</sup> g<sup>-1</sup> (Zhao et al., 2020) for PBS, 0.207 – 3.327 m<sup>2</sup> g<sup>-1</sup> for PP (J. Wang et al., 2019), and 0.164 m<sup>2</sup> g<sup>-1</sup> for PET (Lončarski et al., 2021). The only available pore volume in the relevant sorption studies is given in the literature by Zhao et al. (2020) for PBS as 0.66E-4 cm<sup>3</sup> g<sup>-1</sup>.

In the general literature, the glass transition temperature for LDPE is -118.1 °C (Khonakdar et al., 2007), for PBS between -28.5 °C (L. Wang et al., 2019) and -33.8 °C (Qiu et al., 2003), for PP from -11.15 °C (Gan et al., 1985) to -8.85 °C (Nitta and Takayanagi, 1999), and for PET is 78 °C (Lotti et al., 2013). In addition, published melting temperature is between 106 °C (Prasad, 1998) and 120.08 °C (Zaky and Mohamed, 2010) for LDPE, between 100 °C (Shen, 2023) and 116.4 °C (L. Wang et al., 2019) for PBS, 164.85 °C (Nitta and Takayanagi, 1999) for PP and 252 °C (Lotti et al., 2013) for PET. In further studies, the crystallinity for LDPE, PBS, PP and PET is given in the range between 33.6 % (Chen et al., 2020) and 60.0 % (Lambert and Wagner, 2018), 35.0 % (Zhang et al., 2012) and 65.6 % (Jin et al., 2014), 33.6 % (Thumsorn and Srisawat, 2014) and 58.1 % (Yang et al., 2016), and 2.0 % (Mishra and Deopura, 1989) and 40.0 % (Ehrenstein, 2012), respectively.

The SFE is specified in the literature between 21.15 (Phokhaphaiboonsuk et al., 2012) and 33.8 mN m<sup>-1</sup> (Aktas et al., 2023), 46.4 mN m<sup>-1</sup> (Valerio et al., 2018) and 48.6 mN m<sup>-1</sup> (Wu et al., 2012), 20.2 mN m<sup>-1</sup> (Fenouillot et al., 2009) and 30.75 mN m<sup>-1</sup> (Krásný et al., 2012), 26.84 mN m<sup>-1</sup> (Pandiyaraj et al., 2012) and 48.2 mN m<sup>-1</sup> (Struller et al., 2014) for LDPE, PBS, PP and PET. All literature values are summarised in Table 13.

### 6.1.2. Measured plastic properties of this thesis compared with literature plastic properties

Four types of pre-production plastic resin pellets, PBS, LDPE, PP and PET, and their density were provided by CARAT GmbH (Germany) and are listed in Table 13.

The d<sub>50</sub> of the plastic particles were measured with a Malvern Mastersizer 3000 (Malvern Panalytical Ltd, United Kingdom) at the Technical University of Darmstadt (Germany). All four different plastic type samples were measured in a solution of technical grade Sodium dodecylbenzenesulfonate from Sigma Aldrich (USA) 0.5 weight-% and Milli-Q water (conductivity < 0.056 µS cm<sup>-1</sup> at 25 °C) at 1700 rpm propeller rotation and 10 % ultra sonic ratio. In this case Sodium dodecylbenzenesulfonate was used in order to reduce surface tensions and increase wetting behaviour of the microplastic particles. Particle proportion was measured with shadowing of the Malvern instruments in the range of 5 to 10 % for the whole measurement sequence. Each plastic type sample was measured eight times for 20 seconds. The average d<sub>50</sub> value of each selected plastic material is listed in Table 13.

Brunauer-Emmett-Teller surface area (SA) and pore volume (V<sub>p</sub>) of the plastic particles were determined by 3Flex (Micromeritics, Norcross, USA) at Fraunhofer Institut Alzenau (Germany) with N<sub>2</sub> adsorption-desorption in isotherm measurements. The results are listed in Table 13.

The thermal plastic properties glass transition temperature (T<sub>g</sub>), melting temperature (T<sub>m</sub>) and crystallinity (X<sub>c</sub>) were measured with the Netzsch DSC (200 F3, Germany) at the Technical University of Darmstadt (Germany). The DSC analysis started at a minimum temperature of -100 °C and was heated up to a maximum of 250 °C at a rate of 10 °C/min. The T<sub>g</sub> characterises the state of amorphous regions of a polymer material under a certain temperature. At T<sub>g</sub>, the amorphous domain of a polymer is transformed from a glassy (below T<sub>g</sub>) into a rubbery (above T<sub>g</sub>) state (Endo and Koelmans, 2016; Sørensen et al., 2020; Torres et al., 2021). The T<sub>g</sub> of PP, PBS and PET were -18.5, -28.5 and 78 °C respectively. The T<sub>g</sub> of LDPE could not be measured with DSC. For LDPE, a T<sub>g</sub> literature value was reported at -118.1 °C (Khonakdar et al., 2007). Thus, amorphous domains of LDPE, PP and PBS at ambient temperature are in a rubbery state, whereas that of PET is in a glassy state. The results of this thesis show that polymers whose amorphous domains at ambient temperature are in a rubbery state have a higher crystallinity than polymers in a glassy state. X<sub>c</sub> decreases in order of PBS (59.4 %) > LDPE (47.8 %) > PP (40.1 %) > PET (5.3 %), while T<sub>m</sub> increases in order of PBS (90.3 °C) < LDPE (111.8 °C) < PP (166.3 °C) < PET (251.5 °C). Since all tested polymers had a mixture of crystalline and amorphous structures, they were classified as semicrystalline polymers (Goodship et al., 2015). When the portion of X<sub>c</sub> in a polymer is > 0 % and < 100 %, they are called semicrystalline. The crystallinity was determined by setting the measured melting enthalpy (ΔH<sub>m</sub> - ΔH<sub>c</sub>) in relation to the literature value ΔH<sub>m0</sub> for a completely crystalline material. The X<sub>c</sub> is calculated using the following equation:

$$X_c(\%) = \frac{\Delta H_m - \Delta H_c}{\Delta H_{m0}} \quad \text{equation 21}$$

Where  $\Delta H_m$  ( $J \ g^{-1}$ ) is the heat of melting,  $\Delta H_c$  ( $J \ g^{-1}$ ) is the cold crystallization determined by integrating the peaks and  $\Delta H_{m0}$  is the reference value for a 100 % crystalline polymer.

Regarding other physical properties, PP had the highest pore volume among the four tested polymer materials and a much higher BET surface area (Brunauer, Emmett, Teller) than the other three polymer materials (Figure A6.9-A6.12).

The contact angle was determined with the drop shape analysis system DSA100 Krüss GmbH at Polymer Service GmbH Merseburg (Germany). Distilled water, diiodomethane and ethylene glycol were used as test liquids. The drops were automatically deposited at a volume of  $2 \ \mu\text{L}$ . Each sample was placed on a line of eight drops with 4 mm drop spacing and then measured.

After completing the measurements, the analysed area was cleaned with compressed air and the new row of drops was placed at a distance of approximately 8 mm from the previous row. The measurement of the right and left contact angle of each drop was made 10 times with a time interval of 1 s. The arithmetic mean was obtained from these 10 individual measurements of the contact angle. The surface free energy was calculated based on the Owens, Wendt, Rabel and Kaelble (OWRK) standard model for solid objects from the contact angles of different test liquids. The results, including standard errors of the disperse, polar and sum of disperse, and polar proportions SFE are presented in Table 13.

Furthermore, in Table 13 all physical and thermal plastic properties of this thesis are compared with literature values.

**Table 13:** Physical and thermal properties of polymers used for the sorption experiments and literature values

Sorbent	LDPE		PBS		PP		PET	
	this thesis	literature	this thesis	literature	this thesis	literature	this thesis	literature
$\rho$ ( $\text{g cm}^{-3}$ )	0.92	0.91 - 0.93 <sup>1</sup>	1.24	1.24 - 1.26 <sup>2</sup>	0.91	0.85 - 0.93 <sup>3</sup>	1.34	1.34 <sup>1</sup> - 1.41 <sup>4</sup>
$d_{50}$ ( $\mu\text{m}$ )	455	12 <sup>5</sup> - 100 <sup>6</sup>	535	150 - 200 <sup>7</sup>	536	12.5 <sup>5</sup> - 3,000 <sup>8</sup>	658	3,000 <sup>8</sup>
SA ( $\text{m}^2 \ \text{g}^{-1}$ )	3.16	1.58 <sup>5</sup>	2.77	0.04 <sup>7</sup>	11.44	0.207 - 3.327 <sup>5</sup>	4.24	0.164 <sup>8</sup>
$V_p$ ( $\text{cm}^3 \ \text{g}^{-1}$ )	0.0020	/	0.0018	0.66 E -4 <sup>7</sup>	0.0073	/	0.0028	/
$T_g$ ( $^\circ\text{C}$ )	-118.1 <sup>9</sup>	/	-45.0	-33.8 <sup>10</sup> - -28.5 <sup>11</sup>	-2.6	-11.15 <sup>12</sup> - -8.85 <sup>13</sup>	78.0	78.0 <sup>14</sup>
$T_m$ ( $^\circ\text{C}$ )	111.8	106.00 <sup>15</sup> - 120.08 <sup>16</sup>	90.3	100.00 <sup>17</sup> - 116.40 <sup>10</sup>	166.30	164.85 <sup>13</sup>	251.50	252.00 <sup>14</sup>
$X_c$ (%)	47.8 <sup>18</sup>	33.6 <sup>19</sup> - 60.0 <sup>1</sup>	59.4 <sup>20</sup>	35.0 <sup>21</sup> - 65.6 <sup>22</sup>	40.1 <sup>23</sup>	33.6 <sup>24</sup> - 58.1 <sup>25</sup>	5.3 <sup>26</sup>	2.0 <sup>27</sup> - 40.0 <sup>28</sup>
$\sum \text{SFE}^a$ ( $\text{mN m}^{-1}$ )	$25.4 \pm 0.3$	$21.15^{29}$ - $33.80^{30}$	$58.4 \pm 9.03$	$46.40^{31}$ - $48.60^{32}$	$25.6 \pm 1.29$	$20.20^{33}$ - $30.75^{34}$	$52.8 \pm 8.1$	$26.84^{35}$ - $48.20 \pm 1.3^{36}$
SFE disperse SFE ( $\text{mN m}^{-1}$ )	$25.0 \pm 0.27$	/	$43.8 \pm 5.61$	$32.40^{31}$ - $39.90^{32}$	$24.1 \pm 1.05$	$19.80^{33}$ - $8.25^{34}$	$42.5 \pm 5.33$	$20.95^{35}$ - $38.60 \pm 0.9^{36}$
polar SFE ( $\text{mN m}^{-1}$ )	$0.4 \pm 0.04$	/	$14.6 \pm 3.43$	$14.00^{31}$ - $8.70^{32}$	$1.2 \pm 0.24$	$0.40^{33}$ - $22.50^{34}$	$10.2 \pm 2.77$	$5.89^{35}$ - $9.60 \pm 0.9^{36}$
$R^2$	0.999	/	0.993	/	0.995	/	0.991	/

<sup>1</sup> Lambert and Wagner (2018); <sup>2</sup> Lin et al. (2020); <sup>3</sup> Andradey (2011); <sup>4</sup> Brignac et al. (2019); <sup>5</sup> J. Wang et al. (2019); <sup>6</sup> Cornelissen et al. (2008); <sup>7</sup> Zhao et al. (2020); <sup>8</sup> Lončarski et al. (2021); <sup>9</sup> Khonakdar et al. (2007); <sup>10</sup> Qiu et al. (2003); <sup>11</sup> L. Wang et al. (2019); <sup>12</sup> Gan et al. (1985); <sup>13</sup> Nitta and Takayanagi (1999); <sup>14</sup> Lotti et al. (2013); <sup>15</sup> Prasad (1998); <sup>16</sup> Zaky and Mohamed (2010); <sup>17</sup> Shen (2023); <sup>18</sup> melting enthalpy of 100 % crystalline LDPE  $\Delta H_f^0 = 288 \ J \ g^{-1}$  (Khonakdar et al., 2007); <sup>19</sup> Chen et al. (2020); <sup>20</sup> melting enthalpy of 100 % crystalline PBS  $\Delta H_f^0 = 110.5 \ J \ g^{-1}$  (Xu et al., 2008); <sup>21</sup> Zhang et al. (2012); <sup>22</sup> Jin et al. (2014); <sup>23</sup> melting enthalpy of 100 % crystalline PP homopolymer  $\Delta H_f^0 = 209 \ J \ g^{-1}$  (Gahleitner et al., 1999); <sup>24</sup> Thumsorn and Srivastav (2014); <sup>25</sup> Yang et al. (2016); <sup>26</sup> melting enthalpy of 100 % crystalline PET amorphous  $\Delta H_f^0 = 140 \ J \ g^{-1}$  (Badia et al., 2012); <sup>27</sup> Mishra and Deopura (1989); <sup>28</sup> Ehrenstein (2012); <sup>29</sup> Phokhaphaiboonks et al. (2012); <sup>30</sup> Aktas et al. (2023); <sup>31</sup> Valerio et al. (2018); <sup>32</sup> Wu et al. (2012); <sup>33</sup> Fenouillot et al. (2009); <sup>34</sup> Krásný et al. (2012); <sup>35</sup> Pandiyaraj et al. (2012); <sup>36</sup> Struller et al. (2014)

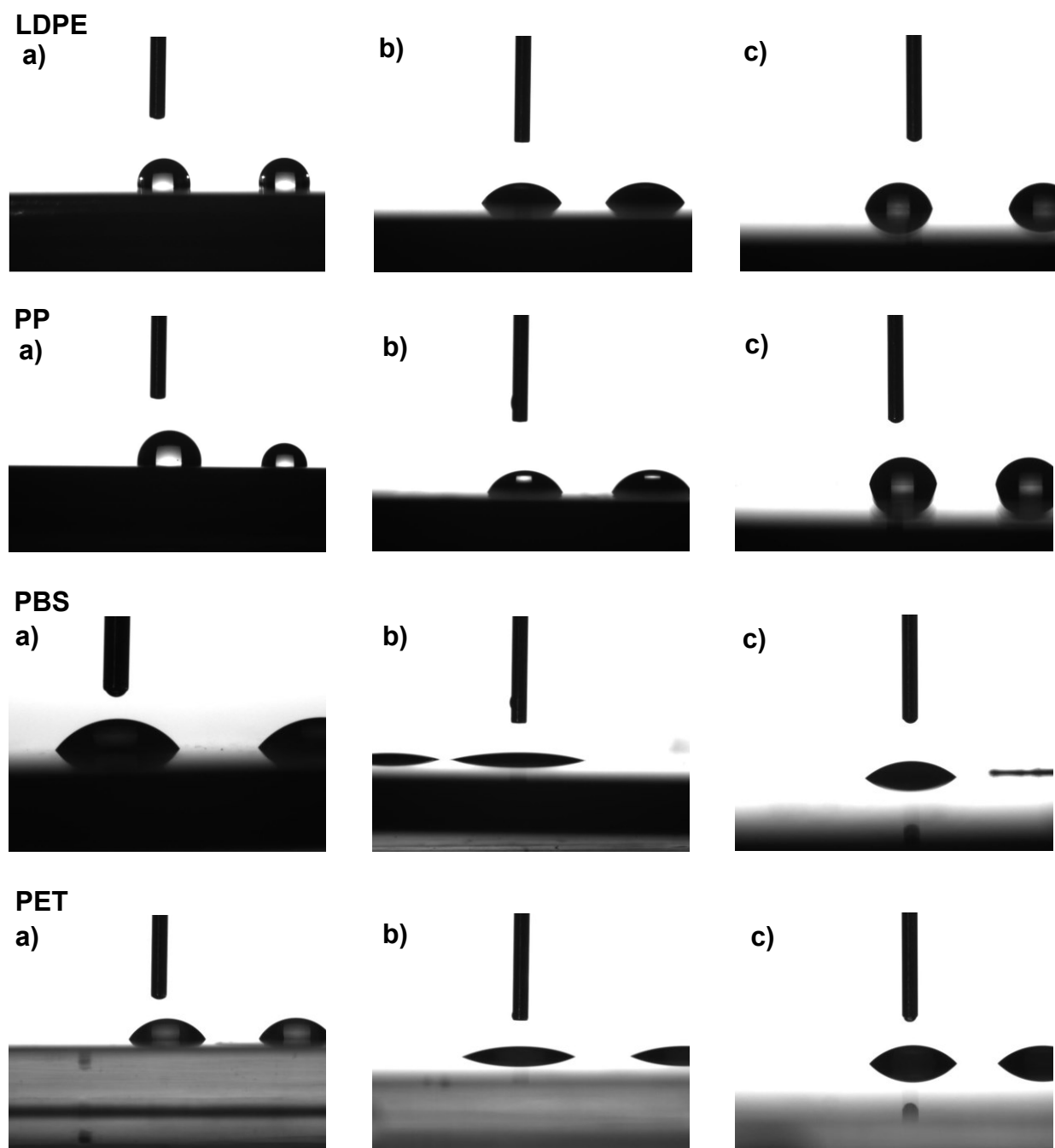
<sup>a</sup>  $\sum \text{SFE}$  = sum of disperse and polar surface free energy

Table 13 shows that the density and crystallinity values of all four different plastic types of this thesis are within the range of the literature values. In case of  $d_{50}$ , only the value of PP is within the range of the literature values. All surface area values of published studies are lower than that of this thesis, and the only available PBS pore volume value of a sorption study was also lower than that of this thesis.

While the  $T_g$  value of PBS and PP in this thesis is outside literature values, the  $T_g$  value of LDPE in this thesis is already a literature value and the value of PET perfectly matches with the literature as well. In addition, the  $T_m$  value of PP and PET only differ from literature values in the single-digit or decimal range and the LDPE value in this thesis is within the range of the literature, with the exception of PBS, which is outside the literature range.

Published surface free energy data of LDPE range from  $21.15$  to  $33.8 \text{ mN m}^{-1}$  (Phokhaphaiboonsuk et al., 2012; Krásný et al., 2012; Chaudhari et al., 2012; Habib et al., 2019; Aktas et al., 2023) for untreated and ungrafted LDPE respectively shows that LDPE as a polymer type can have different surface free energies. The sum of dispersive and polar surface free energy measured for LDPE is within the range of previous data from literature, which indicates that the tested LDPE is an average LDPE material. However,  $\sum \text{SFE}$  of PP is  $5.15$  and  $4.5$  order of magnitude lower than published data by Krásný et al. (2012) and Mamunya et al. (2016) respectively, but  $5.4 \text{ mN m}^{-1}$  higher than the  $\sum \text{SFE}$  by Fenouillot et al. (2009). The tested PP is also within the average of various previously tested PP materials. The results of PBS for the  $\sum \text{SFE}$  listed in Table 13 is higher than the  $\sum \text{SFE}$  from Wu et al. (2012) at  $48.6 \text{ mN m}^{-1}$  and Valerio et al. (2018) at  $46.4 \text{ mN m}^{-1}$ , while the polar SFE by Valerio et al. (2018) is in the same order of magnitude as this thesis, with  $14 \text{ mN m}^{-1}$  and  $14.6 \pm 3.43 \text{ mN m}^{-1}$  respectively. However, Valerio et al. (2018) did not specify any further PBS properties, which makes a comparison difficult. The difference of  $\sum \text{SFE}$  reported by Wu et al. (2012) and this thesis could have been caused by the higher melting temperature of  $112^\circ\text{C}$ , which affects not only the internal structure, but also the surface structure.

In addition, published data for  $\sum \text{SFE}$  of PET is between  $26.84$  and  $48.20 \text{ mN m}^{-1}$  (Pandiyaraj et al., 2012; Giol et al., 2019; Struller et al., 2014), while  $\sum \text{SFE}$  of PET calculated in this thesis is  $4.60 \text{ mN m}^{-1}$  higher ( $52.80 \text{ mN m}^{-1}$ ) than that of published data. While the polar surface free energy of this thesis is  $0.6 \text{ mN m}^{-1}$  higher than that of Struller et al. (2014), it is  $3.9 \text{ mN m}^{-1}$  with disperse surface free energy. Disperse surface free energy of Struller et al. (2014) is  $38.6 \text{ mN m}^{-1}$ . However, Struller et al. (2014) did not further specify the PET in the literature. Both polar and disperse surface free energy of Pandiyaraj et al. (2012) ( $5.89 \text{ mN m}^{-1}$ ,  $20.95 \text{ mN m}^{-1}$ ) and Giol et al. (2019) ( $7.7 \text{ mN m}^{-1}$ ,  $35.9 \text{ mN m}^{-1}$ ) are lower than the surface free energies of PET listed in Table 13. Giol et al. (2019) specifies the PET density between  $1.3$  and  $1.4 \text{ g cm}^{-3}$ , while Pandiyaraj et al. (2012) gives no further details. Figure 19 illustrates the drip image capture of distilled water, diiodomethane and ethylene glycol on the tested polymers LDPE, PP, PBS and PET.



**Figure 19:** drip image capture of a) distilled water b) diiodomethane and c) ethylene glycol on LDPE, PP, PBS and PET

## 6.2. Correlation of film thickness of sorbent materials on $\log K_{p-w}$ of selected PAHs

First, the influence of film thickness and median diameter ( $d_{50}$ ) of polymers on  $\log K_{p-w}$  for PAHs are looked into by comparing relevant available studies and the results from this thesis (Table A6.2 - A6.5).

There are a fair number of studies demonstrating the  $\log K_{LDPE-w}$  of naphthalene, fluorene and phenanthrene using LDPE (Booij et al., 2003; Adams et al., 2007; Cornelissen et al., 2008; Fernandez et al., 2009; Smedes et al., 2009; Hale et al., 2010; Choi et al., 2013; Zhu et al., 2015; J. Wang et al., 2019) with a film thickness between  $12 \mu\text{m}$  and  $100 \mu\text{m}$  (Table 14). These studies are compared to the derived values using LDPE particles with the size of  $d_{50} = 455 \mu\text{m}$ .

The log  $K_{p-w}$  value of naphthalene on LDPE particles was determined to be  $2.93 \pm 0.33$ , showing no significant differences to the data available in other literature ranging from  $2.81$  to  $3.23$  (Cornelissen et al., 2008; Smedes et al., 2009; Choi et al., 2013; Zhu et al., 2015; Wang and Wang, 2019;). With regard to fluorene on LDPE, the log  $K_{LDPE-w}$  was determined to be  $3.88 \pm 0.28$ , which lies between the results from Cornelissen et al. (2008), Smedes et al. (2009), Choi et al. (2013) and Zhu et al. (2015). For phenanthrene, the log  $K_{LDPE-w}$   $4.33 \pm 0.10$  of this thesis was somewhat higher than the results acquired by Booij et al. (2003) at  $30^\circ\text{C}$ , Adams et al. (2007), Cornelissen et al. (2008), Smedes et al. (2009), Hale et al. (2010), Choi et al. (2013), Zhu et al. (2015) and J. Wang et al. (2019). For example, log  $K_{LDPE-w}$  of phenanthrene is  $0.03$  log units higher than that reported by Adams et al. (2007), and  $0.29$  log units higher than calculated by Choi et al. (2013). When compared to Booij et al. (2003), the log  $K_{LDPE-w}$  value for phenanthrene falls between the two determined values by Booij et al. (2003) despite the larger particles used in this thesis. However, all these differences are statistically not significant ( $p < 0.05$ ) in program R.

**Table 14:** Comparison of polyethylene-water partition coefficient

	This thesis	A	B	C	D	E	F	G	H	I
Polyethylene	LDPE	LDPE	LDPE	LDPE	LDPE	LDPE	PE	LDPE	LDPE	LDPE
Film thickness ( $\mu\text{m}$ )	455 <sup>a</sup>	70	51	100	25	70	51	51	76	$12 \mu\text{m}$
$\rho$ ( $\text{g cm}^{-3}$ )	0.92		0.92					0.92		0.92
SA ( $\text{m}^2 \text{g}^{-1}$ )	3.16									1.58
log $K_{LDPE-w/PE-w}$ ( $\text{L kg}^{-1}$ )										
naphthalene	$2.93 \pm 0.33$			$3.04 \pm 0.14$		$2.81 \pm 0.14$		$3.23 \pm 0.06$	$2.94 \pm 0.04$	$2.84 \pm 1.85$
fluorene	$3.88 \pm 0.28$			$3.67 \pm 0.04$		$3.77 \pm 0.11$		$3.78 \pm 0.04$	$4.14 \pm 0.07$	
phenanthrene	$4.33 \pm 0.10$	$4.41 \pm 0.01$ ( $13^\circ\text{C}$ )	$4.12 \pm 0.02$ ( $30^\circ\text{C}$ )	$4.30 \pm 0.1$	$4.14 \pm 0.02$	$4.30 \pm 0.10$	$4.22 \pm 0.11$	$4.13 \pm 0.03$	$4.04 \pm 0.03$	$4.22 \pm 0.07$
										$4.08 \pm 3.70$

References: A (Booij et al., 2003), B (Adams et al., 2007), C (Cornelissen et al., 2008), D (Fernandez et al., 2009), E (Smedes et al., 2009), F (Hale et al., 2010), G (Choi et al., 2013), H (Zhu et al., 2015), I (J. Wang et al., 2019)

<sup>a</sup> median diameter ( $d_{50}$ )

Hence, it can be concluded that the size and shape of LDPE materials has no significant influence on log  $K_{LDPE-w}$  of naphthalene, fluorene and phenanthrene when the particle size or film thickness is in the range of  $12$  to  $455 \mu\text{m}$ .

For PP, the results of Teuten et al. (2007), Karapanagioti and Kloniza (2008), Lee et al. (2014), J. Wang et al. (2019), Zhao et al. (2020) and Lončarski et al. (2021) can be compared to the results of this study.

Lee et al. (2014) conducted a series of sorption experiments in sea water and used a third-phase partitioning method to determine PP-seawater partition coefficients for eight PAHs and other hydrophobic organic compounds. Among these eight PAHs, the only result that is to be compared to this thesis is phenanthrene. For comparison purposes, the PP-seawater partition coefficients (log  $K_{PP-sw}$ ) by Teuten et al. (2007) and Lee et al. (2014) have been converted to PP-freshwater partition coefficients based on the Setschenow constant by Jonker and Muijs (2010), using equation 14.

The log  $K_{p-w}$  of phenanthrene on PP ( $d_{50} = 536 \mu\text{m}$ ) of this thesis was determined to be  $3.83 \pm 0.2$ , which is just  $0.1$  log units higher than the PP-freshwater partition coefficient value of  $3.73$  by Lee et al. (2014) (the median longest dimension:  $320$  -  $440 \mu\text{m}$ ). This comparison outcome shows that log  $K_{p-w}$  values of phenanthrene on PP of these two studies are comparable, with a certain difference in particle size and form. While the PP particle size of Teuten et al. (2007) is also in the three-digit magnitude, the specific surface area is one magnitude lower than in this thesis and the seawater

partition coefficient of Teuten et al. (2007) converted into freshwater is 0.7 log units smaller. Furthermore, published PP partition coefficients of naphthalene and phenanthrene by Karapanagioti and Klontza (2008) and phenanthrene by J. Wang et al. (2019) had a standard error that is one magnitude higher compared to this study, which make a direct comparison difficult. Although, the PP density specified by J. Wang et al. (2019) is comparable to this study, the specific surface area is at least one magnitude lower. The reason for poor comparability with J. Wang et al. (2019) is his use of modified talcum-filled PP versus the unmodified PP of this study. Lončarski et al. (2021) also used PP, but with six times higher film thickness, resulting in a higher partition coefficient compared to this study.

For PBS, a comparison with the study of Zhao et al. (2020), and for PET with the study of Lončarski et al., (2021) can be made. When considering the PBS properties by Zhao et al. (2020), a lower film thickness and a three times lower magnitude of specific surface area result in a lower partition coefficient compared to this study. On the other hand, the one magnitude higher film thickness and two times lower magnitude of specific surface area of Lončarski et al. (2021) resulted in a at least 1.29 higher partition coefficient for naphthalene and fluorene.

**Table 15:** Comparison of polypropylene-water partition coefficient

Polymer	This thesis		A		B		C		D		E		This thesis		F	
	PP	PP	PP	PP	PP	PP	PP	PP	PP	PP	PP	PP	PET	PET	PBS	PBS
Film thickness ( $\mu\text{m}$ )	536 <sup>a</sup>	200-250	< 2000	440	59	12.5	3000		658 <sup>a</sup>	3000		535 <sup>a</sup>	3000	535 <sup>a</sup>	150-200	
density ( $\text{g cm}^{-3}$ )	0.91			0.92	0.91	0.92			1.34				1.24			
specific surface area ( $\text{m}^2 \text{ g}^{-1}$ )	11.44	1.56			3.327	0.201			4.24	0.164		2.77	0.04			
$\log K_{p-w}$ of naphthalene	$2.88 \pm 0.32$						$4.06 \pm 2.03$		$2.72 \pm 1.70$	$4.18^c$	$2.68 \pm 0.13$		$4.39^c$	$3.35 \pm 0.22$		
$\log K_{p-w}$ of fluorene	$3.64 \pm 0.35$								$4.16^c$		$2.81 \pm 0.24$		$4.55^c$	$4.24 \pm 0.17$		
$\log K_{p-w}$ of phenanthrene	$3.83 \pm 0.20$	$3.06^b$	$2.43 \pm 1.90$	$3.73^b$	$4.18 \pm 3.28$	$3.74 \pm 2.42$					$2.82 \pm 1.06$		$5.16 \pm 0.10$	$4.92$		

References: A: (Teuten et al., 2007), B: (Karapanagioti and Klontza 2008), C: (Lee et al., 2014), D: (J. Wang et al., 2019), E: (Lončarski et al., 2021), F: (Zhao et al., 2020)

<sup>a</sup> median diameter ( $d_{50}$ ) in  $\mu\text{m}$ ; <sup>b</sup> seawater  $\log K_{pp,sw}$  values were converted to freshwater  $\log K_{pp,w}$  using the Setschenow constant by Jonker and Muijs (2010); <sup>c</sup>  $\log K_{p-w}$  values were determined in synthetic water enriched with a mixture of salts; values are not converted to fresh water  $\log K_{p-w}$

Since not every study specifies all properties, a tendency can be seen for polymers like PP, PBS and PET with higher particle size or film thickness resulting in higher partition coefficient. However, a combination of particle size and further properties e.g. density or thermal properties could also influence the sorption behaviour of these polymers.

### 6.3. Correlation of log K<sub>p-w</sub> and thermal plastic properties

In the following subchapters, the thermal plastic properties are compared with the log K<sub>p-w</sub> values of this thesis.

#### 6.3.1. Influence of glass transition temperature (T<sub>g</sub>) of the tested plastics on log K<sub>p-w</sub>

According to Endo and Koelmans (2016), Li et al. (2018), Uber et al. (2019), J. Wang et al. (2019) and Wang et al. (2020), sorption affinity of hydrophobic organic compounds for polymers can be, to a certain extent, influenced by thermal properties of polymers, such as crystallinity and glass transition temperature affects. The tendency of this log K<sub>p-w</sub> indicates that the state of amorphous domains of polymers affects the sorption capacity of polymer materials, as Endo and Koelmans (2016) and Zhao et al. (2020) mentioned. For example, PET as a glassy polymer resulted in the lowest log K<sub>p-w</sub> values for all three PAHs in contrast to the rubbery polymers LDPE, PP and PBS.

Based on the results of this thesis, the correlation between log K<sub>p-w</sub> and T<sub>g</sub> (T<sub>g</sub> LDPE = -118.1 °C, T<sub>g</sub> PBS = -45.0 °C, T<sub>g</sub> PP = -2.6 °C, T<sub>g</sub> PET = 78.0 °C) is looked into for naphthalene, fluorene and phenanthrene (Figure 20).

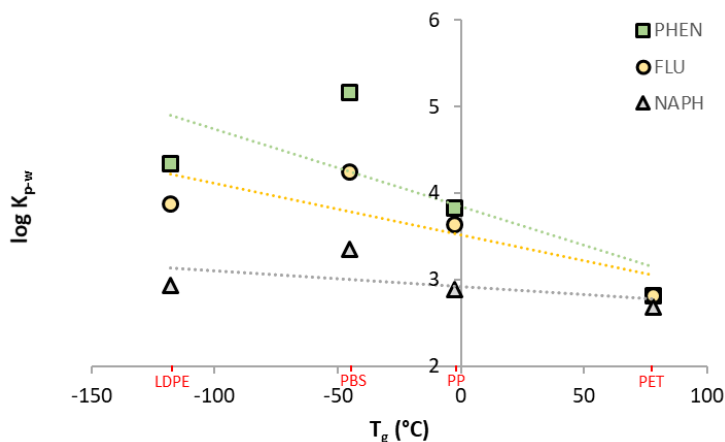


**Figure 20:** correlation between log K<sub>p-w</sub> of selected PAHs and glass transition temperature (T<sub>g</sub>) of the tested polymer materials

NAPH = naphthalene, correlation between log K<sub>p-w</sub> of naphthalene and crystallinity R<sup>2</sup> = 0.275;

FLU = fluorene, correlation of log K<sub>p-w</sub> of fluorene and crystallinity R<sup>2</sup> = 0.644;

PHEN = phenanthrene, correlation of log K<sub>p-w</sub> of phenanthrene and crystallinity R<sup>2</sup> = 0.561

Figure 20 shows a decreasing tendency of log K<sub>p-w</sub> values by increasing T<sub>g</sub>. However, the coefficient of determination (R<sup>2</sup>) of the correlation between log K<sub>p-w</sub> and T<sub>g</sub> for naphthalene, fluorene and phenanthrene was determined to be 0.275, 0.644 and 0.561 respectively, showing there is a lower accuracy for linear correlation between log K<sub>p-w</sub> and T<sub>g</sub>. The equations are as follows:

$$\text{naphthalene: } \log K_{p-w} = -0.002 T_g (\text{°C}) + 2.920 \quad (R^2 = 0.275) \quad \text{equations 22 (a)}$$

$$\text{fluorene: } \log K_{p-w} = -0.006 T_g (\text{°C}) + 3.512 \quad (R^2 = 0.644) \quad \text{equations 22 (b)}$$

$$\text{phenanthrene: } \log K_{p-w} = -0.009 T_g (\text{°C}) + 3.840 \quad (R^2 = 0.561) \quad \text{equations 22 (c)}$$

### 6.3.2. Influence of crystallinity ( $X_c$ ) of the tested plastics on $\log K_{p-w}$

Table 13 listed the crystallinity ( $X_c$ ) of polymers analysed in this thesis in the DSC measurement (Figure A6.1-A6.4). The PET used for this study is labelled “amorphous” PET and possesses the lowest  $X_c$  of 5.3 %, which is in the same range as reported by Wei et al. (2019).  $X_c$  of all rubbery polymers in this study are an order of magnitude higher compared to PET. The  $X_c$  of the rubbery PP homopolymer (40.1 %) in this study was 2.1 % higher than the  $X_c$  of PP homopolymer determined by Eiras and Pessan (2009). The  $X_c$  of the tested polymer materials decreases in the order of PBS (59.4 %) > LDPE (47.8 %) > PP (40.1 %) > PET (5.3 %), which is a similar tendency as the  $\log K_{p-w}$  of all three PAHs. Therefore, the correlation between  $\log K_{p-w}$  and  $X_c$  was determined by plotting a  $\log K_{p-w}$ -crystallinity curve. The results are presented in Figure 21.

As shown in Figure 21,  $\log K_{p-w}$  values correlate well with  $X_c$  of polymer sorbent materials with high  $R^2$  values. A positive correlation between  $\log K_{p-w}$  and  $X_c$  illustrates a greater sorption affinity of selected PAHs for polymers with higher  $X_c$  (Table A6.1).

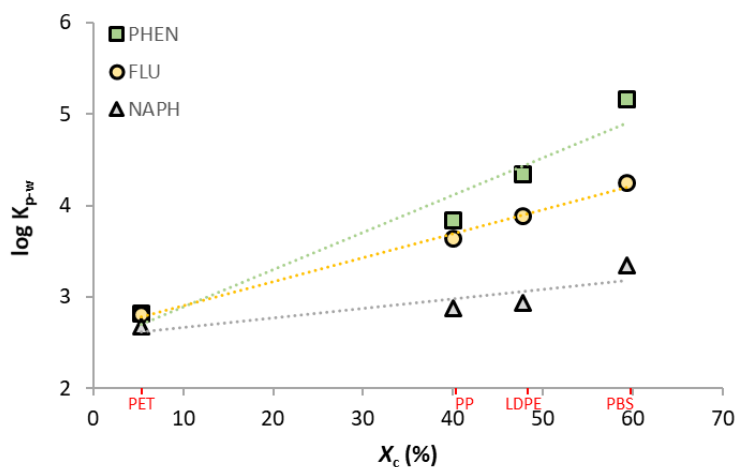


Figure 21: correlation of  $\log K_{p-w}$  and crystallinity ( $X_c$ )

NAPH = naphthalene, correlation of  $\log K_{p-w}$  of naphthalene and crystallinity of four polymers  $R^2 = 0.760$ ;

FLU = fluorene, correlation of  $\log K_{p-w}$  of fluorene and crystallinity of four polymers  $R^2 = 0.994$ ;

PHEN = phenanthrene, correlation of  $\log K_{p-w}$  of phenanthrene and polymer crystallinity of four polymers  $R^2 = 0.940$

Some researchers discussed their results with an assumption that sorption takes place in the amorphous regions of polymers (Endo and Koelmans, 2016; Wang et al., 2020). However, the results of this thesis in Figure 21 show that sorption capacity, i.e.,  $\log K_{p-w}$  of all three tested PAHs, is more clearly influenced by polymer property  $X_c$  than  $T_g$ . Young and Weber (1995) expected that increasing polymer  $X_c$  enhances partition coefficient for organic sorbates. Similarly, Endo and Koelmans (2016), Li et al. (2018) and Uber et al. (2019) mentioned in their studies that an increase of  $X_c$  enhances polymer sorption ability resulting in higher partition coefficients. The results not only support the assumption by Young and Weber (1995), Li et al. (2018), Uber et al. (2019) and Endo and Koelmans (2016), but also demonstrate a positive and significant correlation between  $\log K_{p-w}$  and the  $X_c$  of sorbent polymer materials for the first time to the best of knowledge.

Further, the results in this thesis showed a possibility of predicting the  $\log K_{p-w}$  of the selected PAHs from the  $X_c$  of sorbent polymer materials using the following equations:

naphthalene:  $\log K_{p-w} = 1.05 X_c (\%) + 2.56 (R^2 = 0.760)$  equations 23 (a)

fluorene:  $\log K_{p-w} = 2.61 X_c (\%) + 2.65 (R^2 = 0.994)$  equations 23 (b)

phenanthrene:  $\log K_{p-w} = 4.08 X_c (\%) + 2.48 (R^2 = 0.940)$  equations 23 (c)

### 6.3.3. Influence of melting temperature ( $T_m$ ) of the tested plastics on $\log K_{p-w}$

Melting temperatures ( $T_m$ ) of the tested polymer particles are illustrated in Table 13. Unlike  $T_g$ , at which the glassy state of polymer materials is converted into a rubbery state (Wang et al., 2020; Andrade, 2017; dos Santos et al., 2013; Dominghaus, 2012),  $T_m$  is the temperature at which an ordered crystalline phase of semi-crystalline polymers like PET, PP, LDPE and PBS turns into the disordered amorphous phase (Endo and Koelmans, 2016; Balani, et al., 2015). Overall, the molecular chain topology of the polymers influences the melting temperature. For example, double bonds, aromatic groups and large side groups in the polymer chain can restrict the flexibility of the polymer chains, leading to a high melting temperature.

Among the four polymer materials in this study, the melting point of PET is the highest ( $T_m = 251.5$  °C), followed by PP ( $T_m = 166.3$  °C), LDPE ( $T_m = 111.8$  °C) and PBS ( $T_m = 90.3$  °C). The tendency is contrary to the tendency observed with crystallinity of polymers.

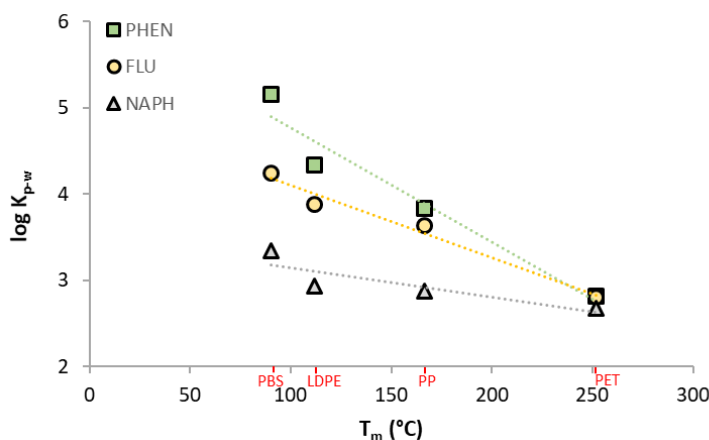


**Figure 22:** correlation between  $\log K_{p-w}$  and melting temperature ( $T_m$ ) of the tested polymer materials

NAPH = naphthalene, correlation of  $\log K_{p-w}$  of naphthalene and  $T_m$  of four polymers,  $R^2 = 0.741$ ;

FLU = fluorene, correlation of  $\log K_{p-w}$  of fluorene and  $T_m$  of four polymers  $R^2 = 0.975$ ;

PHEN = phenanthrene, correlation of  $\log K_{p-w}$  of phenanthrene and  $T_m$  of four polymers  $R^2 = 0.947$

Figure 22 shows correlation between  $\log K_{p-w}$  and melting points of sorbent polymer materials. This thesis found a clear negative correlation for all PAHs between  $\log K_{p-w}$  and  $T_m$ . The highest  $\log K_{p-w}$  values of naphthalene, fluorene and phenanthrene were determined with PBS, which exhibits the lowest melting temperature. Endo et al. (2005) suggested that  $T_m$  may affect the sorption ability of the sorbent. Here the results confirmed that the  $T_m$  of polymers does affect  $\log K_{p-w}$  of selected two-

to three-ring PAHs. Similar to the results for crystallinity, this thesis demonstrates a possibility of predicting  $\log K_{p-w}$  of the selected PAHs from the melting point of sorbent polymer materials using the following equations:

naphthalene:  $\log K_{p-w} = -3.35E-3 T_m (\text{°C}) + 3.48 (R^2 = 0.741)$  equations 24 (a)

fluorene:  $\log K_{p-w} = -8.37E-3 T_m (\text{°C}) + 4.94 (R^2 = 0.975)$  equations 24 (b)

phenanthrene:  $\log K_{p-w} = -1.33E-2 T_m (\text{°C}) + 6.09 (R^2 = 0.947)$  equations 24 (c)

Furthermore, a negative tendency of crystalline polymer values plotted against polymer  $T_m$  was found (Figure 23) and resulted in equation 25.

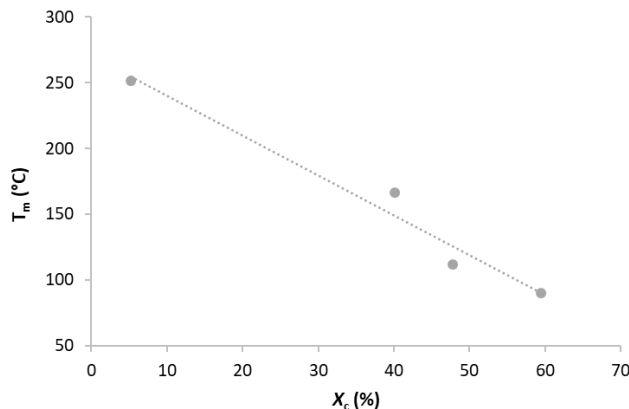


Figure 23: correlation of plastic properties  $T_m$  and  $X_c$

$$T_m = -3.03 X_c (\%) + 270.73 (R^2 = 0.97) \quad \text{equation 25}$$

### Summary

The results of the linear regressions of semi-crystalline plastic-water partition coefficients and polymer crystallinity as well as melting temperature of the tested polymers LDPE, PP, PBS and PET correlate well for 2- and 3-ring PAHs, resulting in an  $R^2$  between 0.76 - 0.99 and 0.74 - 0.98 respectively. However, glass transition temperature value did not correlate well with plastic-water partition coefficients. Furthermore, polymer crystallinity and melting temperature turned out to have a strong correlation in the investigated polymers. This was the first time thermodynamic polymer properties related to PAH plastic-water partition coefficients.

#### 6.4. Correlation of $\log K_{p-w}$ and physical polymer properties

Über et al. (2019) demonstrated for HDPE that the sorption of organic compounds depends on the molar volume and therefore on the density as well as the crystallinity of the polymer. However, the correlation of the partition coefficient and the density for HDPE was not directly applicable across different polymer types. As shown in Figure 24 the tested polymer materials resulted in a low coefficient of determination ( $R^2$ ), from 0.001 for NAPH < 0.053 for PHEN < 0.152 for FLN for linear correlation. These results underscored the thesis that several physicochemical properties affect the sorption behaviour of dissolved hydrophobic compounds on plastic materials.

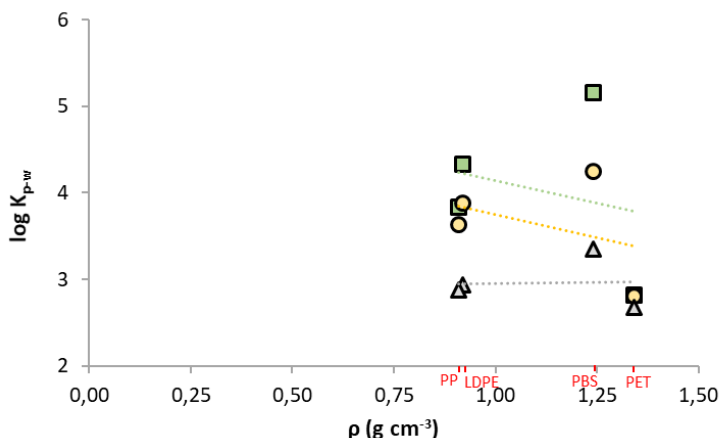
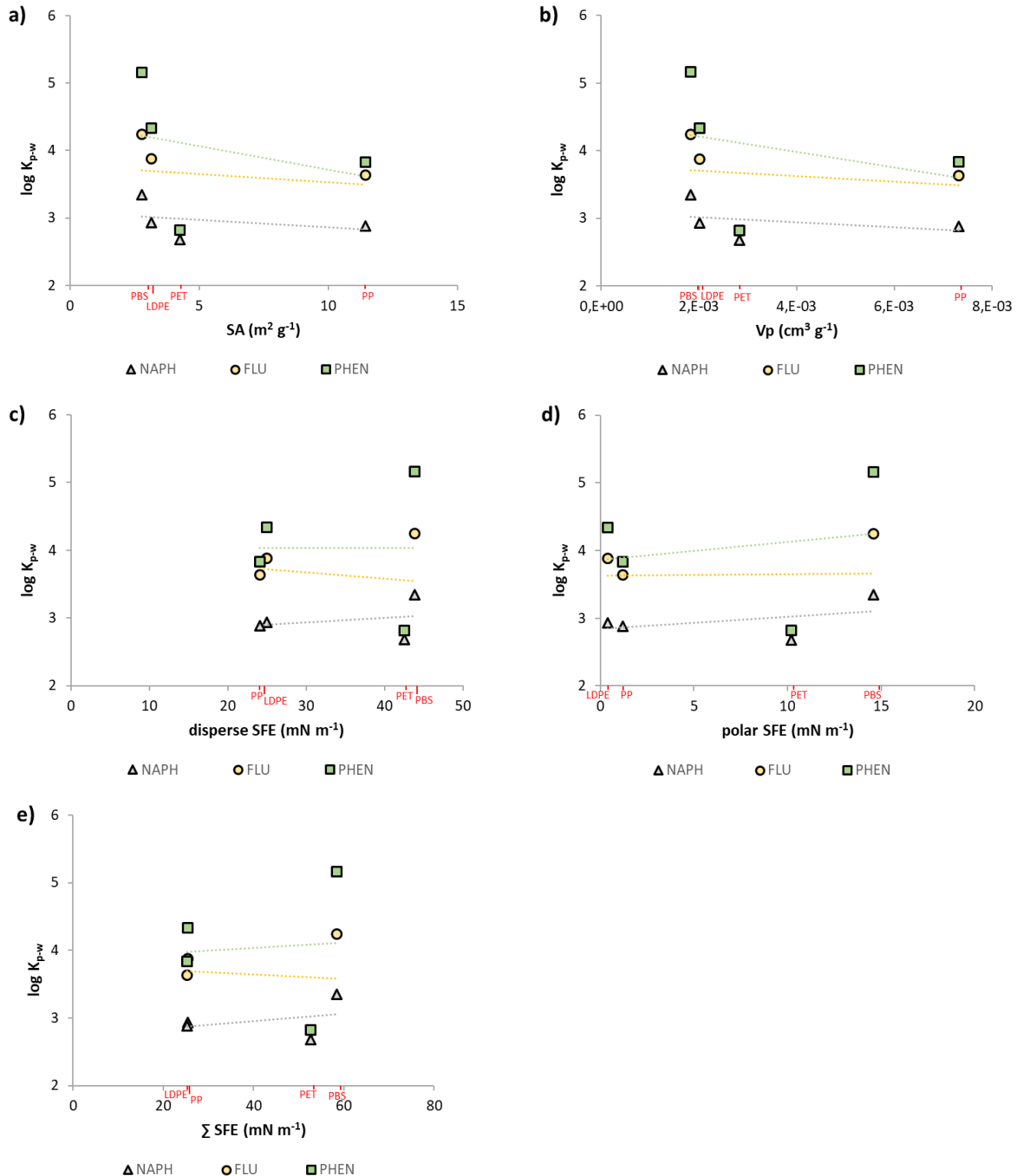


Figure 24: Correlation of density and  $\log K_{p-w}$

The surface area, pore volume, disperse and polar proportion of surface free energy (SFE), as well as the sum of disperse and polar surface free energy resulted in pure correlations. The coefficient of determination for surface area (SA) and pore volume (Vp) ranged from 0.03 to 0.10 and 0.03 to 0.11 respectively (Table A6.6). In addition, the  $R^2$  of disperse, polar and sum of disperse and polar surface free energy was between 3.20E-7 and 0.21 (Figure 25). However, the influence of physical polymer properties such as surface area and hydrophobicity assumed by Praveena and Aris (2020) could not be confirmed by the four different polymer materials of this thesis.



**Figure 25:** Linear regression of SA a), Vp b), disperse SFE c), polar SFE d) and sum of SFE e)

### Summary

The given results of linear regression of polymer density, surface area, pore volume, disperse/polar SFE as well as sum of SFE demonstrated inadequate accuracy for the deployed polymers, represented by a coefficient of determination between 3.20E-7 and 0.21.

## 7. Development of an equation to predict $\log K_{p-w}$

This chapter lays out how the equation for predicting polymer water partition coefficients based on physicochemical properties of PAHs and plastics is developed. The two methods used to develop the equation were 1) linear correlation consisting of the product of various combinations of plastic and PAH properties and 2) individual correlations of plastic and PAH properties. The results from the previous two chapters were used for this purpose.

In method 1, the physicochemical properties of PAHs and polymers as well as their reciprocals were multiplied together. The linear correlation started with the product of one PAH property and one plastic property and increased up to the product of two PAH properties and up to three plastic properties.

For method 2, an individual combination of polymer and PAH properties was chosen, which did not correspond to the linear approach in method 1. An evaluation of the developed equations from method 1 and 2 with the laboratory values from Chapter 4 was performed using the Dikbaş (2017) method. In the course of the evaluation of Dikbaş (2017), a range of accuracy was set to identify the equations with a high accuracy. Subsequently, fitting parameters were determined and incorporated into each individual equation. In the end, published regression models were compared to the best results from the equations of this thesis.

### 7.1. Polymer properties and PAH properties versus values of this thesis – method 1

To compare each equation of method 1 and 2 with the polymer-water partition coefficient of chapter 4, the results of each model and the polymer-water partition coefficient were presented in a matrix consisting of four rows and three columns (4 x 3). The four rows represent the plastic properties and the three columns represent the properties of the PAHs. Table 16 shows, for example, the results from the product of polymer density ( $\rho$ ) and  $\log K_{ow}$  of the PAHs of method 1 in a matrix. Furthermore, the results of chapter 4 are represented in a matrix in Table 17.

**Table 16:** Matrix (A) of polymer density and  $\log K_{ow}$  of PAHs

$\rho \text{ (g cm}^{-3}\text{)} * \log K_{ow} \text{ (-)}$		NAPH $\log K_{ow} \text{ (-)}$ 3.37	FLN $\log K_{ow} \text{ (-)}$ 4.18	PHEN $\log K_{ow} \text{ (-)}$ 4.46	$\bar{A}_m$
LDPE	$\rho \text{ (g cm}^{-3}\text{)}$	0.92	3.10	3.85	4.10
PP	$\rho \text{ (g cm}^{-3}\text{)}$	0.91	3.07	3.80	4.06
PBS	$\rho \text{ (g cm}^{-3}\text{)}$	1.24	4.18	5.18	5.53
PET	$\rho \text{ (g cm}^{-3}\text{)}$	1.34	4.52	5.60	5.98
$\bar{A}_n$		3.72	4.61	4.92	

**Table 17:** Matrix (B) of  $\log K_{p-w}$  from chapter 4

$\log K_{p-w} \text{ (L kg}^{-1}\text{)}$	NAPH	FLN	PHEN	$\bar{B}_m$
LDPE	2.93	3.88	4.33	3.72
PP	2.88	3.64	3.83	3.45
PBS	3.35	4.24	5.16	4.25
PET	2.68	2.81	2.82	2.77
$\bar{B}_n$	2.96	3.64	4.04	

According to Dikbaş' (2017) method, two identical matrices can be compared and two correlation coefficients can be calculated, which is represented by a horizontal ( $r_h$ ) and a vertical correlation coefficient ( $r_v$ ). The horizontal correlation coefficients ( $r_h$ ) and the vertical correlation coefficients ( $r_v$ ) were calculated according to equation 12 and equation 13, respectively, where  $\bar{A}_m$  and  $\bar{B}_m$  were the average of  $m^{\text{th}}$  row while  $\bar{A}_n$  and  $\bar{B}_n$  were the average of  $n^{\text{th}}$  column of matrix A and B.

In the following, an example calculation is carried out for  $r_v$  and  $r_h$  using matrix A from Table 16 and matrix B from Table 17 and the transformation in  $R_v^2$  and  $R_h^2$ .

For  $r_v$ , the differences between each individual column values and the corresponding column mean values ( $\bar{A}_n$ ) from matrix A are multiplied by the differences between the column values with identical positions and the corresponding column mean values ( $\bar{B}_n$ ) from matrix B, and summed up in the end. This resulting sum is divided by the square root of the summed squared differences of all individual column values and the corresponding column mean values ( $\bar{A}_n$ ) from matrix A, multiplied by the summed squared differences of all individual column values and the corresponding column mean values ( $\bar{B}_n$ ) from matrix B.

$$r_v = \frac{\sum_m \sum_n (A_{mn} - \bar{A})(B_{mn} - \bar{B})}{\sqrt{[\sum_m \sum_n (A_{mn} - \bar{A})^2][\sum_m \sum_n (B_{mn} - \bar{B})^2]}} = \frac{(3.10 - 3.72) * (2.93 - 2.96) + (3.07 - 3.72) * (2.88 - 2.96) + \dots}{\sqrt{[(3.10 - 3.72)^2 + (3.07 - 3.72)^2 + \dots] * [(2.93 - 2.96)^2 + (2.88 - 2.96)^2 + \dots]}} = -0.24$$

For  $r_h$ , the differences between each individual row values and the corresponding row mean values ( $\bar{A}_m$ ) from matrix A are multiplied by the differences between the row values with identical positions and the corresponding row mean values ( $\bar{B}_m$ ) from matrix B, and then added up. This sum is divided by the square root of the summed squared differences of all individual row values and the corresponding row mean values ( $\bar{A}_m$ ) from matrix A, multiplied by the summed squared differences of all individual row values and the corresponding row mean values ( $\bar{B}_m$ ) from matrix B.

$$r_h = \frac{\sum_m \sum_n (A_{mn} - \bar{A})(B_{mn} - \bar{B})}{\sqrt{[\sum_m \sum_n (A_{mn} - \bar{A})^2][\sum_m \sum_n (B_{mn} - \bar{B})^2]}} = \frac{(3.10 - 3.68) * (2.93 - 3.74) + (3.07 - 3.64) * (2.88 - 3.45) + \dots}{\sqrt{[(3.10 - 3.68)^2 + (3.07 - 3.64)^2 + \dots] * [(2.93 - 3.74)^2 + (2.88 - 3.45)^2 + \dots]}} = 0.81$$

In order to better compare the results, the  $r_v$  and the  $r_h$  values were squared, which resulted in coefficients of determination  $R_v^2$  and  $R_h^2$ , respectively.

$$\rightarrow R_v^2 = r_v^2 = -0.24^2 = 0.06$$

$$\rightarrow R_h^2 = r_h^2 = 0.81^2 = 0.66$$

In the example of matrix A from Table 16 and matrix B from Table 17, the calculated  $R_v^2$  and  $R_h^2$  values are 0.06 and 0.66.

### 7.1.1. Calculation of the equations of method 1

First, each plastic property was multiplied with each PAH property as well as their reciprocal values (Table 18) and examined for high accuracy with the  $\log K_{p-w}$  values derived from this study according to the matrix comparison of chapter 7.1. In Table 18 the combinations of individual PAH properties ( $\log K_{ow}$ , MW,  $\log C_w^{sat}$ ,  $\log K_{hdw}$ ) as well as the plastic properties ( $\rho$ ,  $d_{50}$ ,  $T_m$ ,  $T_g$ ,  $X_c$ , SA, Vp,  $\sum SFE$ ) were included as well as  $R_v^2$  and  $R_h^2$  were shown.

**Table 18:**  $R_v^2$  and  $R_h^2$  calculation of the matrix of one PAH and one plastic properties with the  $\log K_{p-w}$  matrix

plastic properties	PAH properties															
	$\log K_{ow}$ (-)		$\log K_{ow}^{-1}$ (-)		MW (g mol <sup>-1</sup> )		MW <sup>-1</sup> (mol g <sup>-1</sup> )		$\log C_w^{sat\ -1}$ (mol m <sup>-3</sup> )		$\log C_w^{sat\ -1}$ (m <sup>3</sup> mol <sup>-1</sup> )		$\log K_{hdw}^{-2}$ (-)		$\log K_{hdw}^{-1}$ (-)	
	$R_v^2$	$R_h^2$	$R_v^2$	$R_h^2$	$R_v^2$	$R_h^2$	$R_v^2$	$R_h^2$	$R_v^2$	$R_h^2$	$R_v^2$	$R_h^2$	$R_v^2$	$R_h^2$	$R_v^2$	$R_h^2$
$\rho^{*3}$ (g cm <sup>-3</sup> )	0.06	0.66	0.04	0.65	0.06	0.66	0.04	0.64	0.07	0.66	0.00	0.58	0.06	0.58	0.04	0.65
$\rho^{-1}$ (cm <sup>3</sup> g <sup>-1</sup> )	0.04	0.76	0.02	0.75	0.04	0.76	0.02	0.74	0.05	0.76	0.00	0.68	0.04	0.68	0.02	0.75
$d_{50}^{*4}$ ( $\mu$ m)	0.45	0.64	0.35	0.63	0.45	0.63	0.34	0.62	0.51	0.63	0.01	0.56	0.44	0.56	0.34	0.63
$d_{50}^{-1}$ ( $\mu$ m <sup>-1</sup> )	0.37	0.80	0.28	0.79	0.38	0.80	0.28	0.78	0.42	0.80	0.01	0.71	0.37	0.71	0.28	0.79
$T_m^{*5}$ (K)	0.84	0.61	0.67	0.60	0.85	0.61	0.65	0.60	0.90	0.61	0.05	0.54	0.82	0.54	0.66	0.60
$T_m^{-1}$ (K <sup>-1</sup> )	0.85	0.83	0.68	0.82	0.86	0.83	0.66	0.81	0.90	0.83	0.05	0.73	0.83	0.73	0.67	0.82
$T_g^{*6}$ (K)	0.30	0.48	0.23	0.47	0.30	0.47	0.22	0.47	0.34	0.47	0.01	0.42	0.29	0.42	0.23	0.47
$T_g^{-1}$ (K <sup>-1</sup> )	0.11	0.74	0.08	0.73	0.11	0.74	0.08	0.73	0.13	0.74	0.00	0.66	0.11	0.66	0.08	0.73
$X_c^{*7}$ (%)	0.84	0.95	0.67	0.94	0.85	0.95	0.65	0.93	0.90	0.95	0.05	0.83	0.83	0.83	0.66	0.93
$X_c^{-1}$ (% <sup>-1</sup> )	0.66	0.05	0.52	0.05	0.67	0.05	0.51	0.05	0.72	0.05	0.03	0.05	0.65	0.05	0.51	0.05
SA <sup>*8</sup> (m <sup>2</sup> g <sup>-1</sup> )	0.06	0.43	0.05	0.43	0.06	0.43	0.05	0.43	0.06	0.43	0.01	0.40	0.06	0.40	0.05	0.43
SA <sup>-1</sup> (g m <sup>-2</sup> )	0.24	0.78	0.20	0.76	0.24	0.77	0.19	0.75	0.25	0.77	0.02	0.67	0.24	0.67	0.19	0.76
Vp <sup>*9</sup> (cm <sup>3</sup> g <sup>-1</sup> )	0.06	0.43	0.05	0.43	0.06	0.43	0.05	0.43	0.06	0.43	0.01	0.40	0.06	0.40	0.05	0.43
Vp <sup>-1</sup> (g cm <sup>-3</sup> )	0.25	0.78	0.20	0.77	0.25	0.78	0.20	0.76	0.26	0.78	0.02	0.68	0.25	0.67	0.20	0.77
$\Sigma SFE^{*10}$ (mN m <sup>-1</sup> )	0.00	0.62	0.00	0.61	0.00	0.61	0.00	0.60	0.00	0.61	0.01	0.53	0.00	0.53	0.00	0.60
$\Sigma SFE^{-1}$ (m Nm <sup>-1</sup> )	0.00	0.69	0.00	0.68	0.00	0.69	0.00	0.68	0.00	0.69	0.00	0.62	0.00	0.62	0.00	0.68

\*<sup>1</sup>  $\log C_w^{sat}$ : aqueous solubility of PAHs according to Ma et al. et al. (2010); \*<sup>2</sup>  $\log K_{hdw}$ : hexadecane-water partition coefficient of PAHs according to Schwarzenbach et al. (2003); \*<sup>3</sup>  $\rho$ : plastic density; \*<sup>4</sup>  $d_{50}$ : median diameter of plastics; \*<sup>5</sup>  $T_m$ : melting temperature of plastics; \*<sup>6</sup>  $T_g$ : glass transition temperature of plastics; \*<sup>7</sup>  $X_c$ : crystallinity of plastics; \*<sup>8</sup> SA: surface area; \*<sup>9</sup> Vp: pore volume; \*<sup>10</sup>  $\sum SFE$ : sum of polar and disperse surface free energy of plastics

According to the two-dimensional calculation of  $R_v^2$  and  $R_h^2$ , not only the accuracies of the plastic rows of the horizontal values but also the accuracies of the PAH columns of the vertical values were considered.

In many cases, the  $R_v^2$  values were found to be significantly smaller (more than 20x smaller) than the corresponding  $R_h^2$  value. An example of this is the  $R_v^2$  value of the product of plastic density and  $\log K_{ow}$  ( $R_v^2 = 0.02$ ) to the corresponding  $R_h^2$  value ( $R_h^2 = 0.76$ ), which was 38 times smaller and thus exhibited a high inaccuracy in relation to the  $R_v^2$ -value. Furthermore, the product of  $\log C_w^{sat\ -1}$  and the plastic properties of  $R_v^2$  resulted in values smaller than 0.05. In contrast, the results of  $T_m$  and  $T_m^{-1}$  as well as  $X_c$  showed high accuracies for both  $R_v^2$ -values and  $R_h^2$ -values for all PAH properties except  $\log C_w^{sat}$  (Table 18). Further results of the product of polymer properties and PAH properties were listed in Table 19 and Table 20. Table 19 shows the results of the product of single physicochemical properties of PAHs and two polymer properties with density as fixed parameter. Furthermore, Table 20 shows the results of the product of two physicochemical properties of PAHs  $\log K_{ow}$  and MW and three polymer properties with  $\rho$  and  $X_c$  of the plastics as fixed parameter.

**Table 19:**  $R_v^2$  and  $R_h^2$  calculation of the matrix of one PAH and two plastic properties ( $\rho$  as fixed parameter) with the log  $K_{p-w}$  matrix

plastic property product		PAH properties															
1 <sup>st</sup> fixed parameter	2 <sup>nd</sup> variable parameter	log $K_{ow}$ (-)		log $K_{ow}^{-1}$ (-)		MW (g mol <sup>-1</sup> )		MW <sup>1</sup> (mol g <sup>-1</sup> )		log $C_w^{sat}$ (mol m <sup>-3</sup> )		log $C_w^{sat-1}$ (m <sup>3</sup> mol <sup>-1</sup> )		log $K_{kdw}$ (-)		log $K_{kdw}^{-1}$ (-)	
		$R_v^2$	$R_h^2$	$R_v^2$	$R_h^2$	$R_v^2$	$R_h^2$	$R_v^2$	$R_h^2$	$R_v^2$	$R_h^2$	$R_v^2$	$R_h^2$	$R_v^2$	$R_h^2$	$R_v^2$	$R_h^2$
	$d_{50}$ ( $\mu\text{m}$ )	0.23	0.54	0.18	0.54	0.24	0.54	0.17	0.53	0.27	0.54	0.00	0.48	0.23	0.48	0.17	0.53
	$d_{50}^{-1}$ ( $\mu\text{m}^{-1}$ )	0.15	0.79	0.11	0.78	0.15	0.79	0.10	0.78	0.17	0.79	0.00	0.71	0.14	0.71	0.11	0.78
	$T_m$ (K)	0.47	0.52	0.36	0.51	0.47	0.52	0.35	0.51	0.52	0.52	0.02	0.46	0.46	0.46	0.36	0.51
	$T_m^{-1}$ (K <sup>-1</sup> )	0.30	0.78	0.25	0.77	0.30	0.78	0.25	0.76	0.29	0.78	0.04	0.68	0.29	0.68	0.25	0.76
	$T_g$ (K)	0.39	0.42	0.30	0.42	0.39	0.42	0.29	0.41	0.44	0.42	0.01	0.37	0.38	0.37	0.29	0.42
	$T_g^{-1}$ (K <sup>-1</sup> )	0.40	0.83	0.32	0.82	0.41	0.83	0.31	0.81	0.44	0.83	0.02	0.73	0.40	0.73	0.31	0.82
$\rho$ (g cm <sup>-3</sup> )	$X_c$ (%) *	0.87	0.94	0.71	0.92	0.88	0.93	0.69	0.91	0.91	0.93	0.06	0.81	0.86	0.81	0.70	0.92
	$X_c^{-1}$ (%) <sup>-1</sup>	0.63	0.04	0.50	0.04	0.64	0.04	0.49	0.04	0.69	0.04	0.03	0.04	0.63	0.04	0.49	0.04
	SA (m <sup>2</sup> g <sup>-1</sup> )	0.14	0.45	0.11	0.44	0.14	0.45	0.11	0.44	0.15	0.45	0.01	0.41	0.14	0.41	0.11	0.44
	SA <sup>-1</sup> (g m <sup>-2</sup> )	0.14	0.70	0.11	0.69	0.14	0.70	0.11	0.68	0.13	0.70	0.02	0.60	0.13	0.60	0.11	0.69
	Vp (cm <sup>3</sup> g <sup>-1</sup> )	0.15	0.45	0.12	0.44	0.16	0.45	0.12	0.44	0.16	0.45	0.01	0.41	0.15	0.41	0.12	0.44
	Vp <sup>-1</sup> (g cm <sup>-3</sup> )	0.15	0.71	0.12	0.70	0.15	0.71	0.12	0.69	0.15	0.71	0.02	0.61	0.15	0.61	0.12	0.70
	$\sum SFE$ (mN m <sup>-1</sup> )	0.00	0.52	0.00	0.51	0.00	0.52	0.00	0.50	0.01	0.52	0.00	0.45	0.00	0.44	0.00	0.51
	$\sum SFE^{-1}$ (m Nm <sup>-1</sup> )	0.02	0.70	0.02	0.69	0.02	0.70	0.02	0.69	0.01	0.70	0.01	0.63	0.02	0.63	0.02	0.69

**Table 20:**  $R_v^2$  and  $R_h^2$  calculation of the matrix of one/two PAH and three plastic properties ( $X_c * \rho$  as fixed parameters) with the log  $K_{p-w}$  matrix

plastic property product		PAH properties											
1 <sup>st</sup> * 2 <sup>nd</sup> fixed parameters	3 <sup>rd</sup> variable parameter	log $K_{ow}$ (-)		MW (g mol <sup>-1</sup> )		log $K_{ow} * MW$ (g mol <sup>-1</sup> )		MW * log $K_{ow}^{-1}$ (g mol <sup>-1</sup> )		log $K_{ow} * MW^1$ (mol g <sup>-1</sup> )		(log $K_{ow} * MW$ ) <sup>-1</sup> (mol g <sup>-1</sup> )	
		$R_v^2$	$R_h^2$	$R_v^2$	$R_h^2$	$R_v^2$	$R_h^2$	$R_v^2$	$R_h^2$	$R_v^2$	$R_h^2$	$R_v^2$	$R_h^2$
	$d_{50}$ ( $\mu\text{m}$ )	0.83	0.92	0.84	0.91	0.88	0.93	0.78	0.85	0.75	0.85	0.56	0.89
	$d_{50}^{-1}$ ( $\mu\text{m}^{-1}$ )	0.88	0.95	0.89	0.95	0.94	0.96	0.82	0.88	0.79	0.88	0.58	0.92
	$T_m$ (K)	0.86	0.94	0.87	0.94	0.92	0.95	0.81	0.87	0.78	0.87	0.57	0.91
	$T_m^{-1}$ (K <sup>-1</sup> )	0.86	0.93	0.87	0.92	0.92	0.94	0.81	0.86	0.78	0.85	0.57	0.89
	$T_g$ (K)	0.72	0.88	0.73	0.88	0.76	0.89	0.68	0.81	0.65	0.81	0.49	0.85
$X_c$ (%) *	$T_g^{-1}$ (K <sup>-1</sup> )	0.81	0.94	0.82	0.94	0.87	0.95	0.76	0.87	0.73	0.87	0.53	0.91
$\rho$ (g cm <sup>-3</sup> )	SA (m <sup>2</sup> g <sup>-1</sup> )	0.11	0.63	0.11	0.63	0.11	0.64	0.10	0.60	0.09	0.60	0.07	0.62
	SA <sup>-1</sup> (g m <sup>-2</sup> )	0.73	0.84	0.74	0.83	0.78	0.84	0.69	0.76	0.66	0.76	0.49	0.80
	Vp (cm <sup>3</sup> g <sup>-1</sup> )	0.11	0.64	0.11	0.64	0.12	0.64	0.10	0.61	0.10	0.60	0.07	0.62
	Vp <sup>-1</sup> (g cm <sup>-3</sup> )	0.74	0.84	0.75	0.83	0.78	0.85	0.69	0.77	0.67	0.76	0.49	0.80
	$\sum SFE$ (mN m <sup>-1</sup> )	0.65	0.77	0.66	0.76	0.69	0.78	0.61	0.70	0.59	0.70	0.45	0.73
	$\sum SFE^{-1}$ (m Nm <sup>-1</sup> )	0.47	0.88	0.48	0.88	0.51	0.89	0.44	0.83	0.42	0.83	0.29	0.86

An accuracy criterion for the results was established to filter out the combinations of plastic and PAH properties that achieved a high correlation with the laboratory log  $K_{p-w}$  values. For this purpose, the accuracy criterion was set at greater than or equal to 0.95 for the  $r_v$  and  $r_h$  results of the original equation. Accordingly, the accuracy criterion for  $R_v^2$  and  $R_h^2$  was 0.90 and has been marked in green in Table 19 as well as Table 20. However only the polymer and PAH products from method 1 and 2 whose  $R_v^2$  and  $R_h^2$  were greater than 0.90, were used to determine the regression models. All other combination results of method 1 are listed in the appendix (Table A7.1 - A7.105).

In Table 18, no combination had an accuracy of at least 0.90 for  $R_v^2$  and  $R_h^2$ . However, in Table 19, the product of the two polymer properties density and crystallinity with the PAH property aqueous solubility achieved this accuracy for both  $R_v^2$  and  $R_h^2$ . Therefore, the parameter calculation was performed for this combination. In Table 20, the accuracy criterion was also met for the following products: i) crystallinity, density and  $d_{50}^{-1}$  of polymer properties with log  $K_{ow}$  and MW of PAH properties; ii) crystallinity, density and  $T_m$  of polymer properties with log  $K_{ow}$  and MW of PAH properties.

properties; and iii) crystallinity, density and  $T_m^{-1}$  of polymer properties with  $\log K_{ow}$  and MW of PAH properties. The parameters were also calculated for each of these products. Following these results, the coefficients of the equations with high accuracy for both  $R_v^2$  and  $R_h^2$  must be determined.

### 7.1.2. Selection of equations from method 1

In total, 48 equations were developed through method 1 in fulfilment with the accuracy criteria for both  $R_v^2$  and  $R_h^2$ . These results were obtained from the product of a minimum of two polymer properties and one PAH property, and a maximum of three polymer properties and two PAH properties. An accuracy of  $> 0.90$  for both  $R_v^2$  and  $R_h^2$  was not achieved for the product of one polymer property and one PAH property.

Notably, the plastic property of crystallinity is involved in every one of the plastic-PAH product combinations of the equations listed below (equations 26 – 73). This indicates that crystallinity is an important criterion for the sorption capacity of plastics, as it provides information about the structural composition of plastics.

#### Equations based on method 1

$\log K_{p-w} = -1.90 * \log C_w^{sat PAH} * X_{c_p} * \rho_p + 2.90$	equation 26
$\log K_{p-w} = -685.00 * \log C_w^{sat PAH} * X_{c_p} * T_{m_p}^{-1} + 2.93$	equation 27
$\log K_{p-w} = 6.37E-3 * \log K_{ow PAH} * MW_{PAH} * X_{c_p} * \rho_p + 1.98$	equation 28
$\log K_{p-w} = 2.26 * \log K_{ow PAH} * MW_{PAH} * X_{c_p} * T_{m_p}^{-1} + 1.98$	equation 29
$\log K_{p-w} = 0.18 * \log K_{ow PAH} * \log K_{hdw PAH} * X_{c_p} * \rho_p + 2.28$	equation 30
$\log K_{p-w} = 68.90 * \log K_{ow PAH} * \log K_{hdw PAH} * X_{c_p} * T_{m_p}^{-1} + 2.36$	equation 31
$\log K_{p-w} = -0.26 * \log K_{ow PAH} * \log C_w^{sat PAH} * X_{c_p} * \rho_p + 2.90$	equation 32
$\log K_{p-w} = -11.50 * \log C_w^{sat PAH} * \log K_{ow PAH}^{-1} * X_{c_p} * \rho_p + 2.90$	equation 33
$\log K_{p-w} = -93.37 * \log C_w^{sat PAH} * \log K_{ow PAH} * X_{c_p} * T_{m_p}^{-1} + 2.90$	equation 34
$\log K_{p-w} = -4562.02 * \log C_w^{sat PAH} * \log K_{ow PAH}^{-1} * X_{c_p} * T_{m_p}^{-1} + 2.90$	equation 35
$\log K_{p-w} = -523.44 * \log C_w^{sat PAH} * MW_{PAH}^{-1} * X_{c_p} * \rho_p + 2.90$	equation 36
$\log K_{p-w} = -1.98E+5 * \log C_w^{sat PAH} * MW_{PAH}^{-1} * X_{c_p} * T_{m_p}^{-1} + 2.90$	equation 37
$\log K_{p-w} = -0.25 * \log C_w^{sat PAH} * \log K_{hdw PAH} * X_{c_p} * \rho_p + 2.90$	equation 38
$\log K_{p-w} = -15.20 * \log C_w^{sat PAH} * \log K_{hdw PAH}^{-1} * X_{c_p} * \rho_p + 2.90$	equation 39
$\log K_{p-w} = -89.50 * \log C_w^{sat PAH} * \log K_{hdw PAH} * X_{c_p} * T_{m_p}^{-1} + 2.90$	equation 40
$\log K_{p-w} = -5521.82 * \log C_w^{sat PAH} * \log K_{hdw PAH}^{-1} * X_{c_p} * T_{m_p}^{-1} + 2.90$	equation 41
$\log K_{p-w} = 2.90E-3 * \log K_{ow PAH} * MW_{PAH} * X_{c_p} * \rho_p * d_{50 p}^{-1} + 1.98$	equation 42
$\log K_{p-w} = 0.11 * \log K_{ow PAH} * \log K_{hdw PAH} * X_{c_p} * \rho_p * d_{50 p}^{-1} + 1.88$	equation 43
$\log K_{p-w} = -0.87 * \log C_w^{sat PAH} * X_{c_p} * \rho_p * d_{50 p}^{-1} + 2.95$	equation 44
$\log K_{p-w} = -0.15 * \log K_{ow PAH} * \log C_w^{sat PAH} * X_{c_p} * \rho_p * d_{50 p}^{-1} + 2.95$	equation 45

$\log K_{p-w} = 8.89E-3 * \log K_{ow PAH} * \log C_w^{sat PAH^{-1}} * X_{c,p} * \rho_p * d_{50,p}^{-1} + 5.37$	equation 46
$\log K_{p-w} = 1.00E+6 * MW_{PAH} * \log C_w^{sat PAH^{-1}} * X_{c,p} * \rho_p * d_{50,p}^{-1} + 5.25$	equation 47
$\log K_{p-w} = -0.12 * \log K_{hdw PAH} * \log C_w^{sat PAH^{-1}} * X_{c,p} * \rho_p * d_{50,p}^{-1} + 3.14$	equation 48
$\log K_{p-w} = 4.96 * \log K_{hdw PAH} * \log C_w^{sat PAH^{-1}} * X_{c,p} * d_{50,p} * T_{m,p} + 1.98$	equation 49
$\log K_{p-w} = 183.99 * \log K_{ow PAH} * \log K_{hdw PAH} * X_{c,p} * d_{50,p} * T_{m,p}^{-1} + 1.88$	equation 50
$\log K_{p-w} = -1510.00 * \log C_w^{sat PAH^{-1}} * X_{c,p} * d_{50,p} * T_{m,p}^{-1} + 2.92$	equation 51
$\log K_{p-w} = -235.00 * \log K_{ow PAH} * \log C_w^{sat PAH^{-1}} * X_{c,p} * d_{50,p} * T_{m,p}^{-1} + 2.99$	equation 52
$\log K_{p-w} = 0.50E-5 * MW_{PAH} * \log C_w^{sat PAH^{-1}} * X_{c,p} * \rho_p * d_{50,p}^{-1} + 5.43$	equation 53
$\log K_{p-w} = 1.67E-5 * \log K_{ow PAH} * MW_{PAH} * X_{c,p} * \rho_p * T_{m,p} + 1.98$	equation 54
$\log K_{p-w} = 6.14E-4 * \log K_{ow PAH} * \log K_{hdw PAH} * X_{c,p} * \rho_p * T_{m,p} + 1.88$	equation 55
$\log K_{p-w} = 0.50E-2 * \log C_w^{sat PAH^{-1}} * X_{c,p} * \rho_p * T_{m,p} + 2.93$	equation 56
$\log K_{p-w} = -7.54E-4 * \log K_{ow PAH} * \log C_w^{sat PAH^{-1}} * X_{c,p} * \rho_p * T_{m,p} + 2.92$	equation 57
$\log K_{p-w} = -0.70E-3 * \log K_{hdw PAH} * \log C_w^{sat PAH^{-1}} * X_{c,p} * \rho_p * T_{m,p} + 2.90$	equation 58
$\log K_{p-w} = 1.26E-4 * \log K_{ow PAH} * MW_{PAH} * X_{c,p} * \rho_p * T_{m,p}^{-1} + 9.56$	equation 59
$\log K_{p-w} = 91.00 * \log K_{ow PAH} * \log K_{hdw PAH} * X_{c,p} * \rho_p * T_{m,p}^{-1} + 1.88$	equation 60
$\log K_{p-w} = 106.42 * \log K_{ow PAH} * \log C_w^{sat PAH^{-1}} * X_{c,p} * \rho_p * T_{m,p}^{-1} + 3.32$	equation 61
$\log K_{p-w} = 0.50E-5 * \log K_{ow PAH} * \log C_w^{sat PAH^{-1}} * X_{c,p} * \rho_p * T_{m,p}^{-1} + 5.23$	equation 62
$\log K_{p-w} = -89.00 * \log K_{hdw PAH} * \log C_w^{sat PAH^{-1}} * X_{c,p} * \rho_p * T_{m,p}^{-1} + 3.43$	equation 63
$\log K_{p-w} = 0.82E-2 * \log K_{hdw PAH} * \log C_w^{sat PAH^{-1}} * X_{c,p} * \rho_p * d_{50,p}^{-1} + 5.38$	equation 64
$\log K_{p-w} = 15.19 * \log K_{ow PAH} * \log C_w^{sat PAH^{-1}} * X_{c,p} * d_{50,p} * T_{m,p}^{-1} + 5.37$	equation 65
$\log K_{p-w} = 0.40 * MW_{PAH} * \log C_w^{sat PAH^{-1}} * X_{c,p} * d_{50,p} * T_{m,p}^{-1} + 5.38$	equation 66
$\log K_{p-w} = 0.11 * \log K_{hdw PAH} * \log C_w^{sat PAH^{-1}} * X_{c,p} * d_{50,p} * T_{m,p}^{-1} + 3.43$	equation 67
$\log K_{p-w} = 71.41 * \log K_{ow PAH} * MW_{PAH} * X_{c,p} * V_{p,p} * \sum SFE_{p^{-1}} + 2.10$	equation 68
$\log K_{p-w} = 2641.17 * \log K_{ow PAH} * \log K_{hdw PAH} * X_{c,p} * V_{p,p} * \sum SFE_{p^{-1}} + 2.01$	equation 69
$\log K_{p-w} = 2.35E+4 * \log C_w^{sat PAH^{-1}} * X_{c,p} * V_{p,p} * \sum SFE_{p^{-1}} + 2.93$	equation 70
$\log K_{p-w} = 3500.00 * \log K_{ow PAH} * \log C_w^{sat PAH^{-1}} * X_{c,p} * V_{p,p} * SFE_{p^{-1}} + 2.93$	equation 71
$\log K_{p-w} = -1.57E+5 * \log K_{ow PAH} * \log C_w^{sat PAH^{-1}} * X_{c,p} * V_{p,p} * \sum SFE_{p^{-1}} + 2.93$	equation 72
$\log K_{p-w} = -3045.00 * \log K_{hdw PAH} * \log C_w^{sat PAH^{-1}} * X_{c,p} * V_{p,p} * \sum SFE_{p^{-1}} + 2.94$	equation 73

where  $\log K_{ow PAH}$ ,  $MW_{PAH}$ ,  $\log C_w^{sat PAH}$ ,  $\log K_{hdw PAH}$  represented the properties of PAHs and crystallinity ( $X_{c,p}$ ), density ( $\rho_p$ ), melting temperature ( $T_{m,p}$ ), particle size distribution of 50 % ( $d_{50,p}$ ), pore volume ( $V_{p,p}$ ), and sum of surface free energy ( $\sum SFE_p$ ) represented the polymer properties.

The determination of the coefficients for equations 26 to 73 was done by means of the Excel Add-Ins Solver. Here, the 48 selected products of the plastic and PAH properties were compared with the  $\log K_{Fr}$  values derived from the laboratory experiments and the coefficients were calculated.

## 7.2. Polymer properties and PAH properties versus values of this thesis – method 2

For method 2, a free approach was chosen, which was first set up on the basis of different combinations of the plastic properties and added with an adjustment of the PAH properties. The basic structure of the formula for method 2 is shown in equation 74.

$$\log K_{p-w} = (a * \text{properties}_{PAH} + b) * \text{properties}_p + c \quad \text{equation 74}$$

The equation was adjusted the three coefficients “a”, “b” and “c” shown in equation 74. These were determined by the Excel Add-in Solver. The results of the equations from method 2 were evaluated analogously to the results of method 1 using the two-dimensional method of Dikbaş (2017). In the following, only the three equations from method 2 whose results achieved a minimum discrepancy of 0.90 for both  $R_v^2$  and  $R_h^2$  when using  $\log K_{p-w}$  values from the laboratory experiments are represented. Table 21 details the equations, as well as the exact accuracy of  $R_v^2$  and  $R_h^2$  corresponding to each equation:

**Table 21:** Equations derived through method 2

equation	$R_v^2$	$R_h^2$	
$\log K_{p-w} = (-1.85 * \log C_w^{\text{sat}}_{PAH} + 1.00) * X_{c,p} * \rho_p + 2.50$	0,95	0,93	equation 75
$\log K_{p-w} = (60 * MW_{PAH} - 6.75) * X_{c,p} * \rho_p + 2.50$	0,95	0,93	equation 76
$\log K_{p-w} = (6.14 * \log K_{ow,PAH} * MW_{PAH} - 1.00) * X_{c,p} * \rho_p + 2.50$	0,95	0,95	equation 77

where aqueous solubility ( $\log C_w^{\text{sat}}_{PAH}$ ),  $\log K_{ow,PAH}$  and molar weight  $MW_{PAH}$  were PAH properties, while crystallinity ( $X_{c,p}$ ) and density ( $\rho_p$ ) were polymer properties. The three equations based on the polymer properties  $X_{c,p}$  and  $\rho_p$  and the intercept 2.5 with the PAH properties  $\log C_w^{\text{sat}}_{PAH}$ ,  $\log K_{ow,PAH}$  and  $\log K_{ow,PAH}$  times  $MW_{PAH}$  resulted in the required accuracy. From the results, it seems equation 77 has the comparatively highest accuracy. However, the following chapter will determine whether this result can be confirmed after evaluation and comparison with literature values.

### 7.3. Evaluating the final equation from method 1 and 2

The goal of this chapter is to identify a final equation from equations 26 - 73 from method 1 and 75 - 77 from method 2. For this purpose, equations 26 - 73 and 75 - 77 are compared with an already published equation as a reference equation. The final equation should achieve an equivalent or higher accuracy when compared to the selected reference equation.

For example, Lohmann (2012) determined correlations of the different PAH properties octanol-water partition coefficient ( $\log K_{ow}$ ), molar weight (MW), aqueous solubility ( $\log C_w^{sat}$ ), hexadecane-water partition coefficient ( $\log K_{hdw}$ ) with  $n = 65$  published  $\log K_{LDPE-w}$  values. This published  $\log K_{LDPE-w}$  values were determined by Booij et al. (2003), Adams et al. (2007), Cornelissen et al. (2008), Fernandez et al. (2009), Smedes et al. (2009), Perron et al. (2009) and Hale et al. (2010). As a result, from Lohmann (2012), aqueous solubility ( $\log C_w^{sat}$ ) published by Ma et al. (2010) was best correlated with the published data shown by equation 78.

$$\log K_{PE-w} = -0.85 (\pm 0.023) * \log C_w^{sat} + 2.85 (\pm 0.071) \quad \text{equation 78}$$

While Lohmann (2012) was the only study to establish equations for PAH properties and plastic-water partition coefficients generated by multiple studies for LDPE, equations 26 - 73 and 75 - 77 can only be compared to equation 78 as the reference equation. Extensive published studies for PP, PBS and PET polymer type were still pending and could not be compared in this thesis.

To assess the accuracy of equations 26 - 73 and 75 - 77 against the reference equation by Lohmann (2012), the root mean square error of  $n = 100$  published  $\log K_{LDPE-w}$ -values (Table A7.106) with similar experimental settings was calculated for each of these equations (Table A7.107). The equation of RMSE is as follows:

$$RMSE = \sqrt{\sum_{i=1}^n \frac{(\hat{y}_i - y_i)^2}{n}} \quad \text{equation 79}$$

where  $\hat{y}_i$  are the predicted values for properties  $i$  of an equation-dependent variable  $y_i$  and  $n$  corresponds to the number of  $\log K_{LDPE-w}$  values. The RMSE is the absolute error indicator and describes how much a prediction deviates on average from the actual data. The smaller the RMSE, the smaller the deviation and the greater the accuracy to the actual  $n = 100$  published  $\log K_{LDPE-w}$ .

The aim of the RMSE comparison was to obtain one final equation from equations 26 - 73 and 75 - 77 with a higher accuracy than the reference equation of Lohmann (2012). The following table listed all the equations which had a higher accuracy than the reference equation of Lohmann (2012).

**Table 22:** RMSE calculation of the selected equations of method 1 and 2

	selected equations of method 1 and 2		RMSE
Ref. Lohmann (2012)	$\log K_{PE-w} = -0.85 (\pm 0.023) * \log C_w^{sat} + 2.85 (\pm 0.071)$	equation 78	0.3097
	$\log K_{p-w} = -1.90 * \log C_w^{sat}_{PAH} * X_{c,p} * \rho_p + 2.90$	equation 26	0.3026
	$\log K_{p-w} = -685.00 * \log C_w^{sat}_{PAH} * X_{c,p} * T_{mp}^{-1} + 2.93$	equation 27	0.2964
method 1	$\log K_{p-w} = -0.87 * \log C_w^{sat}_{PAH} * X_{c,p} * \rho_p * d_{50,p}^{-1} + 2.95$	equation 44	0.2952
	$\log K_{p-w} = -1510.00 * \log C_w^{sat}_{PAH} * X_{c,p} * d_{50,p} * T_{mp}^{-1} + 2.92$	equation 51	0.2968
	$\log K_{p-w} = 0.50 * 10E-2 * \log C_w^{sat}_{PAH} * X_{c,p} * \rho_p * T_{mp} + 2.93$	equation 56	0.2964
method 2	$\log K_{p-w} = (-1.85 * \log C_w^{sat}_{PAH} + 1.00) * X_{c,p} * \rho_p + 2.50$	equation 75	0.3079
	$\log K_{p-w} = (60 * MW_{PAH} - 6.75) * X_{c,p} * \rho_p + 2.50$	equation 76	0.3092

The equations 26, 27, 44, 51, 56, 75 and 76 listed in Table 22 resulted in lower RMSE than the reference equation of Lohmann (2012). This shows that methods 1 and 2 yield suitable equations that satisfy the accuracy criterion. In the selected equations in Table 22 from method 1 as well as equation 75, it stands out that the PAH property aqueous solubility ( $\log C_w^{sat}$ ) was included in each equation in addition to the plastic property crystallinity ( $X_c$ ). This finding coincided with the equation determined by Lohmann (2012), which was also based on the PAH property  $\log C_w^{sat}$ .

Each of the seven equations resulted in a higher accuracy than the reference equation 78 with a RMSE ranged from 0.2952 - 0.3092, compared to a RMSE of 0.3097 for the reference equation by Lohmann (2012). The highest accuracy was determined for equation 44 with a RMSE of 0.2952. However, for all five equations in method 1, the intercept indicating the lowest partition coefficient that can be calculated was greater than 2.90. Therefore, a lower partition coefficient than 2.90 cannot be calculated for equations 26, 27, 44, 51 and 56. For example, the  $\log K_{p-w}$  for PET of naphthalene (2.68), fluorene (2.81) and phenanthrene (2.82) determined from the laboratory tests cannot be calculated with these equations (26, 27, 44, 51, 56) since its intercept is larger. Therefore, not all equations are considered further, which is not due to the selection of properties, but due to the determined parameters that can result from this consideration.

However, equations 75 and 76 of method 2 satisfy the conditions i) a partition coefficient of theoretically 2.5 can be calculated and ii) it has a higher accuracy than the reference equation of Lohmann (2012). Since equation 75 had a higher accuracy than equation 76, equation 75 was set as the final equation of this work to predict  $\log K_{p-w}$ .

#### 7.4. Proof of concept: comparison of modelled values versus published data

After choosing equation 75 to work with going forward, the next step was to determine whether the previously published  $\log K_{p-w}$  values could be mapped using equation 75. For this purpose, the upper and lower limits of equation 75 were determined with the minimum and maximum literature values of the polymer properties for all four plastic types tested in this thesis, while the PAH property  $\log C_w^{sat}$  based on molar weight remains as constant. In addition, the  $\log K_{p-w}$  of PAHs were also mapped whose molar weight were greater than that of phenanthrene. The following sections examined whether published  $\log K_{p-w}$  values were within the plastic-specific limits of Equation 75. For this purpose, the 16 EPA PAHs were used.

Since the fitting accuracy of equation 75 depends on the type of plastic used, equations 80 to 83 list the plastic-specific equations, including the uncertainties of the regression coefficients and the coefficient of determination ( $R^2$ ) for the plastic-water partition coefficients determined in the laboratory. The coefficient uncertainties were included in the respective equations in the following four subsections in order to map the smallest and largest possible confidence band below and above the plastic-specific trend line.

$$\log K_{LDPE-w} = -0.81 (\pm 0.082) * \log C_w^{sat} + 2.94 (\pm 0.090) \quad (R^2 = 0.99) \quad \text{equation 80}$$

$$\log K_{PP-w} = -0.67 (\pm 0.133) * \log C_w^{sat} + 2.86 (\pm 0.146) \quad (R^2 = 0.96) \quad \text{equation 81}$$

$$\log K_{PBS-w} = -1.36 (\pm 0.937) * \log C_w^{sat} + 3.24 (\pm 1.034) \quad (R^2 = 0.68) \quad \text{equation 82}$$

$$\log K_{PET-w} = -0.13 (\pm 0.187) * \log C_w^{sat} + 2.57 (\pm 0.207) \quad (R^2 = 0.33) \quad \text{equation 83}$$

#### 7.4.1. Proof of concept for LDPE

The standard property of LDPE for density = 0.92 g cm<sup>-3</sup> and crystallinity = 0.48 % from the previous section has shown that modelled values based on equation 75 resulted in a lower RMSE compared to reference equation 78 of Lohmann (2012). This indicates a higher accuracy and therefore, equation 75 was applied to published studies that determined at least three log K<sub>LDPE-w</sub>.

For LDPE the lower and upper limits were determined by the minimum and maximum crystallinities 33.6 (Chen et al., 2020) and 60 % (Lambert and Wagner, 2018) as well as minimum and maximum densities, 0.91 and 0.93 g cm<sup>-3</sup> (Lambert and Wagner, 2018) that were found in the literature. Furthermore, the trendline of equation 80 and the confidence band of equation 80 can be seen in Figure 26. The lowest number of published log K<sub>LDPE-w</sub> - values that had been compared with the final equation was five (Adams et al., 2007) and the highest 16 (Smedes et al., 2009; Zhu et al., 2015), as well as log K<sub>LDPE-w</sub> determined in this thesis. For display purposes, the constant of water solubility (log C<sub>w</sub><sup>sat</sup>) was mapped on the abscissa and the plastic property on the ordinate shown in the following figure:

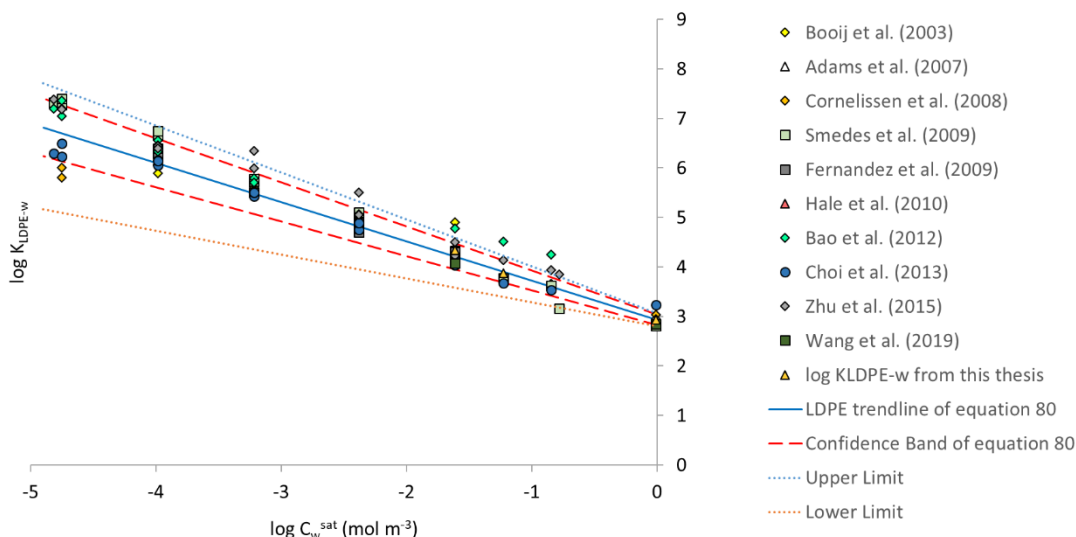


Figure 26: Results of literature LDPE-water partition coefficients within upper and lower limits of equation 75

As shown in Figure 26, the lower and upper limits of equation 75 are undershot or exceeded in individual cases. Overall, seven published  $\log K_{LDPE-W}$  values out of 100 were not within the limits of equation 75, which means that 93 % of the considered LDPE-water partition coefficients from the literature could be calculated. For example, the value for acenaphthylene from Smedes et al. (2009) is 0.09 log units below the lower limit, whereas all other 15 partition coefficients from Smedes et al. (2009) are within the limits of equation 75. Furthermore, one partition coefficient of Booij et al. (2003) anthracene was 0.18 and three partition coefficients of Bao et al. (2012) acenaphthene, fluorene and phenanthrene were 0.32, 0.18 and 0.06 log units above the upper limit. Moreover,  $\log K_{LDPE-W}$  of naphthalene by Choi et al. (2013) and acenaphthene by Zhu et al. (2015) were 0.16 and 0.01 log units above the upper limit of equation 75. Since the confidence band of equation 80 lies within the upper and lower limits of equation 75, this reflects the high accuracy of the laboratory values determined for equation 80.

In all literatures no information about crystallinity was given, therefore a verification with exact crystallinity values was not possible. However, it had been shown that equation 75 can be applied to many LDPE-water partition coefficients, including PAHs whose molar mass was greater than that of phenanthrene. This allowed a prediction of PAHs outside the considered study range of naphthalene and phenanthrene.

#### 7.4.2. Proof of concept for PP

For PP, publications by Lee et al. (2014) and Lončarski et al. (2021) are available to compare modelled values of equation 75, having at least three different partition coefficients for PAH. For example, Lee et al. (2014) tested eight different PAH (phenanthrene, anthracene, fluoranthene, pyrene, chrysene, benzo(a)pyrene, dibenz(a,h)anthracene, benzo(g,h,i)perylene) in artificial sea water and Lončarski et al. (2021) determined partition coefficients of four PAHs (naphthalene, fluorene, fluoranthene, pyrene) in a synthetic water matrix. Both data sets were transferred to freshwater according to Jonker and Muijs (2010). However, the focus of both publications was not on determining polymer properties, therefore there is no data on crystallinity for either publication. In the following, it was verified whether the published partition coefficients were within the limits of equation 75, as the results from the previous chapter were mostly found to be. For this purpose, the upper and lower limits of plastic properties were compiled from various publications. Published polymer crystallinities for PP were in the range of 33.6 % (Thumsorn and Srisawat, 2014) to 58.1 % (Yang et al., 2016), and the polymer density was between 0.85 – 0.93 g cm<sup>-3</sup> (Andrady, 2011). Furthermore, the trendline of equation 81, the confidence band of equation 81, and the  $\log K_{PP-W}$  of this thesis can be seen in Figure 27. The results are shown in the following figure:

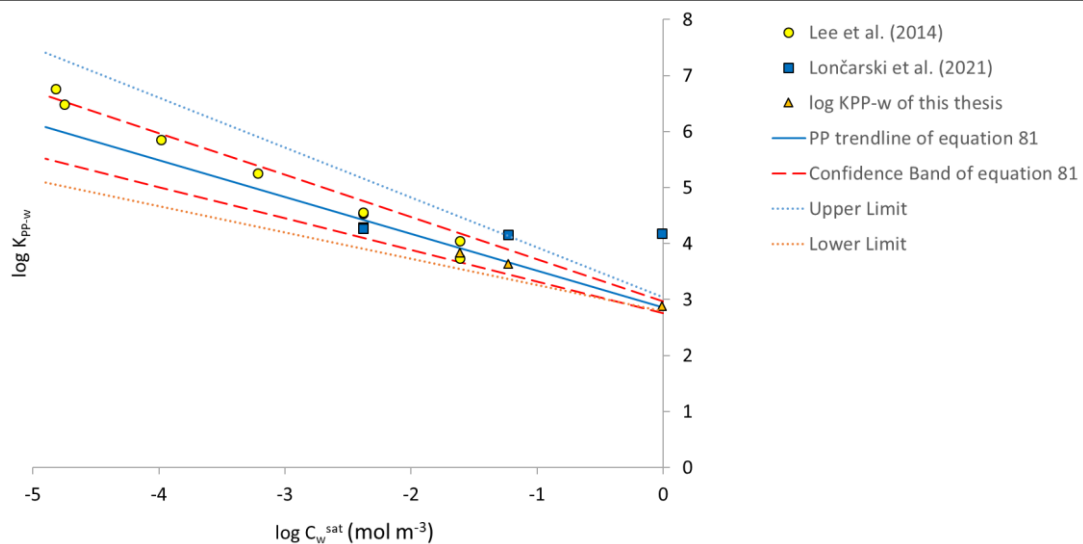


**Figure 27:** Results of literature PP-water partition coefficients  $\log K_{\text{PP}-\text{w}}$  within upper and lower limits of equation 75

The results of Figure 27 show that all partition coefficients of Lee et al. (2014) that had been converted into fresh-water partition coefficients, were within the limits of equation 75, as well as three partition coefficients of Lončarski et al. (2021). Only the value of naphthalene by Lončarski et al. (2021) was above the determined limit of equation 75. In total, eleven values were within the limits, which corresponds to 91,7 %, and one value was above the limit. The upper confidence band of equation 81 is within the limit range of equation 75, but the lower confidence band of equation 81 is only within the limits of equation 75 again from a  $\log C_w^{\text{sat}}$  value of less than -0.27 mol m<sup>-3</sup>.

Since Lončarski et al. (2021) did not specify any properties for PP other than surface properties, no further statements can be made on the validation or accuracy of equation 75.

As a special feature, it should be mentioned that the eight partition coefficients determined by Lee et al. (2014) had a molar mass greater than that of phenanthrene and no PAHs were determined to be less than this. Thus, the range of a molar mass greater than 178.24 g mol<sup>-1</sup> already represented a prediction of the values and can be applied due to its compliance with the lower and upper limits.

However, there were no other publications that had determined at least three PP-water partition coefficients, so the studies by Lee et al. (2014) and by Lončarski et al. (2021) were the only two studies of comparison value.

### 7.4.3. Proof of concept for PBS

Bioplastics such as PBS have not yet become the focus of sorption experiments, therefore available publications were limited. For PBS, no publication was available that had determined three partition coefficients for PAHs. However, Zhao et al. (2020) published a  $\log K_{\text{PBS-W}}$  for phenanthrene and pyrene that can be compared to the modelled values based on equation 75. Since Zhao et al. (2020) gave no information about polymer density and crystallinity, the results were presented with both properties unknown, as in the previous chapters.

Published polymer crystallinities were in the range of 35.0 % (Zhang et al., 2012) to 65.6 % (Jin et al., 2014) and polymer density between 1.24 - 1.26 g cm<sup>-3</sup> (Lin et al., 2020). The upper and lower limits were determined based on these values. The results of the lower and upper limit of equation 75 for the polymer type PBS, as well as the trendline of equation 82, the confidence band of equation 82, and the  $\log K_{\text{PBS-W}}$  of this thesis were shown in Figure 28.

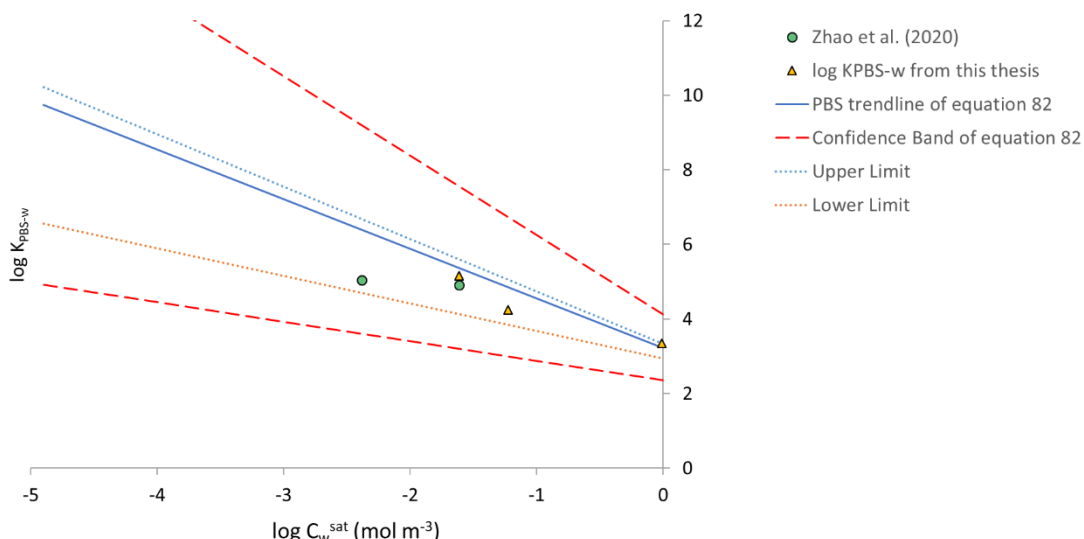


Figure 28: Results of literature PBS-water partition coefficients  $\log K_{\text{PBS-W}}$  within upper and lower limits of equation 75

The only published partition coefficients of phenanthrene and pyrene by Zhao et al. (2020) were within the limits of equation 75 shown in Figure 28. Since the molar weight and hence aqueous solubility ( $\log C_w^{\text{sat}}$ ) of pyrene is greater than that of phenanthrene, and both phenanthrene and pyrene partition coefficients were within the estimated limits of this equation, it follows that it might be possible to apply the equation to the publication of Zhao et al. (2020). However, there were only two partition coefficients available, which is why no further conclusions can be drawn about the applicability of this equation for PBS. Due to the higher inaccuracy of equation 82, the upper and lower confidence bands lie outside the upper and lower limit of equation 75. Further  $\log K_{\text{PBS-W}}$ -values would be needed to confirm the accuracy and the applicability of the equation 75. In addition to the partition coefficients of the individual plastics, further information on the used plastic properties would be useful to specify equation 75.

#### 7.4.4. Proof of concept for PET

Publications of PAH sorption experiments on PET were also limited. However, Lončarski et al. (2021) published PET-water partition coefficients for naphthalene, fluorene, fluoranthene and pyrene that can be used to compare modelled values based on equation 75 and to verify if they were within the lower and upper limits. The study by Lončarski et al. (2021) was the only one available for PET. Since Lončarski et al. (2021) performed sorption experiments in a synthetic water matrix the data set was transferred to freshwater according to Jonker and Muijs (2010).

However, further information on plastic properties was not provided by Lončarski et al. (2021). The minimum and maximum values for density and the crystallinity were researched from other publications to determine the lower and upper limits of equation 75 for PET. Published polymer crystallinities were in the range of 2.0 % (Mishra and Deopura, 1989) to 40.0 % (Ehrenstein, 2012) and polymer density between the lower and upper limits of 1.34 (Lambert and Wagner, 2018) - 1.41 g cm<sup>-3</sup> (Brignac et al., 2019). The log K<sub>PET-w</sub> of Lončarski et al. (2021) as well as the lower and upper limits of equation 75 for PET and the log K<sub>PET-w</sub> from this thesis, as well as the trendline of equation 83 and the associated confidence band were shown in the following figure:

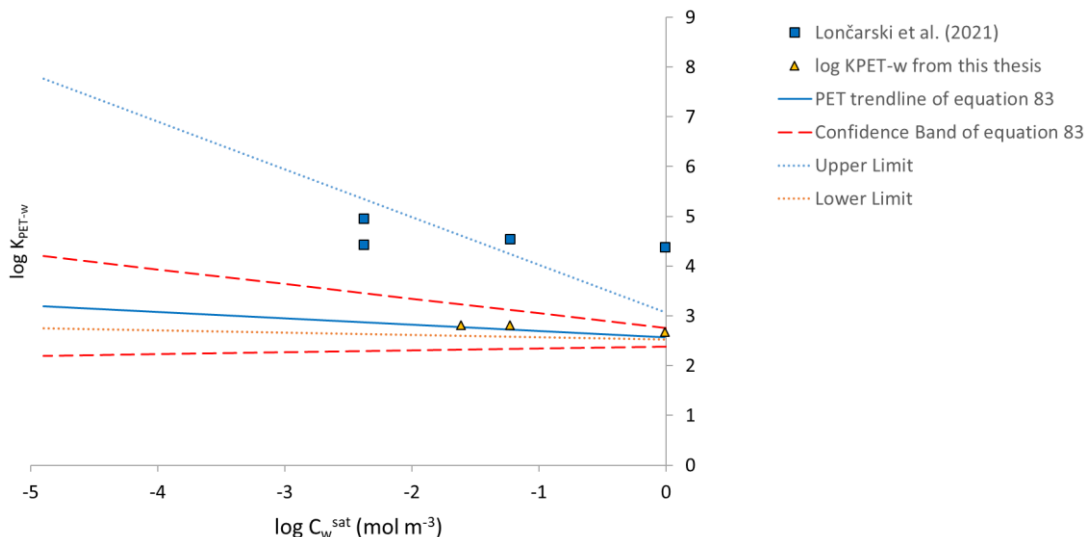


Figure 29: Results of literature PET-water partition coefficients log K<sub>PET-w</sub> within upper and lower limits of equation 75

Figure 29 shows partition coefficients of Lončarski et al. (2021) that were within the limits of equation 75 for fluoranthene, and pyrene, but the partition coefficients of naphthalene and fluorene were above the upper limit of this equation. If all four partition coefficients of Lončarski et al. (2021) were connected with a linear regression line, it runs nearly parallel to the lower limit but shifted upward by about 2.0 log units. This suggests a similar combination of the plastic properties represented by the parallelism of the slopes. Since Lončarski et al. (2021) did not specify the plastic properties, a modified plastic may have been used. Furthermore, the upper confidence band of equation 83 lies within the limits of equation 75, but the lower confidence band is outside these limits. For PET, there were no other partition coefficients available. In order to be able to make equation 75 more precise for PET as well, further partition coefficients and the associated plastic properties are required from future publications.

### Summary

Equation 75 showed that of the 100 published LDPE water partition coefficients, 93 % fell within the upper and lower limits of this equation, according to the lower and upper plastic property values found in the literature. Concerning the partition coefficients that were not within the limits of this equation, there was no further information on the polymer properties, so it is not possible within the scope of this thesis to analyse in detail what may have caused this. When looking at the plastics PP, PBS and PET, only few publications were available for comparison. Since the studies by Lee et al. (2014), Zhao et al. (2020) and Lončarski et al. (2021) did not provide information on the plastic properties, the equation of this study can only give a potential prediction for the plastics PP, PBS and PET. The inaccuracies of the equations for PBS and PET, equations 82 and 83, have shown that more published data is needed to be able to make a better statement about the accuracy and adequacy of equation 75. However, a foundation stone has been laid with this equation and can be optimized by further studies.

## 8. Conclusion and outlook

The problem of pollutant accumulation on plastics is present in the marine environment. Such contaminated plastic particles may have greater ecotoxicological impact on marine organisms compare to the plastic particles themselves. To understand sorption behaviours of pollutants on plastics in aquatic milieu, plastic-water partition coefficient ( $\log K_{p-w}$ ) is often determined and compared. However,  $\log K_{p-w}$  values are available for limited combinations of pollutants and polymers. For hydrophobic pollutants, it is not easy to implement the experiment to determine  $\log K_{p-w}$  values, since such pollutants may be adsorbed also on the surfaces other than polymer to be tested.

Therefore, the aim of my dissertation was to develop a mathematical equation based on physicochemical properties of PAHs and plastics to estimate the plastic-water partition coefficient ( $\log K_{p-w}$ ). This makes it possible to estimate the sorption potential and potential environmental impact of existing or newly developed plastic materials based on their PAH accumulation properties.

The plastic-water partition coefficients were first determined on a series of small laboratory scale experiments. Following this, the second step consisted of correlating single physicochemical properties of PAHs and plastics with the  $\log K_{p-w}$  of the laboratory experiments. Afterwards physicochemical properties of PAHs and plastics were combined and also correlated against  $\log K_{p-w}$  of the laboratory experiments. Finally, selected equations were compared with a published equation for LDPE from Lohmann (2012), since it was the only such equation available. This resulted in the formulation of one final equation that would be tested against literature data.

In the first step a series of sorption isotherm experiments was conducted to determine the plastic-water partition coefficients of three PAHs, naphthalene, fluorene, and phenanthrene on three conventional plastics (LDPE, PP, and PET) and one biodegradable plastic (PBS). A total of 12 sorption experiments were performed. The  $\log K_{p-w}$  of Freundlich isotherm increased in the order of PET < PP < LDPE < PBS for all PAH tested. A comparison of the laboratory-determined partition coefficients for LDPE with published partition coefficients confirmed the validity of the experimental setup and its results. The same setup was therefore used for the other plastics. Since the published data base for the other plastics (PP, PBS, PET) was not so large, the results could only be partially confirmed. The partition coefficients that could not be confirmed had little or no published data to be compared to. Therefore, further investigations need to carry out.

In the second step, individual physicochemical properties of the investigated PAHs and plastics were correlated with the 12  $\log K_{p-w}$  determined from the laboratory experiments. In this thesis significant linear correlations were observed between these 12  $\log K_{p-w}$  and the octanol-water partition coefficient ( $\log K_{ow}$ ), molar mass (MW), aqueous solubility ( $\log C_w^{sat}$ ) by Ma et al. (2010) and hexadecane-water partition coefficient of the tested PAHs for LDPE, PP, PBS and PET with  $R^2 > 0.914$ . With respect to LDPE, the  $\log K_{LDPE-w} - \log K_{ow}$  equation of this thesis showed no significant difference compared to the six published studies, confirming the validity of the experimental settings. For PP, PBS, and PET,  $\log K_{p-w} - \log K_{ow}$  and  $\log K_{p-w} - MW$  regression models were developed for the first time, to the best of knowledge. These models can be applied to estimate  $\log K_{p-w}$  values of other PAHs with relatively high accuracy, especially three-ring PAHs with  $\log K_{ow}$  values between 3.35 and 4.45, for LDPE, PBS, PP, and PET.

Furthermore, the influence of physical, thermodynamic and surface plastic properties of the four different types of plastics (LDPE, PP, PBS, PET) on the  $\log K_{p-w}$  of naphthalene, fluorene and phenanthrene was analysed. For this purpose, the 12  $\log K_{p-w}$  from the laboratory experiments were initially correlated with thermodynamic plastic properties (crystallinity, melting temperature ( $T_m$ )),

glass transition temperature ( $T_g$ ) which were measured through differential scanning calorimetry (DSC). The results of crystallinity as well as melting temperature of the tested plastics LDPE, PP, PBS and PET correlate well for 2- and 3-ring PAHs, resulting in  $R^2$  between 0.76 - 0.99 and 0.74 - 0.98, respectively. However, from the present results, no correlation of  $\log K_{p-w}$  greater than  $R^2 = 0.21$  could be found for neither individual surface plastic properties nor physical plastic properties.

In the third step, a final equation was developed that allows an estimation of the  $\log K_{p-w}$  while the physicochemical properties of each plastic and PAH taking into account. The different PAH and plastic properties from step one were first combined with each other and compared to the  $\log K_{p-w}$  from the laboratory experiments. Only a small number of the combinations of plastic and PAH properties ( $n = 51$ ) met the accuracy specifications to establish the final equation. The PAH properties  $\log K_{ow}$ , MW,  $\log C_w^{sat}$  and  $\log K_{hdw}$  as well as the plastic properties crystallinity and melting temperature were found to be suitable to determine the partition coefficients of LDPE, PP, PBS and PET. In addition to the accuracy comparison of the selected equations ( $n = 51$ ) with each other, the reference equation by Lohmann (2012) was included as a minimum accuracy criterion for the  $n = 100$  published  $\log K_{LDPE-w}$  values. Finally, an equation derived from the physicochemical properties of plastics ( $X_{c pi} =$  crystallinity of plastic i,  $\rho_{pi}$  = density of plastic i) and PAH ( $\log C_w^{sat}_{PAHj} = \log$  water solubility of PAH j) was identified whose modelled plastic-water partition coefficients ( $\log K_{pi-w}$ ) had higher accuracy than the equation from Lohmann (2012). The final equation was as follows:

$$\log K_{pi-w} \text{ of } PAH_j = (-1.85 * \log C_w^{sat}_{PAHj} + 1.00) * X_{c pi} * \rho_{pi} + 2.50 \quad \text{equation 75}$$

Finally, a transferability of equation 75 to previously published  $\log K_{p-w}$  was performed and showed that 93.0 % (93 out of 100 published  $\log K_{LDPE-w}$  values), 91.7 % (11 out of 12 published  $\log K_{PP-w}$  values), 100 % (2 out of 2 published  $\log K_{PBS-w}$  values), and 50 % (2 out of 4 published  $\log K_{PET-w}$  values) of the  $\log K_{p-w}$  of LDPE, PP, PBS, and PET were within the limits of this equation. Comparatively few  $\log K_{p-w}$  values were published for PP, PBS, and PET, so a literature comparison was limited.

However, the equation can be used for future planning of experiments concerning the plastic types used in this thesis and to estimate the ecotoxicological impact of these plastics in the marine environment. In the future, this universal equation can be optimized by i) pollutants other than PAHs and with a  $\log K_{ow}$  lower than 3.37 and higher than 6.70, ii) plastic properties measured for further  $\log K_{p-w}$  experiments, iii) individual correlation between  $\log K_{p-w}$  and plastic properties (within the same type of plastic, or different plastics).

## 9. References

- Adams, R. G., Lohmann, R., Fernandez, L. A., MacFarlane, J. K., Gschwend, P. M. (2007). Polyethylene Devices: Passive Samplers for Measuring Dissolved Hydrophobic Organic Compounds in Aquatic Environments. *Environmental Science Technology*. Vol. 41, 1317-1323.
- Agency for Toxic Substances and Disease Registry (ATSDR) (1995). Toxicological profile for polycyclic aromatic hydrocarbons (PAHs). Atlanta, GA: US Department of Health and Human.
- Aktas, C., Polat, O., Beitollahpoor, M., Farzam, M., Pesika, N. S., & Sahiner, N. (2023). Force-Based Characterization of the Wetting Properties of LDPE Surfaces Treated with CF4 and H2 Plasmas. *Polymers*, 15(9), 2132.
- Andrady A. L. (2011). Microplastics in the marine environment. *Marine Pollution Bulletin*. Vol. 62, 1596-05.
- Andrady, A. L. (2017). The plastic in microplastics: A review. *Marine Pollution Bulletin*. Vol. 119 (1), 12-22.
- Badia, J. D., Srömberg, E., Karlsson, S., Ribes-Greus, A. (2012). The role of crystalline, mobile amorphous and rigid amorphous fractions in the performance of recycled poly (ethylene terephthalate) (PET). *Polymer Degradation and Stability*. Vol. 97, 98-107.
- Balani, K., Verma, V., Agarwal, A., Narayan, R. (2015). *Biosurfaces: A Material Science and Engineering Perspective*. John Wiley & Sons, Inc., Hoboken, New Jersey.
- Bao, L. J., Xu, S. P., Liang, Y., Zang, E. Y. (2012). Development of a low-density polyethylene-containing passive sampler for measuring dissolved hydrophobic organic compounds in open waters. *Environmental Toxicology and Chemistry*. Vol. 31, (5), 1012–1018.
- Baur, E., Harsch, G., Moneke, M. (2019). *Werkstoff-Führer Kunststoffe. Eigenschaften - Prüfungen - Kennwerte*, 11. Aufl., München: Carl Hanser Verlag.
- Bonnet, M. (2016). *Kunststofftechnik. Grundlagen, Verarbeitung, Werkstoffauswahl und Fallbeispiele*, 3. Aufl., Wiesbaden: Springer Vieweg.
- Booij, K., Hofmans, H. E., Fischer C. V., Van Weerlee, E. M. (2003). Temperature-dependent uptake rates of nonpolar organic compounds by semipermeable membrane devices and low-density polyethylene membranes. *Environmental Science and Technology*. Vol. 37, 361-366.
- Brignac, K. C., Jung, M. R., King, C., Royer, S. J., Blickley, L., Lamson, M. R., Potemra, J. T., Lynch, J. M. (2019). Marine debris polymers on main Hawaiian Island beaches, sea surface, and seafloor. *Environmental science & technology*, 53(21), 12218-12226.
- Burant, A., Lowry, G.V., Karamalidis, A.K. (2016). Measurement of Setschenow constants for six hydrophobic compounds in simulated brines and use in predictive modeling for oil and gas systems. *Chemosphere*. Vol. 144, 2247–2256.
- Camacho, M., Herrera, A., Gómez, M., Acosta-Dacal, A., Martínez, I., Henríquez-Hernández, L. A., Lizardo, O. P. (2019). Organic pollutants in marine plastic debris from Canary Islands beaches. *Science of The Total Environment*. Vol. 662, 22-31.
- Camarda, D. S., Lampe, M. J., Desbois, P., Stoll, K., Gabriel, C., Konradi, R. (2021). Upcycling by grafting onto semi-crystalline polymers using supercritical CO<sub>2</sub>. *Journal of Applied Polymer Science*. Vol. 138 (41), 51203.
- Chaudhari, C. V., Dubey, K. A., Goel, N. K., Bhardwaj, Y. K., Varshney, L. (2012). Correlation between surface energy and uptake behavior of radiation-grafted methacrylic acid-g-LDPE. *Polymer Bulletin*, 69, 779-793.
- Chen, J. Q., Wang, X., Sun, W. F., Zhao, H. (2020). Improved Water-Tree Resistances of SEBS/PP Semi-Crystalline Composites under Crystallization Modifications. *Molecules*, 25, 3669.

- Cheung, K. C., Leung, H. M., Kong, K. Y., Wong, M. H. (2007). Residual levels of DDTs and PAHs in freshwater and marine fish from Hong Kong markets and their health risk assessment. *Chemosphere*. Vol. 66 (3), 460-468.
- Choi, Y., Cho, Y. M., Luthy R. G. (2013). Polyethylen-Water Partitioning Coefficients for Parent- and Alkylated-Polycyclic Aromatic Hydrocarbons and Polychlorinated Biphenyls. *Environmental Science & Technology*. Vol. 47, 6943-6950.
- Cornelissen, G., Pettersen, A., Broman, D., Mayer, P., Breedveld, G. D. (2008). Field testing equilibrium passive samplers to determine freely dissolved native polycyclic aromatic hydrocarbon concentrations. *Environmental Toxicology Chemistry*. Vol. 27 (3), 499-508.
- Corsolini, S., Sarà, G. (2017). The trophic transfer of persistent pollutants (HCB, DDTs, PCBs) within polar marine food webs. *Chemosphere*. Vol. 177, 189-199.
- Domininghaus, H. (2012). *Kunststoffe. Eigenschaften und Anwendungen*, Elsner, P., Eyerer P., Hirth, T., (Hrsg.), 8. Aufl., Berlin: Springer-Verlag.
- Dikbaş, F. (2017). A novel two-dimensional correlation coefficient for assessing associations in time series data. *International Journal of Climatology*, 37(11), 4065-4076.
- dos Santos, W. N., de Sousa, J. A., Gregorio Jr. R. (2013). Thermal conductivity behaviour of polymers around glass transition and crystalline melting temperatures. *Polymer Testing*. Vol. 32 (5), 987-994.
- Ehrenstein, G.W. (2012). *Polymeric materials: structure, properties, applications*. Hanser Gardner Publications, Inc., München.
- Eiras, D., Pessan, L. A. (2009). Influence of calcium carbonate nanoparticles on the crystallization of polypropylene. *Materials Research*. Vol. 12 (4).
- Endo, S., Koelmans, A. A. (2016). Sorption of Hydrophobic Organic Compounds to Plastics in the Marine Environment: Equilibrium. In: Takada H., Karapanagioti H. (eds) *Hazardous Chemicals Associated with Plastics in the Marine Environment. The Handbook of Environmental Chemistry*. Vol 78. Springer, Cham.
- Endo, S., Takizawa, R., Okuda, K., Takada, H., Chiba, K., Kanehiro, H., Ogi, H., Yamashita, R., Date, T. (2005). Concentration of polychlorinated biphenyls (PCBs) in beached resin pellets: Variability among individual particles and regional differences. *Marine Pollution Bulletin*. Vol. 50, 1103-1114.
- Eriksen, M., Lebreton, L. C. M., Carson, H. S., Thiel, M., Moore, C. J., Borerro, J. C., Galgani, F., Ryan, P. G., Reisser, J. (2014). Plastic Pollution in the World's Oceans: More than 5 Trillion Plastic Pieces Weighing over 250,000 Tons Afloat at Sea. *PLoS ONE*. Vol. 9 (12), 111913.
- European Bioplastics, nova-Institute (2019). Bioplastics market data 2019. Available online: <https://www.european-bioplastics.org/new-market-data-2019-bioplastics-industry-shows-dynamic-growth/> (accessed 17th June 2023).
- European Bioplastics, nova-Institute (2020). Bioplastics Market Data 2020 - 2026. 2021, Volume 2020 - 2021. Available online: <https://www.european-bioplastics.org/market/> (accessed 17th June 2023).
- Fenouillot, F., Cassagnau, P., Majesté, J. C. (2009). Uneven distribution of nanoparticles in immiscible fluids: Morphology development in polymer blends. *Polymer*. Vol. 50 (6), 1333-1350.
- Fernandez, L. A., MacFarlane, J. K., Tcaciuc, A. P., Gschwend, P. M. (2009). Measurement of freely dissolved PAH concentrations in sediment beds using passive sampling with low-density polyethylene strips. *Environmental Science and Technology*. Vol. 43, 1430 – 1436.
- Gahleitner, M., Bachner, C., Ratajski, E., Rohazcek, G., Neißl, W. (1999). Effects of the Catalyst System on the Crystallization of Polypropylene. *Journal of Applied Polymer Science*. Vol. 73, 2507-2515.

- Gan, S. N., Burfield, D. R., Soga, K. (1985). Differential scanning calorimetry studies of ethylene-propylene copolymers. *Macromolecules*, 18(12), 2684-2688.
- Geyer, R., Jambeck, J. R., Law, K. L. (2017). Production, use, and fate of all plastics ever made. *Science Advances*. Vol. 3 (7), 1700782.
- Girol, E. D., Van Vlierberghe, S., Unger, R. E., Kersemans, K., de Vos, F., Kirkpatrick, C. J., Dubrule, P. (2019). Biomimetic strategy towards gelatin coatings on PET. Effect of protocol on coating stability and cell-interactive properties. *Journal of materials chemistry B*. Vol. 7(8), 1258-1269.
- González-Dávila, M., Santana-Casiano, J. M., González, A. G., Pérez, N., Millero, F. J. (2009). Oxidation of copper(I) in seawater at nanomolar levels. *Marine Chemistry*. Vol. 115 (1-2) 118-124.
- Goodship, V., Middleton, B., Cherrington, R. (2015). Design and Manufacture of Plastic Components for Multifunctionality Structural Composites, Injection Molding, and 3D Printing. Kidlington, Oxford, UK: Waltham, MA: William Andrew.
- Gray, J. S. (2002). Biomagnification in marine systems: the perspective of an ecologist. *Marine Pollution Bulletin*. Vol. 45 (1-12), 46-52.
- Habib, S., Lehocky, M., Vesela, D., Humpolíček, P., Krupa, I., Popelka, A. (2019). Preparation of Progressive Antibacterial LDPE Surface via Active Biomolecule Deposition Approach. *Polymers*. Vol. 11 (10), 1704.
- Hale, S. E., Martin, T. J., Goss, K. U., Arp, H. P. H., Werner, D. (2010). Partitioning of organochlorine pesticides from water to polyethylene passive samplers. *Environmental Pollution*. Vol. 158 (7), 2511-2517.
- Harvey, R. G. (1997). Polycyclic aromatic hydrocarbons. Weinheim u.a. Wiley-VCH.
- Haskett, M., Takada, H., Yamashita, R., Yuyama, M., Yeo, M., Geok, B., Ogata, Y., Kwan, C., Heckhausen, A., Taylor, H., Powell, T., Morishige, C., Young, D., Patterson, H., Robertson, B., Bailey, E., Mermoz, J. (2012). Measurement of persistent organic pollutants (POPs) in plastic resin pellets from remote islands: Toward establishment of background concentrations for International Pellet Watch. *Marine Pollution Bulletin*. Vol. 64 (2), 445-448.
- Hirai, H., Takada, H., Ogata, Y., Yamashita, R., Mizukawa, K., Sahaa, M., Kwan, C., Moo, C., Gray, H., Laursen, D., Zettler, E. R., Farrington, J. W., Reddy, C. M., Peacock, E. E., Ward, M. W. (2011). Organic micropollutants in marine plastics debris from the open ocean and remote and urban beaches. *Marine Pollution Bulletin*. Vol. 62 (8) 1683-1692.
- Ho, Y. S. (1995). Adsorption of heavy metals from waste streams by peat. Dissertation for the Doctoral Degree. Birmingham: University of Birmingham.
- Hüffer, T., Hofmann, T. (2016). Sorption of non-polar organic compounds by micro-sized plastic particles in aqueous solution. *Environmental Pollution*. Vol. 214, 194-201.
- Ibrahim, N. I., Shahar, F. S., Sultan, M. T. H., Shah, A. U. M., Safri, S. N. A., Mat Yazik, M. H. (2021). Overview of Bioplastic Introduction and Its Applications in Product Packaging. *Coatings*. Vol. 11, 1423.
- Jambeck, J. R., Geyer, R., Wilcox, C., Siegler, T. R., Perryman, M., Andrade, A., Narayan, R., Law, K. L. (2015). Plastic waste inputs from land into the ocean. *Marine Pollution*. Vol. 347, 768-771.
- Jin, T. X., Zhou, M., Hu, S. D., Chen, F., Fu, Q. (2014). Effect of Molecular Weight on the Properties of Poly(butylene succinate). *Chinese Journal of Polymer Science*. Vol. 32 (7), 953-960.
- Jonker, M. T. O., Muijs, B. (2010). Using solid phase micro extraction to determine salting-out (Setschenow) constants for hydrophobic organic chemicals. *Chemosphere*. Vol. 80 (3), 223-227.

- Karapanagioti, H. K., Klontza, I. (2008). Testing phenanthrene distribution properties of virgin plastic pellets and plastic eroded pellets found on Lesvos island beaches (Greece). *Marine Environmental Research*. Vol. 65, 283–290.
- Koltzenburg, S., Maskos, M., Nuyken, O. (2014). *Polymere. Synthese, Eigenschaften und Anwendungen*, Berlin: Springer Spektrum.
- Khonakdar, H. A., Jafari, S. H., Hässler, R. (2007). Glass-Transition-Temperature Depression in Chemically Crosslinked Low-Density Polyethylene and High-Density Polyethylene and their Blends with Ethylene Vinyl Acetate Copolymer. *Journal of Applied Polymer Science*. Vol. 104, 1654-1660.
- Krásný, I., Kupská, I., Lapčík, L. (2012). Effect of Glow-Discharge Air Plasma Treatment on Wettability of Synthetic Polymers. *Journal of Surface Engineered Materials and Advanced Technology*. Vol. 2 (3), 142-148.
- Lagergren, S. (1898). About the theory of so-called adsorption of soluble substances. *Kungliga Svenska Vetenskapsakademiens Handlingar*. Vol. 24, 1-39.
- Lambert, S., Wagner, M. (2018). Microplastics are contaminants of emerging concern in freshwater environments: an overview. *Freshwater microplastics*, 1-23.
- Lee, H., Shim, W.J., Kwon, J. H. (2014). Sorption capacity of plastic debris for hydrophobic organic chemicals. *Science of the total environment*. Vol. 470-471, 1545-1552.
- Li, D., Zhou, L., Wang, X., He, L., Yang, X. (2019). Effect of Crystallinity of Polyethylene with Different Densities on Breakdown Strength and Conductance Property. *Materials*. Vol. 12, 1746.
- Li, J., Zhang, K., Zhang, H, (2018). Adsorption of antibiotics on microplastics. *Environmental pollution*. Vol. 237, 460-467.
- Lin, C., Liu, L., Liu, Y., Leng, J. (2020). The compatibility of polylactic acid and polybutylene succinate blends by molecular and mesoscopic dynamics. *International Journal of Smart and Nano Materials*, 11(1), 24-37.
- Lin, J., Wang, L. (2009). Comparison between linear and non-linear forms of pseudo-first-order and pseudo-second-order adsorption kinetic models for the removal of methylene blue by activated carbon. *Frontiers of Environmental Science & Engineering in China*. Vol. 3 (3), 320-324.
- Lohmann, R. (2012). Critical Review of Low-Density Polyethylene's Partitioning and Diffusion Coefficients for Trace Organic Contaminants and Implications for Its Use as a Passive Sampler. *Environmental Science & Technology*. Vol. 47, 46, 606 – 618.
- Lončarski, M., Gvoić, V., Prica, M., Cveticanin, L., Agbaba, J., Tubić, A. (2021). Sorption behavior of polycyclic aromatic hydrocarbons on biodegradable polylactic acid and various nondegradable microplastics: Model fitting and mechanism analysis. *Science of the Total Environment*. Vol. 785, 147289.
- Lotti, N., Colonna, M., Fiorini, M., Finelli, L., Berti, C. (2013). Poly (ethylene terephthalate), modified with bisphenol S units, with increased glass transition temperature. *Journal of applied polymer science*, 128(1), 416-423.
- Ma, Y. G., Lei, Y. D., Xiao, H., Wania, F., Wang, W. H. (2010). Critical review and recommended values for the physical-chemical property data of 15 polycyclic aromatic hydrocarbons at 25 C. *Journal of Chemical & Engineering Data*. Vol. 55(2), 819-825.
- Mackay, D., Shiu, W. Y., Ma, K. C. (1992). *Illustrated Handbook of Physical-Chemical Properties and Environmental Fate for Organic Chemicals. Volume II: Polynuclear Aromatic Hydrocarbons, Polychlorinated Dioxins, and Dibenzofurans*. Lewis Publishers, Boca Raton, FL.
- Mamunya, Y., Levchenko, V., Boiteux, G., Seytre, G., Zanoaga, M., Tanasa, F., Lebedev, E. (2016). Controlling morphology, electrical, and mechanical properties of polymer blends by heterogeneous distribution of carbon nanotubes. *Polym. Compos.* Vol. 37, 2467-2477.

- Mato, Y., Isobe, T., Takada, H., Otake, C., Kaminuma, T. (2001). Plastic Resin Pellets as a Transport Medium for Toxic Chemicals in the Marine Environment. *Environmental Science & Technology*. Vol. 35, 318-324.
- Mishra, S. P., Deopura, B. L. (1989). Modification of poly (ethylene terephthalate) fibre by polymer blending with poly (butylene terephthalate) fibre: Part V-Extrusion behaviour.
- Mwakalapa, E. B., Mmochi, A. J., Müller, M. H. B., Mdegela, R. H., Lyche, J. L., Polder, A. (2018). Occurrence and levels of persistent organic pollutants (POPs) in farmed and wild marine fish from Tanzania. A pilot study. *Chemosphere*. Vol. 191, 438-449.
- Nitta, K. H., Takayanagi, M. (1999). Role of tie molecules in the yielding deformation of isotactic polypropylene. *Journal of Polymer Science Part B: Polymer Physics*, 37(4), 357-368.
- Ogata, Y., Takada, H., Mizukawa, K., Hirai, H., Iwasa, S., Endo, S., Mato, Y., Saha, M., Okuda, K., Nakashima, A., Murakami, M., Zurcher, N., Booyatumano, R., Zakaria, M.P., Dung, L. Q., Gordon, M., Miguez, C., Suzuki, S., Moore, C., Karapanagioti, H., Weerts, S., McClurg, T., Burres, E., Smith, W., Van Velkenburg, M., Lang, J. S., Lang, R.C., Laursen, D., Danner, B., Stewardson, N., Thompson, R.C. (2009). International pellet watch: Global monitoring of persistent organic pollutants (POPs) in coastal waters. 1. Initial phase data on PCBs, DDTs, and HCHs. *Marine Pollution Bulletin*. Vol. 58, 1437-1446.
- Pandiyaraj, K. N., Heeg, J., Lampka, A., Junge, F., Barfels, T., Wienecke, M., Rhee, Y. H., Kim, H. W. (2012). In vitro cyto and blood compatibility of titanium containing diamond-like carbon prepared by hybrid sputtering method. *Plasma Science and Technology*, 14(9), 829.
- Phokhaphaiboonsuk, D., Jarupan, L., Pechyen, C., Nandhivajrin, C. (2012). Surface Treatment on Low Density Polyethylene with TiO<sub>2</sub> Nano-Particles for Packaging Printing. *Advanced Materials Research*. Vol. 506, 615–618.
- Prasad, A. (1998). A quantitative analysis of low density polyethylene and linear low density polyethylene blends by differential scanning calorimetry and fourier transform infrared spectroscopy methods. *Polymer Engineering & Science*, 38(10), 1716-1728.
- Praveena, S. M., Aris, A. Z. (2020). Sorptive Properties of Microplastics Extracted from Cosmetics. In: Rocha-Santos T., Costa M., Mouneyrac C. (eds) *Handbook of Microplastics in the Environment*. Springer, Cham. 1-12.
- Qiu, Z., Ikebara, T., Nishi, T. (2003). Poly (hydroxybutyrate)/poly (butylene succinate) blends: miscibility and nonisothermal crystallization. *Polymer*, 44(8), 2503-2508.
- Rios, L. M., Moore, C., Jones, P. R. (2007). Persistent organic pollutants carried by synthetic polymers in the ocean environment. *Marine Pollution Bulletin*. Vol. 54, 1230-1237.
- Ritchie, H., Roser, M. (2018). Plastic Pollution. Published online at OurWorldInData.org. Retrieved from: '<https://ourworldindata.org/plastic-pollution>' [Online Resource].
- Rochman, C. M., Hoh, E., Hentschel, B. T., Kaye, S. (2013). Long-term field measurement of sorption of organic contaminants to five types of plastic Pellets: Implications for plastic marine debris. *Environmental Science & Technology*. Vol. 47, 1646-1654.
- Rodrigues, J. P., Duarte, A. C., Santos-Echeandía, J., Rocha-Santos, T. (2019). Significance of interactions between microplastics and POPs in the marine environment: A critical overview. *TrAC Trends in Analytical Chemistry*. Vol. 111, 252-260.
- Rujnić-Sokele, M. (2015). Plastic waste - A global environmental problem. *Environmental protection*. Vol. 36, 1-2.
- Schwarzenbach, R. P., Gschwend, P. M., Imboden, D. M. (2003). *Environmental Organic Chemistry*, 2nd ed.; Wiley-Interscience: New Jersey.

- Shen, K. (2023). Synthesis, Properties and Applications of Poly (Butylene Succinate). In MATEC Web of Conferences (Vol. 386, p. 01005). EDP Sciences.)
- Smedes, F., Geertsma, R. W., van der Zande, T., Booij, K. (2009). Polymer-water partition coefficients of hydrophobic compounds for passive sampling: Application of cosolvent models for validation. *Environmental Science & Technology*. Vol. 43 (18), 7047-7054.
- Sonne, C., Siebert, U., Gonnen, K., Desforges, J. P., Eulaers, I., Persson, S., Roos, A., Bäcklin, B. M., Kauhala, K., Olsen, M. T., Harding, K. C., Treu, G., Galatius, A., Andersen-Ranberg, E., Gross, S., Lakemeyer, J., Lehnert, K., Lam, S. S., Peng, W., Dietz, R. (2020). Health effects from contaminant exposure in Baltic Sea birds and marine mammals: A review. *Environment International*. Vol. 139, 105725.
- Sørensen, L., Rogers, E., Altin, D., Salaberria, I., Booth, A. M. (2020). Sorption of PAHs to microplastic and their bioavailability and toxicity to marine copepods under co-exposure conditions. *Environmental Pollution*. Vol. 258, 118344.
- Struller, C. F., Kelly, P. J., Copeland, N. J. (2014). Aluminum oxide barrier coatings on polymer films for food packaging applications. *Surface and Coatings Technology*, 241, 130-137.
- Teuten, E. L., Rowland, S. J., Galloway, T. S., Thompson, R. C. (2007). Potential for plastics to transport hydrophobic contaminants. *Environmental Science & Technology*. Vol. 41 (22), 7759-7764.
- Thumsorn, S., Srisawat, N. (2014). Influence of Ethylene Vinyl Acetate Contents on Properties and Crease Recovery of Slit Yarn from Polypropylene/High Density Polyethylene Blend. *Energy Procedia*, 56, 334-341.
- Torres, F.G., Díoses-Salinas, D.C., Pizarro-Ortega, C.I., De-la-Torre, G.E. (2021). Sorption of chemical contaminants on degradable and non-degradable microplastics: Recent progress and research trends. *Science of The Total Environment*. Vol. 757, 143875.
- Türk, O. (2014). Stoffliche Nutzung nachwachsender Rohstoffe. Grundlagen - Werkstoffe - Anwendungen. Wiesbaden: Springer Vieweg.
- Über, T. H. (2019). Adsorption and desorption process on polymers in aquatic system. Dissertation.
- United Nations, Department of Economic and Social Affairs, Population Division (2019). World Population Prospects 2019. Online Edition. Rev. 1.
- Valerio, O., Misra, M., Mohanty, A. K. (2018). Statistical design of sustainable thermoplastic blends of poly (glycerol succinate-co-maleate) (PGSMA), poly (lactic acid) (PLA) and poly (butylene succinate)(PBS). *Polymer Testing*. Vol. 65, 420-428.
- Van, A., Rochmann, C. M., Flores, E. M., Hill, K. L., Vargas, E., Vargas, S. A., Hoh, E. (2012). Persistent organic pollutants in plastic marine debris found on beaches in San Diego, California. *Chemosphere*. Vol. 86, 258–263.
- Verla, A. W., Enyoh, C. E., Verla, E. N. (2019). Microplastics, an Emerging Concern: A Review of Analytical Techniques for Detecting and Quantifying Microplastics Accepted in Analytical Methods in Environmental Chemistry Journal 2(2).
- Wang, F., Zhang, M., Sha, W., Wang, Y., Hao, H., Dou, Y., Li, Y. (2020). Sorption Behavior and Mechanisms of Organic Contaminants to Nano and Microplastics. *Molecules*. Vol. 25 (8), 1827.
- Wang, J., Liu, X., Liu, G. (2019). Sorption behaviors of phenanthrene, nitrobenzene, and naphthalene on mesoplastics and microplastics. *Environmental Science and Pollution Research*. Vol. 26, 12563–12573.
- Wang, L., Zhang, M., Lawson, T., Kanwal, A., Miao, Z. (2019). Poly (butylene succinate-co-salicylic acid) copolymers and their effect on promoting plant growth. *Royal Society Open Science*, 6(7), 190504.

- Wang, W., Wang, J. (2018). Different partition of polycyclic aromatic hydrocarbon on environmental particulates in freshwater: Microplastics in comparison to natural sediment. Ecotoxicity and Environmental Safety. Vol. 147, 648-655.
- Wei, R., Breite, D., Song, C., Gräsing, D., Ploss, T., Hille, P., Schwerdtfeger, R., Matysik, J., Schulze, A., Zimmermann, W. (2019). Biocatalytic Degradation Efficiency of Postconsumer Polyethylene Terephthalate Packaging Determined by Their Polymer Microstructures. Advanced Science. Vol. 6 (14).
- Wu, D., Yuan, L., Laredo, E., Zhang, M., Zhou, W. (2012). Interfacial properties, viscoelasticity, and thermal behaviors of poly (butylene succinate)/polylactide blend. Industrial & engineering chemistry research. Vol. 51(5), 2290-2298.
- Xu, Y., Xu, J., Liu, D., Guo, B., Xie, X., 2008. Synthesis and Characterization of Biodegradable Poly(butylene succinate-co-propylene succinate)s. Journal of Applied Polymer Science. Vol. 109, 1881-1889.
- Yamashita, R., Tanaka, K., Geok Yeo, B., Takada, H., van Franeker, J.A., Dalton, M., Dale, E. (2018). Hazardous Chemicals in Plastics in Marine Environments: International Pellet Watch. The Handbook of Environmental Chemistry. Vol. 78, Springer, Berlin, Heidelberg.
- Yan, J., Wang, L. (2004). Photomutagenicity of 16 polycyclic aromatic hydrocarbons from the USEPA priority pollutant list. Mutation Research. Vol. 557, 99-108.
- Yang, C. G., Wang, M. H., Zhang, M. X., Li, X. H., Wang, H. L., Xing, Z., Ye, L. F., Wu, G. Z. (2016). Supercritical CO<sub>2</sub> foaming of radiation cross-linked isotactic polypropylene in the presence of TAIC. Molecules. Vol. 21(12), 1660.
- Yang, C. H. (1998). Statistical mechanical study on the Freundlich isotherm equation. Journal of colloid and interface science, 208(2), 379-387.
- Yang, L., Chen, J., Guo, Y., Zhang, Z. (2009). Surface modification of a biomedical polyethylene terephthalate (PET) by air plasma. Applied Surface Science. Volume 255 (8), 4446-4451.
- Yeo, B. G., Takada, H., Hosoda, J., Kondo, A., Yamashita, R., Saha, M., Maes, T. (2017). Polycyclic aromatic hydrocarbons (PAHs) and hopanes in plastic resin pellets as markers of oil pollution via international pellet watch monitoring. Archives of environmental contamination and toxicology, 73, 196-206.
- Young, T. M., Weber Jr., W. J. (1995). A distributed reactivity model for sorption by soils and sediments. 3. Effects of diagenetic processes on sorption energetics. Environmental Science and Technology. Vol. 29, 92-97.
- Zaky, M. T., Mohamed, N. H. (2010). Influence of low-density polyethylene on the thermal characteristics and crystallinity of high melting point macro-and micro-crystalline waxes. Thermochimica acta, 499(1-2), 79-84.)
- Zhang, Y., Lu, B., Lv, F., Guo, W., Ji, J., Chu, P. K., Zhang, C. (2012). Effect of processing conditions on poly (butylene succinate) foam materials. Journal of applied polymer science, 126(2), 756-761.
- Zhao, L., Rong, L., Xu, J., Lian, J., Wang, L., Sun, H. (2020). Sorption of five organic compounds by polar and nonpolar microplastics. Chemosphere. Vol. 257, 127206.
- Zhu, T., Jafvert, C. T., Fu, D., Hu, Y. (2015). A novel method for measuring polymer-water partition coefficients. Chemosphere. Vol. 138, 973-979.
- Zuo, L. Z., Li, H. X., Lin, L., Sun, Y. X., Diao, Z. H., Liu, S., Zhang, Z. Y., Xu, X. R. (2019). Sorption and desorption of phenanthrene on biodegradable poly(butylene adipate co-terephthalate) microplastics. Chemosphere. Vol. 215, 25-32.

---

## 10. List of posters (June 2023)

---

Gottschling, M., Zhou, Y., Schwabe, I., Bui, T.Q., Oyen, A. van, Schebek, L., Sakaguchi-Söder, K., (2018). *Comparison of one-time spiking, multiple spiking and dialysis tubing methods for the determination of plastic-water partition coefficient of one polycyclic hydrocarbons on microplastic.* In: MICRO 2018 Fate and Impact of Microplastics: Knowledge, Actions and Solutions; conference proceedings, S. 312-312, Lanzarote, Spain, MICRO 2018, Fate and Impact of Microplastics: Knowledge, Actions and Solutions, Lanzarote, Spain. [Konferenzveröffentlichung]

Gottschling, M., Zhou, Y., Schwabe, I., Sakaguchi-Söder, K., Oyen, A. van, Schebek, L., (2018). *Comparison of spiking and dialysis tubing methods for the determination of sorption capacity and plastic-water partition coefficient of three different polycyclic hydrocarbons on microplastic.* Rom, SETAC. [Konferenzveröffentlichung]

Gottschling, M., Sakaguchi-Söder, K., Oyen, A. van, Schebek, L. (2017). *Investigation of the effect of plastic additives on the plastic-water partition coefficient of selected persistent organic pollutants (POPs) in batch tests.* SETAC Europe 28th Annual Meeting, Brüssel. [Konferenzveröffentlichung]

Gottschling, M., Zhou, Y., Schwabe, I., Bui T.Q., Heide, J., Oyen, A. van, Sakaguchi-Söder, Schebek, L., K., (2018). *Wie lassen sich aus einem Zusammenhang stoffspezifischer Parameter ausgewählter Schadstoffe und MP Verteilungskoeffizienten ableiten?* In: Umwelt 2018: Tagungsband, S. 123, Münster, SETAC GLB: Umwelt 2018. [Konferenzveröffentlichung]

---

## 11. Appendices

---

<b>Chapter 1</b> .....	A-IX
Table A1.1: log $K_{PE-w}$ of selected PAHs ( $L \text{ kg}^{-1}$ ) .....	A-IX
Table A1.2: polymer-water partition coefficient of selected PAHs ( $L \text{ kg}^{-1}$ ) .....	A-IX
<b>Chapter 2</b> .....	A-X
Table A2.1: values of $\log K_{ow}$ , MW, $\log C_w^{\text{sat}}$ and $\log K_{hdw}$ used in this thesis .....	A-X
<b>Chapter 4</b> .....	A-XI
Table A4.1: pseudo-first-order and pseudo-second-order model parameters for PAH adsorption on MP.....	A-XI
Table A4.2: Glass adsorption determination of each concentration series and experimental series for naphthalene (NAPH) in duplicates.....	A-XII
Table A4.3: Glass adsorption determination of each concentration series and experimental series for fluorene (FLN) in duplicates .....	A-XII
Table A4.4: Glass adsorption determination of each concentration series and experimental series for phenanthrene (PHEN) in duplicates .....	A-XII
<b>Chapter 5</b> .....	A-XIII
Table A5.1: $\log K_{ow}$ and $\log K_{LDPE-w}$ ( $L \text{ kg}^{-1}$ ) of selected PAHs .....	A-XIII
Table A5.2: $\log K_{ow}$ and $\log K_{PP-w}$ ( $L \text{ kg}^{-1}$ ) of selected PAHs .....	A-XIII
Table A5.3: $\log K_{ow}$ and $\log K_{PET-w}$ ( $L \text{ kg}^{-1}$ ) of selected PAHs .....	A-XIV
Table A5.4: MW ( $\text{g mol}^{-1}$ ) and $\log K_{LDPE-w}$ ( $L \text{ kg}^{-1}$ ) of selected PAHs .....	A-XIV
Table A5.5: MW ( $\text{g mol}^{-1}$ ) and $\log K_{PP-w}$ ( $L \text{ kg}^{-1}$ ) of selected PAHs .....	A-XV
Table A5.6: MW ( $\text{g mol}^{-1}$ ) and $\log K_{PET-w}$ ( $L \text{ kg}^{-1}$ ) of selected PAHs .....	A-XV
<b>Chapter 6</b> .....	A-XVI
Figure A6.1: DSC Analysis of LDPE .....	A-XVI
Figure A6.2: DSC Analysis of PP .....	A-XVI
Figure A6.3: DSC Analysis of PBS .....	A-XVII
Figure A6.4: DSC Analysis of PET .....	A-XVII
Table A6.1: Results of DSC Analysis for LDPE, PP, PBS and PET .....	A-XVIII
Figure A6.5: Evaluating the BET surface area of LDPE .....	A-XVIII
Figure A6.6: Evaluating the BET surface area of PP .....	A-XIX
Figure A6.7: Evaluating the BET surface area of PBS .....	A-XIX
Figure A6.8: Evaluating the BET surface area of PET .....	A-XX
Figure A6.9: Evaluating the pore volume of LDPE .....	A-XX
Figure A6.10: Evaluating the pore volume of PP .....	A-XX
Figure A6.11: Evaluating the pore volume of PBS .....	A-XXI
Figure A6.12: Evaluating the pore volume of PET .....	A-XXII
Appendices	A-II

Table A6.2: Results of particle size distribution ( $d_{50}$ ) with Malvern Unit for LDPE .....	A-XXII
Table A6.3: Results of particle size distribution ( $d_{50}$ ) with Malvern Unit for PP .....	A-XXII
Table A6.4: Results of particle size distribution ( $d_{50}$ ) with Malvern Unit for PBS .....	A-XXIII
Table A6.5: Results of particle size distribution ( $d_{50}$ ) with Malvern Unit for PET .....	A-XXIII
Table A6.6: Determination of correlation coefficients for plastic properties and $\log K_{p-w}$ values .....	A-XXIII
<b>Chapter 7 .....</b>	<b>A-XXIV</b>
Table A7.1 Calculation of $R_h^2$ and $R_v^2$ with the matrix of one PAH property multiplied with two plastic properties ( $\rho^{-1}$ as fixed parameter) and the $\log K_{p-w}$ matrix .....	A-XXIV
Table A7.2: Calculation of $R_h^2$ and $R_v^2$ with the matrix of one PAH property multiplied with two plastic properties ( $d_{50}^{-1}$ as fixed parameter) and the $\log K_{p-w}$ matrix .....	A-XXIV
Table A7.3: Calculation of $R_h^2$ and $R_v^2$ with the matrix of one PAH property multiplied with two plastic properties ( $d_{50}^{-1}$ as fixed parameter), and the $\log K_{p-w}$ matrix .....	A-XXIV
Table A7.4: Calculation of $R_h^2$ and $R_v^2$ with the matrix of one PAH property multiplied with two plastic properties ( $T_m$ as fixed parameter), and the $\log K_{p-w}$ matrix .....	A-XXV
Table A7.5: Calculation of $R_h^2$ and $R_v^2$ with the matrix of one PAH property multiplied with two plastic properties ( $T_m^{-1}$ as fixed parameter) and the $\log K_{p-w}$ matrix.....	A-XXV
Table A7.6: Calculation of $R_h^2$ and $R_v^2$ with the matrix of one PAH property multiplied with two plastic properties ( $T_g$ as fixed parameter) and the $\log K_{p-w}$ matrix .....	A-XXV
Table A7.7: Calculation of $R_h^2$ and $R_v^2$ with the matrix of one PAH property multiplied with two plastic properties ( $T_g^{-1}$ as fixed parameter) and the $\log K_{p-w}$ matrix .....	A-XXVI
Table A7.8: Calculation of $R_h^2$ and $R_v^2$ with the matrix of one PAH property multiplied with two plastic properties ( $X_c$ as fixed parameter) and the $\log K_{p-w}$ matrix .....	A-XXVI
Table A7.9: Calculation of $R_h^2$ and $R_v^2$ with the matrix of one PAH property multiplied with two plastic properties ( $X_c^{-1}$ as fixed parameter) and the $\log K_{p-w}$ matrix .....	A-XXVI
Table A7.10: Calculation of $R_h^2$ and $R_v^2$ with the matrix of one PAH property multiplied with two plastic properties (SA as fixed parameter), and the $\log K_{p-w}$ matrix .....	A-XXVII
Table A7.11: Calculation of $R_h^2$ and $R_v^2$ with the matrix of one PAH property multiplied with two plastic properties (SA $^{-1}$ as fixed parameter) and the $\log K_{p-w}$ matrix .....	A-XXVII
Table A7.12: Calculation of $R_h^2$ and $R_v^2$ with the matrix of one PAH property multiplied with two plastic properties (Vp as fixed parameter) and the $\log K_{p-w}$ matrix .....	A-XXVII
Table A7.13: Calculation of $R_h^2$ and $R_v^2$ with the matrix of one PAH property multiplied with two plastic properties (Vp $^{-1}$ as fixed parameter) and the $\log K_{p-w}$ matrix .....	A-XXVIII
Table A7.14: Calculation of $R_h^2$ and $R_v^2$ with the matrix of one PAH property multiplied with two plastic properties ( $\sum SFE$ as fixed parameter) and the $\log K_{p-w}$ matrix .....	A-XXVIII
Table A7.15: Calculation of $R_h^2$ and $R_v^2$ with the matrix of one PAH property multiplied with two plastic properties ( $\sum SFE^{-1}$ as fixed parameter) and the $\log K_{p-w}$ matrix .....	A-XXVIII
Table A7.16: Calculation of $R_h^2$ and $R_v^2$ with the matrix of two PAH properties ( $\log K_{ow}$ , MW) multiplied with two plastic properties ( $X_c$ as fixed parameter) and the $\log K_{p-w}$ matrix .....	A-XXIX
Table A7.17: Calculation of $R_h^2$ and $R_v^2$ with the matrix of two PAH properties ( $\log K_{ow}$ , $\log K_{hdw}$ ) multiplied with two plastic properties ( $X_c$ as fixed parameter) and the $\log K_{p-w}$ matrix .....	A-XXIX

- Table A7.18: Calculation of  $R_h^2$  and  $R_v^2$  with the matrix of two PAH properties ( $\log K_{ow}$ ,  $\log C_w^{sat}$ ) multiplied with two plastic properties ( $X_c$  as fixed parameter), and the  $\log K_{p-w}$  matrix ..... A-XXIX
- Table A7.19: Calculation of  $R_h^2$  and  $R_v^2$  with the matrix of two PAH properties (MW,  $\log K_{hdw}$ ) multiplied with two plastic properties ( $X_c$  as fixed parameter) and the  $\log K_{p-w}$  matrix ..... A-XXX
- Table A7.20: Calculation of  $R_h^2$  and  $R_v^2$  with the matrix of two PAH properties (MW,  $\log C_w^{sat}$ ) multiplied with two plastic properties ( $X_c$  as fixed parameter) and the  $\log K_{p-w}$  matrix ..... A-XXX
- Table A7.21: Calculation of  $R_h^2$  and  $R_v^2$  with the matrix of two PAH properties ( $\log K_{hdw}$ ,  $\log C_w^{sat}$ ) multiplied with two plastic properties ( $X_c$  as fixed parameter) and the  $\log K_{p-w}$  matrix ..... A-XXX
- Table A7.22: Calculation of  $R_h^2$  and  $R_v^2$  with the matrix of two PAH properties ( $\log K_{ow}$ , MW,) multiplied with two plastic properties ( $T_m$  as fixed parameter) and the  $\log K_{p-w}$  matrix ..... A-XXXI
- Table A7.23: Calculation of  $R_h^2$  and  $R_v^2$  with the matrix of two PAH properties ( $\log K_{ow}$ ,  $\log K_{hdw}$ ) multiplied with two plastic properties ( $T_m$  as fixed parameter) and the  $\log K_{p-w}$  matrix ..... A-XXXI
- Table A7.24: Calculation of  $R_h^2$  and  $R_v^2$  with the matrix of two PAH properties ( $\log K_{ow}$ ,  $\log C_w^{sat}$ ) multiplied with two plastic properties ( $T_m$  as fixed parameter) and the  $\log K_{p-w}$  matrix ..... A-XXXI
- Table A7.25: Calculation of  $R_h^2$  and  $R_v^2$  with the matrix of two PAH properties (MW,  $\log K_{hdw}$ ) multiplied with two plastic properties ( $T_m$  as fixed parameter) and the  $\log K_{p-w}$  matrix ..... A-XXXII
- Table A7.26: Calculation of  $R_h^2$  and  $R_v^2$  with the matrix of two PAH properties (MW,  $\log C_w^{sat}$ ) multiplied with two plastic properties ( $T_m$  as fixed parameter) and the  $\log K_{p-w}$  matrix ..... A-XXXII
- Table A7.27: Calculation of  $R_h^2$  and  $R_v^2$  with the matrix of two PAH properties ( $\log K_{hdw}$ ,  $\log C_w^{sat}$ ) multiplied with two plastic properties ( $T_m$  as fixed parameter) and the  $\log K_{p-w}$  matrix ..... A-XXXII
- Table A7.28: Calculation of  $R_h^2$  and  $R_v^2$  with the matrix of two PAH properties ( $\log K_{ow}$  , MW,) multiplied with two plastic properties ( $T_m^{-1}$  as fixed parameter) and the  $\log K_{p-w}$  matrix ..... A-XXXIII
- Table A7.29: Calculation of  $R_h^2$  and  $R_v^2$  with the matrix of two PAH properties ( $\log K_{ow}$ ,  $\log K_{hdw}$ ) multiplied with two plastic properties ( $T_m^{-1}$  as fixed parameter) and the  $\log K_{p-w}$  matrix ..... A-XXXIII
- Table A7.30: Calculation of  $R_h^2$  and  $R_v^2$  with the matrix of two PAH properties ( $\log K_{ow}$ ,  $\log C_w^{sat}$ ) multiplied with two plastic properties ( $T_m^{-1}$  as fixed parameter) and the  $\log K_{p-w}$  matrix ..... A-XXXIII
- Table A7.31: Calculation of  $R_h^2$  and  $R_v^2$  with the matrix of two PAH properties (MW,  $\log K_{hdw}$ ) multiplied with two plastic properties ( $T_m^{-1}$  as fixed parameter) and the  $\log K_{p-w}$  matrix ..... A-XXXIV
- Table A7.32: Calculation of  $R_h^2$  and  $R_v^2$  with the matrix of two PAH properties (MW,  $\log C_w^{sat}$ ) multiplied with two plastic properties ( $T_m^{-1}$  as fixed parameter) and the  $\log K_{p-w}$  matrix ..... A-XXXIV
- Table A7.33: Calculation of  $R_h^2$  and  $R_v^2$  with the matrix of two PAH properties ( $\log K_{hdw}$ ,  $\log C_w^{sat}$ ) multiplied with two plastic properties ( $T_m^{-1}$  as fixed parameter) and the  $\log K_{p-w}$  matrix ..... A-XXXIV
- Table A7.34: Calculation of  $R_h^2$  and  $R_v^2$  with the matrix of two PAH properties ( $\log K_{ow}$ , MW,) multiplied with three plastic properties ( $X_c * \rho$  as fixed parameters) and the  $\log K_{p-w}$  matrix ... A-XXXV
- Table A7.35: Calculation of  $R_h^2$  and  $R_v^2$  with the matrix of two PAH properties ( $\log K_{ow}$ ,  $\log K_{hdw}$ ) multiplied with three plastic properties ( $X_c * \rho$  as fixed parameters) and the  $\log K_{p-w}$  matrix ... A-XXXV
- Table A7.36: Calculation of  $R_h^2$  and  $R_v^2$  with the matrix of two PAH properties ( $\log K_{ow}$ ,  $\log C_w^{sat}$ ) multiplied with three plastic properties ( $X_c * \rho$  as fixed parameters) and the  $\log K_{p-w}$  matrix ... A-XXXV
- Table A7.37: Calculation of  $R_h^2$  and  $R_v^2$  with the matrix of two PAH properties (MW,  $\log K_{hdw}$ ) multiplied with three plastic properties ( $X_c * \rho$  as fixed parameters) and the  $\log K_{p-w}$  matrix ... A-XXXVI
- Table A7.38: Calculation of  $R_h^2$  and  $R_v^2$  with the matrix of two PAH properties (MW,  $\log C_w^{sat}$ ) multiplied with three plastic properties ( $X_c * \rho$  as fixed parameters) and the  $\log K_{p-w}$  matrix ... A-XXXVI

Table A7.39: Calculation of $R_h^2$ and $R_v^2$ with the matrix of two PAH properties ( $\log K_{hdw}$ , $\log C_w^{sat}$ ) multiplied with three plastic properties ( $X_c * \rho$ as fixed parameters) and the $\log K_{p-w}$ matrix ...	A-XXXVI
Table A7.40: Calculation of $R_h^2$ and $R_v^2$ with the matrix of two PAH properties ( $\log K_{ow}$ , MW,) multiplied with three plastic properties ( $X_c * \rho^{-1}$ as fixed parameters) and the $\log K_{p-w}$ matrix .....	A-XXXVII
Table A7.41: Calculation of $R_h^2$ and $R_v^2$ with the matrix of two PAH properties ( $\log K_{ow}$ , $\log K_{hdw}$ ) multiplied with three plastic properties ( $X_c * \rho^{-1}$ as fixed parameters) and the $\log K_{p-w}$ matrix .....	A-XXXVII
Table A7.42: Calculation of $R_h^2$ and $R_v^2$ with the matrix of two PAH properties ( $\log K_{ow}$ , $\log C_w^{sat}$ ) multiplied with three plastic properties ( $X_c * \rho^{-1}$ as fixed parameters) and the $\log K_{p-w}$ matrix .....	A-XXXVII
Table A7.43: Calculation of $R_h^2$ and $R_v^2$ with the matrix of two PAH properties (MW, $\log K_{hdw}$ ) multiplied with three plastic properties ( $X_c * \rho^{-1}$ as fixed parameters) and the $\log K_{p-w}$ matrix .....	A-XXXVIII
Table A7.44: Calculation of $R_h^2$ and $R_v^2$ with the matrix of two PAH properties (MW, $\log C_w^{sat}$ ) multiplied with three plastic properties ( $X_c * \rho^{-1}$ as fixed parameters) and the $\log K_{p-w}$ matrix .....	A-XXXVIII
Table A7.45: Calculation of $R_h^2$ and $R_v^2$ with the matrix of two PAH properties ( $\log K_{hdw}$ , $\log C_w^{sat}$ ) multiplied with three plastic properties ( $X_c * \rho^{-1}$ as fixed parameters) and the $\log K_{p-w}$ matrix .....	A-XXXVIII
Table A7.46: Calculation of $R_h^2$ and $R_v^2$ with the matrix of two PAH properties ( $\log K_{ow}$ , MW,) multiplied with three plastic properties ( $X_c * d_{50}$ as fixed parameters) and the $\log K_{p-w}$ matrix .....	A-XXXIX
Table A7.47: Calculation of $R_h^2$ and $R_v^2$ with the matrix of two PAH properties ( $\log K_{ow}$ , $\log K_{hdw}$ ) multiplied with three plastic properties ( $X_c * d_{50}$ as fixed parameters) and the $\log K_{p-w}$ matrix .....	A-XXXIX
Table A7.48: Calculation of $R_h^2$ and $R_v^2$ with the matrix of two PAH properties ( $\log K_{ow}$ , $\log C_w^{sat}$ ) multiplied with three plastic properties ( $X_c * d_{50}$ as fixed parameters) and the $\log K_{p-w}$ matrix .....	A-XXXIX
Table A7.49: Calculation of $R_h^2$ and $R_v^2$ with the matrix of two PAH properties (MW, $\log K_{hdw}$ ) multiplied with three plastic properties ( $X_c * d_{50}$ as fixed parameters) and the $\log K_{p-w}$ matrix ....	A-XL
Table A7.50: Calculation of $R_h^2$ and $R_v^2$ with the matrix of two PAH properties (MW, $\log C_w^{sat}$ ) multiplied with three plastic properties ( $X_c * d_{50}$ as fixed parameters) and the $\log K_{p-w}$ matrix ....	A-XL
Table A7.51: Calculation of $R_h^2$ and $R_v^2$ with the matrix of two PAH properties ( $\log K_{hdw}$ , $\log C_w^{sat}$ ) multiplied with three plastic properties ( $X_c * d_{50}$ as fixed parameters) and the $\log K_{p-w}$ matrix ....	A-XL
Table A7.52: Calculation of $R_h^2$ and $R_v^2$ with the matrix of two PAH properties ( $\log K_{ow}$ , MW,) multiplied with three plastic properties ( $X_c * d_{50}^{-1}$ as fixed parameters) and the $\log K_{p-w}$ matrix ..	A-XLI
Table A7.53: Calculation of $R_h^2$ and $R_v^2$ with the matrix of two PAH properties ( $\log K_{ow}$ , $\log K_{hdw}$ ) multiplied with three plastic properties ( $X_c * d_{50}^{-1}$ as fixed parameters) and the $\log K_{p-w}$ matrix ..	A-XLI
Table A7.54: Calculation of $R_h^2$ and $R_v^2$ with the matrix of two PAH properties ( $\log K_{ow}$ , $\log C_w^{sat}$ ) multiplied with three plastic properties ( $X_c * d_{50}^{-1}$ as fixed parameters) and the $\log K_{p-w}$ matrix ..	A-XLI
Table A7.55: Calculation of $R_h^2$ and $R_v^2$ with the matrix of two PAH properties (MW, $\log K_{hdw}$ ) multiplied with three plastic properties ( $X_c * d_{50}^{-1}$ as fixed parameters) and the $\log K_{p-w}$ matrix ..	A-XLII

Table A7.56: Calculation of $R_h^2$ and $R_v^2$ with the matrix of two PAH properties (MW, $\log C_w^{\text{sat}}$ ) multiplied with three plastic properties ( $X_c * d_{50}^{-1}$ as fixed parameters) and the $\log K_{p-w}$ matrix ..	A-XLII
Table A7.57: Calculation of $R_h^2$ and $R_v^2$ with the matrix of two PAH properties ( $\log K_{\text{hdw}}$ , $\log C_w^{\text{sat}}$ ) multiplied with three plastic properties ( $X_c * d_{50}^{-1}$ as fixed parameters) and the $\log K_{p-w}$ matrix ..	A-XLII
Table A7.58: Calculation of $R_h^2$ and $R_v^2$ with the matrix of two PAH properties ( $\log K_{\text{ow}}$ , MW,) multiplied with three plastic properties ( $X_c * T_m$ as fixed parameters) and the $\log K_{p-w}$ matrix ..	A-XLIII
Table A7.59: Calculation of $R_h^2$ and $R_v^2$ with the matrix of two PAH properties ( $\log K_{\text{ow}}$ , $\log K_{\text{hdw}}$ ) multiplied with three plastic properties ( $X_c * T_m$ as fixed parameters) and the $\log K_{p-w}$ matrix ..	A-XLIII
Table A7.60: Calculation of $R_h^2$ and $R_v^2$ with the matrix of two PAH properties ( $\log K_{\text{ow}}$ , $\log C_w^{\text{sat}}$ ) multiplied with three plastic properties ( $X_c * T_m$ as fixed parameters) and the $\log K_{p-w}$ matrix ..	A-XLIII
Table A7.61: Calculation of $R_h^2$ and $R_v^2$ with the matrix of two PAH properties (MW, $\log K_{\text{hdw}}$ ) multiplied with three plastic properties ( $X_c * T_m$ as fixed parameters) and the $\log K_{p-w}$ matrix ..	A-XLIV
Table A7.62: Calculation of $R_h^2$ and $R_v^2$ with the matrix of two PAH properties (MW, $\log C_w^{\text{sat}}$ ) multiplied with three plastic properties ( $X_c * T_m$ as fixed parameters) and the $\log K_{p-w}$ matrix ..	A-XLIV
Table A7.63: Calculation of $R_h^2$ and $R_v^2$ with the matrix of two PAH properties ( $\log K_{\text{hdw}}$ , $\log C_w^{\text{sat}}$ ) multiplied with three plastic properties ( $X_c * T_m$ as fixed parameters) and the $\log K_{p-w}$ matrix ..	A-XLIV
Table A7.64: Calculation of $R_h^2$ and $R_v^2$ with the matrix of two PAH properties ( $\log K_{\text{ow}}$ , MW,) multiplied with three plastic properties ( $X_c * T_m^{-1}$ as fixed parameters) and the $\log K_{p-w}$ matrix ..	A-XLV
Table A7.65: Calculation of $R_h^2$ and $R_v^2$ with the matrix of two PAH properties ( $\log K_{\text{ow}}$ , $\log K_{\text{hdw}}$ ) multiplied with three plastic properties ( $X_c * T_m^{-1}$ as fixed parameters) and the $\log K_{p-w}$ matrix ..	A-XLV
Table A7.66: Calculation of $R_h^2$ and $R_v^2$ with the matrix of two PAH properties ( $\log K_{\text{ow}}$ , $\log C_w^{\text{sat}}$ ) multiplied with three plastic properties ( $X_c * T_m^{-1}$ as fixed parameters) and the $\log K_{p-w}$ matrix ..	A-XLV
Table A7.67: Calculation of $R_h^2$ and $R_v^2$ with the matrix of two PAH properties (MW, $\log K_{\text{hdw}}$ ) multiplied with three plastic properties ( $X_c * T_m^{-1}$ as fixed parameters) and the $\log K_{p-w}$ matrix ..	A-XLVI
Table A7.68: Calculation of $R_h^2$ and $R_v^2$ with the matrix of two PAH properties (MW, $\log C_w^{\text{sat}}$ ) multiplied with three plastic properties ( $X_c * T_m^{-1}$ as fixed parameters) and the $\log K_{p-w}$ matrix ..	A-XLVI
Table A7.69: Calculation of $R_h^2$ and $R_v^2$ with the matrix of two PAH properties ( $\log K_{\text{hdw}}$ , $\log C_w^{\text{sat}}$ ) multiplied with three plastic properties ( $X_c * T_m^{-1}$ as fixed parameters) and the $\log K_{p-w}$ matrix ..	A-XLVI
Table A7.70: Calculation of $R_h^2$ and $R_v^2$ with the matrix of two PAH properties ( $\log K_{\text{ow}}$ , MW,) multiplied with three plastic properties ( $X_c * T_g$ as fixed parameters) and the $\log K_{p-w}$ matrix ..	A-XLVII
Table A7.71: Calculation of $R_h^2$ and $R_v^2$ with the matrix of two PAH properties ( $\log K_{\text{ow}}$ , $\log K_{\text{hdw}}$ ) multiplied with three plastic properties ( $X_c * T_g$ as fixed parameters) and the $\log K_{p-w}$ matrix ..	A-XLVII
Table A7.72: Calculation of $R_h^2$ and $R_v^2$ with the matrix of two PAH properties ( $\log K_{\text{ow}}$ , $\log C_w^{\text{sat}}$ ) multiplied with three plastic properties ( $X_c * T_g$ as fixed parameters) and the $\log K_{p-w}$ matrix ..	A-XLVII
Table A7.73: Calculation of $R_h^2$ and $R_v^2$ with the matrix of two PAH properties (MW, $\log K_{\text{hdw}}$ ) multiplied with three plastic properties ( $X_c * T_g$ as fixed parameters) and the $\log K_{p-w}$ matrix ..	A-XLVII



Table A7.93: Calculation of $R_h^2$ and $R_v^2$ with the matrix of two PAH properties ( $\log K_{hdw}$ , $\log C_w^{sat}$ ) multiplied with three plastic properties ( $X_c * SA^{-1}$ as fixed parameters) and the $\log K_{p-w}$ matrix ..	A-LII
Table A7.94: Calculation of $R_h^2$ and $R_v^2$ with the matrix of two PAH properties ( $\log K_{ow}$ , MW,) multiplied with three plastic properties ( $X_c * Vp$ as fixed parameters) and the $\log K_{p-w}$ matrix ..	A-LIII
Table A7.95: Calculation of $R_h^2$ and $R_v^2$ with the matrix of two PAH properties ( $\log K_{ow}$ , $\log K_{hdw}$ ) multiplied with three plastic properties ( $X_c * Vp$ as fixed parameters) and the $\log K_{p-w}$ matrix ...	A-LIII
Table A7.96: Calculation of $R_h^2$ and $R_v^2$ with the matrix of two PAH properties ( $\log K_{ow}$ , $\log C_w^{sat}$ ) multiplied with three plastic properties ( $X_c * Vp$ as fixed parameters) and the $\log K_{p-w}$ matrix ...	A-LIII
Table A7.97: Calculation of $R_h^2$ and $R_v^2$ with the matrix of two PAH properties (MW, $\log K_{hdw}$ ) multiplied with three plastic properties ( $X_c * Vp$ as fixed parameters) and the $\log K_{p-w}$ matrix ...	A-LIII
Table A7.98: Calculation of $R_h^2$ and $R_v^2$ with the matrix of two PAH properties (MW, $\log C_w^{sat}$ ) multiplied with three plastic properties ( $X_c * Vp$ as fixed parameters) and the $\log K_{p-w}$ matrix ...	A-LIII
Table A7.99: Calculation of $R_h^2$ and $R_v^2$ with the matrix of two PAH properties ( $\log K_{hdw}$ , $\log C_w^{sat}$ ) multiplied with three plastic properties ( $X_c * Vp$ as fixed parameters) and the $\log K_{p-w}$ matrix ...	A-LIV
Table A7.100: Calculation of $R_h^2$ and $R_v^2$ with the matrix of two PAH properties ( $\log K_{ow}$ , MW,) multiplied with three plastic properties ( $X_c * Vp^{-1}$ as fixed parameters) and the $\log K_{p-w}$ matrix .	A-LIV
Table A7.101: Calculation of $R_h^2$ and $R_v^2$ with the matrix of two PAH properties ( $\log K_{ow}$ , $\log K_{hdw}$ ) multiplied with three plastic properties ( $X_c * Vp^{-1}$ as fixed parameters) and the $\log K_{p-w}$ matrix .	A-LIV
Table A7.102: Calculation of $R_h^2$ and $R_v^2$ with the matrix of two PAH properties ( $\log K_{ow}$ , $\log C_w^{sat}$ ) multiplied with three plastic properties ( $X_c * Vp^{-1}$ as fixed parameters) and the $\log K_{p-w}$ matrix .	A-LIV
Table A7.103: Calculation of $R_h^2$ and $R_v^2$ with the matrix of two PAH properties (MW, $\log K_{hdw}$ ) multiplied with three plastic properties ( $X_c * Vp^{-1}$ as fixed parameters) and the $\log K_{p-w}$ matrix .	A-LIV
Table A7.104: Calculation of $R_h^2$ and $R_v^2$ with the matrix of two PAH properties (MW, $\log C_w^{sat}$ ) multiplied with three plastic properties ( $X_c * Vp^{-1}$ as fixed parameters) and the $\log K_{p-w}$ matrix ..	A-LV
Table A7.105: Calculation of $R_h^2$ and $R_v^2$ with the matrix of two PAH properties ( $\log K_{hdw}$ , $\log C_w^{sat}$ ) multiplied with three plastic properties ( $X_c * Vp^{-1}$ as fixed parameters) and the $\log K_{p-w}$ matrix ..	A-LV
Table A7.106: n = 100 published $\log K_{LDPE-w/PE-w}$ ( $L \text{ kg}^{-1}$ ), which are the basis for the calculation of the RMSE .....	A-LV
Table A7.107: Calculation of RMSE for selected equations from method 1 and n = 100 published data listed in Table A7.106 .....	A-LVI
Table A7.108: plastic-water partition coefficient of selected PAHs for PP, PBS and PET .....	A-LVII
<b>References of Appendix .....</b>	<b>A-LVIII</b>

## Chapter 1

Table A1.1: log K<sub>PE-W</sub> of selected PAHs (L kg<sup>-1</sup>)

Compound	Booij et al., 2003		Adams et al., 2007	Karapanagioti et al., 2008	Cornelissen et al., 2008	Fernandez et al., 2009	Smedes et al., 2009	Hale et al., 2010	Bao et al., 2012	Choi et al., 2013	Zhu et al., 2015	Wang et al., 2019
	13 °C	30 °c										
naphthalene					3.04		2.81			3.23	2.94	2.84
acenaphthylene						3.16					3.85	
acenaphthene	3.81	3.52				3.62		4.25	3.53	3.94		
fluorene					3.78		3.77	4.51	3.67	4.14		
phenanthrene	4.41	4.12	4.30	3.96	4.14	4.30	4.22	4.20	4.78	4.04	4.22	4.08
anthracene	5.09	4.71			4.37	4.30	4.33	4.40		4.15	4.50	
fluoranthene			4.90		4.85	4.90	4.93		4.93	4.75	5.05	
pyrene	5.23	4.86	5.00			4.70	5.10	5.10	5.07	4.89	5.50	
benzo(a)anthracene	5.53	5.48	5.70		5.62	5.50	5.73		5.79	5.43	6.35	
chrysene	5.64	5.49	5.70		5.56	5.50	5.78		5.70	5.51	5.99	
benzo(b)fluoranthene					6.06	6.30	6.66		6.33	6.06	6.46	
benzo(k)fluoranthene					6.07	6.30	6.66		6.56	6.16	6.44	
benzo(a)pyrene	5.73	6.06			6.22	6.50	6.75			6.14	6.39	
dibenz(a,h)anthracene							7.32		7.20	6.30	7.39	
benzo(g,h,i)perylene					5.81		7.27		7.36	6.23	7.20	
indeno(1,2,3-cd)pyrene					6.01		7.40		7.04	6.50	7.19	

Table A1.2: polymer-water partition coefficient of selected PAHs (L kg<sup>-1</sup>)

Compound	Teuten et al., 2007	Karapanagioti et al., 2008	Lee et al., 2014 <sup>a</sup>	Wang et al., 2019	Zhao et al., 2020	Lončarski et al., 2021 <sup>b</sup>
	log K <sub>PP-W</sub>	log K <sub>PP-W</sub>	log K <sub>PP-W</sub>	log K <sub>PP-W</sub>	log K <sub>PBS-W</sub>	log K <sub>PET-W</sub>
naphthalene				4.06		4.39
fluorene						4.55
phenanthrene	3.33	2.43	3.73	4.18	4.92	
anthracene			4.05			
fluoranthene			4.54			4.43
pyrene			4.55		5.04	4.95
chrysene			5.25			
benzo(a)pyrene			5.85			
dibenz(a,h)anthracene			6.76			
benzo(g,h,i)perylene			6.49			

<sup>a</sup> seawater log K<sub>PP-SW</sub> values were converted to freshwater log K<sub>PP-W</sub> using the Setschenow constant by Jonker and Muijs (2010); <sup>b</sup> Freundlich partition coefficient was selected

## Chapter 2

Table A2.1: values of log K<sub>ow</sub>, MW, log C<sub>w</sub><sup>sat</sup> and log K<sub>hdw</sub> used in this thesis

no.	PAH	log K <sub>ow</sub> <sup>1</sup> (-)	MW (g mol <sup>-1</sup> )	log C <sub>w</sub> <sup>sat</sup> (mol m <sup>-3</sup> )	log K <sub>hdw</sub> (-)
1	naphthalene	3.37	128.18	-0.01	3.65
2	acenaphthylene	3.93	152.20	-0.78	4.33
3	acenaphthene	3.92	154.20	-0.84	4.31
4	fluorene	4.18	166.23	-1.23	4.63
5	phenanthrene	4.46	178.24	-1.61	4.97
6	anthracene	4.60	178.24	-1.61	5.14
7	fluoranthene	5.22	202.26	-2.38	5.89
8	pyrene	5.18	202.26	-2.38	5.84
9	benzo(a)anthracene	5.61	228.30	-3.22	6.36
10	chrysene	5.61	228.30	-3.22	6.36
11	benzo(b)fluoranthene	5.78	252.32	-3.98	6.56
12	benzo(k)fluoranthene	6.11	252.32	-3.98	6.96
13	benzo(a)pyrene	6.20	252.32	-3.98	7.07
14	dibenz(a,h)anthracene	6.50	278.35	-4.82	7.44
15	benzo(g,h,i)perylene	6.63	276.34	-4.75	7.59
16	indeno(1,2,3-cd)pyrene	6.70	276.33	-4.75	7.68

<sup>1</sup> log K<sub>ow</sub>-values by Mackay et al. (1992)

## Chapter 4

Table A4.1: pseudo-first-order and pseudo-second-order model parameters for PAH adsorption on MP

sorbate	sample	PFO				PSO				$\sigma q_e$ (experimental) ( $\mu\text{g/g}$ )
		$k_1$ (1/d)	$q_e$ (theoretical) ( $\mu\text{g/g}$ )	$R^2$	$t_{95}$ (d)	$k_2$ ( $\text{g}/(\mu\text{g d})$ )	$q_e$ (theoretical) ( $\mu\text{g/g}$ )	$R^2$	$t_{95}$ (d)	
naphthalene	LDPE 1	2.71E+01	19.4	0.999	0.11	1.15E+01	19.5	0.999	0.08	19.8
	LDPE 2	1.97E+01	68.9	0.995	0.15	1.22E+00	69.4	0.997	0.22	75.9
	LDPE 3	1.23E+01	1,032.4	0.900	0.24	2.58E-02	1,052.1	0.916	0.70	1,566.0
	LDPE 4	2.05E+01	321.6	0.987	0.15	2.72E-01	323.3	0.990	0.22	355.7
	LDPE 5	1.06E+01	4,776.3	0.835	0.28	4.03E-03	4,898.1	0.863	0.96	9,176.9
	LDPE 6	1.98E+01	1,953.1	0.990	0.15	4.03E-02	1,970.1	0.993	0.24	2,263.2
	LDPE 7	6.61E+00	30,386.3	0.675	0.45	2.65E-04	31,321.5	0.728	2.29	44,291.2
	PP 1	2.02E+00	19.0	0.994	1.48	2.76E-01	19.4	0.999	3.54	19.8
	PP 2	1.05E+00	51.7	0.960	2.85	2.98E-02	54.8	0.988	11.63	61.6
	PP 3	1.05E+00	875.6	0.838	9.56	1.27E-03	955.9	0.903	15.65	1,663.7
	PP 4	1.11E+00	287.8	0.970	2.70	5.93E-03	303.5	0.994	10.56	344.9
	PP 5	2.99E-01	3,818.8	0.816	10.03	1.15E-04	4,141.0	0.896	39.91	7,675.5
	PP 6	1.06E+00	1,425.9	0.948	2.82	1.06E-03	1,514.6	0.984	11.85	1,777.6
	PP 7	6.61E-02	35,779.1	0.811	45.31	2.54E-06	39,959.1	0.875	187.29	44,024.1
	PBS 1	3.48E+01	75.1	0.986	0.09	9.76E-01	76.3	0.998	0.26	78.7
	PBS 2	2.62E+01	142.2	0.967	0.11	3.36E-01	144.8	0.992	0.39	160.9
	PBS 3	1.39E+01	628.7	0.882	0.22	3.69E-02	640.0	0.925	0.81	989.0
	PBS 4	3.09E+01	1,059.3	0.990	0.10	6.03E-02	1,074.9	0.999	0.29	1,138.6
	PBS 5	2.47E+01	4,850.6	0.921	0.12	5.10E-03	5,492.9	0.718	0.68	7,073.3
	PBS 6	2.68E+01	5,352.9	0.988	0.11	9.67E-03	5,437.4	0.999	0.36	5,942.4
	PBS 7	9.93E+00	26,248.9	0.711	0.30	4.90E-04	26,822.2	0.758	1.44	37,634.8
	PET 1	1.16E-01	8.1	0.934	25.72	1.67E-02	9.1	0.975	124.36	9.2
	PET 2	4.53E-02	21.6	0.881	66.08	2.51E-03	24.7	0.923	306.14	26.9
	PET 3	9.14E-02	26.9	0.935	32.77	3.87E-03	30.6	0.974	160.50	33.9
	PET 4	3.57E-02	89.6	0.922	83.84	4.06E-04	106.2	0.948	440.80	98.1
	PET 5	8.20E-02	98.2	0.935	36.54	9.47E-04	112.2	0.971	178.81	114.1
	PET 6	4.49E-02	259.8	0.907	66.65	1.92E-04	302.0	0.941	328.42	330.7
	PET 7	4.38E-02	748.7	0.878	68.33	7.19E-05	852.1	0.920	310.21	781.4
fluorene	LDPE 1	2.62E+01	233.6	0.927	0.11	1.59E+00	233.9	0.928	0.05	300.2
	LDPE 2	1.35E+01	494.0	0.942	0.22	8.98E-02	497.3	0.948	0.43	552.8
	LDPE 3	5.96E+00	1,694.9	0.669	0.50	3.22E-03	1,760.7	0.724	3.35	2,444.3
	LDPE 4	1.23E+01	2,091.1	0.960	0.24	2.05E-02	2,102.6	0.964	0.44	2,229.7
	LDPE 5	1.05E+01	3,638.9	0.929	0.28	6.94E-03	3,675.5	0.941	0.75	4,131.8
	LDPE 6	5.83E+00	7,629.5	0.735	0.51	7.36E-04	7,912.1	0.793	3.26	9,592.6
	LDPE 7	4.69E+00	13,496.3	0.694	0.64	2.79E-04	14,137.2	0.765	4.81	17,969.0
	PP 1	2.90E+01	138.9	0.939	0.10	1.96E-02	150.0	0.996	6.45	152.8
	PP 2	1.89E+01	403.3	0.680	0.16	1.90E-03	470.0	0.988	21.32	561.3
	PP 3	1.71E-01	1,612.9	0.800	17.47	1.58E-04	1,762.7	0.868	68.01	2,593.6
	PP 4	1.69E+01	1,609.8	0.829	0.18	6.90E-04	1,866.5	0.985	14.76	2,171.2
	PP 5	5.51E+01	3,226.8	0.921	5.44	2.27E-04	3,490.9	0.973	23.95	4,110.5
	PP 6	3.52E+01	7,156.8	0.892	8.52	6.68E-05	7,800.1	0.953	36.49	9,694.3
	PP 7	1.18E-01	13,568.8	0.889	25.39	1.09E-05	15,120.0	0.942	114.81	18,981.9
	PBS 1	2.98E+01	593.8	0.988	0.10	1.03E-01	602.3	0.993	0.30	609.2
	PBS 2	2.04E+01	1,273.5	0.947	0.15	2.74E-02	1,298.3	0.981	0.53	1,402.7
	PBS 3	1.47E+01	2,268.8	0.961	0.20	1.06E-02	2,309.0	0.983	0.77	2,522.9
	PBS 4	6.33E+01	2,269.2	0.999	0.05	1.24E-01	2,280.6	1.000	0.07	2,359.6
	PBS 5	4.48E+01	4,114.6	0.993	0.07	2.87E-02	4,159.8	0.999	0.16	4,431.8
	PBS 6	2.84E+01	9,315.7	0.969	0.11	5.62E-03	9,490.7	0.991	0.36	10,730.8
	PBS 7	1.10E+01	17,191.6	0.934	0.27	1.01E-03	17,511.3	0.971	1.07	18,092.8
	PET 1	1.10E-01	37.2	0.936	27.16	4.11E-03	40.5	0.969	114.19	43.7
	PET 2	5.16E-02	87.7	0.942	58.06	6.55E-04	101.5	0.972	285.85	101.6
	PET 3	5.51E-02	168.8	0.937	54.37	3.71E-04	194.2	0.966	263.78	191.7
	PET 4	3.90E-02	454.3	0.968	76.81	8.33E-05	544.1	0.979	419.09	456.6
	PET 5	3.04E-02	418.3	0.988	98.54	5.85E-05	525.9	0.993	617.79	454.4
	PET 6	2.43E-02	888.9	0.997	123.14	1.88E-05	1,170.7	0.996	861.84	861.2
	PET 7	4.10E-02	1,689.8	0.915	73.02	3.77E-05	1,806.0	0.948	278.85	1,798.0
phenanthrene	LDPE 1	1.02E+01	191.9	1.000	0.29	1.44E+00	192.1	1.000	0.07	177.9
	LDPE 2	1.01E+01	448.2	1.000	0.30	6.08E-01	448.7	1.000	0.07	418.2
	LDPE 3	1.09E+01	625.8	1.000	0.28	4.88E-01	626.5	1.000	0.06	564.9
	LDPE 4	1.07E+01	878.6	1.000	0.28	3.06E-01	878.9	1.000	0.07	805.6
	LDPE 5	8.48E+00	1,507.8	0.999	0.35	5.17E-02	1,515.4	1.000	0.24	1,382.6
	LDPE 6	6.36E+00	3,253.2	0.991	0.47	8.01E-03	3,300.4	0.994	0.72	2,453.8
	LDPE 7	3.49E+00	5,396.2	0.992	0.86	1.61E-03	5,534.1	0.996	2.14	6,522.4
	PP 1	2.42E+00	60.3	0.998	1.24	1.31E-01	61.4	1.000	2.36	57.9
	PP 2	2.36E-01	2,134.9	0.932	12.69	1.26E-04	2,441.8	0.968	61.79	2,220.5
	PP 3	2.46E+00	116.9	0.999	1.22	7.39E-02	118.9	1.000	2.16	131.3
	PP 4	1.71E-01	3,909.2	0.922	17.50	4.83E-05	4,524.9	0.958	86.88	5,182.7
	PP 5	2.78E+00	185.7	0.999	1.08	6.60E-02	187.9	1.000	1.53	192.9
	PP 6	1.03E+00	5,864.3	0.894	2.90	2.01E-04	6,450.7	0.944	14.66	9,288.7
	PPS 1	7.50E+00	334.7	1.000	0.40	2.19E-01	336.2	1.000	0.26	315.4
	PPS 2	7.36E+00	479.2	1.000	0.41	1.40E-01	481.6	1.000	0.28	491.7
	PPS 3	5.16E+00	644.7	0.999	0.58	3.43E-02	653.3	1.000	0.85	575.7
	PPS 4	5.73E+00	881.3	1.000	0.52	3.43E-02	890.0	1.000	0.62	956.5
	PPS 5	3.56E+00	1,918.3	0.998	0.84	4.88E-03	1,969.7	0.999	1.98	1,644.5
	PPS 6	3.37E+00	3,892.8	0.997	0.89	2.14E-03	4,007.5	0.999	2.21	3,395.5
	PPS 7	2.14E+00	5,485.4	0.975	1.40	6.64E-04	5,787.0	0.997	4.94	7,688.2
	PET 1	2.28E-01	21.4	0.982	13.12	7.36E-03	28.0	0.990	92.32	19.2
	PET 2	2.97E-01	117.4	0.958	10.09	1.55E-03	160.9	0.965	76.34	343.8
	PET 3	1.06E-01	200.9	0.957	28.32	4.15E-04	253.5	0.974	180.78	186.1
	PET 4	1.50E-01	368.2	0.973	20.01	1.55E-04	604.5	0.972	202.99	615.2
	PET 5	1.06E-01	2,367.5	0.732	28.32	1.18E-05	4,078.5	0.968	395.01	2,905.7
	PET 6	3.13E-01	1,501.2	0.780	9.58	2.04E-04	1,754.7	0.856	52.98	1,551.4
	PET 7	3.11E-01	3,360.5	0.879	9.62	9.14E-05	3,923.4	0.933	52.97	3,810.0

Table A4.2: Glass adsorption determination of each concentration series and experimental series for naphthalene (NAPH) in duplicates

NAPH on PBS		NAPH on PET		NAPH on LDPE		NAPH on PP	
Sample Name	Area	Sample Name	Area	Sample Name	Area	Sample Name	Area
NAPH, PBS, E 1.1	NF	NAPH, PET, E 1.1	NF	NAPH, LDPE, E 1.1	NF	NAPH, PP, E 1.1	NF
NAPH, PBS, E 1.1	NF	NAPH, PET, E 1.1	NF	NAPH, LDPE, E 1.1	NF	NAPH, PP, E 1.1	NF
NAPH, PBS, E 1.2	NF	NAPH, PET, E 1.2	NF	NAPH, LDPE, E 1.2	NF	NAPH, PP, E 1.2	NF
NAPH, PBS, E 1.2	NF	NAPH, PET, E 1.2	NF	NAPH, LDPE, E 1.2	NF	NAPH, PP, E 1.2	NF
NAPH, PBS, E 1.3	NF	NAPH, PET, E 1.4	NF	NAPH, LDPE, E 1.3	NF	NAPH, PP, E 1.3	NF
NAPH, PBS, E 1.3	NF	NAPH, PET, E 1.4	NF	NAPH, LDPE, E 1.3	NF	NAPH, PP, E 1.3	NF
NAPH, PBS, E 1.5	NF	NAPH, PET, E 1.5	NF	NAPH, LDPE, E 1.5	NF	NAPH, PP, E 1.5	NF
NAPH, PBS, E 1.5	NF	NAPH, PET, E 1.5	NF	NAPH, LDPE, E 1.5	NF	NAPH, PP, E 1.5	NF
NAPH, PBS, E 1.6	NF	NAPH, PET, E 1.7	NF	NAPH, LDPE, E 1.6	NF	NAPH, PP, E 1.6	NF
NAPH, PBS, E 1.6	NF	NAPH, PET, E 1.7	NF	NAPH, LDPE, E 1.6	NF	NAPH, PP, E 1.6	NF
NAPH, PBS, E 1.8	NF	NAPH, PET, E 1.8	NF	NAPH, LDPE, E 1.8	NF	NAPH, PP, E 1.8	NF
NAPH, PBS, E 1.8	NF	NAPH, PET, E 1.8	NF	NAPH, LDPE, E 1.8	NF	NAPH, PP, E 1.8	NF
NAPH, PBS, E 1.9	NF	NAPH, PET, E 1.10	NF	NAPH, LDPE, E 1.9	NF	NAPH, PP, E 1.9	NF
NAPH, PBS, E 1.9	NF	NAPH, PET, E 1.10	NF	NAPH, LDPE, E 1.9	NF	NAPH, PP, E 1.9	NF

Abbreviation: NF = not found

Table A4.3: Glass adsorption determination of each concentration series and experimental series for fluorene (FLN) in duplicates

FLN on PBS		FLN on PET		FLN on LDPE		FLN on PP	
Sample Name	Area	Sample Name	Area	Sample Name	Area	Sample Name	Area
FLN, PBS, E 2.1	NF	FLN, PET, E 1.1	NF	FLN, LDPE, E 2.1	NF	FLN, PP, E 2.1	NF
FLN, PBS, E 2.1	NF	FLN, PET, E 1.1	NF	FLN, LDPE, E 2.1	NF	FLN, PP, E 2.1	NF
FLN, PBS, E 2.2	NF	FLN, PET, E 1.2	NF	FLN, LDPE, E 2.2	NF	FLN, PP, E 2.2	NF
FLN, PBS, E 2.2	NF	FLN, PET, E 1.2	NF	FLN, LDPE, E 2.2	NF	FLN, PP, E 2.2	NF
FLN, PBS, E 2.3	NF	FLN, PET, E 1.4	NF	FLN, LDPE, E 2.3	NF	FLN, PP, E 2.3	NF
FLN, PBS, E 2.3	NF	FLN, PET, E 1.4	NF	FLN, LDPE, E 2.3	NF	FLN, PP, E 2.3	NF
FLN, PBS, E 2.5	NF	FLN, PET, E 1.5	NF	FLN, LDPE, E 3.5	NF	FLN, PP, E 2.5	NF
FLN, PBS, E 2.5	NF	FLN, PET, E 1.5	NF	FLN, LDPE, E 3.5	NF	FLN, PP, E 2.5	NF
FLN, PBS, E 2.6	NF	FLN, PET, E 1.7	NF	FLN, LDPE, E 2.6	NF	FLN, PP, E 2.6	NF
FLN, PBS, E 2.6	NF	FLN, PET, E 1.7	NF	FLN, LDPE, E 2.6	NF	FLN, PP, E 2.6	NF
FLN, PBS, E 2.7	NF	FLN, PET, E 1.8	NF	FLN, LDPE, E 2.7	NF	FLN, PP, E 2.7	NF
FLN, PBS, E 2.7	NF	FLN, PET, E 1.8	NF	FLN, LDPE, E 2.7	NF	FLN, PP, E 2.7	NF
FLN, PBS, E 2.8	NF	FLN, PET, E 1.10	NF	FLN, LDPE, E 2.8	NF	FLN, PP, E 2.8	NF
FLN, PBS, E 2.8	NF	FLN, PET, E 1.10	NF	FLN, LDPE, E 2.8	NF	FLN, PP, E 2.8	NF

Abbreviation: NF = not found

Table A4.4: Glass adsorption determination of each concentration series and experimental series for phenanthrene (PHEN) in duplicates

PHEN on PBS		PHEN on PET		PHEN on LDPE		PHEN on PP	
Sample Name	Area	Sample Name	Area	Sample Name	Area	Sample Name	Area
PHEN, PBS, 1 E	NF	PHEN, PET, 1 E	NF	PHEN, LDPE, 1 E	NF	PHEN, PP, 1 E	NF
PHEN, PBS, 1 E	NF	PHEN, PET, 1 E	NF	PHEN, LDPE, 1 E	NF	PHEN, PP, 1 E	NF
PHEN, PBS, 2 E	NF	PHEN, PET, 2 E	NF	PHEN, LDPE, 2 E	NF	PHEN, PP, 2 E	NF
PHEN, PBS, 2 E	NF	PHEN, PET, 2 E	NF	PHEN, LDPE, 2 E	NF	PHEN, PP, 2 E	NF
PHEN, PBS, 3 E	NF	PHEN, PET, 4 E	NF	PHEN, LDPE, 3 E	NF	PHEN, PP, 4 E	NF
PHEN, PBS, 3 E	NF	PHEN, PET, 4 E	NF	PHEN, LDPE, 3 E	NF	PHEN, PP, 4 E	NF
PHEN, PBS, 4 E	NF	PHEN, PET, 5 E	NF	PHEN, LDPE, 4 E	NF	PHEN, PP, 5 E	NF
PHEN, PBS, 4 E	NF	PHEN, PET, 5 E	NF	PHEN, LDPE, 4 E	NF	PHEN, PP, 5 E	NF
PHEN, PBS, 5 E	NF	PHEN, PET, 6 E	NF	PHEN, LDPE, 5 E	NF	PHEN, PP, 7 E	NF
PHEN, PBS, 5 E	NF	PHEN, PET, 6 E	NF	PHEN, LDPE, 5 E	NF	PHEN, PP, 7 E	NF
PHEN, PBS, 6 E	NF	PHEN, PET, 8 E	NF	PHEN, LDPE, 6 E	NF	PHEN, PP, 8 E	NF
PHEN, PBS, 6 E	NF	PHEN, PET, 8 E	NF	PHEN, LDPE, 6 E	NF	PHEN, PP, 8 E	NF
PHEN, PBS, 7 E	NF	PHEN, PET, 9 E	NF	PHEN, LDPE, 7 E	NF	PHEN, LDPE, 1 E	NF
PHEN, PBS, 7 E	NF	PHEN, PET, 9 E	NF	PHEN, LDPE, 7 E	NF	PHEN, LDPE, 1 E	NF
						PHEN, LDPE, 2 E	NF
						PHEN, LDPE, 3 E	NF
						PHEN, LDPE, 3 E	NF
						PHEN, LDPE, 4 E	NF
						PHEN, LDPE, 4 E	NF
						PHEN, LDPE, 5 E	NF
						PHEN, LDPE, 5 E	NF
						PHEN, LDPE, 6 E	NF
						PHEN, LDPE, 6 E	NF

Abbreviation: NF = not found

## Chapter 5

Table A5.1:  $\log K_{ow}$  and  $\log K_{LDPE-w}$  ( $L \text{ kg}^{-1}$ ) selected PAHs

PAHs	Booij et al. (2003)		Adams et al. (2007)		Smedes et al. (2009)		Choi et al. (2013) <sup>a</sup>		Zhu et al. (2015)	
	$\log K_{ow}$	$\log K_{LDPE-w}$	$\log K_{ow}$	$\log K_{LDPE-w}$	$\log K_{ow}$	$\log K_{LDPE-w}$	$\log K_{ow}$	$\log K_{LDPE-w}$	$\log K_{ow}$	$\log K_{LDPE-w}$
naphthalene					3.37	2.81	3.3	3.23	3.37	2.94
acenaphthylene					4	3.16			4	3.85
acenaphthene	3.92	3.7			3.92	3.62	3.92	3.53	3.92	3.94
fluorene					4.18	3.77	4.18	3.67	4.18	4.14
phenanthrene	4.57	4.3	4.5	4.3	4.57	4.22	4.46	4.04	4.57	4.22
anthracene					4.54	4.33	4.45	4.15	4.54	4.50
fluoranthene	5.22	4.9	5.1	4.9	5.22	4.93	5.16	4.75	5.22	5.05
pyrene	5.18	5.1	5	5	5.18	5.1	4.88	4.89	5.18	5.50
benzo(a)anthracene	5.91	5.5	5.62	5.7	5.91	5.73	5.76	5.43	5.91	5.99
chrysene	5.86	5.6	5.9	5.7	5.86	5.78	5.81	5.51	5.9	6.66
benzo(b)fluoranthene					5.9	6.66	5.78	6.06	5.9	6.66
benzo(k)fluoranthene					5.9	6.66	6.11	6.16	5.9	6.66
benzo(a)pyrene	6.04	5.9			6.04	6.75	6.13	6.14	6.04	6.46
dibenz(a,h)anthracene					6.75	7.32	6.8	6.3	6.75	7.32
benzo(g,h,i)perylene					6.5	7.27	6.7	6.23	6.5	7.27
indeno(1,2,3-cd)pyrene					6.5	7.4	6.7	6.5	6.5	7.4
benzo(e)pyrene	5.9	6.04	5.3	6.2			6.44	6.04		
2-methyl phenanthrene			5.2	4.8						
perylene			6.3	6.5			6.25	5.92		

<sup>a</sup>  $\log K_{LDPE-w}$  of 17 parent PAHs were presented

Table A5.2:  $\log K_{ow}$  and  $\log K_{PP-w}$  ( $L \text{ kg}^{-1}$ ) selected PAHs

PAHs	Lee et al. (2014) <sup>a</sup>		Lončarski et al. (2021) <sup>b</sup>	
	$\log K_{ow}$	$\log K_{PP-w}$	$\log K_{ow}$	$\log K_{PP-w}$
naphthalene			3.37	4.18
acenaphthylene				
acenaphthene				
fluorene			4.18	4.16
phenanthrene	4.57	3.73		
anthracene	4.54	4.05		
fluoranthene	5.22	4.54	5.22	4.29
pyrene	5.18	4.55	5.18	4.27
benzo(a)anthracene				
chrysene	5.86	5.25		
benzo(b)fluoranthene				
benzo(k)fluoranthene				
benzo(a)pyrene	6.04	5.85		
dibenz(a,h)anthracene	6.75	6.76		
benzo(g,h,i)perylene	6.5	6.49		
indeno(1,2,3-cd)pyrene				

<sup>a</sup> converted to  $\log K_{PP-w}$  in fresh water based on the Setschenow constant from Jonker and Muijs (2010); <sup>b</sup> converted to  $\log K_{PP-w}$  in fresh water based on the Setschenow constant from Burant et al. (2016) and Jonker and Muijs (2010)

Table A5.3: log  $K_{ow}$  and log  $K_{PET-w}$  ( $L \text{ kg}^{-1}$ ) selected PAHs

PAHs	Lončarski et al. (2021) <sup>a</sup>	
	log $K_{ow}$	log $K_{PET-w}$
naphthalene	3.37	4.39
acenaphthylene		
acenaphthene		
fluorene	4.18	4.55
phenanthrene		
anthracene		
fluoranthene	5.22	4.43
pyrene	5.18	4.95
benzo(a)anthracene		
chrysene		
benzo(b)fluoranthene		
benzo(k)fluoranthene		
benzo(a)pyrene		
dibenz(a,h)anthracene		
benzo(g,h,i)perylene		
indeno(1,2,3-cd)pyrene		

<sup>a</sup> log  $K_{PET-w}$  values of four PAHs in synthetic water by Lončarski 2021 were converted to log  $K_{PET-w}$  in fresh water, based on the Setschenow constant from Burant et al. (2016) and Jonker and Muijs (2010)

Table A5.4: MW ( $\text{g mol}^{-1}$ ) and log  $K_{LDPE-w}$  ( $L \text{ kg}^{-1}$ ) selected PAHs

PAHs	MW	Smedes et al. (2007)	Choi et al. (2013) <sup>a</sup>
		log $K_{LDPE-w}$	log $K_{LDPE-w}$
naphthalene	128.2	2.81	3.23
acenaphthylene	152.2	3.16	
acenaphthene	154.2	3.62	3.53
fluorene	166.2	3.77	3.67
phenanthrene	178.2	4.22	4.04
anthracene	178.2	4.33	4.15
fluoranthene	202.3	4.93	4.75
pyrene	202.3	5.1	4.89
benzo(a)anthracene	228.3	5.73	5.43
chrysene	228.3	5.78	5.51
benzo(b)fluoranthene	252.3	6.66	6.06
benzo(k)fluoranthene	252.3	6.66	6.16
benzo(a)pyrene	252.3	6.75	6.14
dibenz(a,h)anthracene	278.4	7.32	6.3
benzo(g,h,i)perylene	276.3	7.27	6.23
indeno(1,2,3-cd)pyrene	276.3	7.4	6.5
perylene	252.32		5.92

<sup>a</sup> log  $K_{LDPE-w}$  of 17 parent PAHs were presented

Table A5.5: MW (g mol<sup>-1</sup>) and log K<sub>PP-W</sub> (L kg<sup>-1</sup>) selected PAHs

PAHs	MW	Lee et al. (2014) <sup>a</sup>	Lončarski et al. (2021) <sup>b</sup>
		log K <sub>PP-W</sub>	log K <sub>PP-W</sub>
naphthalene	128.2		4.18
acenaphthylene	152.2		
acenaphthene	154.2		
fluorene	166.2		4.16
phenanthrene	178.2	3.73	
anthracene	178.2	4.05	
fluoranthene	202.3	4.54	4.29
pyrene	202.3	4.55	4.27
benzo(a)anthracene	228.3		
chrysene	228.3	5.25	
benzo(b)fluoranthene	252.3		
benzo(k)fluoranthene	252.3		
benzo(a)pyrene	252.3	5.85	
dibenz(a,h)anthracene	278.4	6.76	
benzo(g,h,i)perylene	276.3	6.49	
indeno(1,2,3-cd)pyrene	276.3		

<sup>a</sup> converted to log K<sub>PP-W</sub> in fresh water based on the Setschenow constant from Jonker and Muijs (2010); <sup>b</sup> converted to log K<sub>PP-W</sub> in fresh water based on the Setschenow constant from Burant et al. (2016) and Jonker and Muijs (2010)

Table A5.6: MW (g mol<sup>-1</sup>) and log K<sub>PET-W</sub> (L kg<sup>-1</sup>) selected PAHs

PAHs	MW	Lončarski et al. (2021) <sup>a</sup>
		log K <sub>PET-W</sub>
naphthalene	128.2	4.39
acenaphthylene	152.2	
acenaphthene	154.2	
fluorene	166.2	4.55
phenanthrene	178.2	
anthracene	178.2	
fluoranthene	202.3	4.43
pyrene	202.3	4.95
benzo(a)anthracene	228.3	
chrysene	228.3	
benzo(b)fluoranthene	252.3	
benzo(k)fluoranthene	252.3	
benzo(a)pyrene	252.3	
dibenz(a,h)anthracene	278.4	
benzo(g,h,i)perylene	276.3	
indeno(1,2,3-cd)pyrene	276.3	

<sup>a</sup> Log K<sub>PET-W</sub> values of four PAHs in synthetic water by Lončarski et al. 2021 were converted to log K<sub>PET-W</sub> in fresh water, based on the Setschenow constant from Burant et al. (2016) and Jonker and Muijs (2010)

## Chapter 6

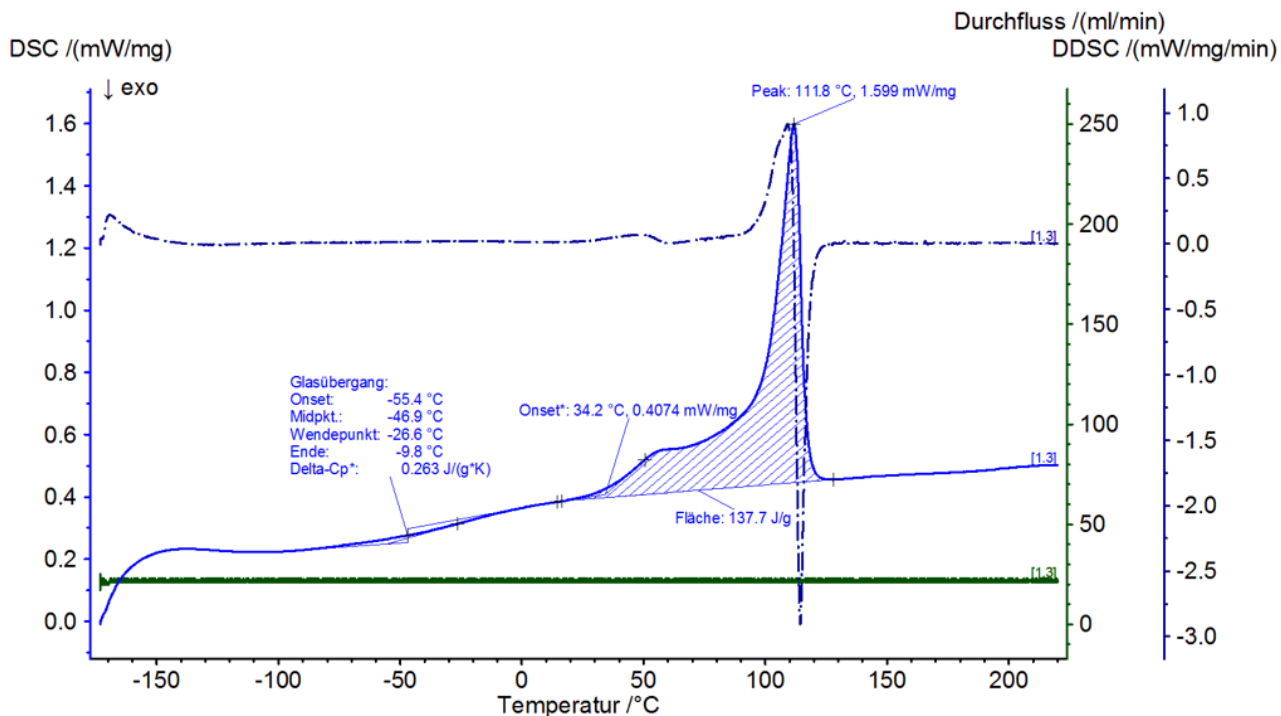


Figure A6.1: DSC Analysis of LDPE

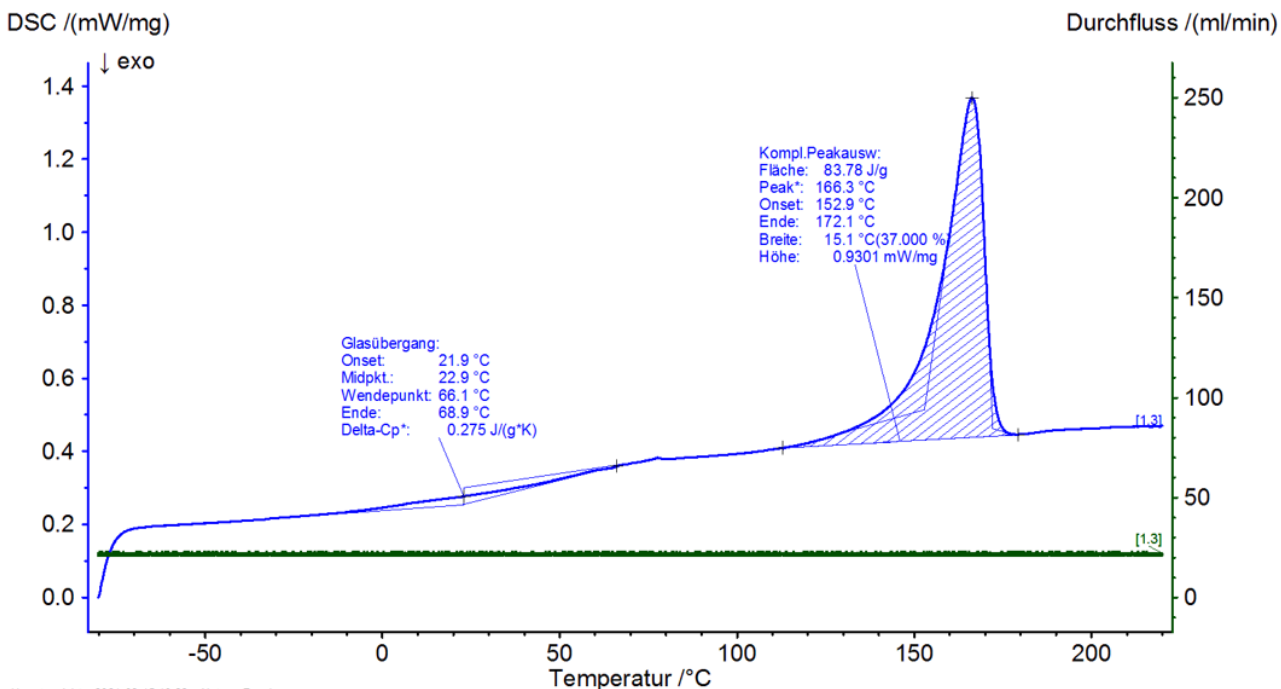


Figure A6.2: DSC Analysis of PP

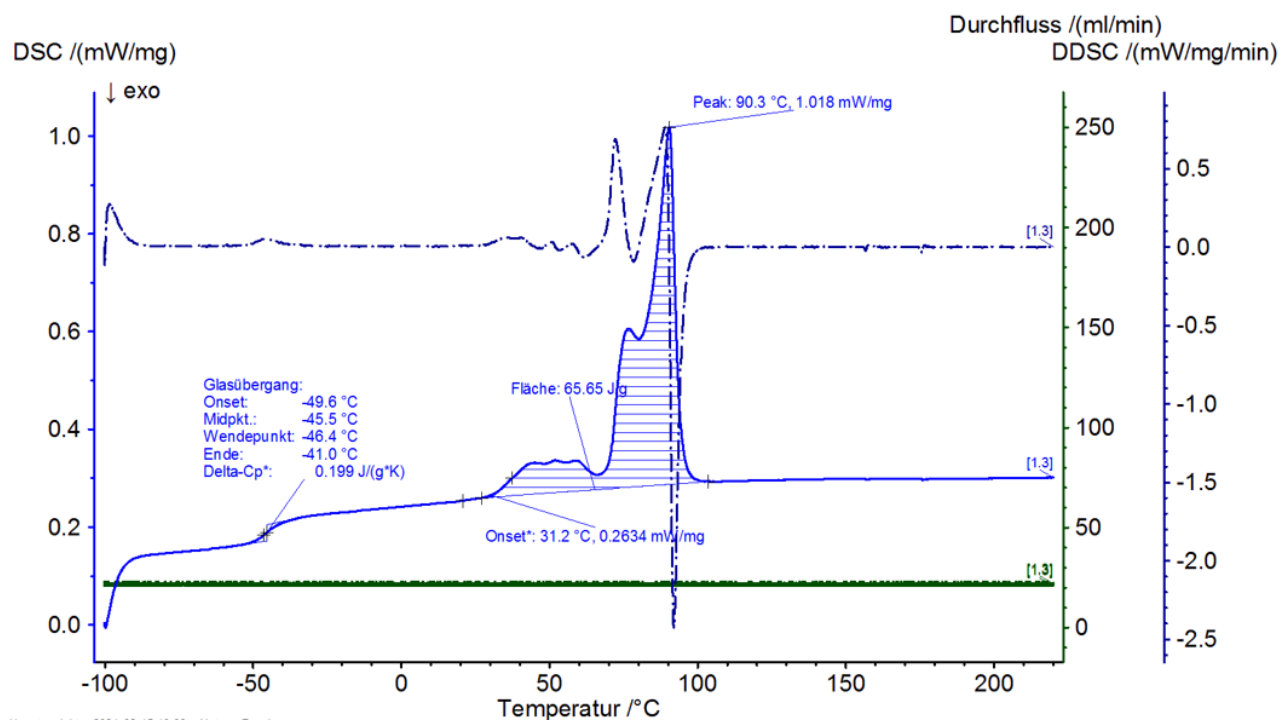


Figure A6.3: DSC Analysis of PBS

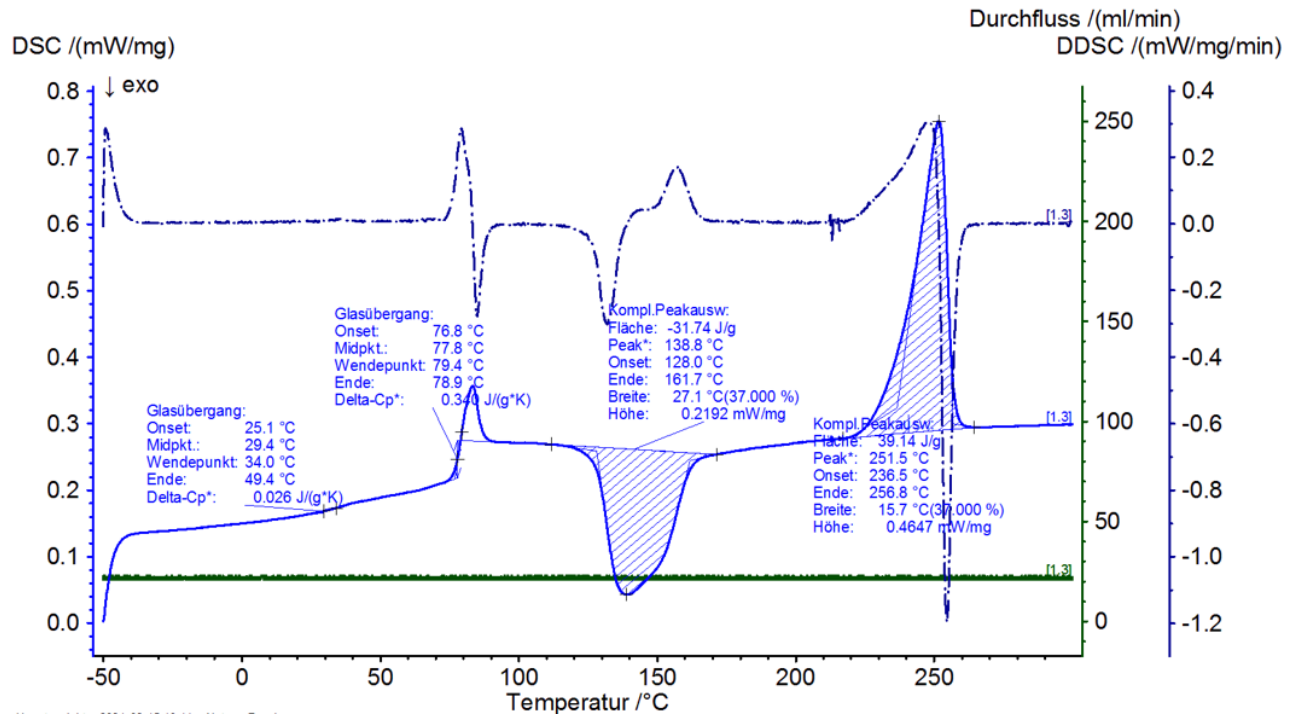


Figure A6.4: DSC Analysis of PET

From the DSC analyses, the thermal properties such as  $T_g$ ,  $X_c$  and  $T_m$  were obtained (Table A6.1)

Table A6.1: Results of DSC Analysis for LDPE, PP, PBS and PET

plastic type	$\rho$ (g cm <sup>-3</sup> )	$T_g$ with DSC (°C)	$T_m$ with DSC (°C)	Melting enthalpy of 100 % crystalline polymer (J g <sup>-1</sup> )	$X_c$ with DSC (%)
LDPE	0.92	-46.9 (Midp.)	111.8	288 <sup>1</sup>	47.81
PP	0.91	22.9 (Midp.)	166.3	209 <sup>2</sup>	40.09
PBS	1.24	-45.5 (Midp.)	90.3	110.5 <sup>3</sup>	59.40
PET	1.34	77.8 (Midp.)	251.5	140 <sup>4</sup>	5.29

<sup>1</sup> Khonakdar et al. (2006)

<sup>2</sup> Gahleitner et al. (1999)

<sup>3</sup> Xu et al. (2008)

<sup>4</sup> Badia et al. (2012)

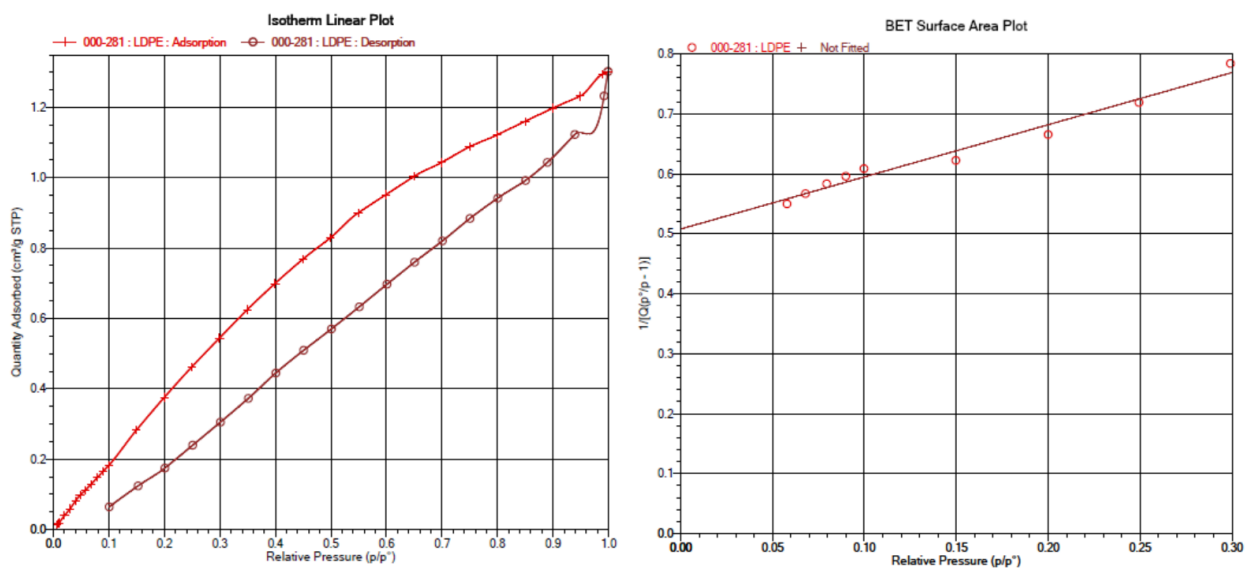


Figure A6.5: Evaluating the BET surface area of LDPE

The adsorbed and desorbed amount of N<sub>2</sub>-gas in an isothermal state on the LDPE particles was investigated (left Figure), so the BET surface plots could be derived (right Figure) and the BET surface area of 3.1586 m<sup>2</sup> g<sup>-1</sup> could be determined.

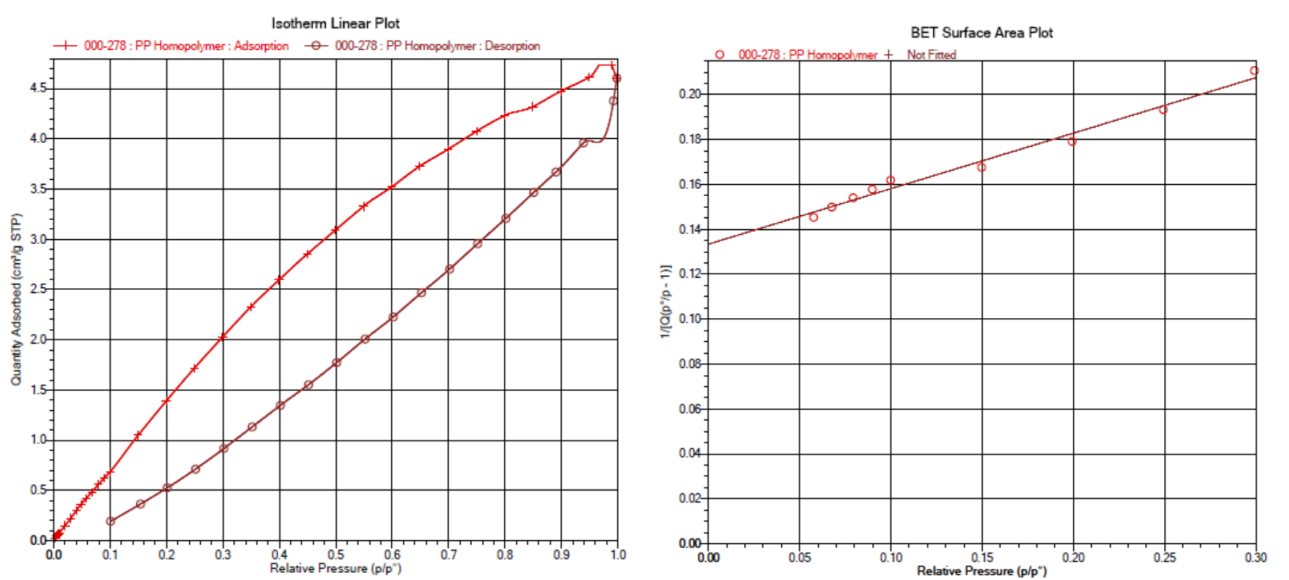


Figure A6.6: Evaluating the BET surface area of PP

The adsorbed and desorbed amount of N<sub>2</sub>-gas in an isothermal state on the PP particles was investigated (**left Figure**), so the BET surface plots could be derived (**right Figure**) and the BET surface area of 11.4393 m<sup>2</sup> g<sup>-1</sup> could be determined.

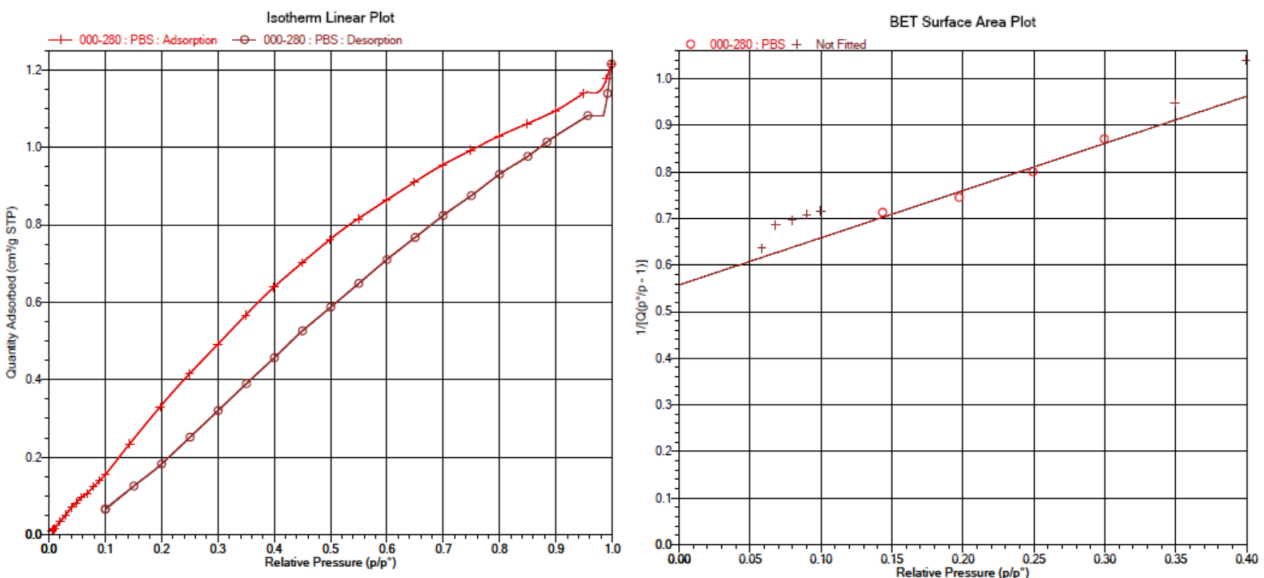


Figure A6.7: Evaluating the BET surface area of PBS

The adsorbed and desorbed amount of N<sub>2</sub>-gas in an isothermal state on the PBS particles was investigated (**left Figure**), so the BET surface plots could be derived (**right Figure**) and the BET surface area of 2.7728 m<sup>2</sup> g<sup>-1</sup> could be determined.

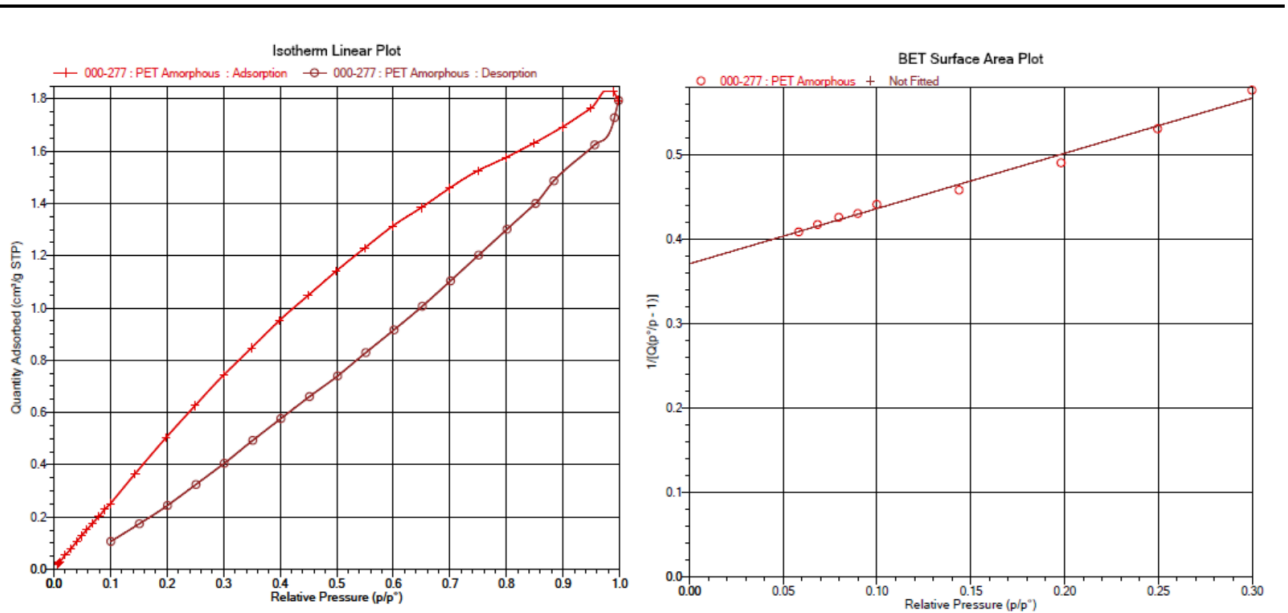


Figure A6.8: Evaluating the BET surface area of PET

The adsorbed and desorbed amount of N<sub>2</sub>-gas in an isothermal state on the PET particles was investigated (**left Figure**), so the BET surface plots could be derived (**right Figure**) and the BET surface area of 4.2438 m<sup>2</sup> g<sup>-1</sup> could be determined.

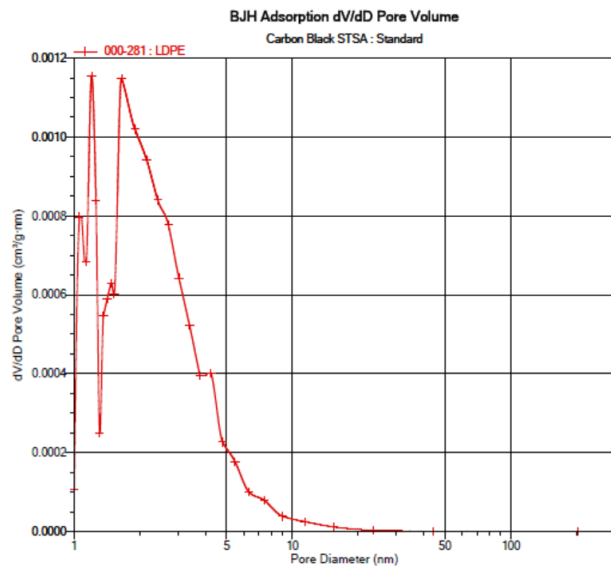


Figure A6.9: Evaluating the pore volume of LDPE

While the BET surface area was measured, the pore volume of LDPE was also recorded at the same time, which is 0.002009 cm<sup>3</sup> g<sup>-1</sup>.

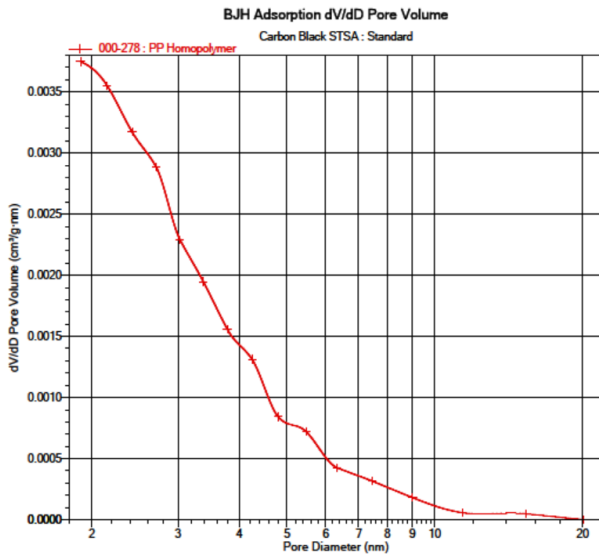


Figure A6.10: Evaluating the pore volume of PP

While the BET surface area was measured, the pore volume of PP was also recorded at the same time, which is  $0.007317 \text{ cm}^3 \text{ g}^{-1}$ .

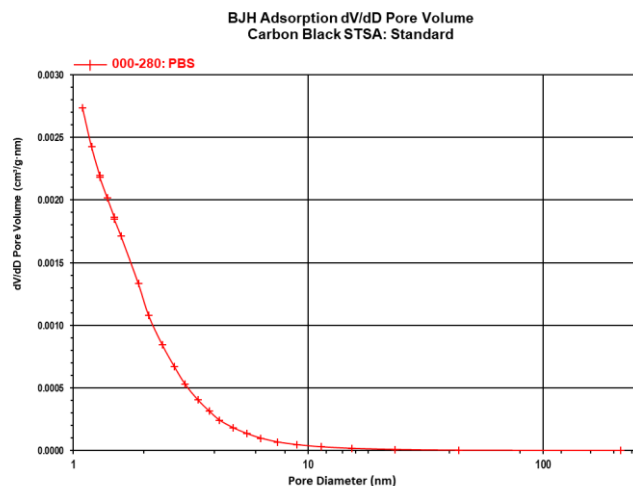


Figure A6.11: Evaluating the pore volume of PBS

While the BET surface area was measured, the pore volume of PBS was also recorded at the same time, which is  $0.001826 \text{ cm}^3 \text{ g}^{-1}$ .

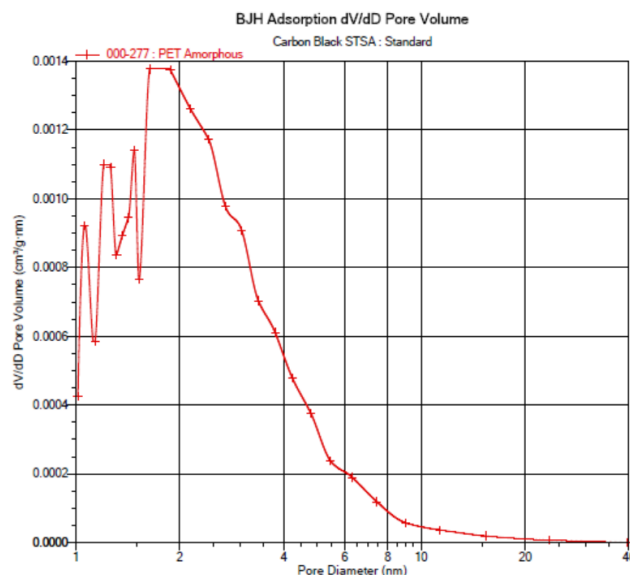


Figure A6.12: Evaluating the pore volume of PET

While the BET surface area was measured, the pore volume of PET was also recorded at the same time, which is  $0.002828 \text{ cm}^3 \text{ g}^{-1}$ .

Table A6.2: Results of particle size distribution ( $d_{50}$ ) with Malvern Unit for LDPE

Trend	Messdatensatz-Nr.	Probenname	Dx (10) ( $\mu\text{m}$ )	Dx (50) ( $\mu\text{m}$ )	Dx (90) ( $\mu\text{m}$ )	Gewichtete Abweichung (%)	Laserabschattung (%)
	19	201217_LDPE102.50_sdbs	145	459	894	0,54	6,97
	20	201217_LDPE102.50_sdbs	146	477	951	0,57	7,08
	21	201217_LDPE102.50_sdbs	135	435	856	0,57	6,68
	22	201217_LDPE102.50_sdbs	138	458	898	0,59	6,75
	23	201217_LDPE102.50_sdbs	139	466	909	0,56	6,74
	24	201217_LDPE102.50_sdbs	137	453	901	0,58	6,67
	25	201217_LDPE102.50_sdbs	133	441	856	0,58	6,57
	26	201217_LDPE102.50_sdbs	133	447	885	0,59	6,52
<b>Mittel</b>			<b>138</b>	<b>455</b>	<b>894</b>	<b>0,57</b>	<b>6,75</b>
<b>1xStd. Abw.</b>			<b>4,75</b>	<b>13,6</b>	<b>30,6</b>	<b>0,02</b>	<b>0,19</b>
<b>1xRSD (%)</b>			<b>3,43</b>	<b>3,00</b>	<b>3,42</b>	<b>2,66</b>	<b>2,85</b>
<b>Min.</b>			<b>133</b>	<b>435</b>	<b>856</b>	<b>0,54</b>	<b>6,52</b>
<b>Max.</b>			<b>146</b>	<b>477</b>	<b>951</b>	<b>0,59</b>	<b>7,08</b>

Table A6.3: Results of particle size distribution ( $d_{50}$ ) with Malvern Unit for PP

Trend	Messdatensatz-Nr.	Probenname	Dx (10) ( $\mu\text{m}$ )	Dx (50) ( $\mu\text{m}$ )	Dx (90) ( $\mu\text{m}$ )	Gewichtete Abweichung (%)	Laserabschattung (%)
	11	201217_PP200.00	190	541	1000	0,62	5,94
	12	201217_PP200.00	179	525	1010	0,58	5,63
	13	201217_PP200.00	177	516	975	0,62	5,61
	14	201217_PP200.00	193	554	1020	0,64	6,11
	15	201217_PP200.00	194	536	995	0,63	6,20
	16	201217_PP200.00	190	544	1010	0,69	6,02
	17	201217_PP200.00	181	532	995	0,66	5,67
<b>Mittel</b>			<b>186</b>	<b>536</b>	<b>1000</b>	<b>0,64</b>	<b>5,88</b>
<b>1xStd. Abw.</b>			<b>7,14</b>	<b>12,5</b>	<b>14,6</b>	<b>0,03</b>	<b>0,25</b>
<b>1xRSD (%)</b>			<b>3,84</b>	<b>2,33</b>	<b>1,46</b>	<b>5,06</b>	<b>4,18</b>
<b>Min.</b>			<b>177</b>	<b>516</b>	<b>975</b>	<b>0,58</b>	<b>5,61</b>
<b>Max.</b>			<b>194</b>	<b>554</b>	<b>1020</b>	<b>0,69</b>	<b>6,20</b>

Table A6.4: Results of particle size distribution ( $d_{50}$ ) with Malvern Unit for PBS

Trend							
	Messdatensatz-Nr.	Probenname	Dx (10) ( $\mu\text{m}$ )	Dx (50) ( $\mu\text{m}$ )	Dx (90) ( $\mu\text{m}$ )	Gewichtete Abweichung (%)	Laserabschattung (%)
	28	201217_PBS900_sdbs	143	532	1130	0,49	9,75
	29	201217_PBS900_sdbs	144	546	1190	0,48	10,03
	30	201217_PBS900_sdbs	141	524	1110	0,53	10,27
	31	201217_PBS900_sdbs	142	529	1120	0,54	10,48
	32	201217_PBS900_sdbs	140	534	1160	0,48	10,63
	33	201217_PBS900_sdbs	141	544	1190	0,49	10,85
	34	201217_PBS900_sdbs	140	528	1090	0,66	10,94
	35	201217_PBS900_sdbs	141	542	1170	0,55	11,18
	<b>Mittel</b>		<b>141</b>	<b>535</b>	<b>1140</b>	<b>0,53</b>	<b>10,52</b>
	<b>1xStd. Abw.</b>		<b>1,36</b>	<b>8,31</b>	<b>38,2</b>	<b>0,06</b>	<b>0,48</b>
	<b>1xRSD (%)</b>		<b>0,965</b>	<b>1,55</b>	<b>3,33</b>	<b>11,78</b>	<b>4,59</b>
	<b>Min.</b>		<b>140</b>	<b>524</b>	<b>1090</b>	<b>0,48</b>	<b>9,75</b>
	<b>Max.</b>		<b>144</b>	<b>546</b>	<b>1190</b>	<b>0,66</b>	<b>11,18</b>

Table A6.5: Results of particle size distribution ( $d_{50}$ ) with Malvern Unit for PET

Trend							
	Messdatensatz-Nr.	Probenname	Dx (10) ( $\mu\text{m}$ )	Dx (50) ( $\mu\text{m}$ )	Dx (90) ( $\mu\text{m}$ )	Gewichtete Abweichung (%)	Laserabschattung (%)
	37	201217_PET400_sdbs	293	677	1170	1,05	7,37
	38	201217_PET400_sdbs	302	696	1220	1,10	7,53
	39	201217_PET400_sdbs	295	681	1200	0,94	7,53
	40	201217_PET400_sdbs	296	681	1200	1,04	7,72
	41	201217_PET400_sdbs	295	685	1200	1,00	7,80
	42	201217_PET400_sdbs	300	680	1170	1,16	7,96
	43	201217_PET400_sdbs	290	691	1240	1,04	7,88
	44	201217_PET400_sdbs	297	689	1210	1,07	8,18
	<b>Mittel</b>		<b>296</b>	<b>685</b>	<b>1200</b>	<b>1,05</b>	<b>7,75</b>
	<b>1xStd. Abw.</b>		<b>3,92</b>	<b>6,67</b>	<b>23,8</b>	<b>0,07</b>	<b>0,26</b>
	<b>1xRSD (%)</b>		<b>1,32</b>	<b>0,974</b>	<b>1,99</b>	<b>6,22</b>	<b>3,39</b>
	<b>Min.</b>		<b>290</b>	<b>677</b>	<b>1170</b>	<b>0,94</b>	<b>7,37</b>
	<b>Max.</b>		<b>302</b>	<b>696</b>	<b>1240</b>	<b>1,16</b>	<b>8,18</b>

Table A6.6: Determination of correlation coefficients for plastic properties and  $\log K_{p-w}$  values

	SA	Vp	dispers SFE	polar SFE	$\sum$ SFE
	R <sup>2</sup>				
NAPH	0.10	0.11	0.07	0.21	0.12
FLU	0.03	0.03	0.03	8.97E-04	0.01
PHEN	0.08	0.09	3.20E-07	0.04	0.01

## Chapter 7

Table A7.1 Calculation of  $R_h^2$  and  $R_v^2$  with the matrix of one PAH property multiplied with two plastic properties ( $\rho^{-1}$  as fixed parameter) and the  $\log K_{p-w}$  matrix

plastic property product		PAH properties																
1 <sup>st</sup> fixed parameter	2 <sup>nd</sup> variable parameter	$\log K_{ow}$		$\log K_{ow}^{-1}$		MW (g mol <sup>-1</sup> )		MW <sup>1</sup> (mol g <sup>-1</sup> )		$\log C_w^{sat}$ (mol m <sup>-3</sup> )		$\log C_w^{sat-1}$ (m <sup>3</sup> mol <sup>-1</sup> )		$\log K_{ndw}$		$\log K_{hdw}^{-1}$		
		$R_v^2$	$R_h^2$	$R_v^2$	$R_h^2$	$R_v^2$	$R_h^2$	$R_v^2$	$R_h^2$	$R_v^2$	$R_h^2$	$R_v^2$	$R_h^2$	$R_v^2$	$R_h^2$	$R_v^2$	$R_h^2$	
$d_{50}$ ( $\mu\text{m}$ )		0.15	0.69	0.13	0.69	0.16	0.69	0.13	0.68	0.15	0.69	0.02	0.62	0.15	0.62	0.13	0.68	
$d_{50}^{-1}$ ( $\mu\text{m}^{-1}$ )		0.13	0.80	0.10	0.79	0.13	0.79	0.09	0.78	0.16	0.79	0.00	0.71	0.13	0.71	0.09	0.78	
$T_m$ (K)		0.22	0.66	0.19	0.65	0.22	0.66	0.18	0.65	0.21	0.66	0.03	0.59	0.22	0.59	0.18	0.65	
$T_m^{-1}$ (K <sup>-1</sup> )		0.35	0.84	0.27	0.82	0.36	0.83	0.26	0.82	0.41	0.83	0.01	0.74	0.35	0.74	0.27	0.82	
$T_g$ (K)		0.38	0.58	0.30	0.57	0.38	0.58	0.29	0.57	0.41	0.58	0.02	0.52	0.37	0.52	0.29	0.57	
$T_g^{-1}$ (K <sup>-1</sup> )		0.17	0.80	0.13	0.79	0.17	0.80	0.12	0.79	0.21	0.80	0.00	0.71	0.17	0.71	0.12	0.79	
$\rho$ ( $\text{cm}^3 \text{g}^{-1}$ )	*	$X_c$ (%)	0.65	0.93	0.52	0.91	0.66	0.92	0.50	0.90	0.72	0.92	0.03	0.81	0.65	0.81	0.51	0.91
	$X_c^{-1}$ (% <sup>-1</sup> )	0.70	0.08	0.56	0.08	0.71	0.08	0.54	0.08	0.76	0.08	0.03	0.08	0.69	0.08	0.55	0.08	
$SA$ (m <sup>2</sup> g <sup>-1</sup> )		0.02	0.41	0.02	0.40	0.02	0.41	0.02	0.40	0.02	0.41	0.00	0.38	0.02	0.38	0.02	0.40	
$SA^{-1}$ (g m <sup>-2</sup> )		0.29	0.81	0.23	0.80	0.29	0.81	0.22	0.79	0.31	0.81	0.01	0.71	0.28	0.70	0.22	0.80	
$V_p$ (cm <sup>3</sup> g <sup>-1</sup> )		0.03	0.41	0.02	0.41	0.03	0.41	0.02	0.40	0.03	0.41	0.00	0.38	0.03	0.38	0.02	0.41	
$V_p^{-1}$ (g cm <sup>-3</sup> )		0.29	0.81	0.23	0.80	0.29	0.81	0.22	0.79	0.31	0.81	0.01	0.71	0.28	0.71	0.22	0.80	
$\sum SFE$ (mN m <sup>-1</sup> )		0.06	0.72	0.05	0.70	0.06	0.71	0.05	0.70	0.05	0.71	0.02	0.62	0.06	0.62	0.05	0.70	
$\sum SFE^{-1}$ (m Nm <sup>-1</sup> )		0.00	0.65	0.00	0.65	0.00	0.65	0.00	0.64	0.01	0.65	0.00	0.59	0.00	0.59	0.00	0.65	

Table A7.2: Calculation of  $R_h^2$  and  $R_v^2$  with the matrix of one PAH property multiplied with two plastic properties ( $d_{50}$  as fixed parameter) and the  $\log K_{p-w}$  matrix

plastic property product		PAH properties																
1 <sup>st</sup> fixed parameter	2 <sup>nd</sup> variable parameter	$\log K_{ow}$		$\log K_{ow}^{-1}$		MW (g mol <sup>-1</sup> )		MW <sup>1</sup> (mol g <sup>-1</sup> )		$\log C_w^{sat}$ (mol m <sup>-3</sup> )		$\log C_w^{sat-1}$ (m <sup>3</sup> mol <sup>-1</sup> )		$\log K_{ndw}$		$\log K_{hdw}^{-1}$		
		$R_v^2$	$R_h^2$	$R_v^2$	$R_h^2$	$R_v^2$	$R_h^2$	$R_v^2$	$R_h^2$	$R_v^2$	$R_h^2$	$R_v^2$	$R_h^2$	$R_v^2$	$R_h^2$	$R_v^2$	$R_h^2$	
$\rho$ (g cm <sup>-3</sup> )		0.23	0.54	0.18	0.54	0.24	0.54	0.17	0.53	0.27	0.54	0.00	0.48	0.23	0.48	0.17	0.53	
$\rho^{-1}$ (cm <sup>3</sup> g <sup>-1</sup> )		0.15	0.69	0.13	0.69	0.16	0.69	0.13	0.68	0.15	0.69	0.02	0.62	0.15	0.62	0.13	0.68	
$T_m$ (K)		0.70	0.50	0.55	0.49	0.71	0.50	0.54	0.49	0.76	0.50	0.03	0.44	0.69	0.44	0.54	0.49	
$T_m^{-1}$ (K <sup>-1</sup> )		0.15	0.69	0.13	0.69	0.16	0.69	0.13	0.68	0.15	0.69	0.02	0.62	0.15	0.62	0.13	0.68	
$T_g$ (K)		0.54	0.41	0.42	0.40	0.54	0.41	0.41	0.40	0.60	0.41	0.02	0.36	0.53	0.36	0.41	0.40	
$T_g^{-1}$ (K <sup>-1</sup> )		0.29	0.81	0.22	0.80	0.29	0.81	0.22	0.79	0.33	0.81	0.01	0.71	0.29	0.71	0.22	0.80	
$d_{50}$ ( $\mu\text{m}$ )	*	$X_c$ (%)	0.84	0.94	0.68	0.93	0.85	0.94	0.66	0.92	0.89	0.94	0.05	0.82	0.83	0.82	0.67	0.93
	$X_c^{-1}$ (% <sup>-1</sup> )	0.65	0.04	0.52	0.04	0.66	0.04	0.50	0.04	0.71	0.04	0.03	0.04	0.64	0.04	0.51	0.04	
$SA$ (m <sup>2</sup> g <sup>-1</sup> )		0.12	0.40	0.09	0.39	0.12	0.40	0.09	0.39	0.12	0.40	0.01	0.37	0.11	0.36	0.09	0.39	
$SA^{-1}$ (g m <sup>-2</sup> )		0.08	0.70	0.07	0.69	0.08	0.70	0.07	0.68	0.08	0.70	0.01	0.60	0.08	0.60	0.07	0.68	
$V_p$ (cm <sup>3</sup> g <sup>-1</sup> )		0.13	0.40	0.10	0.39	0.13	0.40	0.10	0.39	0.13	0.40	0.01	0.36	0.12	0.36	0.10	0.39	
$V_p^{-1}$ (g cm <sup>-3</sup> )		0.09	0.71	0.08	0.70	0.09	0.71	0.08	0.69	0.09	0.71	0.01	0.61	0.09	0.61	0.08	0.69	
$\sum SFE$ (mN m <sup>-1</sup> )		0.04	0.51	0.02	0.50	0.04	0.51	0.02	0.49	0.05	0.51	0.00	0.44	0.04	0.44	0.02	0.50	
$\sum SFE^{-1}$ (m Nm <sup>-1</sup> )		0.04	0.65	0.04	0.64	0.04	0.65	0.04	0.64	0.03	0.65	0.01	0.59	0.04	0.59	0.04	0.64	

Table A7.3: Calculation of  $R_h^2$  and  $R_v^2$  with the matrix of one PAH property multiplied with two plastic properties ( $d_{50}^{-1}$  as fixed parameter) and the  $\log K_{p-w}$  matrix

plastic property product		PAH properties																
1 <sup>st</sup> fixed parameter	2 <sup>nd</sup> variable parameter	$\log K_{ow}$		$\log K_{ow}^{-1}$		MW (g mol <sup>-1</sup> )		MW <sup>1</sup> (mol g <sup>-1</sup> )		$\log C_w^{sat}$ (mol m <sup>-3</sup> )		$\log C_w^{sat-1}$ (m <sup>3</sup> mol <sup>-1</sup> )		$\log K_{ndw}$		$\log K_{hdw}^{-1}$		
		$R_v^2$	$R_h^2$	$R_v^2$	$R_h^2$	$R_v^2$	$R_h^2$	$R_v^2$	$R_h^2$	$R_v^2$	$R_h^2$	$R_v^2$	$R_h^2$	$R_v^2$	$R_h^2$	$R_v^2$	$R_h^2$	
$\rho$ (g cm <sup>-3</sup> )		0.21	0.76	0.17	0.75	0.21	0.76	0.17	0.74	0.20	0.76	0.02	0.67	0.20	0.67	0.17	0.75	
$\rho^{-1}$ (cm <sup>3</sup> g <sup>-1</sup> )		0.13	0.80	0.10	0.79	0.13	0.79	0.09	0.78	0.16	0.79	0.00	0.71	0.13	0.71	0.09	0.78	
$T_m$ (K)		0.28	0.70	0.23	0.69	0.28	0.70	0.23	0.69	0.26	0.70	0.04	0.62	0.27	0.62	0.23	0.69	
$T_m^{-1}$ (K <sup>-1</sup> )		0.65	0.87	0.51	0.86	0.65	0.87	0.49	0.85	0.71	0.87	0.03	0.77	0.64	0.77	0.50	0.86	
$T_g$ (K)		0.39	0.62	0.30	0.61	0.40	0.62	0.29	0.61	0.44	0.62	0.01	0.55	0.38	0.55	0.30	0.61	
$T_g^{-1}$ (K <sup>-1</sup> )		0.26	0.83	0.20	0.82	0.27	0.83	0.19	0.81	0.30	0.83	0.01	0.73	0.26	0.73	0.20	0.82	
$d_{50}$ ( $\mu\text{m}$ )	*	$X_c$ (%)	0.79	0.95	0.63	0.94	0.80	0.95	0.61	0.93	0.86	0.95	0.04	0.83	0.78	0.83	0.62	0.93
	$X_c^{-1}$ (% <sup>-1</sup> )	0.67	0.08	0.53	0.08	0.68	0.08	0.52	0.08	0.73	0.08	0.03	0.07	0.66	0.07	0.52	0.08	
$SA$ (m <sup>2</sup> g <sup>-1</sup> )		0.02	0.47	0.02	0.46	0.02	0.47	0.02	0.46	0.02	0.47	0.00	0.43	0.02	0.43	0.02	0.46	
$SA^{-1}$ (g m <sup>-2</sup> )		0.35	0.82	0.28	0.80	0.35	0.81	0.27	0.79									

Table A7.4: Calculation of  $R_h^2$  and  $R_v^2$  with the matrix of one PAH property multiplied with two plastic properties ( $T_m$  as fixed parameter) and the log  $K_{p-w}$  matrix

plastic property product			PAH properties															
1 <sup>st</sup> fixed parameter	*	2 <sup>nd</sup> variable parameter	log $K_{ow}$ (-)		log $K_{ow}^{-1}$ (-)		MW (g mol <sup>-1</sup> )		MW <sup>1</sup> (mol g <sup>-1</sup> )		log $C_w^{sat}$ (mol m <sup>-3</sup> )		log $C_w^{sat-1}$ (m <sup>3</sup> mol <sup>-1</sup> )		log $K_{ndw}$ (-)		log $K_{ndw}^{-1}$ (-)	
	R <sub>v</sub> <sup>2</sup>	R <sub>b</sub> <sup>2</sup>	R <sub>v</sub> <sup>2</sup>	R <sub>b</sub> <sup>2</sup>	R <sub>v</sub> <sup>2</sup>	R <sub>b</sub> <sup>2</sup>	R <sub>v</sub> <sup>2</sup>	R <sub>b</sub> <sup>2</sup>	R <sub>v</sub> <sup>2</sup>	R <sub>b</sub> <sup>2</sup>	R <sub>v</sub> <sup>2</sup>	R <sub>b</sub> <sup>2</sup>	R <sub>v</sub> <sup>2</sup>	R <sub>b</sub> <sup>2</sup>	R <sub>v</sub> <sup>2</sup>	R <sub>b</sub> <sup>2</sup>		
$T_m$ (K)	$\rho$ (g cm <sup>-3</sup> )	0.47	0.52	0.36	0.51	0.47	0.52	0.35	0.51	0.52	0.52	0.02	0.46	0.46	0.46	0.36	0.51	
	$p^1$ (cm <sup>3</sup> g <sup>-1</sup> )	0.35	0.84	0.27	0.82	0.36	0.83	0.26	0.82	0.41	0.83	0.01	0.74	0.35	0.74	0.27	0.82	
	$d_{50}$ (μm)	0.70	0.50	0.55	0.49	0.71	0.50	0.54	0.49	0.76	0.50	0.03	0.44	0.69	0.44	0.54	0.49	
	$d_{50}^{-1}$ (μm <sup>-1</sup> )	0.65	0.87	0.51	0.86	0.65	0.87	0.49	0.85	0.71	0.87	0.03	0.77	0.64	0.77	0.50	0.86	
	$T_g$ (K)	0.66	0.38	0.52	0.38	0.67	0.38	0.50	0.37	0.72	0.38	0.03	0.34	0.65	0.34	0.51	0.38	
	$T_g^{-1}$ (K <sup>-1</sup> )	0.44	0.88	0.34	0.86	0.44	0.87	0.33	0.85	0.49	0.87	0.02	0.77	0.43	0.77	0.34	0.86	
	$X_c$ (%)	0.77	0.94	0.62	0.92	0.78	0.93	0.60	0.91	0.83	0.93	0.04	0.82	0.76	0.82	0.61	0.92	
	$X_c^{-1}$ (%) <sup>-1</sup>	0.65	0.08	0.52	0.08	0.66	0.08	0.50	0.08	0.71	0.08	0.03	0.08	0.64	0.08	0.51	0.08	
	SA (m <sup>2</sup> g <sup>-2</sup> )	0.13	0.38	0.10	0.38	0.13	0.38	0.10	0.37	0.13	0.38	0.01	0.35	0.12	0.35	0.10	0.37	
	SA <sup>1</sup> (g m <sup>-2</sup> )	0.44	0.83	0.36	0.81	0.45	0.83	0.35	0.80	0.46	0.83	0.03	0.71	0.43	0.71	0.35	0.81	
	Vp (cm <sup>3</sup> g <sup>-1</sup> )	0.14	0.38	0.11	0.37	0.14	0.38	0.11	0.37	0.14	0.38	0.01	0.35	0.14	0.35	0.11	0.37	
	Vp <sup>1</sup> (g cm <sup>-3</sup> )	0.45	0.83	0.36	0.82	0.45	0.83	0.35	0.81	0.47	0.83	0.03	0.72	0.44	0.72	0.36	0.82	
	$\sum SFE$ (mN m <sup>-1</sup> )	0.13	0.48	0.10	0.47	0.13	0.48	0.09	0.47	0.16	0.48	0.00	0.42	0.13	0.42	0.10	0.47	
	$\sum SFE^1$ (m Nm <sup>-1</sup> )	0.05	0.74	0.03	0.74	0.05	0.74	0.03	0.73	0.07	0.74	0.00	0.67	0.05	0.67	0.03	0.73	

Table A7.5: Calculation of  $R_h^2$  and  $R_v^2$  with the matrix of one PAH property multiplied with two plastic properties ( $T_m^{-1}$  as fixed parameter) and the log  $K_{p-w}$  matrix

plastic property product			PAH properties															
1 <sup>st</sup> fixed parameter	*	2 <sup>nd</sup> variable parameter	log $K_{ow}$ (-)		log $K_{ow}^{-1}$ (-)		MW (g mol <sup>-1</sup> )		MW <sup>1</sup> (mol g <sup>-1</sup> )		log $C_w^{sat}$ (mol m <sup>-3</sup> )		log $C_w^{sat-1}$ (m <sup>3</sup> mol <sup>-1</sup> )		log $K_{ndw}$ (-)		log $K_{ndw}^{-1}$ (-)	
	R <sub>v</sub> <sup>2</sup>	R <sub>b</sub> <sup>2</sup>	R <sub>v</sub> <sup>2</sup>	R <sub>b</sub> <sup>2</sup>	R <sub>v</sub> <sup>2</sup>	R <sub>b</sub> <sup>2</sup>	R <sub>v</sub> <sup>2</sup>	R <sub>b</sub> <sup>2</sup>	R <sub>v</sub> <sup>2</sup>	R <sub>b</sub> <sup>2</sup>	R <sub>v</sub> <sup>2</sup>	R <sub>b</sub> <sup>2</sup>	R <sub>v</sub> <sup>2</sup>	R <sub>b</sub> <sup>2</sup>	R <sub>v</sub> <sup>2</sup>	R <sub>b</sub> <sup>2</sup>		
$T_m^{-1}$ (K <sup>-1</sup> )	$\rho$ (g cm <sup>-3</sup> )	0.30	0.78	0.25	0.77	0.30	0.78	0.25	0.76	0.29	0.78	0.04	0.68	0.29	0.68	0.25	0.76	
	$p^1$ (cm <sup>3</sup> g <sup>-1</sup> )	0.35	0.84	0.27	0.82	0.36	0.83	0.26	0.82	0.41	0.83	0.01	0.74	0.35	0.74	0.27	0.82	
	$d_{50}$ (μm)	0.31	0.76	0.26	0.75	0.31	0.76	0.26	0.74	0.30	0.76	0.04	0.67	0.31	0.67	0.26	0.75	
	$d_{50}^{-1}$ (μm <sup>-1</sup> )	0.65	0.87	0.51	0.86	0.65	0.87	0.49	0.85	0.71	0.87	0.03	0.77	0.64	0.77	0.50	0.86	
	$T_g$ (K)	0.09	0.65	0.07	0.64	0.09	0.64	0.06	0.63	0.12	0.64	0.00	0.57	0.09	0.57	0.06	0.64	
	$T_g^{-1}$ (K <sup>-1</sup> )	0.44	0.88	0.34	0.86	0.44	0.87	0.33	0.85	0.49	0.87	0.02	0.77	0.43	0.77	0.34	0.86	
	$X_c$ (%)	0.87	0.96	0.70	0.94	0.88	0.95	0.68	0.93	0.93	0.95	0.05	0.83	0.86	0.83	0.69	0.94	
	$X_c^{-1}$ (%) <sup>-1</sup>	0.65	0.08	0.52	0.08	0.66	0.08	0.50	0.08	0.71	0.08	0.03	0.08	0.64	0.08	0.51	0.08	
	SA (m <sup>2</sup> g <sup>-1</sup> )	0.01	0.49	0.01	0.49	0.01	0.49	0.01	0.49	0.01	0.49	0.00	0.45	0.01	0.45	0.01	0.49	
	SA <sup>1</sup> (g m <sup>-2</sup> )	0.44	0.83	0.36	0.81	0.45	0.83	0.35	0.80	0.46	0.83	0.03	0.71	0.43	0.71	0.35	0.81	
	Vp (cm <sup>3</sup> g <sup>-1</sup> )	0.01	0.50	0.01	0.49	0.01	0.50	0.01	0.49	0.01	0.50	0.00	0.45	0.01	0.45	0.01	0.49	
	Vp <sup>1</sup> (g cm <sup>-3</sup> )	0.45	0.83	0.36	0.82	0.45	0.83	0.35	0.81	0.47	0.83	0.03	0.72	0.44	0.72	0.36	0.82	
	$\sum SFE$ (mN m <sup>-1</sup> )	0.19	0.72	0.16	0.71	0.19	0.72	0.16	0.70	0.18	0.72	0.03	0.62	0.19	0.62	0.16	0.70	
	$\sum SFE^1$ (m Nm <sup>-1</sup> )	0.05	0.74	0.03	0.74	0.05	0.74	0.03	0.73	0.07	0.74	0.00	0.67	0.05	0.67	0.03	0.73	

Table A7.6: Calculation of  $R_h^2$  and  $R_v^2$  with the matrix of one PAH property multiplied with two plastic properties ( $T_g$  as fixed parameter) and the log  $K_{p-w}$  matrix

plastic property product			PAH properties															
1 <sup>st</sup> fixed parameter	*	2 <sup>nd</sup> variable parameter	log $K_{ow}$ (-)		log $K_{ow}^{-1}$ (-)		MW (g mol <sup>-1</sup> )		MW <sup>1</sup> (mol g <sup>-1</sup> )		log $C_w^{sat}$ (mol m <sup>-3</sup> )		log $C_w^{sat-1}$ (m <sup>3</sup> mol <sup>-1</sup> )		log $K_{ndw}$ (-)		log $K_{ndw}^{-1}$ (-)	
	R <sub>v</sub> <sup>2</sup>	R <sub>b</sub> <sup>2</sup>	R <sub>v</sub> <sup>2</sup>	R <sub>b</sub> <sup>2</sup>	R <sub>v</sub> <sup>2</sup>	R <sub>b</sub> <sup>2</sup>	R <sub>v</sub> <sup>2</sup>	R <sub>b</sub> <sup>2</sup>	R <sub>v</sub> <sup>2</sup>	R <sub>b</sub> <sup>2</sup>	R <sub>v</sub> <sup>2</sup>	R <sub>b</sub> <sup>2</sup>	R <sub>v</sub> <sup>2</sup>	R <sub>b</sub> <sup>2</sup>	R <sub>v</sub> <sup>2</sup>	R <sub>b</sub> <sup>2</sup>		
$T_g$ (K)	$\rho$ (g cm <sup>-3</sup> )	0.39	0.42	0.30	0.42	0.39	0.42	0.29	0.41	0.44	0.42	0.01	0.37	0.38	0.37	0.29	0.42	
	$p^1$ (cm <sup>3</sup> g <sup>-1</sup> )	0.38	0.58	0.30	0.57	0.38	0.58	0.29	0.57	0.41	0.58	0.02	0.52	0.37	0.52	0.29	0.57	
	$d_{50}$ (μm)	0.54	0.41	0.42	0.40	0.54	0.41	0.41	0.40	0.60	0.41	0.02	0.36	0.53	0.36	0.41	0.40	
	$d_{50}^{-1}$ (μm <sup>-1</sup> )	0.39	0.62	0.30	0.61	0.40	0.62	0.29	0.61	0.44	0.62	0.01	0.55	0.38	0.55	0.30	0.61	
	$T_m$ (K)	0.66	0.38	0.52	0.38	0.67	0.38	0.50	0.37	0.72	0.38	0.03	0.34	0.65	0.34	0.51	0.38	
	$T_m^{-1}$ (K <sup>-1</sup> )	0.09	0.65	0.07	0.64	0.09	0.64	0.06	0.63	0.12	0.64	0.00	0.57	0.09	0.57	0.06	0.64	
	$X_c$ (%)	0.70	0.90	0.57	0.88	0.71	0.89	0.55	0.87	0.73	0.89	0.05	0.78	0.69	0.78	0.56	0.88	
	$X_c^{-1}$ (%) <sup>-1</sup>	0.65	0.03	0.52														

Table A7.7: Calculation of  $R_h^2$  and  $R_v^2$  with the matrix of one PAH property multiplied with two plastic properties ( $T_g^{-1}$  as fixed parameter) and the log  $K_{p-w}$  matrix

plastic property product		PAH properties															
1 <sup>st</sup> fixed parameter	* variable parameter	log $K_{ow}$ (-)		log $K_{ow}^{-1}$ (-)		MW (g mol <sup>-1</sup> )		MW <sup>1</sup> (mol g <sup>-1</sup> )		log $C_w^{sat}$ (mol m <sup>-3</sup> )		log $C_w^{sat-1}$ (m <sup>3</sup> mol <sup>-1</sup> )		log $K_{ndw}$ (-)		log $K_{ndw}^{-1}$ (-)	
		$R_h^2$	$R_h^2$	$R_v^2$	$R_v^2$	$R_v^2$	$R_h^2$	$R_v^2$	$R_h^2$	$R_v^2$	$R_h^2$	$R_v^2$	$R_h^2$	$R_v^2$	$R_h^2$	$R_v^2$	
	$\rho$ (g cm <sup>-3</sup> )	0.40	0.83	0.32	0.82	0.41	0.83	0.31	0.81	0.44	0.83	0.02	0.73	0.40	0.73	0.31	0.82
	$\rho^1$ (cm <sup>3</sup> g <sup>-1</sup> )	0.17	0.80	0.13	0.79	0.17	0.80	0.12	0.79	0.21	0.80	0.00	0.71	0.17	0.71	0.12	0.79
	$d_{50}$ (μm)	0.29	0.81	0.22	0.80	0.29	0.81	0.22	0.79	0.33	0.81	0.01	0.71	0.29	0.71	0.22	0.80
	$d_{50}^{-1}$ (μm <sup>-1</sup> )	0.26	0.83	0.20	0.82	0.27	0.83	0.19	0.81	0.30	0.83	0.01	0.73	0.26	0.73	0.20	0.82
	$T_m$ (K)	0.07	0.77	0.05	0.76	0.07	0.77	0.04	0.76	0.09	0.77	0.00	0.69	0.06	0.68	0.05	0.76
	$T_m^{-1}$ (K <sup>-1</sup> )	0.44	0.88	0.34	0.86	0.44	0.87	0.33	0.85	0.49	0.87	0.02	0.77	0.43	0.77	0.34	0.86
$T_g$ <sup>3</sup> (K <sup>1</sup> )	$X_c$ (%)	0.67	0.93	0.53	0.91	0.68	0.92	0.52	0.90	0.74	0.92	0.03	0.81	0.66	0.80	0.52	0.91
	$X_c^{-1}$ (%) <sup>-1</sup>	0.66	0.12	0.53	0.12	0.67	0.12	0.51	0.12	0.72	0.12	0.03	0.11	0.66	0.11	0.52	0.12
	SA (m <sup>2</sup> g <sup>-1</sup> )	0.00	0.56	0.00	0.56	0.00	0.56	0.00	0.55	0.00	0.56	0.00	0.51	0.00	0.51	0.00	0.56
	SA <sup>1</sup> (g m <sup>-2</sup> )	0.34	0.81	0.27	0.79	0.34	0.80	0.26	0.78	0.37	0.80	0.02	0.70	0.33	0.70	0.26	0.79
	Vp (cm <sup>3</sup> g <sup>-1</sup> )	0.00	0.56	0.00	0.56	0.00	0.56	0.00	0.56	0.00	0.56	0.00	0.51	0.00	0.51	0.00	0.56
	Vp <sup>1</sup> (g cm <sup>-3</sup> )	0.33	0.80	0.26	0.79	0.34	0.80	0.25	0.78	0.37	0.80	0.02	0.70	0.33	0.70	0.26	0.79
	$\sum SFE$ (mN m <sup>-1</sup> )	0.38	0.81	0.32	0.79	0.39	0.80	0.31	0.78	0.38	0.80	0.04	0.69	0.37	0.69	0.31	0.79
	$\sum SFE^1$ (m Nm <sup>-1</sup> )	0.05	0.70	0.04	0.69	0.06	0.70	0.04	0.68	0.07	0.70	0.00	0.63	0.05	0.63	0.04	0.69

Table A7.8: Calculation of  $R_h^2$  and  $R_v^2$  with the matrix of one PAH property multiplied with two plastic properties ( $X_c$  as fixed parameter) and the log  $K_{p-w}$  matrix

plastic property product		PAH properties																
1 <sup>st</sup> fixed parameter	* variable parameter	log $K_{ow}$ (-)		log $K_{ow}^{-1}$ (-)		MW (g mol <sup>-1</sup> )		MW <sup>1</sup> (mol g <sup>-1</sup> )		log $C_w^{sat}$ (mol m <sup>-3</sup> )		log $C_w^{sat-1}$ (m <sup>3</sup> mol <sup>-1</sup> )		log $K_{ndw}$ (-)		log $K_{ndw}^{-1}$ (-)		
		$R_h^2$	$R_h^2$	$R_v^2$	$R_v^2$	$R_v^2$	$R_h^2$	$R_v^2$	$R_h^2$	$R_v^2$	$R_h^2$	$R_v^2$	$R_h^2$	$R_v^2$	$R_h^2$	$R_v^2$		
	$\rho$ (g cm <sup>-3</sup> )	0.87	0.94	0.71	0.92	0.88	0.93	0.69	0.91	0.91	0.93	0.06	0.81	0.86	0.81	0.70	0.92	
	$\rho^1$ (cm <sup>3</sup> g <sup>-1</sup> )	0.65	0.93	0.52	0.91	0.66	0.92	0.50	0.90	0.72	0.92	0.03	0.81	0.65	0.81	0.51	0.91	
	$d_{50}$ (μm)	0.84	0.94	0.68	0.93	0.85	0.94	0.66	0.92	0.89	0.94	0.05	0.82	0.83	0.82	0.67	0.93	
	$d_{50}^{-1}$ (μm <sup>-1</sup> )	0.79	0.95	0.63	0.94	0.80	0.95	0.61	0.93	0.86	0.95	0.04	0.83	0.78	0.83	0.62	0.93	
	$T_m$ (K)	0.77	0.94	0.62	0.92	0.78	0.93	0.60	0.91	0.83	0.93	0.04	0.82	0.76	0.82	0.61	0.92	
	$T_m^{-1}$ (K <sup>-1</sup> )	0.87	0.96	0.70	0.94	0.88	0.95	0.68	0.93	0.93	0.95	0.05	0.83	0.86	0.83	0.69	0.94	
$X_c$ (%)	*	$T_g$ (K)	0.70	0.90	0.57	0.88	0.71	0.89	0.55	0.87	0.73	0.89	0.05	0.78	0.69	0.78	0.56	0.88
		$T_g^{-1}$ (K <sup>-1</sup> )	0.67	0.93	0.53	0.91	0.68	0.92	0.52	0.90	0.74	0.92	0.03	0.81	0.66	0.80	0.52	0.91
	SA (m <sup>2</sup> g <sup>-1</sup> )	0.05	0.56	0.04	0.56	0.05	0.56	0.04	0.55	0.06	0.56	0.00	0.51	0.05	0.51	0.04	0.55	
	SA <sup>1</sup> (g m <sup>-2</sup> )	0.75	0.88	0.61	0.86	0.76	0.87	0.59	0.85	0.79	0.87	0.05	0.75	0.74	0.75	0.60	0.86	
	Vp (cm <sup>3</sup> g <sup>-1</sup> )	0.05	0.57	0.04	0.56	0.05	0.56	0.04	0.56	0.06	0.56	0.00	0.51	0.05	0.51	0.04	0.56	
	Vp <sup>1</sup> (g cm <sup>-3</sup> )	0.75	0.88	0.60	0.86	0.76	0.87	0.59	0.85	0.79	0.87	0.05	0.75	0.74	0.75	0.60	0.86	
	$\sum SFE$ (mN m <sup>-1</sup> )	0.74	0.84	0.60	0.82	0.74	0.83	0.59	0.81	0.75	0.83	0.06	0.71	0.73	0.71	0.60	0.82	
	$\sum SFE^1$ (m Nm <sup>-1</sup> )	0.28	0.81	0.21	0.80	0.28	0.81	0.21	0.80	0.32	0.81	0.01	0.72	0.28	0.72	0.21	0.80	

Table A7.9: Calculation of  $R_h^2$  and  $R_v^2$  with the matrix of one PAH property multiplied with two plastic properties ( $X_c^{-1}$  as fixed parameter) and the log  $K_{p-w}$  matrix

plastic property product		PAH properties																
1 <sup>st</sup> fixed parameter	* variable parameter	log $K_{ow}$ (-)		log $K_{ow}^{-1}$ (-)		MW (g mol <sup>-1</sup> )		MW <sup>1</sup> (mol g <sup>-1</sup> )		log $C_w^{sat}$ (mol m <sup>-3</sup> )		log $C_w^{sat-1}$ (m <sup>3</sup> mol <sup>-1</sup> )		log $K_{ndw}$ (-)		log $K_{ndw}^{-1}$ (-)		
		$R_h^2$	$R_h^2$	$R_v^2$	$R_v^2$	$R_v^2$	$R_h^2$	$R_v^2$	$R_h^2$	$R_v^2$	$R_h^2$	$R_v^2$	$R_h^2$	$R_v^2$	$R_h^2$	$R_v^2$		
	$\rho$ (g cm <sup>-3</sup> )	0.63	0.04	0.50	0.04	0.64	0.04	0.49	0.04	0.69	0.04	0.03	0.04	0.63	0.04	0.49	0.04	
	$\rho^1$ (cm <sup>3</sup> g <sup>-1</sup> )	0.70	0.08	0.56	0.08	0.71	0.08	0.54	0.08	0.76	0.08	0.03	0.08	0.69	0.08	0.55	0.08	
	$d_{50}$ (μm)	0.65	0.04	0.52	0.04	0.66	0.04	0.50	0.04	0.71	0.04	0.03	0.04	0.64	0.04	0.51	0.04	
	$d_{50}^{-1}$ (μm <sup>-1</sup> )	0.67	0.08	0.53	0.08	0.68	0.08	0.52	0.08	0.73	0.08	0.03	0.07	0.66	0.07	0.52	0.08	
	$T_m$ (K)	0.66	0.04	0.53	0.04	0.67	0.04	0.51	0.04	0.72	0.04	0.03	0.03	0.65	0.03	0.52	0.04	
	$T_m^{-1}$ (K <sup>-1</sup> )	0.65	0.08	0.52	0.08	0.66	0.08	0.50	0.08	0.71	0.08	0.03	0.08	0.64	0.08	0.51	0.08	
$X_c$ (%) <sup>-1</sup>	*	$T_g$ (K)	0.65	0.03	0.52	0.03	0.66	0.03	0.50	0.03	0.71	0.03	0.03	0.03	0.65	0.03	0.51	0.03
		$T_g^{-1}$ (K <sup>-1</sup> )	0.66	0.12	0.53	0.12	0.67	0.12	0.51	0.12	0.72	0.12	0.03	0.11	0.66	0.11	0.52	0.12
	SA (m <sup>2</sup> g <sup>-1</sup> )	0.77	0.07	0.62	0.07	0.78	0.07	0.60	0.07	0.84	0.07	0.04	0.07	0.76	0.07	0.61	0.07	
	SA <sup>1</sup> (g m <sup>-2</sup> )	0.57	0.06	0.45	0.06	0.58	0.06	0.44	0.06	0.62	0.06	0.02	0.06	0.56	0.06	0.44	0.06	
	Vp (cm <sup>3</sup> g <sup>-1</sup> )	0.77	0.07	0.61	0.07	0.78	0.07	0.59	0.07	0.83	0.07	0.04	0.07	0.76	0.07	0.60	0.07	
	Vp <sup>1</sup> (g cm <sup>-3</sup> )	0.57	0.07	0.45	0.07	0.58	0.07	0.44	0.07	0.62	0.07	0.02	0.06	0.56	0.06	0.44	0.07	
	$\sum SFE$ (mN m <sup>-1</sup> )	0.60	0.03	0.47	0.03	0.61	0.03	0.46	0.03	0.66	0.03	0.03	0.03	0.59	0.03	0.47	0.03	
	$\sum SFE^1$ (m Nm <sup>-1</sup> )	0.77	0.11	0.62	0.11	0.78												

Table A7.10: Calculation of  $R_h^2$  and  $R_v^2$  with the matrix of one PAH property multiplied with two plastic properties (SA as fixed parameter) and the log  $K_{p-w}$  matrix

plastic property product		PAH properties																
1 <sup>st</sup> fixed parameter	2 <sup>nd</sup> variable parameter	log $K_{ow}$ (-)		log $K_{ow}^{-1}$ (-)		MW (g mol <sup>-1</sup> )		MW <sup>1</sup> (mol g <sup>-1</sup> )		log $C_w^{sat}$ (mol m <sup>-3</sup> )		log $C_w^{sat-1}$ (m <sup>3</sup> mol <sup>-1</sup> )		log $K_{ndw}$ (-)		log $K_{ndw}^{-1}$ (-)		
		$R_q^2$	$R_h^2$	$R_q^2$	$R_h^2$	$R_q^2$	$R_h^2$	$R_q^2$	$R_h^2$	$R_q^2$	$R_h^2$	$R_q^2$	$R_h^2$	$R_q^2$	$R_h^2$	$R_q^2$	$R_h^2$	
	$\rho$ (g cm <sup>-3</sup> )	0.14	0.45	0.11	0.44	0.14	0.45	0.11	0.44	0.15	0.45	0.01	0.41	0.14	0.41	0.11	0.44	
	$\rho^{-1}$ (cm <sup>3</sup> g <sup>-1</sup> )	0.02	0.41	0.02	0.40	0.02	0.41	0.02	0.40	0.02	0.41	0.00	0.38	0.02	0.38	0.02	0.40	
	$d_{50}$ (μm)	0.12	0.40	0.09	0.39	0.12	0.40	0.09	0.39	0.12	0.40	0.01	0.37	0.11	0.36	0.09	0.39	
	$d_{50}^{-1}$ (μm <sup>-1</sup> )	0.02	0.47	0.02	0.46	0.02	0.47	0.02	0.46	0.02	0.47	0.00	0.43	0.02	0.43	0.02	0.46	
	$T_m$ (K)	0.13	0.38	0.10	0.38	0.13	0.38	0.10	0.37	0.13	0.38	0.01	0.35	0.12	0.35	0.10	0.37	
	$T_m^{-1}$ (K <sup>-1</sup> )	0.01	0.49	0.01	0.49	0.01	0.49	0.01	0.49	0.01	0.49	0.00	0.45	0.01	0.45	0.01	0.49	
SA	*	$T_g$ (K)	0.16	0.33	0.13	0.33	0.16	0.33	0.12	0.33	0.17	0.33	0.01	0.31	0.15	0.31	0.12	0.33
(m <sup>2</sup> g <sup>-1</sup> )	*	$T_g^{-1}$ (K <sup>-1</sup> )	0.00	0.56	0.00	0.56	0.00	0.56	0.00	0.55	0.00	0.56	0.00	0.51	0.00	0.51	0.00	0.56
	$X_c$ (%)	0.05	0.56	0.04	0.56	0.05	0.56	0.04	0.55	0.06	0.56	0.00	0.51	0.05	0.51	0.04	0.55	
	$X_c^{-1}$ (%) <sup>-1</sup>	0.77	0.07	0.62	0.07	0.78	0.07	0.60	0.07	0.84	0.07	0.04	0.07	0.76	0.07	0.61	0.07	
	$V_p$ (cm <sup>3</sup> g <sup>-1</sup> )	0.03	0.23	0.02	0.23	0.03	0.23	0.02	0.23	0.03	0.23	0.00	0.22	0.03	0.22	0.02	0.23	
	$V_p^{-1}$ (g cm <sup>-3</sup> )	0.08	0.74	0.06	0.73	0.08	0.74	0.05	0.72	0.10	0.74	0.00	0.66	0.08	0.65	0.06	0.73	
	$\sum SFE$ (mN m <sup>-1</sup> )	0.18	0.49	0.14	0.48	0.18	0.49	0.14	0.48	0.20	0.49	0.01	0.44	0.18	0.44	0.14	0.48	
	$\sum SFE^{-1}$ (m Nm <sup>-1</sup> )	0.02	0.36	0.02	0.36	0.02	0.36	0.02	0.36	0.00	0.34	0.02	0.34	0.02	0.36	0.02	0.36	

Table A7.11: Calculation of  $R_h^2$  and  $R_v^2$  with the matrix of one PAH property multiplied with two plastic properties (SA<sup>-1</sup> as fixed parameter) and the log  $K_{p-w}$  matrix

plastic property product		PAH properties																
1 <sup>st</sup> fixed parameter	2 <sup>nd</sup> variable parameter	log $K_{ow}$ (-)		log $K_{ow}^{-1}$ (-)		MW (g mol <sup>-1</sup> )		MW <sup>1</sup> (mol g <sup>-1</sup> )		log $C_w^{sat}$ (mol m <sup>-3</sup> )		log $C_w^{sat-1}$ (m <sup>3</sup> mol <sup>-1</sup> )		log $K_{ndw}$ (-)		log $K_{ndw}^{-1}$ (-)		
		$R_q^2$	$R_h^2$	$R_q^2$	$R_h^2$	$R_q^2$	$R_h^2$	$R_q^2$	$R_h^2$	$R_q^2$	$R_h^2$	$R_q^2$	$R_h^2$	$R_q^2$	$R_h^2$	$R_q^2$	$R_h^2$	
	$\rho$ (g cm <sup>-3</sup> )	0.14	0.70	0.11	0.69	0.14	0.70	0.11	0.68	0.13	0.70	0.02	0.60	0.13	0.60	0.11	0.69	
	$\rho^{-1}$ (cm <sup>3</sup> g <sup>-1</sup> )	0.29	0.81	0.23	0.80	0.29	0.81	0.22	0.79	0.31	0.81	0.01	0.71	0.28	0.70	0.22	0.80	
	$d_{50}$ (μm)	0.08	0.70	0.07	0.69	0.08	0.70	0.07	0.68	0.08	0.70	0.01	0.60	0.08	0.60	0.07	0.68	
	$d_{50}^{-1}$ (μm <sup>-1</sup> )	0.35	0.82	0.28	0.80	0.35	0.81	0.27	0.79	0.37	0.81	0.02	0.71	0.34	0.71	0.27	0.80	
	$T_m$ (K)	0.02	0.68	0.02	0.67	0.02	0.68	0.02	0.66	0.02	0.68	0.00	0.59	0.02	0.59	0.02	0.67	
	$T_m^{-1}$ (K <sup>-1</sup> )	0.44	0.83	0.36	0.81	0.45	0.83	0.35	0.80	0.46	0.83	0.03	0.71	0.43	0.71	0.35	0.81	
SA <sup>-1</sup>	*	$T_g$ (K)	0.00	0.59	0.00	0.58	0.00	0.59	0.00	0.57	0.00	0.59	0.00	0.51	0.00	0.51	0.00	0.58
(g m <sup>-2</sup> )	*	$T_g^{-1}$ (K <sup>-1</sup> )	0.34	0.81	0.27	0.79	0.34	0.80	0.26	0.78	0.37	0.80	0.02	0.70	0.33	0.70	0.26	0.79
	$X_c$ (%)	0.75	0.88	0.61	0.86	0.76	0.87	0.59	0.85	0.79	0.87	0.05	0.75	0.74	0.75	0.60	0.86	
	$X_c^{-1}$ (%) <sup>-1</sup>	0.57	0.06	0.45	0.06	0.58	0.06	0.44	0.06	0.62	0.06	0.02	0.06	0.56	0.06	0.44	0.06	
	$V_p$ (cm <sup>3</sup> g <sup>-1</sup> )	0.08	0.73	0.06	0.72	0.08	0.72	0.06	0.71	0.11	0.72	0.00	0.64	0.08	0.64	0.06	0.71	
	$V_p^{-1}$ (g cm <sup>-3</sup> )	0.38	0.78	0.31	0.76	0.39	0.78	0.30	0.76	0.40	0.78	0.03	0.67	0.37	0.66	0.31	0.76	
	$\sum SFE$ (mN m <sup>-1</sup> )	0.16	0.64	0.14	0.63	0.16	0.64	0.13	0.62	0.15	0.64	0.02	0.54	0.16	0.54	0.14	0.63	
	$\sum SFE^{-1}$ (m Nm <sup>-1</sup> )	0.12	0.74	0.09	0.73	0.12	0.74	0.08	0.73	0.14	0.74	0.00	0.66	0.11	0.66	0.08	0.73	

Table A7.12: Calculation of  $R_h^2$  and  $R_v^2$  with the matrix of one PAH property multiplied with two plastic properties (Vp as fixed parameter) and the log  $K_{p-w}$  matrix

plastic property product		PAH properties																
1 <sup>st</sup> fixed parameter	2 <sup>nd</sup> variable parameter	log $K_{ow}$ (-)		log $K_{ow}^{-1}$ (-)		MW (g mol <sup>-1</sup> )		MW <sup>1</sup> (mol g <sup>-1</sup> )		log $C_w^{sat}$ (mol m <sup>-3</sup> )		log $C_w^{sat-1}$ (m <sup>3</sup> mol <sup>-1</sup> )		log $K_{ndw}$ (-)		log $K_{ndw}^{-1}$ (-)		
		$R_q^2$	$R_h^2$	$R_q^2$	$R_h^2$	$R_q^2$	$R_h^2$	$R_q^2$	$R_h^2$	$R_q^2$	$R_h^2$	$R_q^2$	$R_h^2$	$R_q^2$	$R_h^2$	$R_q^2$	$R_h^2$	
	$\rho$ (g cm <sup>-3</sup> )	0.15	0.45	0.12	0.44	0.16	0.45	0.12	0.44	0.16	0.45	0.01	0.41	0.15	0.41	0.12	0.44	
	$\rho^{-1}$ (cm <sup>3</sup> g <sup>-1</sup> )	0.03	0.41	0.02	0.41	0.03	0.41	0.02	0.40	0.03	0.41	0.00	0.38	0.03	0.38	0.02	0.41	
	$d_{50}$ (μm)	0.13	0.40	0.10	0.39	0.13	0.40	0.10	0.39	0.13	0.40	0.01	0.36	0.12	0.36	0.10	0.39	
	$d_{50}^{-1}$ (μm <sup>-1</sup> )	0.02	0.47	0.02	0.47	0.02	0.47	0.02	0.46	0.02	0.47	0.00	0.43	0.02	0.43	0.02	0.47	
	$T_m$ (K)	0.14	0.38	0.11	0.37	0.14	0.38	0.11	0.37	0.14	0.38	0.01	0.35	0.14	0.35	0.11	0.37	
	$T_m^{-1}$ (K <sup>-1</sup> )	0.01	0.50	0.01	0.49	0.01	0.50	0.01	0.49	0.01	0.50	0.00	0.45	0.01	0.45	0.01	0.49	
Vp	*	$T_g$ (K)	0.17	0.33	0.14	0.33	0.17	0.33	0.13	0.33	0.18	0.33	0.01	0.31	0.17	0.31	0.13	0.33
(cm <sup>3</sup> g <sup>-1</sup> )	*	$T_g^{-1}$ (K <sup>-1</sup> )	0.00	0.56	0.00	0.56	0.00	0.56	0.00	0.56	0.00	0.56	0.00	0.51	0.00	0.51	0.00	0.56
	$X_c$ (%)	0.05	0.57	0.04	0.56	0.05	0.56	0.04	0.56	0.06	0.56	0.00	0.51	0.05	0.51	0.04	0.56	
	$X_c^{-1}$ (%) <sup>-1</sup>	0.77	0.07	0.61	0.07	0.78	0.07	0.59	0.07	0.83	0.07	0.04	0.07	0				

Table A7.13: Calculation of  $R_h^2$  and  $R_v^2$  with the matrix of one PAH property multiplied with two plastic properties ( $Vp^{-1}$  as fixed parameter) and the  $\log K_{p-w}$  matrix

plastic property product		PAH properties																
1 <sup>st</sup> fixed parameter	2 <sup>nd</sup> variable parameter	$\log K_{ow}$		$\log K_{ow}^{-1}$		MW (g mol <sup>-1</sup> )		MW <sup>1</sup> (mol g <sup>-1</sup> )		$\log C_w^{sat}$ (mol m <sup>-3</sup> )		$\log C_w^{sat-1}$ (m <sup>3</sup> mol <sup>-1</sup> )		$\log K_{hdw}$		$\log K_{hdw}^{-1}$		
		$R_v^2$	$R_n^2$	$R_v^2$	$R_n^2$	$R_v^2$	$R_n^2$	$R_v^2$	$R_n^2$	$R_v^2$	$R_n^2$	$R_v^2$	$R_n^2$	$R_v^2$	$R_n^2$	$R_v^2$	$R_n^2$	
	$\rho$ (g cm <sup>-3</sup> )	0.15	0.71	0.12	0.70	0.15	0.71	0.12	0.69	0.15	0.71	0.02	0.61	0.15	0.61	0.12	0.70	
	$\rho^1$ (cm <sup>3</sup> g <sup>-1</sup> )	0.29	0.81	0.23	0.80	0.29	0.81	0.22	0.79	0.31	0.81	0.01	0.71	0.28	0.71	0.22	0.80	
	$d_{50}$ (μm)	0.09	0.71	0.08	0.70	0.09	0.71	0.08	0.69	0.09	0.71	0.01	0.61	0.09	0.61	0.08	0.69	
	$d_{50}^{-1}$ (μm <sup>-1</sup> )	0.35	0.82	0.28	0.80	0.35	0.82	0.27	0.80	0.37	0.82	0.02	0.71	0.34	0.71	0.27	0.80	
	$T_m$ (K)	0.03	0.69	0.02	0.68	0.03	0.69	0.02	0.67	0.03	0.69	0.00	0.60	0.03	0.60	0.02	0.68	
	$T_m^{-1}$ (K <sup>-1</sup> )	0.45	0.83	0.36	0.82	0.45	0.83	0.35	0.81	0.47	0.83	0.03	0.72	0.44	0.72	0.36	0.82	
$Vp^{-1}$ (g cm <sup>-3</sup> )	*	$T_g$ (K)	0.00	0.60	0.00	0.59	0.00	0.60	0.00	0.59	0.00	0.60	0.00	0.52	0.00	0.52	0.00	0.59
		$T_g^{-1}$ (K <sup>-1</sup> )	0.33	0.80	0.26	0.79	0.34	0.80	0.25	0.78	0.37	0.80	0.02	0.70	0.33	0.70	0.26	0.79
	$X_c$ (%)	0.75	0.88	0.60	0.86	0.76	0.87	0.59	0.85	0.79	0.87	0.05	0.75	0.74	0.75	0.60	0.86	
	$X_c^{-1}$ (% <sup>-1</sup> )	0.57	0.07	0.45	0.07	0.58	0.07	0.44	0.07	0.62	0.07	0.02	0.06	0.56	0.06	0.44	0.07	
	SA (m <sup>2</sup> g <sup>-1</sup> )	0.08	0.74	0.06	0.73	0.08	0.74	0.05	0.72	0.10	0.74	0.00	0.66	0.08	0.65	0.06	0.73	
	SA <sup>1</sup> (g m <sup>-2</sup> )	0.38	0.78	0.31	0.76	0.39	0.78	0.30	0.76	0.40	0.78	0.03	0.67	0.37	0.66	0.31	0.76	
	$\sum SFE$ (mN m <sup>-1</sup> )	0.17	0.65	0.15	0.64	0.17	0.65	0.14	0.63	0.16	0.65	0.02	0.55	0.17	0.55	0.14	0.64	
	$\sum SFE^1$ (m N m <sup>-1</sup> )	0.11	0.74	0.08	0.73	0.12	0.74	0.08	0.72	0.14	0.74	0.00	0.65	0.11	0.65	0.08	0.73	

Table A7.14: Calculation of  $R_h^2$  and  $R_v^2$  with the matrix of one PAH property multiplied with two plastic properties ( $\sum SFE$  as fixed parameter) and the  $\log K_{p-w}$  matrix

plastic property product		PAH properties																
1 <sup>st</sup> fixed parameter	2 <sup>nd</sup> variable parameter	$\log K_{ow}$		$\log K_{ow}^{-1}$		MW (g mol <sup>-1</sup> )		MW <sup>1</sup> (mol g <sup>-1</sup> )		$\log C_w^{sat}$ (mol m <sup>-3</sup> )		$\log C_w^{sat-1}$ (m <sup>3</sup> mol <sup>-1</sup> )		$\log K_{hdw}$		$\log K_{hdw}^{-1}$		
		$R_v^2$	$R_n^2$	$R_v^2$	$R_n^2$	$R_v^2$	$R_n^2$	$R_v^2$	$R_n^2$	$R_v^2$	$R_n^2$	$R_v^2$	$R_n^2$	$R_v^2$	$R_n^2$	$R_v^2$	$R_n^2$	
	$\rho$ (g cm <sup>-3</sup> )	0.00	0.52	0.00	0.51	0.00	0.52	0.00	0.50	0.01	0.52	0.00	0.45	0.00	0.44	0.00	0.51	
	$\rho^1$ (cm <sup>3</sup> g <sup>-1</sup> )	0.06	0.72	0.05	0.70	0.06	0.71	0.05	0.70	0.05	0.71	0.02	0.62	0.06	0.62	0.05	0.70	
	$d_{50}$ (μm)	0.04	0.51	0.02	0.50	0.04	0.51	0.02	0.49	0.05	0.51	0.00	0.44	0.04	0.44	0.02	0.50	
	$d_{50}^{-1}$ (μm <sup>-1</sup> )	0.12	0.72	0.11	0.71	0.12	0.72	0.11	0.70	0.11	0.72	0.02	0.62	0.12	0.62	0.11	0.70	
	$T_m$ (K)	0.13	0.48	0.10	0.47	0.13	0.48	0.09	0.47	0.16	0.48	0.00	0.42	0.13	0.42	0.10	0.47	
	$T_m^{-1}$ (K <sup>-1</sup> )	0.19	0.72	0.16	0.71	0.19	0.72	0.16	0.70	0.18	0.72	0.03	0.62	0.19	0.62	0.16	0.70	
$\sum SFE$ (m N m <sup>-1</sup> )	*	$T_g$ (K)	0.16	0.40	0.12	0.39	0.16	0.40	0.11	0.39	0.19	0.40	0.00	0.35	0.15	0.35	0.11	0.39
		$T_g^{-1}$ (K <sup>-1</sup> )	0.38	0.81	0.32	0.79	0.39	0.80	0.31	0.78	0.38	0.80	0.04	0.69	0.37	0.69	0.31	0.79
	$X_c$ (%)	0.74	0.84	0.60	0.82	0.74	0.83	0.59	0.81	0.75	0.83	0.06	0.71	0.73	0.71	0.60	0.82	
	$X_c^{-1}$ (% <sup>-1</sup> )	0.60	0.03	0.47	0.03	0.61	0.03	0.46	0.03	0.66	0.03	0.03	0.03	0.59	0.03	0.47	0.03	
	SA (m <sup>2</sup> g <sup>-1</sup> )	0.18	0.49	0.14	0.48	0.18	0.49	0.14	0.48	0.20	0.49	0.01	0.44	0.18	0.44	0.14	0.48	
	SA <sup>1</sup> (g m <sup>-2</sup> )	0.16	0.64	0.14	0.63	0.16	0.64	0.13	0.62	0.15	0.64	0.02	0.54	0.16	0.54	0.14	0.63	
	$Vp$ (cm <sup>3</sup> g <sup>-1</sup> )	0.20	0.49	0.15	0.48	0.20	0.48	0.15	0.48	0.22	0.48	0.01	0.44	0.19	0.43	0.15	0.48	
	$Vp^1$ (g cm <sup>-3</sup> )	0.17	0.65	0.15	0.64	0.17	0.65	0.14	0.63	0.16	0.65	0.02	0.55	0.17	0.55	0.14	0.64	

Table A7.15: Calculation of  $R_h^2$  and  $R_v^2$  with the matrix of one PAH property multiplied with two plastic properties ( $\sum SFE^{-1}$  as fixed parameter) and the  $\log K_{p-w}$  matrix

plastic property product		PAH properties																
1 <sup>st</sup> fixed parameter	2 <sup>nd</sup> variable parameter	$\log K_{ow}$		$\log K_{ow}^{-1}$		MW (g mol <sup>-1</sup> )		MW <sup>1</sup> (mol g <sup>-1</sup> )		$\log C_w^{sat}$ (mol m <sup>-3</sup> )		$\log C_w^{sat-1}$ (m <sup>3</sup> mol <sup>-1</sup> )		$\log K_{hdw}$		$\log K_{hdw}^{-1}$		
		$R_v^2$	$R_n^2$	$R_v^2$	$R_n^2$	$R_v^2$	$R_n^2$	$R_v^2$	$R_n^2$	$R_v^2$	$R_n^2$	$R_v^2$	$R_n^2$	$R_v^2$	$R_n^2$	$R_v^2$	$R_n^2$	
	$\rho$ (g cm <sup>-3</sup> )	0.02	0.70	0.02	0.69	0.02	0.70	0.02	0.69	0.01	0.70	0.01	0.63	0.02	0.63	0.02	0.69	
	$\rho^1$ (cm <sup>3</sup> g <sup>-1</sup> )	0.00	0.65	0.00	0.65	0.00	0.65	0.00	0.64	0.01	0.65	0.00	0.59	0.00	0.59	0.00	0.65	
	$d_{50}$ (μm)	0.00	0.69	0.00	0.68	0.00	0.69	0.00	0.68	0.00	0.69	0.00	0.62	0.00	0.62	0.00	0.68	
	$d_{50}^{-1}$ (μm <sup>-1</sup> )	0.02	0.70	0.01	0.70	0.02	0.70	0.01	0.69	0.03	0.70	0.00	0.64	0.02	0.63	0.01	0.70	
	$T_m$ (K)	0.06	0.62	0.05	0.61	0.06	0.62	0.05	0.61	0.05	0.62	0.01	0.56	0.06	0.56	0.05	0.61	
	$T_m^{-1}$ (K <sup>-1</sup> )	0.05	0.74	0.03	0.74	0.05	0.74	0.03	0.73	0.07	0.74	0.00	0.67	0.05	0.67	0.03	0.73	
$\sum SFE$ (m N m <sup>-1</sup> )	*	$T_g$ (K)	0.19	0.55	0.16	0.55	0.19	0.55	0.15	0.54	0.19	0.55	0.02	0.50	0.18	0.50	0.15	0.55
		$T_g^{-1}$ (K <sup>-1</sup> )	0.05	0.70	0.04	0.69	0.06	0.70	0.04	0.68	0.07	0.70	0.00	0.63	0.05	0.63	0.04	0.69
	$X_c$ (%)	0.28	0.81	0.21	0.80	0.28	0.81	0.21	0.80	0.32	0.81	0.01	0.72	0.28	0.72	0.21	0.80	
	$X_c^{-1}$ (% <sup>-1</sup> )	0.77	0.11	0.62	0.11	0.78	0.11	0.60	0.11	0.83	0.11	0.04	0.10	0.76	0.10	0.61	0.11	
	SA (m <sup>2</sup> g <sup>-1</sup> )	0.02																

Table A7.16: Calculation of  $R_h^2$  and  $R_v^2$  with the matrix of two PAH properties ( $\log K_{ow}$ , MW) multiplied with two plastic properties ( $X_c$  as fixed parameter) and the  $\log K_{p-w}$  matrix

plastic property product		PAH properties											
1 <sup>st</sup> fixed parameter	2 <sup>nd</sup> variable parameter	$\log K_{ow}$ (-)		MW (g mol <sup>-1</sup> )		$\log K_{ow} * MW$ (g mol <sup>-1</sup> )		$MW * \log K_{ow}^{-1}$ (g mol <sup>-1</sup> )		$\log K_{ow} * MW^1$ (mol g <sup>-1</sup> )		$(\log K_{ow} * MW)^{-1}$ (mol g <sup>-1</sup> )	
	$R_v^2$	$R_h^2$	$R_v^2$	$R_h^2$	$R_v^2$	$R_h^2$	$R_v^2$	$R_h^2$	$R_v^2$	$R_h^2$	$R_v^2$	$R_h^2$	
$\rho$ (g cm <sup>-3</sup> )	0.87	0.94	0.88	0.93	0.93	0.95	0.81	0.87	0.79	0.87	0.58	0.91	
$\rho^{-1}$ (cm <sup>3</sup> g <sup>-1</sup> )	0.65	0.93	0.66	0.92	0.70	0.93	0.61	0.86	0.58	0.86	0.41	0.90	
$d_{50}$ (μm)	0.84	0.94	0.85	0.94	0.90	0.95	0.79	0.88	0.76	0.87	0.55	0.91	
$d_{50}^{-1}$ (μm <sup>-1</sup> )	0.79	0.95	0.80	0.95	0.85	0.96	0.74	0.89	0.71	0.88	0.51	0.92	
$T_m$ (K)	0.77	0.94	0.78	0.93	0.82	0.94	0.72	0.88	0.69	0.87	0.50	0.91	
$T_m^{-1}$ (K <sup>-1</sup> )	0.87	0.96	0.88	0.95	0.93	0.96	0.81	0.89	0.78	0.88	0.57	0.92	
$X_c$ (%) *	$T_g$ (K)	0.70	0.90	0.71	0.89	0.74	0.90	0.65	0.83	0.63	0.83	0.46	0.87
	$T_g^{-1}$ (K <sup>-1</sup> )	0.67	0.93	0.68	0.92	0.72	0.93	0.62	0.86	0.60	0.86	0.43	0.89
SA (m <sup>2</sup> g <sup>-1</sup> )	0.05	0.56	0.05	0.56	0.05	0.56	0.05	0.53	0.04	0.53	0.03	0.55	
SA <sup>-1</sup> (g m <sup>-2</sup> )	0.75	0.88	0.76	0.87	0.80	0.89	0.70	0.81	0.68	0.80	0.50	0.84	
Vp (cm <sup>3</sup> g <sup>-1</sup> )	0.05	0.57	0.05	0.56	0.06	0.57	0.05	0.54	0.05	0.54	0.03	0.55	
Vp <sup>-1</sup> (g cm <sup>-3</sup> )	0.75	0.88	0.76	0.87	0.80	0.89	0.70	0.81	0.67	0.81	0.49	0.84	
$\sum SFE$ (mN m <sup>-1</sup> )	0.74	0.84	0.74	0.83	0.78	0.85	0.69	0.77	0.67	0.77	0.50	0.80	
$\sum SFE^{-1}$ (m Nm <sup>-1</sup> )	0.28	0.81	0.28	0.81	0.30	0.82	0.26	0.77	0.24	0.77	0.17	0.79	

Table A7.17: Calculation of  $R_h^2$  and  $R_v^2$  with the matrix of two PAH properties ( $\log K_{ow}$ ,  $\log K_{hdw}$ ) multiplied with two plastic properties ( $X_c$  as fixed parameter) and the  $\log K_{p-w}$  matrix

plastic property product		PAH properties											
1 <sup>st</sup> fixed parameter	2 <sup>nd</sup> variable parameter	$\log K_{ow}$ (-)		$\log K_{hdw}$ (-)		$\log K_{ow} * \log K_{hdw}$ (-)		$\log K_{hdw} * \log K_{ow}^{-1}$ (-)		$\log K_{ow} * \log K_{hdw}^{-1}$ (-)		$(\log K_{ow} * \log K_{hdw})^{-1}$ (-)	
	$R_v^2$	$R_h^2$	$R_v^2$	$R_h^2$	$R_v^2$	$R_h^2$	$R_v^2$	$R_h^2$	$R_v^2$	$R_h^2$	$R_v^2$	$R_h^2$	
$\rho$ (g cm <sup>-3</sup> )	0.87	0.94	0.64	0.94	0.92	0.95	0.81	0.92	0.79	0.92	0.59	0.91	
$\rho^{-1}$ (cm <sup>3</sup> g <sup>-1</sup> )	0.65	0.93	0.66	0.93	0.70	0.93	0.60	0.91	0.59	0.91	0.42	0.90	
$d_{50}$ (μm)	0.84	0.94	0.85	0.94	0.90	0.95	0.79	0.88	0.76	0.87	0.55	0.91	
$d_{50}^{-1}$ (μm <sup>-1</sup> )	0.79	0.95	0.80	0.95	0.85	0.96	0.74	0.89	0.71	0.88	0.51	0.92	
$T_m$ (K)	0.77	0.94	0.78	0.93	0.82	0.94	0.72	0.88	0.69	0.87	0.50	0.91	
$T_m^{-1}$ (K <sup>-1</sup> )	0.87	0.96	0.88	0.95	0.93	0.96	0.81	0.89	0.78	0.88	0.57	0.92	
$X_c$ (%) *	$T_g$ (K)	0.70	0.90	0.71	0.89	0.74	0.90	0.65	0.83	0.63	0.83	0.46	0.87
	$T_g^{-1}$ (K <sup>-1</sup> )	0.67	0.93	0.68	0.92	0.72	0.93	0.62	0.86	0.60	0.86	0.43	0.89
SA (m <sup>2</sup> g <sup>-1</sup> )	0.05	0.56	0.05	0.56	0.05	0.56	0.05	0.53	0.04	0.53	0.03	0.55	
SA <sup>-1</sup> (g m <sup>-2</sup> )	0.75	0.88	0.76	0.87	0.80	0.89	0.70	0.81	0.68	0.80	0.50	0.84	
Vp (cm <sup>3</sup> g <sup>-1</sup> )	0.05	0.57	0.05	0.56	0.06	0.57	0.05	0.54	0.05	0.54	0.03	0.55	
Vp <sup>-1</sup> (g cm <sup>-3</sup> )	0.75	0.88	0.76	0.87	0.80	0.89	0.70	0.81	0.67	0.81	0.49	0.84	
$\sum SFE$ (mN m <sup>-1</sup> )	0.74	0.84	0.74	0.83	0.78	0.85	0.69	0.77	0.67	0.77	0.50	0.80	
$\sum SFE^{-1}$ (m Nm <sup>-1</sup> )	0.28	0.81	0.28	0.81	0.30	0.82	0.26	0.77	0.24	0.77	0.17	0.79	

Table A7.18: Calculation of  $R_h^2$  and  $R_v^2$  with the matrix of two PAH properties ( $\log K_{ow}$ ,  $\log C_w^{sat}$ ) multiplied with two plastic properties ( $X_c$  as fixed parameter) and the  $\log K_{p-w}$  matrix

plastic property product		PAH properties											
1 <sup>st</sup> fixed parameter	2 <sup>nd</sup> variable parameter	$\log K_{ow}$ (-)		$\log C_w^{sat}$ (mol m <sup>-3</sup> )		$\log K_{ow} * \log C_w^{sat}$ (mol m <sup>-3</sup> )		$\log C_w^{sat} * \log K_{ow}^{-1}$ (mol m <sup>-3</sup> )		$\log K_{ow} * \log C_w^{sat-1}$ (m <sup>3</sup> mol <sup>-1</sup> )		$(\log K_{ow} * \log C_w^{sat})^{-1}$ (m <sup>3</sup> mol <sup>-1</sup> )	
	$R_v^2$	$R_h^2$	$R_v^2$	$R_h^2$	$R_v^2$	$R_h^2$	$R_v^2$	$R_h^2$	$R_v^2$	$R_h^2$	$R_v^2$	$R_h^2$	
$\rho$ (g cm <sup>-3</sup> )	0.87	0.94	0.14	0.93	0.92	0.95	0.91	0.91	0.06	0.81	0.06	0.81	
$\rho^{-1}$ (cm <sup>3</sup> g <sup>-1</sup> )	0.65	0.93	0.72	0.92	0.72	0.93	0.71	0.90	0.03	0.81	0.03	0.81	
$d_{50}$ (μm)	0.84	0.94	0.89	0.94	0.90	0.95	0.89	0.92	0.05	0.82	0.05	0.82	
$d_{50}^{-1}$ (μm <sup>-1</sup> )	0.79	0.95	0.86	0.95	0.86	0.96	0.85	0.93	0.04	0.83	0.04	0.83	
$T_m$ (K)	0.77	0.94	0.83	0.93	0.83	0.95	0.82	0.92	0.04	0.82	0.04	0.82	
$T_m^{-1}$ (K <sup>-1</sup> )	0.87	0.96	0.93	0.95	0.93	0.97	0.92	0.93	0.05	0.83	0.05	0.83	
$X_c$ (%) *	$T_g$ (K)	0.70	0.90	0.73	0.89	0.73	0.91	0.73	0.87	0.05	0.78	0.04	0.78
	$T_g^{-1}$ (K <sup>-1</sup> )	0.67	0.93	0.74	0.92	0.74	0.93	0.73	0.90	0.03	0.81	0.03	0.81
SA (m <sup>2</sup> g <sup>-1</sup> )	0.05	0.56	0.06	0.56	0.06	0.56	0.06	0.55	0.00	0.51	0.00	0.51	
SA <sup>-1</sup> (g m <sup>-2</sup> )	0.75	0.88	0.79	0.87	0.80	0.89	0.79	0.85	0.05	0.75	0.05	0.75	
Vp (cm <sup>3</sup> g <sup>-1</sup> )	0.05	0.57	0.06	0.56	0.06	0.57	0.06	0.56	0.00	0.51	0.00	0.51	
Vp <sup>-1</sup> (g cm <sup>-3</sup> )	0.75	0.88	0.79	0.87	0.80	0.89	0.79	0.85	0.05	0.75	0.05	0.75	
$\sum SFE$ (mN m <sup>-1</sup> )	0.74	0.84	0.75	0.83	0.76	0.85	0.75	0.81	0.06	0.71	0.06	0.71	
$\sum SFE^{-1}$ (m Nm <sup>-1</sup> )	0.28	0.81	0.32	0.81	0.32	0.82	0.32	0.80	0.01	0.72	0.01	0.72	

Table A7.19: Calculation of  $R_h^2$  and  $R_v^2$  with the matrix of two PAH properties (MW,  $\log K_{hdw}$ ) multiplied with two plastic properties ( $X_c$  as fixed parameter) and the  $\log K_{p-w}$  matrix

plastic property product		PAH properties											
1 <sup>st</sup> fixed parameter	2 <sup>nd</sup> variable parameter	MW (g mol <sup>-1</sup> )		$\log K_{hdw}$ (-)		MW * log $K_{hdw}$ (g mol <sup>-1</sup> )		MW * log $K_{p-w}^{-1}$ (g mol <sup>-1</sup> )		$\log K_{hdw} * MW^{-1}$ (mol g <sup>-1</sup> )		$(MW * \log K_{hdw})^{-1}$ (mol g <sup>-1</sup> )	
		$R_v^2$	$R_h^2$	$R_v^2$	$R_h^2$	$R_v^2$	$R_h^2$	$R_v^2$	$R_h^2$	$R_v^2$	$R_h^2$		
	$\rho$ (g cm <sup>-3</sup> )	0.88	0.93	0.14	0.94	0.32	0.25	0.79	0.78	0.81	0.78	0.57	0.90
	$\rho^{-1}$ (cm <sup>3</sup> g <sup>-1</sup> )	0.66	0.92	0.66	0.93	0.26	0.21	0.59	0.79	0.60	0.79	0.41	0.90
	$d_{50}$ (μm)	0.85	0.94	0.85	0.94	0.32	0.23	0.77	0.79	0.78	0.79	0.54	0.91
	$d_{50}^{-1}$ (μm <sup>-1</sup> )	0.80	0.95	0.80	0.95	0.30	0.23	0.72	0.80	0.73	0.80	0.50	0.92
	$T_m$ (K)	0.78	0.93	0.78	0.94	0.30	0.22	0.70	0.79	0.71	0.79	0.49	0.91
	$T_m^{-1}$ (K <sup>-1</sup> )	0.88	0.95	0.88	0.96	0.32	0.24	0.79	0.80	0.80	0.80	0.56	0.92
$X_c$ (%)	$T_g$ (K)	0.71	0.89	0.70	0.90	0.27	0.22	0.64	0.75	0.65	0.75	0.46	0.87
	$T_g^{-1}$ (K <sup>-1</sup> )	0.68	0.92	0.68	0.93	0.25	0.22	0.61	0.78	0.62	0.78	0.42	0.89
	SA (m <sup>2</sup> g <sup>-1</sup> )	0.05	0.56	0.05	0.56	0.03	0.10	0.04	0.49	0.04	0.49	0.03	0.55
	SA <sup>-1</sup> (g m <sup>2</sup> )	0.76	0.87	0.76	0.88	0.27	0.25	0.68	0.72	0.69	0.72	0.49	0.84
	Vp (cm <sup>3</sup> g <sup>-1</sup> )	0.05	0.56	0.05	0.57	0.03	0.10	0.05	0.50	0.05	0.50	0.03	0.55
	Vp <sup>-1</sup> (g cm <sup>3</sup> )	0.76	0.87	0.76	0.88	0.27	0.25	0.68	0.72	0.69	0.72	0.48	0.84
	$\sum SFE$ (mN m <sup>-1</sup> )	0.74	0.83	0.74	0.84	0.26	0.25	0.68	0.68	0.68	0.68	0.49	0.80
	$\sum SFE^{-1}$ (m Nm <sup>-1</sup> )	0.28	0.81	0.28	0.81	0.12	0.16	0.25	0.70	0.25	0.70	0.16	0.79

Table A7.20: Calculation of  $R_h^2$  and  $R_v^2$  with the matrix of two PAH properties (MW,  $\log C_w^{sat}$ ) multiplied with two plastic properties ( $X_c$  as fixed parameter) and the  $\log K_{p-w}$  matrix

plastic property product		PAH properties											
1 <sup>st</sup> fixed parameter	2 <sup>nd</sup> variable parameter	MW (g mol <sup>-1</sup> )		$\log C_w^{sat}$ (mol m <sup>-3</sup> )		MW * log $C_w^{sat}$ (g m <sup>-3</sup> )		$\log C_w^{sat} * MW^{-1}$ (mol <sup>2</sup> m <sup>-3</sup> g <sup>-1</sup> )		MW * log $C_w^{sat-1}$ (g m <sup>-3</sup> mol <sup>-2</sup> )		$(\log K_{ow} * \log C_w^{sat})^{-1}$ (m <sup>3</sup> g <sup>-1</sup> )	
		$R_v^2$	$R_h^2$	$R_v^2$	$R_h^2$	$R_v^2$	$R_h^2$	$R_v^2$	$R_h^2$	$R_v^2$	$R_h^2$	$R_v^2$	$R_h^2$
	$\rho$ (g cm <sup>-3</sup> )	0.88	0.93	0.16	0.93	0.28	0.02	0.91	0.91	0.06	0.81	0.06	0.81
	$\rho^{-1}$ (cm <sup>3</sup> g <sup>-1</sup> )	0.66	0.92	0.72	0.92	0.25	0.03	0.71	0.90	0.03	0.81	0.03	0.81
	$d_{50}$ (μm)	0.85	0.94	0.89	0.94	0.29	0.02	0.89	0.92	0.05	0.82	0.05	0.82
	$d_{50}^{-1}$ (μm <sup>-1</sup> )	0.80	0.95	0.86	0.95	0.28	0.02	0.85	0.93	0.04	0.83	0.04	0.83
	$T_m$ (K)	0.78	0.93	0.83	0.93	0.28	0.02	0.82	0.91	0.04	0.82	0.04	0.82
	$T_m^{-1}$ (K <sup>-1</sup> )	0.88	0.95	0.93	0.95	0.29	0.02	0.92	0.93	0.05	0.83	0.05	0.83
$X_c$ (%)	$T_g$ (K)	0.71	0.89	0.73	0.89	0.24	0.02	0.73	0.87	0.05	0.78	0.04	0.78
	$T_g^{-1}$ (K <sup>-1</sup> )	0.68	0.92	0.74	0.92	0.24	0.02	0.73	0.90	0.03	0.81	0.03	0.81
	SA (m <sup>2</sup> g <sup>-1</sup> )	0.05	0.56	0.06	0.56	0.03	0.03	0.06	0.55	0.00	0.51	0.00	0.51
	SA <sup>-1</sup> (g m <sup>2</sup> )	0.76	0.87	0.79	0.87	0.23	0.01	0.79	0.85	0.05	0.75	0.05	0.75
	Vp (cm <sup>3</sup> g <sup>-1</sup> )	0.05	0.56	0.06	0.56	0.03	0.03	0.06	0.56	0.00	0.51	0.00	0.51
	Vp <sup>-1</sup> (g cm <sup>3</sup> )	0.76	0.87	0.79	0.87	0.23	0.01	0.78	0.85	0.05	0.75	0.05	0.75
	$\sum SFE$ (mN m <sup>-1</sup> )	0.74	0.83	0.75	0.83	0.22	0.01	0.75	0.81	0.06	0.71	0.06	0.71
	$\sum SFE^{-1}$ (m Nm <sup>-1</sup> )	0.28	0.81	0.32	0.81	0.13	0.03	0.32	0.80	0.01	0.72	0.01	0.72

Table A7.21: Calculation of  $R_h^2$  and  $R_v^2$  with the matrix of two PAH properties ( $\log K_{hdw}$ ,  $\log C_w^{sat}$ ) multiplied with two plastic properties ( $X_c$  as fixed parameter) and the  $\log K_{p-w}$  matrix

plastic property product		PAH properties											
1 <sup>st</sup> fixed parameter	2 <sup>nd</sup> variable parameter	$\log K_{hdw}$		$\log C_w^{sat}$ (mol m <sup>-3</sup> )		$\log K_{hdw} * \log C_w^{sat}$ (mol m <sup>-3</sup> )		$\log C_w^{sat} * \log K_{hdw}^{-1}$ (mol m <sup>-3</sup> )		$\log K_{hdw} * \log C_w^{sat-1}$ (m <sup>3</sup> mol <sup>-1</sup> )		$(\log K_{ow} * \log C_w^{sat})^{-1}$ (m <sup>3</sup> mol <sup>-1</sup> )	
		$R_v^2$	$R_h^2$	$R_v^2$	$R_h^2$	$R_v^2$	$R_h^2$	$R_v^2$	$R_h^2$	$R_v^2$	$R_h^2$	$R_v^2$	$R_h^2$
	$\rho$ (g cm <sup>-3</sup> )	0.88	0.94	0.15	0.93	0.92	0.95	0.91	0.91	0.06	0.81	0.06	0.81
	$\rho^{-1}$ (cm <sup>3</sup> g <sup>-1</sup> )	0.66	0.93	0.72	0.92	0.72	0.93	0.71	0.90	0.03	0.81	0.03	0.81
	$d_{50}$ (μm)	0.85	0.94	0.89	0.94	0.90	0.95	0.89	0.92	0.05	0.82	0.05	0.82
	$d_{50}^{-1}$ (μm <sup>-1</sup> )	0.80	0.95	0.86	0.95	0.86	0.96	0.85	0.93	0.04	0.83	0.04	0.83
	$T_m$ (K)	0.78	0.94	0.83	0.93	0.83	0.95	0.82	0.91	0.04	0.82	0.04	0.82
	$T_m^{-1}$ (K <sup>-1</sup> )	0.88	0.96	0.93	0.95	0.93	0.97	0.92	0.93	0.05	0.83	0.05	0.83
$X_c$ (%)	$T_g$ (K)	0.70	0.90	0.73	0.89	0.73	0.91	0.73	0.87	0.05	0.78	0.04	0.78
	$T_g^{-1}$ (K <sup>-1</sup> )	0.68	0.93	0.74	0.92	0.74	0.93	0.73	0.90	0.03	0.81	0.03	0.81
	SA (m <sup>2</sup> g <sup>-1</sup> )	0.05	0.56	0.06	0.56	0.06	0.56	0.06	0.55	0.00	0.51	0.00	0.51
	SA <sup>-1</sup> (g m <sup>2</sup> )	0.76	0.88	0.79	0.87	0.80	0.89	0.79	0.85	0.05	0.75	0.05	0.75
	Vp (cm <sup>3</sup> g <sup>-1</sup> )	0.05	0.57	0.06	0.56	0.06	0.57	0.06	0.56	0.00	0.51	0.00	0.51
	Vp <sup>-1</sup> (g cm <sup>3</sup> )	0.76	0.88	0.79	0.87	0.80	0.89	0.78	0.85	0.05	0.75	0.05	0.75
	$\sum SFE$ (mN m <sup>-1</sup> )	0.74	0.84	0.75	0.83	0.76	0.85	0.75	0.81	0.06	0.71	0.06	0.71
	$\sum SFE^{-1}$ (m Nm <sup>-1</sup> )	0.28	0.81	0.32	0.81	0.32	0.82	0.32	0.80	0.01	0.72	0.01	0.72

Table A7.22: Calculation of  $R_h^2$  and  $R_v^2$  with the matrix of two PAH properties ( $\log K_{ow}$ , MW<sub>w</sub>) multiplied with two plastic properties ( $T_m$  as fixed parameter) and the  $\log K_{p-w}$  matrix

plastic property product		PAH properties											
1 <sup>st</sup> fixed parameter	2 <sup>nd</sup> variable parameter	$\log K_{ow}$ (-)		MW (g mol <sup>-1</sup> )		$\log K_{ow} * MW$ (g mol <sup>-1</sup> )		$MW * \log K_{ow}^{-1}$ (g mol <sup>-1</sup> )		$\log K_{ow} * MW^{-1}$ (mol g <sup>-1</sup> )		$(\log K_{ow} * MW)^{-1}$ (mol g <sup>-1</sup> )	
		$R_v^2$	$R_h^2$	$R_v^2$	$R_h^2$	$R_v^2$	$R_h^2$	$R_v^2$	$R_h^2$	$R_v^2$	$R_h^2$		
$T_m$ (K)	$\rho$ (g cm <sup>-3</sup> )	0.47	0.52	0.00	0.52	0.50	0.52	0.43	0.49	0.41	0.48	0.29	0.50
	$\rho^{-1}$ (cm <sup>3</sup> g <sup>-1</sup> )	0.22	0.66	0.22	0.66	0.23	0.66	0.21	0.63	0.20	0.63	0.16	0.65
	$d_{50}$ (μm)	0.70	0.50	0.71	0.50	0.75	0.50	0.65	0.47	0.62	0.47	0.44	0.48
	$d_{50}^{-1}$ (μm <sup>-1</sup> )	0.28	0.70	0.28	0.70	0.29	0.71	0.26	0.66	0.26	0.66	0.20	0.68
	$T_g$ (K)	0.66	0.38	0.67	0.38	0.71	0.38	0.61	0.36	0.58	0.36	0.42	0.37
	$T_g^{-1}$ (K <sup>-1</sup> )	0.07	0.77	0.07	0.77	0.07	0.78	0.06	0.73	0.06	0.73	0.03	0.75
	SA (m <sup>2</sup> g <sup>-1</sup> )	0.13	0.38	0.13	0.38	0.14	0.38	0.12	0.36	0.11	0.36	0.09	0.37
	SA <sup>-1</sup> (g m <sup>-2</sup> )	0.02	0.68	0.02	0.68	0.02	0.69	0.02	0.63	0.02	0.63	0.02	0.66
	Vp (cm <sup>3</sup> g <sup>-1</sup> )	0.14	0.38	0.14	0.38	0.15	0.38	0.13	0.36	0.13	0.36	0.09	0.37
	Vp <sup>-1</sup> (g cm <sup>-3</sup> )	0.03	0.69	0.03	0.69	0.03	0.69	0.03	0.64	0.03	0.64	0.02	0.67
$\sum SFE$ (mN m <sup>-1</sup> )	$\sum SFE$ (mN m <sup>-1</sup> )	0.13	0.48	0.13	0.48	0.14	0.49	0.12	0.45	0.11	0.45	0.07	0.47
	$\sum SFE^{-1}$ (m Nm <sup>-1</sup> )	0.06	0.62	0.06	0.62	0.06	0.62	0.06	0.59	0.06	0.59	0.05	0.61

Table A7.23: Calculation of  $R_h^2$  and  $R_v^2$  with the matrix of two PAH properties ( $\log K_{ow}$ ,  $\log K_{hdw}$ ) multiplied with two plastic properties ( $T_m$  as fixed parameter) and the  $\log K_{p-w}$  matrix

plastic property product		PAH properties											
1 <sup>st</sup> fixed parameter	2 <sup>nd</sup> variable parameter	$\log K_{ow}$ (-)		$\log K_{hdw}$ (-)		$\log K_{ow} * \log K_{hdw}$ (-)		$\log K_{hdw} * \log K_{ow}^{-1}$ (-)		$\log K_{ow} * \log K_{hdw}^{-1}$ (-)		$(\log K_{ow} * \log K_{hdw})^{-1}$ (-)	
		$R_v^2$	$R_h^2$	$R_v^2$	$R_h^2$	$R_v^2$	$R_h^2$	$R_v^2$	$R_h^2$	$R_v^2$	$R_h^2$		
$T_m$ (K)	$\rho$ (g cm <sup>-3</sup> )	0.47	0.52	0.00	0.52	0.50	0.52	0.43	0.51	0.42	0.51	0.29	0.50
	$\rho^{-1}$ (cm <sup>3</sup> g <sup>-1</sup> )	0.22	0.66	0.22	0.66	0.23	0.66	0.21	0.65	0.20	0.65	0.16	0.65
	$d_{50}$ (μm)	0.70	0.50	0.71	0.50	0.75	0.50	0.65	0.47	0.62	0.47	0.44	0.48
	$d_{50}^{-1}$ (μm <sup>-1</sup> )	0.28	0.70	0.28	0.70	0.29	0.71	0.26	0.66	0.26	0.66	0.20	0.68
	$T_g$ (K)	0.66	0.38	0.67	0.38	0.71	0.38	0.61	0.36	0.58	0.36	0.42	0.37
	$T_g^{-1}$ (K <sup>-1</sup> )	0.07	0.77	0.07	0.77	0.07	0.78	0.06	0.73	0.06	0.73	0.03	0.75
	SA (m <sup>2</sup> g <sup>-1</sup> )	0.13	0.38	0.13	0.38	0.14	0.38	0.12	0.36	0.11	0.36	0.09	0.37
	SA <sup>-1</sup> (g m <sup>-2</sup> )	0.02	0.68	0.02	0.68	0.02	0.69	0.02	0.63	0.02	0.63	0.02	0.66
	Vp (cm <sup>3</sup> g <sup>-1</sup> )	0.14	0.38	0.14	0.38	0.15	0.38	0.13	0.36	0.13	0.36	0.09	0.37
	Vp <sup>-1</sup> (g cm <sup>-3</sup> )	0.03	0.69	0.03	0.69	0.03	0.69	0.03	0.64	0.03	0.64	0.02	0.67
$\sum SFE$ (mN m <sup>-1</sup> )	$\sum SFE$ (mN m <sup>-1</sup> )	0.13	0.48	0.13	0.48	0.14	0.49	0.12	0.45	0.11	0.45	0.07	0.47
	$\sum SFE^{-1}$ (m Nm <sup>-1</sup> )	0.06	0.62	0.06	0.62	0.06	0.62	0.06	0.59	0.06	0.59	0.05	0.61

Table A7.24: Calculation of  $R_h^2$  and  $R_v^2$  with the matrix of two PAH properties ( $\log K_{ow}$ ,  $\log C_w^{sat}$ ) multiplied with two plastic properties ( $T_m$  as fixed parameter) and the  $\log K_{p-w}$  matrix

plastic property product		PAH properties											
1 <sup>st</sup> fixed parameter	2 <sup>nd</sup> variable parameter	$\log K_{ow}$ (-)		$\log C_w^{sat}$ (mol m <sup>-3</sup> )		$\log K_{ow} * \log C_w^{sat}$ (mol m <sup>-3</sup> )		$\log C_w^{sat} * \log K_{ow}^{-1}$ (mol m <sup>-3</sup> )		$\log K_{ow} * \log C_w^{sat-1}$ (m <sup>3</sup> mol <sup>-1</sup> )		$(\log K_{ow} * \log C_w^{sat})^{-1}$ (m <sup>3</sup> mol <sup>-1</sup> )	
		$R_v^2$	$R_h^2$	$R_v^2$	$R_h^2$	$R_v^2$	$R_h^2$	$R_v^2$	$R_h^2$	$R_v^2$	$R_h^2$	$R_v^2$	$R_h^2$
$T_m$ (K)	$\rho$ (g cm <sup>-3</sup> )	0.47	0.52	0.00	0.52	0.52	0.52	0.52	0.51	0.02	0.46	0.02	0.46
	$\rho^{-1}$ (cm <sup>3</sup> g <sup>-1</sup> )	0.22	0.66	0.21	0.66	0.21	0.66	0.21	0.65	0.03	0.59	0.03	0.59
	$d_{50}$ (μm)	0.70	0.50	0.76	0.50	0.77	0.50	0.76	0.49	0.03	0.44	0.03	0.44
	$d_{50}^{-1}$ (μm <sup>-1</sup> )	0.28	0.70	0.26	0.70	0.26	0.71	0.26	0.69	0.04	0.62	0.04	0.62
	$T_g$ (K)	0.66	0.38	0.72	0.38	0.72	0.38	0.72	0.37	0.03	0.34	0.03	0.34
	$T_g^{-1}$ (K <sup>-1</sup> )	0.07	0.77	0.09	0.77	0.09	0.78	0.09	0.76	0.00	0.69	0.00	0.69
	SA (m <sup>2</sup> g <sup>-1</sup> )	0.13	0.38	0.13	0.38	0.13	0.38	0.13	0.37	0.01	0.35	0.01	0.35
	SA <sup>-1</sup> (g m <sup>-2</sup> )	0.02	0.68	0.02	0.68	0.02	0.69	0.02	0.66	0.00	0.59	0.00	0.59
	Vp (cm <sup>3</sup> g <sup>-1</sup> )	0.14	0.38	0.14	0.38	0.15	0.38	0.14	0.37	0.01	0.35	0.01	0.35
	Vp <sup>-1</sup> (g cm <sup>-3</sup> )	0.03	0.69	0.03	0.69	0.03	0.70	0.03	0.67	0.00	0.60	0.00	0.60
$\sum SFE$ (mN m <sup>-1</sup> )	$\sum SFE$ (mN m <sup>-1</sup> )	0.13	0.48	0.16	0.48	0.16	0.49	0.16	0.47	0.00	0.42	0.00	0.42
	$\sum SFE^{-1}$ (m Nm <sup>-1</sup> )	0.06	0.62	0.05	0.62	0.05	0.62	0.05	0.61	0.02	0.56	0.01	0.56

Table A7.25: Calculation of  $R_h^2$  and  $R_v^2$  with the matrix of two PAH properties (MW,  $\log K_{\text{hdw}}$ ) multiplied with two plastic properties ( $T_m$  as fixed parameter) and the  $\log K_{\text{p-w}}$  matrix

plastic property product		PAH properties									
1 <sup>st</sup> fixed parameter	2 <sup>nd</sup> variable parameter	MW (g mol <sup>-1</sup> )		$\log K_{\text{hdw}}$ (-)		MW * $\log K_{\text{hdw}}$ (g mol <sup>-1</sup> )		MW * $\log K_{\text{hdw}}^{-1}$ (g mol <sup>-1</sup> )		$\log K_{\text{hdw}} * \text{MW}^{-1}$ (mol g <sup>-1</sup> )	
		$R_v^2$	$R_h^2$	$R_v^2$	$R_h^2$	$R_v^2$	$R_h^2$	$R_v^2$	$R_h^2$	$R_v^2$	$R_h^2$
$T_m$ (K)	$\rho$ (g cm <sup>-3</sup> )	0.47	0.52	0.00	0.52	0.19	0.11	0.42	0.44	0.42	0.44
	$\rho^{-1}$ (cm <sup>3</sup> g <sup>-1</sup> )	0.22	0.66	0.22	0.66	0.07	0.13	0.20	0.58	0.21	0.58
	$d_{50}$ (μm)	0.71	0.50	0.70	0.50	0.27	0.10	0.63	0.43	0.64	0.43
	$d_{50}^{-1}$ (μm <sup>-1</sup> )	0.28	0.70	0.28	0.70	0.09	0.14	0.26	0.61	0.26	0.61
	$T_g$ (K)	0.67	0.38	0.66	0.38	0.25	0.07	0.59	0.33	0.60	0.33
	$T_g^{-1}$ (K <sup>-1</sup> )	0.07	0.77	0.07	0.77	0.03	0.16	0.06	0.67	0.06	0.67
	SA (m <sup>2</sup> g <sup>-1</sup> )	0.13	0.38	0.13	0.38	0.04	0.06	0.12	0.34	0.12	0.34
	SA <sup>-1</sup> (g m <sup>-2</sup> )	0.02	0.68	0.02	0.68	0.00	0.17	0.02	0.57	0.02	0.57
	Vp (cm <sup>3</sup> g <sup>-1</sup> )	0.14	0.38	0.14	0.38	0.04	0.06	0.13	0.34	0.13	0.34
	Vp <sup>-1</sup> (g cm <sup>-3</sup> )	0.03	0.69	0.03	0.69	0.01	0.17	0.03	0.58	0.03	0.58
$\Sigma$ SFE (mN m <sup>-1</sup> )	0.13	0.48	0.13	0.48	0.06	0.12	0.11	0.40	0.12	0.40	0.07
	$\Sigma$ SFE <sup>-1</sup> (m Nm <sup>-1</sup> )	0.06	0.62	0.06	0.62	0.01	0.11	0.06	0.55	0.06	0.55

Table A7.26: Calculation of  $R_h^2$  and  $R_v^2$  with the matrix of two PAH properties (MW,  $\log C_w^{\text{sat}}$ ) multiplied with two plastic properties ( $T_m$  as fixed parameter) and the  $\log K_{\text{p-w}}$  matrix

plastic property product		PAH properties									
1 <sup>st</sup> fixed parameter	2 <sup>nd</sup> variable parameter	MW (g mol <sup>-1</sup> )		$\log C_w^{\text{sat}}$ (mol m <sup>-3</sup> )		MW * $\log C_w^{\text{sat}}$ (g m <sup>-3</sup> )		$\log C_w^{\text{sat}} * \text{MW}^{-1}$ (mol <sup>2</sup> m <sup>-3</sup> g <sup>-1</sup> )		MW * $\log C_w^{\text{sat}-1}$ (g m <sup>3</sup> mol <sup>-2</sup> )	
		$R_v^2$	$R_h^2$	$R_v^2$	$R_h^2$	$R_v^2$	$R_h^2$	$R_v^2$	$R_h^2$	$R_v^2$	$R_h^2$
$T_m$ (K)	$\rho$ (g cm <sup>-3</sup> )	0.47	0.52	0.00	0.52	0.19	0.02	0.52	0.51	0.02	0.46
	$\rho^{-1}$ (cm <sup>3</sup> g <sup>-1</sup> )	0.22	0.66	0.21	0.66	0.04	0.03	0.21	0.65	0.03	0.59
	$d_{50}$ (μm)	0.71	0.50	0.76	0.50	0.26	0.02	0.76	0.49	0.03	0.44
	$d_{50}^{-1}$ (μm <sup>-1</sup> )	0.28	0.70	0.26	0.70	0.06	0.03	0.26	0.69	0.04	0.62
	$T_g$ (K)	0.67	0.38	0.72	0.38	0.24	0.02	0.72	0.37	0.03	0.34
	$T_g^{-1}$ (K <sup>-1</sup> )	0.07	0.77	0.09	0.77	0.04	0.03	0.09	0.76	0.00	0.69
	SA (m <sup>2</sup> g <sup>-1</sup> )	0.13	0.38	0.13	0.38	0.03	0.03	0.13	0.37	0.01	0.35
	SA <sup>-1</sup> (g m <sup>-2</sup> )	0.02	0.68	0.02	0.68	0.00	0.01	0.02	0.66	0.00	0.59
	Vp (cm <sup>3</sup> g <sup>-1</sup> )	0.14	0.38	0.14	0.38	0.03	0.03	0.14	0.37	0.01	0.35
	Vp <sup>-1</sup> (g cm <sup>-3</sup> )	0.03	0.69	0.03	0.69	0.00	0.01	0.03	0.67	0.00	0.60
$\Sigma$ SFE (mN m <sup>-1</sup> )	0.13	0.48	0.16	0.48	0.08	0.01	0.16	0.47	0.00	0.42	0.00
	$\Sigma$ SFE <sup>-1</sup> (m Nm <sup>-1</sup> )	0.06	0.62	0.05	0.62	0.00	0.03	0.05	0.61	0.02	0.56

Table A7.27: Calculation of  $R_h^2$  and  $R_v^2$  with the matrix of two PAH properties ( $\log K_{\text{hdw}}$ ,  $\log C_w^{\text{sat}}$ ) multiplied with two plastic properties ( $T_m$  as fixed parameter) and the  $\log K_{\text{p-w}}$  matrix

plastic property product		PAH properties									
1 <sup>st</sup> fixed parameter	2 <sup>nd</sup> variable parameter	$\log K_{\text{hdw}}$		$\log C_w^{\text{sat}}$ (mol m <sup>-3</sup> )		$\log K_{\text{hdw}} * \log C_w^{\text{sat}}$ (mol m <sup>-3</sup> )		$\log C_w^{\text{sat}} * \log K_{\text{hdw}}^{-1}$ (mol m <sup>-3</sup> )		$\log K_{\text{hdw}} * \log C_w^{\text{sat}-1}$ (m <sup>3</sup> mol <sup>-1</sup> )	
		$R_v^2$	$R_h^2$	$R_v^2$	$R_h^2$	$R_v^2$	$R_h^2$	$R_v^2$	$R_h^2$	$R_v^2$	$R_h^2$
$T_m$ (K)	$\rho$ (g cm <sup>-3</sup> )	0.47	0.52	0.00	0.52	0.52	0.52	0.52	0.51	0.02	0.46
	$\rho^{-1}$ (cm <sup>3</sup> g <sup>-1</sup> )	0.22	0.66	0.21	0.66	0.21	0.67	0.21	0.65	0.03	0.59
	$d_{50}$ (μm)	0.70	0.50	0.76	0.50	0.77	0.50	0.76	0.49	0.03	0.44
	$d_{50}^{-1}$ (μm <sup>-1</sup> )	0.28	0.70	0.26	0.70	0.26	0.71	0.26	0.69	0.04	0.62
	$T_g$ (K)	0.66	0.38	0.72	0.38	0.72	0.38	0.72	0.37	0.03	0.34
	$T_g^{-1}$ (K <sup>-1</sup> )	0.07	0.77	0.09	0.77	0.09	0.78	0.09	0.76	0.00	0.69
	SA (m <sup>2</sup> g <sup>-1</sup> )	0.13	0.38	0.13	0.38	0.13	0.38	0.13	0.37	0.01	0.35
	SA <sup>-1</sup> (g m <sup>-2</sup> )	0.02	0.68	0.02	0.68	0.02	0.69	0.02	0.66	0.00	0.59
	Vp (cm <sup>3</sup> g <sup>-1</sup> )	0.14	0.38	0.14	0.38	0.15	0.38	0.14	0.37	0.01	0.35
	Vp <sup>-1</sup> (g cm <sup>-3</sup> )	0.03	0.69	0.03	0.69	0.03	0.70	0.03	0.67	0.00	0.60
$\Sigma$ SFE (mN m <sup>-1</sup> )	0.13	0.48	0.16	0.48	0.16	0.49	0.16	0.47	0.00	0.42	0.00
	$\Sigma$ SFE <sup>-1</sup> (m Nm <sup>-1</sup> )	0.06	0.62	0.05	0.62	0.05	0.62	0.05	0.61	0.02	0.56

Table A7.28: Calculation of  $R_h^2$  and  $R_v^2$  with the matrix of two PAH properties ( $\log K_{ow}$ , MW<sub>w</sub>) multiplied with two plastic properties ( $T_m^{-1}$  as fixed parameter) and the  $\log K_{p-w}$  matrix

plastic property product		PAH properties											
1 <sup>st</sup> fixed parameter	2 <sup>nd</sup> variable parameter	$\log K_{ow}$ (-)		MW (g mol <sup>-1</sup> )		$\log K_{ow} * MW$ (g mol <sup>-1</sup> )		$MW * \log K_{ow}^{-1}$ (g mol <sup>-1</sup> )		$\log K_{ow} * MW^{-1}$ (mol g <sup>-1</sup> )		$(\log K_{ow} * MW)^{-1}$ (mol g <sup>-1</sup> )	
		$R_v^2$	$R_h^2$	$R_v^2$	$R_h^2$	$R_v^2$	$R_h^2$	$R_v^2$	$R_h^2$	$R_v^2$	$R_h^2$		
$T_m^{-1}$ (K <sup>-1</sup> )	$\rho$ (g cm <sup>-3</sup> )	0.30	0.78	0.00	0.78	0.31	0.78	0.28	0.73	0.28	0.72	0.21	0.75
	$\rho^{-1}$ (cm <sup>3</sup> g <sup>-1</sup> )	0.35	0.84	0.36	0.83	0.38	0.84	0.33	0.79	0.31	0.78	0.21	0.81
	$d_{50}$ (μm)	0.31	0.76	0.31	0.76	0.32	0.77	0.30	0.71	0.29	0.71	0.22	0.74
	$d_{50}^{-1}$ (μm <sup>-1</sup> )	0.65	0.87	0.65	0.87	0.69	0.88	0.60	0.82	0.57	0.82	0.41	0.85
	$T_g$ (K)	0.09	0.65	0.09	0.64	0.10	0.65	0.08	0.61	0.08	0.61	0.05	0.63
	$T_g^{-1}$ (K <sup>-1</sup> )	0.44	0.88	0.44	0.87	0.47	0.88	0.40	0.82	0.39	0.82	0.27	0.85
	SA (m <sup>2</sup> g <sup>-1</sup> )	0.01	0.49	0.01	0.49	0.01	0.50	0.01	0.47	0.01	0.47	0.01	0.49
	SA <sup>-1</sup> (g m <sup>-2</sup> )	0.44	0.83	0.45	0.83	0.47	0.84	0.41	0.77	0.40	0.76	0.29	0.80
	Vp (cm <sup>3</sup> g <sup>-1</sup> )	0.01	0.50	0.01	0.50	0.02	0.50	0.01	0.48	0.01	0.48	0.01	0.49
	Vp <sup>-1</sup> (g cm <sup>-3</sup> )	0.45	0.83	0.45	0.83	0.48	0.84	0.42	0.77	0.40	0.77	0.30	0.80
$\sum SFE$ (mN m <sup>-1</sup> )	$\sum SFE$ (mN m <sup>-1</sup> )	0.19	0.72	0.19	0.72	0.20	0.73	0.18	0.66	0.18	0.66	0.14	0.69
	$\sum SFE^{-1}$ (m Nm <sup>-1</sup> )	0.05	0.74	0.05	0.74	0.06	0.75	0.04	0.71	0.04	0.70	0.02	0.73

Table A7.29: Calculation of  $R_h^2$  and  $R_v^2$  with the matrix of two PAH properties ( $\log K_{ow}$ ,  $\log K_{hdw}$ ) multiplied with two plastic properties ( $T_m^{-1}$  as fixed parameter) and the  $\log K_{p-w}$  matrix

plastic property product		PAH properties											
1 <sup>st</sup> fixed parameter	2 <sup>nd</sup> variable parameter	$\log K_{ow}$ (-)		$\log K_{hdw}$ (-)		$\log K_{ow} * \log K_{hdw}$ (-)		$\log K_{hdw} * \log K_{ow}^{-1}$ (-)		$\log K_{ow} * \log K_{hdw}^{-1}$ (-)		$(\log K_{ow} * \log K_{hdw})^{-1}$ (-)	
		$R_v^2$	$R_h^2$	$R_v^2$	$R_h^2$	$R_v^2$	$R_h^2$	$R_v^2$	$R_h^2$	$R_v^2$	$R_h^2$		
$T_m^{-1}$ (K <sup>-1</sup> )	$\rho$ (g cm <sup>-3</sup> )	0.30	0.78	0.81	0.78	0.31	0.79	0.28	0.77	0.28	0.76	0.22	0.76
	$\rho^{-1}$ (cm <sup>3</sup> g <sup>-1</sup> )	0.35	0.84	0.36	0.84	0.38	0.84	0.32	0.82	0.31	0.82	0.22	0.82
	$d_{50}$ (μm)	0.31	0.76	0.31	0.76	0.32	0.77	0.30	0.71	0.29	0.71	0.22	0.74
	$d_{50}^{-1}$ (μm <sup>-1</sup> )	0.65	0.87	0.65	0.87	0.69	0.88	0.60	0.82	0.57	0.82	0.41	0.85
	$T_g$ (K)	0.09	0.65	0.09	0.64	0.10	0.65	0.08	0.61	0.08	0.61	0.05	0.63
	$T_g^{-1}$ (K <sup>-1</sup> )	0.44	0.88	0.44	0.87	0.47	0.88	0.40	0.82	0.39	0.82	0.27	0.85
	SA (m <sup>2</sup> g <sup>-1</sup> )	0.01	0.49	0.01	0.49	0.01	0.50	0.01	0.47	0.01	0.47	0.01	0.49
	SA <sup>-1</sup> (g m <sup>-2</sup> )	0.44	0.83	0.45	0.83	0.47	0.84	0.41	0.77	0.40	0.76	0.29	0.80
	Vp (cm <sup>3</sup> g <sup>-1</sup> )	0.01	0.50	0.01	0.50	0.02	0.50	0.01	0.48	0.01	0.48	0.01	0.49
	Vp <sup>-1</sup> (g cm <sup>-3</sup> )	0.45	0.83	0.45	0.83	0.48	0.84	0.42	0.77	0.40	0.77	0.30	0.80
$\sum SFE$ (mN m <sup>-1</sup> )	$\sum SFE$ (mN m <sup>-1</sup> )	0.19	0.72	0.19	0.72	0.20	0.73	0.18	0.66	0.18	0.66	0.14	0.69
	$\sum SFE^{-1}$ (m Nm <sup>-1</sup> )	0.05	0.74	0.05	0.74	0.06	0.75	0.04	0.71	0.04	0.70	0.02	0.73

Table A7.30: Calculation of  $R_h^2$  and  $R_v^2$  with the matrix of two PAH properties ( $\log K_{ow}$ ,  $\log C_w^{sat}$ ) multiplied with two plastic properties ( $T_m^{-1}$  as fixed parameter) and the  $\log K_{p-w}$  matrix

plastic property product		PAH properties											
1 <sup>st</sup> fixed parameter	2 <sup>nd</sup> variable parameter	$\log K_{ow}$ (-)		$\log C_w^{sat}$ (mol m <sup>-3</sup> )		$\log K_{ow} * \log C_w^{sat}$ (mol m <sup>-3</sup> )		$\log C_w^{sat} * \log K_{ow}^{-1}$ (mol m <sup>-3</sup> )		$\log K_{ow} * \log C_w^{sat}^{-1}$ (m <sup>3</sup> mol <sup>-1</sup> )		$(\log K_{ow} * \log C_w^{sat})^{-1}$ (m <sup>3</sup> mol <sup>-1</sup> )	
		$R_v^2$	$R_h^2$	$R_v^2$	$R_h^2$	$R_v^2$	$R_h^2$	$R_v^2$	$R_h^2$	$R_v^2$	$R_h^2$	$R_v^2$	$R_h^2$
$T_m^{-1}$ (K <sup>-1</sup> )	$\rho$ (g cm <sup>-3</sup> )	0.30	0.78	0.81	0.78	0.29	0.79	0.29	0.76	0.04	0.68	0.03	0.68
	$\rho^{-1}$ (cm <sup>3</sup> g <sup>-1</sup> )	0.35	0.84	0.41	0.83	0.40	0.84	0.40	0.82	0.01	0.74	0.01	0.74
	$d_{50}$ (μm)	0.31	0.76	0.30	0.76	0.30	0.77	0.29	0.74	0.04	0.67	0.04	0.67
	$d_{50}^{-1}$ (μm <sup>-1</sup> )	0.65	0.87	0.71	0.87	0.71	0.88	0.71	0.85	0.03	0.77	0.03	0.77
	$T_g$ (K)	0.09	0.65	0.12	0.64	0.12	0.65	0.12	0.63	0.00	0.57	0.00	0.57
	$T_g^{-1}$ (K <sup>-1</sup> )	0.44	0.88	0.49	0.87	0.49	0.88	0.49	0.86	0.02	0.77	0.02	0.77
	SA (m <sup>2</sup> g <sup>-1</sup> )	0.01	0.49	0.01	0.49	0.01	0.50	0.01	0.49	0.00	0.45	0.00	0.45
	SA <sup>-1</sup> (g m <sup>-2</sup> )	0.44	0.83	0.46	0.83	0.47	0.84	0.46	0.81	0.03	0.71	0.03	0.71
	Vp (cm <sup>3</sup> g <sup>-1</sup> )	0.01	0.50	0.01	0.50	0.01	0.50	0.01	0.49	0.00	0.45	0.00	0.45
	Vp <sup>-1</sup> (g cm <sup>-3</sup> )	0.45	0.83	0.47	0.83	0.47	0.84	0.47	0.81	0.03	0.72	0.03	0.72
$\sum SFE$ (mN m <sup>-1</sup> )	$\sum SFE$ (mN m <sup>-1</sup> )	0.19	0.72	0.18	0.72	0.18	0.73	0.17	0.70	0.03	0.62	0.03	0.62
	$\sum SFE^{-1}$ (m Nm <sup>-1</sup> )	0.05	0.74	0.07	0.74	0.07	0.75	0.07	0.73	0.00	0.67	0.00	0.67

Table A7.31: Calculation of  $R_h^2$  and  $R_v^2$  with the matrix of two PAH properties (MW,  $\log K_{hdw}$ ) multiplied with two plastic properties ( $T_m^{-1}$  as fixed parameter) and the  $\log K_{p-w}$  matrix

plastic property product		PAH properties											
1 <sup>st</sup> fixed parameter	2 <sup>nd</sup> variable parameter	MW (g mol <sup>-1</sup> )		$\log K_{hdw}$ (-)		MW * $\log K_{hdw}$ (g mol <sup>-1</sup> )		MW * $\log K_{hdw}^{-1}$ (g mol <sup>-1</sup> )		$\log K_{hdw} * MW^{-1}$ (mol g <sup>-1</sup> )		(MW * $\log K_{hdw}$ ) <sup>-1</sup> (mol g <sup>-1</sup> )	
		$R_v^2$	$R_h^2$	$R_v^2$	$R_h^2$	$R_v^2$	$R_h^2$	$R_v^2$	$R_h^2$	$R_v^2$	$R_h^2$		
$T_m^{-1}$ (K <sup>-1</sup> )	$\rho$ (g cm <sup>-3</sup> )	0.30	0.78	0.50	0.78	0.10	0.19	0.28	0.66	0.28	0.66	0.21	0.75
	$\rho^{-1}$ (cm <sup>3</sup> g <sup>-1</sup> )	0.36	0.83	0.36	0.84	0.14	0.18	0.31	0.72	0.32	0.72	0.21	0.81
	$d_{50}$ (μm)	0.31	0.76	0.31	0.76	0.10	0.17	0.29	0.65	0.29	0.65	0.22	0.74
	$d_{50}^{-1}$ (μm <sup>-1</sup> )	0.65	0.87	0.65	0.87	0.24	0.20	0.58	0.74	0.59	0.74	0.40	0.85
	$T_g$ (K)	0.09	0.64	0.09	0.65	0.04	0.14	0.08	0.55	0.08	0.55	0.05	0.63
	$T_g^{-1}$ (K <sup>-1</sup> )	0.44	0.87	0.44	0.88	0.16	0.20	0.39	0.75	0.40	0.74	0.26	0.85
	SA (m <sup>2</sup> g <sup>-1</sup> )	0.01	0.49	0.01	0.49	0.00	0.08	0.01	0.44	0.01	0.44	0.01	0.49
	SA <sup>-1</sup> (g m <sup>-2</sup> )	0.45	0.83	0.45	0.83	0.15	0.22	0.40	0.69	0.41	0.69	0.29	0.80
	Vp (cm <sup>3</sup> g <sup>-1</sup> )	0.01	0.50	0.01	0.50	0.00	0.08	0.01	0.44	0.01	0.44	0.01	0.49
	Vp <sup>-1</sup> (g cm <sup>-3</sup> )	0.45	0.83	0.45	0.83	0.15	0.22	0.41	0.69	0.41	0.69	0.29	0.80
$\Sigma SFE$ (mN m <sup>-1</sup> )	0.19	0.72	0.19	0.72	0.06	0.20	0.18	0.60	0.18	0.60	0.14	0.69	
	$\Sigma SFE^{-1}$ (m Nm <sup>-1</sup> )	0.05	0.74	0.05	0.74	0.03	0.14	0.04	0.65	0.04	0.65	0.02	0.73

Table A7.32: Calculation of  $R_h^2$  and  $R_v^2$  with the matrix of two PAH properties (MW,  $\log C_w^{sat}$ ) multiplied with two plastic properties ( $T_m^{-1}$  as fixed parameter) and the  $\log K_{p-w}$  matrix

plastic property product		PAH properties											
1 <sup>st</sup> fixed parameter	2 <sup>nd</sup> variable parameter	MW (g mol <sup>-1</sup> )		$\log C_w^{sat}$ (mol m <sup>-3</sup> )		MW * $\log C_w^{sat}$ (g m <sup>-3</sup> )		$\log C_w^{sat} * MW^{-1}$ (mol <sup>2</sup> m <sup>-3</sup> g <sup>-1</sup> )		MW * $\log C_w^{sat-1}$ (g m <sup>3</sup> mol <sup>-2</sup> )		$(\log K_{ow} * \log C_w^{sat})^{-1}$ (m <sup>3</sup> g <sup>-1</sup> )	
		$R_v^2$	$R_h^2$	$R_v^2$	$R_h^2$	$R_v^2$	$R_h^2$	$R_v^2$	$R_h^2$	$R_v^2$	$R_h^2$		
$T_m^{-1}$ (K <sup>-1</sup> )	$\rho$ (g cm <sup>-3</sup> )	0.30	0.78	0.00	0.78	0.06	0.02	0.29	0.76	0.04	0.68	0.03	0.68
	$\rho^{-1}$ (cm <sup>3</sup> g <sup>-1</sup> )	0.36	0.83	0.41	0.83	0.16	0.03	0.40	0.82	0.01	0.74	0.01	0.74
	$d_{50}$ (μm)	0.31	0.76	0.30	0.76	0.07	0.02	0.29	0.74	0.04	0.67	0.04	0.67
	$d_{50}^{-1}$ (μm <sup>-1</sup> )	0.65	0.87	0.71	0.87	0.24	0.03	0.71	0.85	0.03	0.77	0.03	0.77
	$T_g$ (K)	0.09	0.64	0.12	0.64	0.05	0.02	0.12	0.63	0.00	0.57	0.00	0.57
	$T_g^{-1}$ (K <sup>-1</sup> )	0.44	0.87	0.49	0.87	0.16	0.02	0.49	0.85	0.02	0.77	0.01	0.77
	SA (m <sup>2</sup> g <sup>-1</sup> )	0.01	0.49	0.01	0.49	0.00	0.03	0.01	0.49	0.00	0.45	0.00	0.45
	SA <sup>-1</sup> (g m <sup>-2</sup> )	0.45	0.83	0.46	0.83	0.12	0.01	0.46	0.80	0.03	0.71	0.03	0.71
	Vp (cm <sup>3</sup> g <sup>-1</sup> )	0.01	0.50	0.01	0.50	0.00	0.03	0.01	0.49	0.00	0.45	0.00	0.45
	Vp <sup>-1</sup> (g cm <sup>-3</sup> )	0.45	0.83	0.47	0.83	0.13	0.01	0.47	0.81	0.03	0.72	0.03	0.72
$\Sigma SFE$ (mN m <sup>-1</sup> )	0.19	0.72	0.18	0.72	0.03	0.01	0.17	0.70	0.03	0.62	0.03	0.62	
	$\Sigma SFE^{-1}$ (m Nm <sup>-1</sup> )	0.05	0.74	0.07	0.74	0.04	0.03	0.07	0.73	0.00	0.67	0.00	0.67

Table A7.33: Calculation of  $R_h^2$  and  $R_v^2$  with the matrix of two PAH properties ( $\log K_{hdw}$ ,  $\log C_w^{sat}$ ) multiplied with two plastic properties ( $T_m^{-1}$  as fixed parameter) and the  $\log K_{p-w}$  matrix

plastic property product		PAH properties											
1 <sup>st</sup> fixed parameter	2 <sup>nd</sup> variable parameter	$\log K_{hdw}$ (-)		$\log C_w^{sat}$ (mol m <sup>-3</sup> )		$\log K_{hdw} * \log C_w^{sat}$ (mol m <sup>-3</sup> )		$\log C_w^{sat} * \log K_{hdw}^{-1}$ (mol m <sup>-3</sup> )		$\log K_{hdw} * \log C_w^{sat-1}$ (m <sup>3</sup> mol <sup>-1</sup> )		$(\log K_{hdw} * \log C_w^{sat})^{-1}$ (m <sup>3</sup> mol <sup>-1</sup> )	
		$R_v^2$	$R_h^2$	$R_v^2$	$R_h^2$	$R_v^2$	$R_h^2$	$R_v^2$	$R_h^2$	$R_v^2$	$R_h^2$	$R_v^2$	$R_h^2$
$T_m^{-1}$ (K <sup>-1</sup> )	$\rho$ (g cm <sup>-3</sup> )	0.30	0.78	0.00	0.78	0.29	0.79	0.29	0.76	0.04	0.68	0.03	0.68
	$\rho^{-1}$ (cm <sup>3</sup> g <sup>-1</sup> )	0.36	0.84	0.41	0.83	0.40	0.84	0.40	0.82	0.01	0.74	0.01	0.74
	$d_{50}$ (μm)	0.31	0.76	0.30	0.76	0.30	0.77	0.29	0.74	0.04	0.67	0.04	0.67
	$d_{50}^{-1}$ (μm <sup>-1</sup> )	0.65	0.87	0.71	0.87	0.71	0.88	0.71	0.85	0.03	0.77	0.03	0.77
	$T_g$ (K)	0.09	0.64	0.12	0.64	0.12	0.65	0.12	0.63	0.00	0.57	0.00	0.57
	$T_g^{-1}$ (K <sup>-1</sup> )	0.44	0.88	0.49	0.87	0.49	0.88	0.49	0.85	0.02	0.77	0.02	0.77
	SA (m <sup>2</sup> g <sup>-1</sup> )	0.01	0.49	0.01	0.49	0.01	0.50	0.01	0.49	0.00	0.45	0.00	0.45
	SA <sup>-1</sup> (g m <sup>-2</sup> )	0.45	0.83	0.46	0.83	0.47	0.84	0.46	0.80	0.03	0.71	0.03	0.71
	Vp (cm <sup>3</sup> g <sup>-1</sup> )	0.01	0.50	0.01	0.50	0.01	0.50	0.01	0.49	0.00	0.45	0.00	0.45
	Vp <sup>-1</sup> (g cm <sup>-3</sup> )	0.45	0.83	0.47	0.83	0.48	0.84	0.47	0.81	0.03	0.72	0.03	0.72
$\Sigma SFE$ (mN m <sup>-1</sup> )	0.19	0.72	0.18	0.72	0.18	0.72	0.17	0.70	0.03	0.62	0.03	0.62	0.03
	$\Sigma SFE^{-1}$ (m Nm <sup>-1</sup> )	0.05	0.74	0.07	0.74	0.07	0.75	0.07	0.73	0.00	0.67	0.00	0.67

Table A7.34: Calculation of  $R_h^2$  and  $R_v^2$  with the matrix of two PAH properties ( $\log K_{ow}$ , MW<sub>w</sub>) multiplied with three plastic properties ( $X_c * \rho$  as fixed parameters) and the  $\log K_{p-w}$  matrix

plastic property product		PAH properties											
1 <sup>st</sup> * 2 <sup>nd</sup> fixed parameters	3 <sup>rd</sup> variable parameter	$\log K_{ow}$ (-)		MW (g mol <sup>-1</sup> )		$\log K_{ow} * MW$ (g mol <sup>-1</sup> )		MW * $\log K_{ow}^{-1}$ (g mol <sup>-1</sup> )		$\log K_{ow} * MW^{-1}$ (mol g <sup>-1</sup> )		$(\log K_{ow} * MW)^{-1}$ (mol g <sup>-1</sup> )	
		$R_v^2$	$R_h^2$	$R_v^2$	$R_h^2$	$R_v^2$	$R_h^2$	$R_v^2$	$R_h^2$	$R_v^2$	$R_h^2$		
	$d_{50}$ ( $\mu\text{m}$ )	0.83	0.92	0.84	0.91	0.88	0.93	0.78	0.85	0.75	0.85	0.56	0.89
	$d_{50}^{-1}$ ( $\mu\text{m}^{-1}$ )	0.88	0.95	0.89	0.95	0.94	0.96	0.82	0.88	0.79	0.88	0.58	0.92
	$T_m$ (K)	0.86	0.94	0.87	0.94	0.92	0.95	0.81	0.87	0.78	0.87	0.57	0.91
	$T_m^{-1}$ (K <sup>-1</sup> )	0.86	0.93	0.87	0.92	0.92	0.94	0.81	0.86	0.78	0.85	0.57	0.89
	$T_g$ (K)	0.72	0.88	0.73	0.88	0.76	0.89	0.68	0.81	0.65	0.81	0.49	0.85
$X_c$ (%) * $\rho$ (g cm <sup>-3</sup> )	$T_g^{-1}$ (K <sup>-1</sup> )	0.81	0.94	0.82	0.94	0.87	0.95	0.76	0.87	0.73	0.87	0.53	0.91
	SA (m <sup>2</sup> g <sup>-1</sup> )	0.11	0.63	0.11	0.63	0.11	0.64	0.10	0.60	0.09	0.60	0.07	0.62
	SA <sup>-1</sup> (g m <sup>-2</sup> )	0.73	0.84	0.74	0.83	0.78	0.84	0.69	0.76	0.66	0.76	0.49	0.80
	Vp (cm <sup>3</sup> g <sup>-1</sup> )	0.11	0.64	0.11	0.64	0.12	0.64	0.10	0.61	0.10	0.60	0.07	0.62
	Vp <sup>-1</sup> (g cm <sup>-3</sup> )	0.74	0.84	0.75	0.83	0.78	0.85	0.69	0.77	0.67	0.76	0.49	0.80
	$\sum SFE$ (mN m <sup>-1</sup> )	0.65	0.77	0.66	0.76	0.69	0.78	0.61	0.70	0.59	0.70	0.45	0.73
	$\sum SFE^{-1}$ (m Nm <sup>-1</sup> )	0.47	0.88	0.48	0.88	0.51	0.89	0.44	0.83	0.42	0.83	0.29	0.86

Table A7.35: Calculation of  $R_h^2$  and  $R_v^2$  with the matrix of two PAH properties ( $\log K_{ow}$ ,  $\log K_{hdw}$ ) multiplied with three plastic properties ( $X_c * \rho$  as fixed parameters) and the  $\log K_{p-w}$  matrix

plastic property product		PAH properties											
1 <sup>st</sup> * 2 <sup>nd</sup> fixed parameters	3 <sup>rd</sup> variable parameter	$\log K_{ow}$ (-)		$\log K_{hdw}$ (-)		$\log K_{ow} * \log K_{hdw}$ (-)		$\log K_{hdw} * \log K_{ow}^{-1}$ (-)		$\log K_{ow} * \log K_{hdw}^{-1}$ (-)		$(\log K_{ow} * \log K_{hdw})^{-1}$ (-)	
		$R_v^2$	$R_h^2$	$R_v^2$	$R_h^2$	$R_v^2$	$R_h^2$	$R_v^2$	$R_h^2$	$R_v^2$	$R_h^2$		
	$d_{50}$ ( $\mu\text{m}$ )	0.83	0.92	0.84	0.92	0.88	0.93	0.77	0.90	0.76	0.90	0.57	0.89
	$d_{50}^{-1}$ ( $\mu\text{m}^{-1}$ )	0.88	0.95	0.89	0.95	0.94	0.96	0.81	0.93	0.80	0.93	0.59	0.92
	$T_m$ (K)	0.86	0.94	0.87	0.94	0.92	0.95	0.81	0.87	0.78	0.87	0.57	0.91
	$T_m^{-1}$ (K <sup>-1</sup> )	0.86	0.93	0.87	0.92	0.92	0.94	0.81	0.86	0.78	0.85	0.57	0.89
	$T_g$ (K)	0.72	0.88	0.73	0.88	0.76	0.89	0.68	0.81	0.65	0.81	0.49	0.85
$X_c$ (%) * $\rho$ (g cm <sup>-3</sup> )	$T_g^{-1}$ (K <sup>-1</sup> )	0.81	0.94	0.82	0.94	0.87	0.95	0.76	0.87	0.73	0.87	0.53	0.91
	SA (m <sup>2</sup> g <sup>-1</sup> )	0.11	0.63	0.11	0.63	0.11	0.64	0.10	0.60	0.09	0.60	0.07	0.62
	SA <sup>-1</sup> (g m <sup>-2</sup> )	0.73	0.84	0.74	0.83	0.78	0.84	0.69	0.76	0.66	0.76	0.49	0.80
	Vp (cm <sup>3</sup> g <sup>-1</sup> )	0.11	0.64	0.11	0.64	0.12	0.64	0.10	0.61	0.10	0.60	0.07	0.62
	Vp <sup>-1</sup> (g cm <sup>-3</sup> )	0.74	0.84	0.75	0.83	0.78	0.85	0.69	0.77	0.67	0.76	0.49	0.80
	$\sum SFE$ (mN m <sup>-1</sup> )	0.65	0.77	0.66	0.76	0.69	0.78	0.61	0.70	0.59	0.70	0.45	0.73
	$\sum SFE^{-1}$ (m Nm <sup>-1</sup> )	0.47	0.88	0.48	0.88	0.51	0.89	0.44	0.83	0.42	0.83	0.29	0.86

Table A7.36: Calculation of  $R_h^2$  and  $R_v^2$  with the matrix of two PAH properties ( $\log K_{ow}$ ,  $\log C_w^{\text{sat}}$ ) multiplied with three plastic properties ( $X_c * \rho$  as fixed parameters) and the  $\log K_{p-w}$  matrix

plastic property product		PAH properties											
1 <sup>st</sup> * 2 <sup>nd</sup> fixed parameters	3 <sup>rd</sup> variable parameter	$\log K_{ow}$ (-)		$\log C_w^{\text{sat}}$ (mol m <sup>-3</sup> )		$\log K_{ow} * \log C_w^{\text{sat}}$ (mol m <sup>-3</sup> )		$\log C_w^{\text{sat}} * \log K_{ow}^{-1}$ (mol m <sup>-3</sup> )		$\log K_{ow} * \log C_w^{\text{sat}-1}$ (m <sup>3</sup> mol <sup>-1</sup> )		$(\log K_{ow} * \log C_w^{\text{sat}})^{-1}$ (m <sup>3</sup> mol <sup>-1</sup> )	
		$R_v^2$	$R_h^2$	$R_v^2$	$R_h^2$	$R_v^2$	$R_h^2$	$R_v^2$	$R_h^2$	$R_v^2$	$R_h^2$	$R_v^2$	$R_h^2$
	$d_{50}$ ( $\mu\text{m}$ )	0.83	0.92	0.87	0.91	0.87	0.93	0.86	0.89	0.06	0.79	0.06	0.79
	$d_{50}^{-1}$ ( $\mu\text{m}^{-1}$ )	0.88	0.95	0.93	0.95	0.94	0.96	0.93	0.93	0.06	0.82	0.05	0.82
	$T_m$ (K)	0.86	0.94	0.91	0.94	0.91	0.95	0.90	0.92	0.06	0.81	0.05	0.81
	$T_m^{-1}$ (K <sup>-1</sup> )	0.86	0.93	0.90	0.92	0.91	0.94	0.90	0.90	0.06	0.80	0.06	0.80
	$T_g$ (K)	0.72	0.88	0.74	0.88	0.75	0.89	0.74	0.86	0.06	0.76	0.05	0.76
$X_c$ (%) * $\rho$ (g cm <sup>-3</sup> )	$T_g^{-1}$ (K <sup>-1</sup> )	0.81	0.94	0.87	0.94	0.87	0.95	0.86	0.92	0.05	0.81	0.04	0.81
	SA (m <sup>2</sup> g <sup>-1</sup> )	0.11	0.63	0.11	0.63	0.11	0.64	0.11	0.62	0.00	0.57	0.00	0.57
	SA <sup>-1</sup> (g m <sup>-2</sup> )	0.73	0.84	0.76	0.83	0.77	0.85	0.76	0.81	0.06	0.70	0.05	0.70
	Vp (cm <sup>3</sup> g <sup>-1</sup> )	0.11	0.64	0.12	0.64	0.12	0.64	0.12	0.63	0.00	0.57	0.00	0.57
	Vp <sup>-1</sup> (g cm <sup>-3</sup> )	0.74	0.84	0.77	0.83	0.77	0.85	0.76	0.81	0.05	0.71	0.05	0.71
	$\sum SFE$ (mN m <sup>-1</sup> )	0.65	0.77	0.66	0.76	0.67	0.78	0.66	0.74	0.06	0.65	0.06	0.65
	$\sum SFE^{-1}$ (m Nm <sup>-1</sup> )	0.47	0.88	0.53	0.88	0.53	0.89	0.53	0.86	0.02	0.78	0.02	0.78

Table A7.37: Calculation of  $R_h^2$  and  $R_v^2$  with the matrix of two PAH properties (MW,  $\log K_{\text{hdw}}$ ) multiplied with three plastic properties ( $X_c * \rho$  as fixed parameters) and the  $\log K_{\text{p-w}}$  matrix

plastic property product		PAH properties											
1 <sup>st</sup> * 2 <sup>nd</sup> fixed parameter	3 <sup>rd</sup> variable parameter	MW (g mol <sup>-1</sup> )		$\log K_{\text{hdw}}$ (-)		MW * $\log K_{\text{hdw}}$ (g mol <sup>-1</sup> )		MW * $\log K_{\text{hdw}}^{-1}$ (g mol <sup>-1</sup> )		$\log K_{\text{hdw}} * MW^{-1}$ (mol g <sup>-1</sup> )		$(MW * \log K_{\text{hdw}})^{-1}$ (mol g <sup>-1</sup> )	
		$R_v^2$	$R_h^2$	$R_v^2$	$R_h^2$	$R_v^2$	$R_h^2$	$R_v^2$	$R_h^2$	$R_v^2$	$R_h^2$		
$X_c (\%)$ $* \rho (\text{g cm}^{-3})$	$d_{50} (\mu\text{m})$	0.84	0.91	0.84	0.92	0.31	0.25	0.76	0.76	0.77	0.76	0.55	0.88
	$d_{50}^{-1} (\mu\text{m}^{-1})$	0.89	0.95	0.89	0.95	0.32	0.25	0.80	0.79	0.81	0.79	0.57	0.92
	$T_m (\text{K})$	0.87	0.94	0.87	0.94	0.32	0.24	0.79	0.79	0.80	0.79	0.56	0.91
	$T_m^{-1} (\text{K}^{-1})$	0.87	0.92	0.87	0.93	0.31	0.25	0.79	0.77	0.80	0.77	0.56	0.89
	$T_g (\text{K})$	0.73	0.88	0.73	0.88	0.27	0.23	0.66	0.73	0.67	0.73	0.48	0.85
	$T_g^{-1} (\text{K}^{-1})$	0.82	0.94	0.82	0.94	0.30	0.24	0.74	0.79	0.75	0.79	0.52	0.91
	$SA (\text{m}^2 \text{g}^{-1})$	0.11	0.63	0.11	0.63	0.05	0.12	0.09	0.55	0.10	0.55	0.07	0.62
	$SA^{-1} (\text{g m}^{-2})$	0.74	0.83	0.74	0.84	0.26	0.25	0.67	0.68	0.68	0.68	0.48	0.80
	$Vp (\text{cm}^3 \text{g}^{-1})$	0.11	0.64	0.11	0.64	0.05	0.13	0.10	0.56	0.10	0.56	0.07	0.62
	$Vp^{-1} (\text{g cm}^{-3})$	0.75	0.83	0.74	0.84	0.26	0.25	0.67	0.68	0.68	0.68	0.48	0.80
$\sum SFE (\text{mN m}^{-1})$	0.66	0.76	0.66	0.77	0.23	0.24	0.60	0.62	0.61	0.62	0.44	0.73	
	$\sum SFE^{-1} (\text{m Nm}^{-1})$	0.48	0.88	0.48	0.88	0.19	0.19	0.42	0.76	0.43	0.76	0.29	0.86

Table A7.38: Calculation of  $R_h^2$  and  $R_v^2$  with the matrix of two PAH properties (MW,  $\log C_w^{\text{sat}}$ ) multiplied with three plastic properties ( $X_c * \rho$  as fixed parameters) and the  $\log K_{\text{p-w}}$  matrix

plastic property product		PAH properties											
1 <sup>st</sup> * 2 <sup>nd</sup> fixed parameter	3 <sup>rd</sup> variable parameter	MW (g mol <sup>-1</sup> )		$\log C_w^{\text{sat}}$ (mol m <sup>-3</sup> )		MW * $\log C_w^{\text{sat}}$ (g m <sup>-3</sup> )		$\log C_w^{\text{sat}} * MW^{-1}$ (mol <sup>2</sup> m <sup>-3</sup> g <sup>-1</sup> )		MW * $\log C_w^{\text{sat-1}}$ (g m <sup>3</sup> mol <sup>-2</sup> )		$(\log K_{\text{ow}} * \log C_w^{\text{sat}})^{-1}$ (m <sup>3</sup> g <sup>-1</sup> )	
		$R_v^2$	$R_h^2$	$R_v^2$	$R_h^2$	$R_v^2$	$R_h^2$	$R_v^2$	$R_h^2$	$R_v^2$	$R_h^2$		
$X_c (\%)$ $* \rho (\text{g cm}^{-3})$	$d_{50} (\mu\text{m})$	0.84	0.91	0.87	0.91	0.26	0.01	0.86	0.89	0.06	0.79	0.06	0.79
	$d_{50}^{-1} (\mu\text{m}^{-1})$	0.89	0.95	0.93	0.95	0.29	0.02	0.93	0.92	0.06	0.82	0.05	0.82
	$T_m (\text{K})$	0.87	0.94	0.91	0.94	0.28	0.02	0.90	0.91	0.06	0.81	0.05	0.81
	$T_m^{-1} (\text{K}^{-1})$	0.87	0.92	0.90	0.92	0.27	0.01	0.90	0.90	0.06	0.80	0.06	0.80
	$T_g (\text{K})$	0.73	0.88	0.74	0.88	0.23	0.01	0.74	0.86	0.06	0.76	0.05	0.76
	$T_g^{-1} (\text{K}^{-1})$	0.82	0.94	0.87	0.94	0.27	0.02	0.86	0.92	0.05	0.81	0.04	0.81
	$SA (\text{m}^2 \text{g}^{-1})$	0.11	0.63	0.11	0.63	0.05	0.03	0.11	0.62	0.00	0.57	0.00	0.57
	$SA^{-1} (\text{g m}^{-2})$	0.74	0.83	0.76	0.83	0.22	0.01	0.76	0.80	0.06	0.70	0.05	0.70
	$Vp (\text{cm}^3 \text{g}^{-1})$	0.11	0.64	0.12	0.64	0.06	0.03	0.12	0.63	0.00	0.57	0.00	0.57
	$Vp^{-1} (\text{g cm}^{-3})$	0.75	0.83	0.77	0.83	0.22	0.01	0.76	0.81	0.06	0.71	0.05	0.71
$\sum SFE (\text{mN m}^{-1})$	0.66	0.76	0.66	0.76	0.18	0.01	0.66	0.74	0.06	0.65	0.06	0.65	
	$\sum SFE^{-1} (\text{m Nm}^{-1})$	0.48	0.88	0.53	0.88	0.20	0.03	0.53	0.86	0.02	0.78	0.02	0.78

Table A7.39: Calculation of  $R_h^2$  and  $R_v^2$  with the matrix of two PAH properties ( $\log K_{\text{hdw}}$ ,  $\log C_w^{\text{sat}}$ ) multiplied with three plastic properties ( $X_c * \rho$  as fixed parameters) and the  $\log K_{\text{p-w}}$  matrix

plastic property product		PAH properties											
1 <sup>st</sup> * 2 <sup>nd</sup> fixed parameter	3 <sup>rd</sup> variable parameter	$\log K_{\text{hdw}}$ (-)		$\log C_w^{\text{sat}}$ (mol m <sup>-3</sup> )		$\log K_{\text{hdw}} * \log C_w^{\text{sat}}$ (mol m <sup>-3</sup> )		$\log C_w^{\text{sat}} * \log K_{\text{hdw}}^{-1}$ (mol m <sup>-3</sup> )		$\log K_{\text{hdw}} * \log C_w^{\text{sat-1}}$ (m <sup>3</sup> mol <sup>-1</sup> )		$(\log K_{\text{hdw}} * \log C_w^{\text{sat}})^{-1}$ (m <sup>3</sup> mol <sup>-1</sup> )	
		$R_v^2$	$R_h^2$	$R_v^2$	$R_h^2$	$R_v^2$	$R_h^2$	$R_v^2$	$R_h^2$	$R_v^2$	$R_h^2$	$R_v^2$	$R_h^2$
$X_c (\%)$ $* \rho (\text{g cm}^{-3})$	$d_{50} (\mu\text{m})$	0.84	0.92	0.87	0.91	0.87	0.93	0.86	0.89	0.06	0.79	0.06	0.79
	$d_{50}^{-1} (\mu\text{m}^{-1})$	0.89	0.95	0.93	0.95	0.94	0.96	0.92	0.92	0.06	0.82	0.05	0.82
	$T_m (\text{K})$	0.87	0.94	0.91	0.94	0.91	0.95	0.90	0.91	0.06	0.81	0.05	0.81
	$T_m^{-1} (\text{K}^{-1})$	0.87	0.93	0.90	0.92	0.91	0.94	0.90	0.90	0.06	0.80	0.06	0.80
	$T_g (\text{K})$	0.73	0.88	0.74	0.88	0.75	0.89	0.74	0.85	0.06	0.76	0.05	0.76
	$T_g^{-1} (\text{K}^{-1})$	0.82	0.94	0.87	0.94	0.87	0.96	0.86	0.92	0.05	0.81	0.04	0.81
	$SA (\text{m}^2 \text{g}^{-1})$	0.11	0.63	0.11	0.63	0.11	0.64	0.11	0.62	0.00	0.57	0.00	0.57
	$SA^{-1} (\text{g m}^{-2})$	0.74	0.84	0.76	0.83	0.77	0.85	0.75	0.80	0.06	0.70	0.05	0.70
	$Vp (\text{cm}^3 \text{g}^{-1})$	0.11	0.64	0.12	0.64	0.12	0.64	0.12	0.63	0.00	0.57	0.00	0.57
	$Vp^{-1} (\text{g cm}^{-3})$	0.74	0.84	0.77	0.83	0.77	0.85	0.76	0.81	0.06	0.71	0.05	0.71
$\sum SFE (\text{mN m}^{-1})$	0.66	0.77	0.66	0.76	0.67	0.78	0.66	0.74	0.06	0.65	0.06	0.65	
	$\sum SFE^{-1} (\text{m Nm}^{-1})$	0.48	0.88	0.53	0.88	0.53	0.89	0.53	0.86	0.02	0.78	0.02	0.78

Table A7.40: Calculation of  $R_h^2$  and  $R_v^2$  with the matrix of two PAH properties ( $\log K_{ow}$ , MW<sub>w</sub>) multiplied with three plastic properties ( $X_c * \rho^{-1}$  as fixed parameters) and the  $\log K_{p-w}$  matrix

plastic property product		PAH properties											
1 <sup>st</sup> * 2 <sup>nd</sup> fixed parameter	3 <sup>rd</sup> variable parameter	$\log K_{ow}$ (-)		MW (g mol <sup>-1</sup> )		$\log K_{ow} * MW$ (g mol <sup>-1</sup> )		$MW * \log K_{ow}^{-1}$ (g mol <sup>-1</sup> )		$\log K_{ow} * MW^{-1}$ (mol g <sup>-1</sup> )		$(\log K_{ow} * MW)^{-1}$ (mol g <sup>-1</sup> )	
		$R_v^2$	$R_h^2$	$R_v^2$	$R_h^2$	$R_v^2$	$R_h^2$	$R_v^2$	$R_h^2$	$R_v^2$	$R_h^2$	$R_v^2$	$R_h^2$
$X_c$ (%) $* \rho^{-1}$ (cm <sup>3</sup> g <sup>-1</sup> )	$d_{50}$ (μm)	0.69	0.93	0.70	0.92	0.74	0.93	0.64	0.86	0.62	0.86	0.44	0.90
	$d_{50}^{-1}$ (μm <sup>-1</sup> )	0.58	0.91	0.59	0.91	0.63	0.92	0.54	0.85	0.52	0.85	0.37	0.88
	$T_m$ (K)	0.54	0.90	0.54	0.89	0.58	0.90	0.50	0.84	0.48	0.84	0.34	0.87
	$T_m^{-1}$ (K <sup>-1</sup> )	0.74	0.94	0.75	0.94	0.79	0.95	0.68	0.88	0.66	0.88	0.47	0.91
	$T_g$ (K)	0.54	0.87	0.54	0.87	0.57	0.88	0.50	0.82	0.48	0.81	0.35	0.85
	$T_g^{-1}$ (K <sup>-1</sup> )	0.48	0.87	0.48	0.87	0.51	0.88	0.44	0.82	0.42	0.81	0.29	0.85
	SA (m <sup>2</sup> g <sup>-1</sup> )	0.02	0.50	0.02	0.50	0.02	0.50	0.02	0.48	0.02	0.48	0.01	0.49
	SA <sup>-1</sup> (g m <sup>-2</sup> )	0.70	0.89	0.71	0.88	0.75	0.90	0.65	0.82	0.62	0.82	0.45	0.86
	Vp (cm <sup>3</sup> g <sup>-1</sup> )	0.02	0.50	0.02	0.50	0.03	0.50	0.02	0.48	0.02	0.48	0.01	0.49
	Vp <sup>-1</sup> (g cm <sup>-3</sup> )	0.69	0.89	0.70	0.88	0.73	0.90	0.64	0.82	0.61	0.82	0.44	0.86
$\sum SFE$ (mN m <sup>-1</sup> )	$\sum SFE$ (mN m <sup>-1</sup> )	0.83	0.91	0.84	0.90	0.88	0.91	0.77	0.83	0.75	0.83	0.55	0.87
	$\sum SFE^{-1}$ (m Nm <sup>-1</sup> )	0.16	0.74	0.17	0.74	0.18	0.74	0.15	0.70	0.14	0.70	0.09	0.72

Table A7.41: Calculation of  $R_h^2$  and  $R_v^2$  with the matrix of two PAH properties ( $\log K_{ow}$ ,  $\log K_{hdw}$ ) multiplied with three plastic properties ( $X_c * \rho^{-1}$  as fixed parameters) and the  $\log K_{p-w}$  matrix

plastic property product		PAH properties											
1 <sup>st</sup> * 2 <sup>nd</sup> fixed parameter	3 <sup>rd</sup> variable parameter	$\log K_{ow}$ (-)		$\log K_{hdw}$ (-)		$\log K_{ow} * \log K_{hdw}$ (-)		$\log K_{hdw} * \log K_{ow}^{-1}$ (-)		$\log K_{ow} * \log K_{hdw}^{-1}$ (-)		$(\log K_{ow} * \log K_{hdw})^{-1}$ (-)	
		$R_v^2$	$R_h^2$	$R_v^2$	$R_h^2$	$R_v^2$	$R_h^2$	$R_v^2$	$R_h^2$	$R_v^2$	$R_h^2$	$R_v^2$	$R_h^2$
$X_c$ (%) $* \rho^{-1}$ (cm <sup>3</sup> g <sup>-1</sup> )	$d_{50}$ (μm)	0.69	0.93	0.70	0.93	0.74	0.93	0.64	0.91	0.62	0.91	0.45	0.90
	$d_{50}^{-1}$ (μm <sup>-1</sup> )	0.58	0.91	0.59	0.91	0.63	0.92	0.54	0.90	0.52	0.90	0.37	0.89
	$T_m$ (K)	0.54	0.90	0.54	0.89	0.58	0.90	0.50	0.84	0.48	0.84	0.34	0.87
	$T_m^{-1}$ (K <sup>-1</sup> )	0.74	0.94	0.75	0.94	0.79	0.95	0.68	0.88	0.66	0.88	0.47	0.91
	$T_g$ (K)	0.54	0.87	0.54	0.87	0.57	0.88	0.50	0.82	0.48	0.81	0.35	0.85
	$T_g^{-1}$ (K <sup>-1</sup> )	0.48	0.87	0.48	0.87	0.51	0.88	0.44	0.82	0.42	0.81	0.29	0.85
	SA (m <sup>2</sup> g <sup>-1</sup> )	0.02	0.50	0.02	0.50	0.02	0.50	0.02	0.48	0.02	0.48	0.01	0.49
	SA <sup>-1</sup> (g m <sup>-2</sup> )	0.70	0.89	0.71	0.88	0.75	0.90	0.65	0.82	0.62	0.82	0.45	0.86
	Vp (cm <sup>3</sup> g <sup>-1</sup> )	0.02	0.50	0.02	0.50	0.03	0.50	0.02	0.48	0.02	0.48	0.01	0.49
	Vp <sup>-1</sup> (g cm <sup>-3</sup> )	0.69	0.89	0.70	0.88	0.73	0.90	0.64	0.82	0.61	0.82	0.44	0.86
$\sum SFE$ (mN m <sup>-1</sup> )	$\sum SFE$ (mN m <sup>-1</sup> )	0.83	0.91	0.84	0.90	0.88	0.91	0.77	0.83	0.75	0.83	0.55	0.87
	$\sum SFE^{-1}$ (m Nm <sup>-1</sup> )	0.16	0.74	0.17	0.74	0.18	0.74	0.15	0.70	0.14	0.70	0.09	0.72

Table A7.42: Calculation of  $R_h^2$  and  $R_v^2$  with the matrix of two PAH properties ( $\log K_{ow}$ ,  $\log C_w^{sat}$ ) multiplied with three plastic properties ( $X_c * \rho^{-1}$  as fixed parameters) and the  $\log K_{p-w}$  matrix

plastic property product		PAH properties											
1 <sup>st</sup> * 2 <sup>nd</sup> fixed parameter	3 <sup>rd</sup> variable parameter	$\log K_{ow}$ (-)		$\log C_w^{sat}$ (mol m <sup>-3</sup> )		$\log K_{ow} * \log C_w^{sat}$ (mol m <sup>-3</sup> )		$\log C_w^{sat} * \log K_{ow}^{-1}$ (mol m <sup>-3</sup> )		$\log K_{ow} * \log C_w^{sat-1}$ (m <sup>3</sup> mol <sup>-1</sup> )		$(\log K_{ow} * \log C_w^{sat})^{-1}$ (m <sup>3</sup> mol <sup>-1</sup> )	
		$R_v^2$	$R_h^2$	$R_v^2$	$R_h^2$	$R_v^2$	$R_h^2$	$R_v^2$	$R_h^2$	$R_v^2$	$R_h^2$	$R_v^2$	$R_h^2$
$X_c$ (%) $* \rho^{-1}$ (cm <sup>3</sup> g <sup>-1</sup> )	$d_{50}$ (μm)	0.69	0.93	0.75	0.92	0.75	0.93	0.75	0.90	0.03	0.81	0.03	0.81
	$d_{50}^{-1}$ (μm <sup>-1</sup> )	0.58	0.91	0.65	0.91	0.65	0.92	0.65	0.89	0.02	0.80	0.02	0.80
	$T_m$ (K)	0.54	0.90	0.59	0.89	0.59	0.90	0.59	0.88	0.02	0.79	0.02	0.79
	$T_m^{-1}$ (K <sup>-1</sup> )	0.74	0.94	0.80	0.94	0.80	0.95	0.80	0.92	0.04	0.82	0.03	0.82
	$T_g$ (K)	0.54	0.87	0.57	0.87	0.58	0.88	0.57	0.85	0.03	0.77	0.03	0.77
	$T_g^{-1}$ (K <sup>-1</sup> )	0.48	0.87	0.54	0.87	0.54	0.88	0.53	0.85	0.02	0.77	0.02	0.77
	SA (m <sup>2</sup> g <sup>-1</sup> )	0.02	0.50	0.03	0.50	0.03	0.50	0.03	0.49	0.00	0.45	0.00	0.45
	SA <sup>-1</sup> (g m <sup>-2</sup> )	0.70	0.89	0.75	0.88	0.75	0.90	0.74	0.86	0.04	0.76	0.04	0.76
	Vp (cm <sup>3</sup> g <sup>-1</sup> )	0.02	0.50	0.03	0.50	0.03	0.50	0.03	0.50	0.00	0.46	0.00	0.46
	Vp <sup>-1</sup> (g cm <sup>-3</sup> )	0.69	0.89	0.74	0.88	0.74	0.90	0.73	0.86	0.04	0.76	0.04	0.76
$\sum SFE$ (mN m <sup>-1</sup> )	$\sum SFE$ (mN m <sup>-1</sup> )	0.83	0.91	0.86	0.90	0.86	0.92	0.85	0.88	0.06	0.77	0.06	0.77
	$\sum SFE^{-1}$ (m Nm <sup>-1</sup> )	0.16	0.74	0.20	0.74	0.19	0.74	0.20	0.73	0.00	0.67	0.00	0.67

Table A7.43: Calculation of  $R_h^2$  and  $R_v^2$  with the matrix of two PAH properties (MW,  $\log K_{hdw}$ ) multiplied with three plastic properties ( $X_c * \rho^{-1}$  as fixed parameters) and the  $\log K_{p-w}$  matrix

plastic property product		PAH properties											
1 <sup>st</sup> * 2 <sup>nd</sup> fixed parameter	3 <sup>rd</sup> variable parameter	MW (g mol <sup>-1</sup> )		$\log K_{hdw}$ (-)		MW * log $K_{hdw}$ (g mol <sup>-1</sup> )		MW * log $K_{hdw}^{-1}$ (g mol <sup>-1</sup> )		$\log K_{hdw} * MW^{-1}$ (mol g <sup>-1</sup> )		(MW * log $K_{hdw}^{-1}$ ) (mol g <sup>-1</sup> )	
		$R_v^2$	$R_h^2$	$R_v^2$	$R_h^2$	$R_v^2$	$R_h^2$	$R_v^2$	$R_h^2$	$R_v^2$	$R_h^2$		
$X_c$ (%) $* \rho^{-1}$ (cm <sup>3</sup> g <sup>-1</sup> )	d <sub>50</sub> (μm)	0.70	0.92	0.70	0.93	0.27	0.21	0.62	0.79	0.64	0.79	0.43	0.90
	d <sub>50</sub> <sup>-1</sup> (μm <sup>-1</sup> )	0.59	0.91	0.59	0.91	0.23	0.20	0.52	0.78	0.53	0.78	0.36	0.88
	T <sub>m</sub> (K)	0.54	0.89	0.54	0.90	0.21	0.20	0.48	0.77	0.49	0.77	0.33	0.87
	T <sub>m</sub> <sup>-1</sup> (K <sup>-1</sup> )	0.75	0.94	0.74	0.94	0.28	0.22	0.66	0.80	0.68	0.80	0.46	0.91
	T <sub>g</sub> (K)	0.54	0.87	0.54	0.87	0.22	0.20	0.49	0.74	0.49	0.74	0.34	0.84
	T <sub>g</sub> <sup>-1</sup> (K <sup>-1</sup> )	0.48	0.87	0.48	0.87	0.18	0.20	0.43	0.74	0.43	0.74	0.29	0.85
	SA (m <sup>2</sup> g <sup>-1</sup> )	0.02	0.50	0.02	0.50	0.01	0.08	0.02	0.44	0.02	0.44	0.01	0.49
	SA <sup>-1</sup> (g m <sup>-2</sup> )	0.71	0.88	0.70	0.89	0.25	0.24	0.63	0.74	0.64	0.74	0.44	0.85
	Vp (cm <sup>3</sup> g <sup>-1</sup> )	0.02	0.50	0.02	0.50	0.02	0.08	0.02	0.45	0.02	0.45	0.01	0.49
	Vp <sup>-1</sup> (g cm <sup>-3</sup> )	0.70	0.88	0.69	0.89	0.25	0.24	0.62	0.74	0.63	0.74	0.43	0.85
$\sum SFE$ (mN m <sup>-1</sup> )	0.84	0.90	0.83	0.91	0.30	0.25	0.76	0.75	0.77	0.74	0.54	0.87	
	$\sum SFE^{-1}$ (m Nm <sup>-1</sup> )	0.17	0.74	0.16	0.74	0.07	0.14	0.14	0.65	0.15	0.65	0.09	0.72

Table A7.44: Calculation of  $R_h^2$  and  $R_v^2$  with the matrix of two PAH properties (MW,  $\log C_w^{sat}$ ) multiplied with three plastic properties ( $X_c * \rho^{-1}$  as fixed parameters) and the  $\log K_{p-w}$  matrix

plastic property product		PAH properties											
1 <sup>st</sup> * 2 <sup>nd</sup> fixed parameter	3 <sup>rd</sup> variable parameter	MW (g mol <sup>-1</sup> )		$\log C_w^{sat}$ (mol m <sup>-3</sup> )		MW * log $C_w^{sat}$ (g m <sup>-3</sup> )		$\log C_w^{sat} * MW^{-1}$ (mol <sup>2</sup> m <sup>-3</sup> g <sup>-1</sup> )		MW * log $C_w^{sat-1}$ (g m <sup>3</sup> mol <sup>-2</sup> )		$(\log K_{ow} * \log C_w^{sat})^{-1}$ (m <sup>3</sup> g <sup>-1</sup> )	
		$R_v^2$	$R_h^2$	$R_v^2$	$R_h^2$	$R_v^2$	$R_h^2$	$R_v^2$	$R_h^2$	$R_v^2$	$R_h^2$		
$X_c$ (%) $* \rho^{-1}$ (cm <sup>3</sup> g <sup>-1</sup> )	d <sub>50</sub> (μm)	0.70	0.92	0.75	0.92	0.26	0.02	0.75	0.90	0.03	0.81	0.03	0.81
	d <sub>50</sub> <sup>-1</sup> (μm <sup>-1</sup> )	0.59	0.91	0.65	0.91	0.23	0.03	0.65	0.89	0.02	0.80	0.02	0.80
	T <sub>m</sub> (K)	0.54	0.89	0.59	0.89	0.22	0.03	0.59	0.87	0.02	0.79	0.02	0.79
	T <sub>m</sub> <sup>-1</sup> (K <sup>-1</sup> )	0.75	0.94	0.80	0.94	0.27	0.02	0.80	0.92	0.04	0.82	0.03	0.82
	T <sub>g</sub> (K)	0.54	0.87	0.57	0.87	0.20	0.02	0.57	0.85	0.03	0.77	0.03	0.77
	T <sub>g</sub> <sup>-1</sup> (K <sup>-1</sup> )	0.48	0.87	0.54	0.87	0.19	0.03	0.53	0.85	0.02	0.77	0.02	0.77
	SA (m <sup>2</sup> g <sup>-1</sup> )	0.02	0.50	0.03	0.50	0.02	0.03	0.03	0.49	0.00	0.45	0.00	0.45
	SA <sup>-1</sup> (g m <sup>-2</sup> )	0.71	0.88	0.75	0.88	0.23	0.01	0.74	0.86	0.04	0.76	0.04	0.76
	Vp (cm <sup>3</sup> g <sup>-1</sup> )	0.02	0.50	0.03	0.50	0.02	0.03	0.03	0.49	0.00	0.46	0.00	0.46
	Vp <sup>-1</sup> (g cm <sup>-3</sup> )	0.70	0.88	0.74	0.88	0.22	0.01	0.73	0.86	0.04	0.76	0.04	0.76
$\sum SFE$ (mN m <sup>-1</sup> )	0.84	0.90	0.86	0.90	0.26	0.01	0.85	0.88	0.06	0.77	0.06	0.77	
	$\sum SFE^{-1}$ (m Nm <sup>-1</sup> )	0.17	0.74	0.20	0.74	0.09	0.03	0.20	0.73	0.00	0.67	0.00	0.67

Table A7.45: Calculation of  $R_h^2$  and  $R_v^2$  with the matrix of two PAH properties ( $\log K_{hdw}$ ,  $\log C_w^{sat}$ ) multiplied with three plastic properties ( $X_c * \rho^{-1}$  as fixed parameters) and the  $\log K_{p-w}$  matrix

plastic property product		PAH properties											
1 <sup>st</sup> * 2 <sup>nd</sup> fixed parameter	3 <sup>rd</sup> variable parameter	$\log K_{hdw}$ (-)		$\log C_w^{sat}$ (mol m <sup>-3</sup> )		$\log K_{hdw} * \log C_w^{sat}$ (mol m <sup>-3</sup> )		$\log C_w^{sat} * \log K_{hdw}^{-1}$ (mol m <sup>-3</sup> )		$\log K_{hdw} * \log C_w^{sat-1}$ (m <sup>3</sup> mol <sup>-1</sup> )		$(\log K_{hdw} * \log C_w^{sat})^{-1}$ (m <sup>3</sup> mol <sup>-1</sup> )	
		$R_v^2$	$R_h^2$	$R_v^2$	$R_h^2$	$R_v^2$	$R_h^2$	$R_v^2$	$R_h^2$	$R_v^2$	$R_h^2$		
$X_c$ (%) $* \rho^{-1}$ (cm <sup>3</sup> g <sup>-1</sup> )	d <sub>50</sub> (μm)	0.70	0.93	0.75	0.92	0.75	0.93	0.75	0.90	0.03	0.81	0.03	0.81
	d <sub>50</sub> <sup>-1</sup> (μm <sup>-1</sup> )	0.59	0.91	0.65	0.91	0.65	0.92	0.65	0.89	0.02	0.80	0.02	0.80
	T <sub>m</sub> (K)	0.54	0.90	0.59	0.89	0.59	0.90	0.59	0.87	0.02	0.79	0.02	0.79
	T <sub>m</sub> <sup>-1</sup> (K <sup>-1</sup> )	0.74	0.94	0.80	0.94	0.80	0.95	0.80	0.92	0.04	0.82	0.03	0.82
	T <sub>g</sub> (K)	0.54	0.87	0.57	0.87	0.58	0.88	0.57	0.85	0.03	0.77	0.03	0.77
	T <sub>g</sub> <sup>-1</sup> (K <sup>-1</sup> )	0.48	0.87	0.54	0.87	0.54	0.88	0.53	0.85	0.02	0.77	0.02	0.77
	SA (m <sup>2</sup> g <sup>-1</sup> )	0.02	0.50	0.03	0.50	0.03	0.50	0.03	0.49	0.00	0.45	0.00	0.45
	SA <sup>-1</sup> (g m <sup>-2</sup> )	0.70	0.89	0.75	0.88	0.75	0.90	0.74	0.86	0.04	0.76	0.04	0.76
	Vp (cm <sup>3</sup> g <sup>-1</sup> )	0.02	0.50	0.03	0.50	0.03	0.50	0.03	0.49	0.00	0.46	0.00	0.46
	Vp <sup>-1</sup> (g cm <sup>-3</sup> )	0.69	0.89	0.74	0.88	0.74	0.90	0.73	0.86	0.04	0.76	0.04	0.76
$\sum SFE$ (mN m <sup>-1</sup> )	0.83	0.91	0.86	0.90	0.86	0.92	0.85	0.88	0.06	0.77	0.06	0.77	
	$\sum SFE^{-1}$ (m Nm <sup>-1</sup> )	0.16	0.74	0.20	0.74	0.19	0.74	0.20	0.73	0.00	0.67	0.00	0.67

Table A7.46: Calculation of  $R_h^2$  and  $R_v^2$  with the matrix of two PAH properties ( $\log K_{ow}$ , MW<sub>w</sub>) multiplied with three plastic properties ( $X_c * d_{50}$  as fixed parameters) and the  $\log K_{p-w}$  matrix

plastic property product		PAH properties											
1 <sup>st</sup> * 2 <sup>nd</sup> fixed parameter	3 <sup>rd</sup> variable parameter	$\log K_{ow}$ (-)		MW (g mol <sup>-1</sup> )		$\log K_{ow} * MW$ (g mol <sup>-1</sup> )		$MW * \log K_{ow}^{-1}$ (g mol <sup>-1</sup> )		$\log K_{ow} * MW^{-1}$ (mol g <sup>-1</sup> )		$(\log K_{ow} * MW)^{-1}$ (mol g <sup>-1</sup> )	
		$R_v^2$	$R_h^2$	$R_v^2$	$R_h^2$	$R_v^2$	$R_h^2$	$R_v^2$	$R_h^2$	$R_v^2$	$R_h^2$		
$X_c$ (%) * $d_{50}$ ( $\mu m$ )	T <sub>m</sub> (K)	0.77	0.93	0.78	0.92	0.82	0.93	0.71	0.86	0.69	0.86	0.50	0.90
	T <sub>m</sub> <sup>-1</sup> (K <sup>-1</sup> )	0.88	0.95	0.89	0.94	0.93	0.95	0.82	0.88	0.79	0.87	0.58	0.91
	T <sub>g</sub> (K)	0.63	0.87	0.64	0.87	0.67	0.88	0.59	0.81	0.57	0.81	0.42	0.84
	T <sub>g</sub> <sup>-1</sup> (K <sup>-1</sup> )	0.77	0.95	0.78	0.94	0.83	0.95	0.72	0.88	0.69	0.88	0.50	0.92
	SA (m <sup>2</sup> g <sup>-1</sup> )	0.04	0.54	0.04	0.54	0.04	0.54	0.04	0.51	0.03	0.51	0.02	0.53
	SA <sup>-1</sup> (g m <sup>-2</sup> )	0.76	0.87	0.77	0.86	0.81	0.88	0.71	0.80	0.68	0.79	0.51	0.83
	V <sub>p</sub> (cm <sup>3</sup> g <sup>-1</sup> )	0.04	0.54	0.04	0.54	0.05	0.54	0.04	0.52	0.04	0.52	0.03	0.53
	V <sub>p</sub> <sup>-1</sup> (g cm <sup>-3</sup> )	0.76	0.87	0.77	0.87	0.81	0.88	0.71	0.80	0.69	0.80	0.51	0.84
	Σ SFE (mN m <sup>-1</sup> )	0.69	0.81	0.70	0.81	0.73	0.82	0.65	0.74	0.63	0.74	0.47	0.78
	Σ SFE <sup>-1</sup> (m Nm <sup>-1</sup> )	0.30	0.82	0.30	0.82	0.32	0.82	0.27	0.78	0.26	0.77	0.18	0.80

Table A7.47: Calculation of  $R_h^2$  and  $R_v^2$  with the matrix of two PAH properties ( $\log K_{ow}$ ,  $\log K_{hdw}$ ) multiplied with three plastic properties ( $X_c * d_{50}$  as fixed parameters) and the  $\log K_{p-w}$  matrix

plastic property product		PAH properties											
1 <sup>st</sup> * 2 <sup>nd</sup> fixed parameter	3 <sup>rd</sup> variable parameter	$\log K_{ow}$ (-)		$\log K_{hdw}$ (-)		$\log K_{ow} * \log K_{hdw}$ (-)		$\log K_{hdw} * \log K_{ow}^{-1}$ (-)		$\log K_{ow} * \log K_{hdw}^{-1}$ (-)			
		$R_v^2$	$R_h^2$	$R_v^2$	$R_h^2$	$R_v^2$	$R_h^2$	$R_v^2$	$R_h^2$	$R_v^2$	$R_h^2$		
$X_c$ (%) * $d_{50}$ ( $\mu m$ )	T <sub>m</sub> (K)	0.77	0.93	0.78	0.92	0.82	0.93	0.71	0.86	0.69	0.86	0.50	0.90
	T <sub>m</sub> <sup>-1</sup> (K <sup>-1</sup> )	0.88	0.95	0.89	0.94	0.93	0.95	0.82	0.88	0.79	0.87	0.58	0.91
	T <sub>g</sub> (K)	0.63	0.87	0.64	0.87	0.67	0.88	0.59	0.81	0.57	0.81	0.42	0.84
	T <sub>g</sub> <sup>-1</sup> (K <sup>-1</sup> )	0.77	0.95	0.78	0.94	0.83	0.95	0.72	0.88	0.69	0.88	0.50	0.92
	SA (m <sup>2</sup> g <sup>-1</sup> )	0.04	0.54	0.04	0.54	0.04	0.54	0.04	0.51	0.03	0.51	0.02	0.53
	SA <sup>-1</sup> (g m <sup>-2</sup> )	0.76	0.87	0.77	0.86	0.81	0.88	0.71	0.80	0.68	0.79	0.51	0.83
	V <sub>p</sub> (cm <sup>3</sup> g <sup>-1</sup> )	0.04	0.54	0.04	0.54	0.05	0.54	0.04	0.52	0.04	0.52	0.03	0.53
	V <sub>p</sub> <sup>-1</sup> (g cm <sup>-3</sup> )	0.76	0.87	0.77	0.87	0.81	0.88	0.71	0.80	0.69	0.80	0.51	0.84
	Σ SFE (mN m <sup>-1</sup> )	0.69	0.81	0.70	0.81	0.73	0.82	0.65	0.74	0.63	0.74	0.47	0.78
	Σ SFE <sup>-1</sup> (m Nm <sup>-1</sup> )	0.30	0.82	0.30	0.82	0.32	0.82	0.27	0.78	0.26	0.77	0.18	0.80

Table A7.48: Calculation of  $R_h^2$  and  $R_v^2$  with the matrix of two PAH properties ( $\log K_{ow}$ ,  $\log C_w^{sat}$ ) multiplied with three plastic properties ( $X_c * d_{50}$  as fixed parameters) and the  $\log K_{p-w}$  matrix

plastic property product		PAH properties											
1 <sup>st</sup> * 2 <sup>nd</sup> fixed parameter	3 <sup>rd</sup> variable parameter	$\log K_{ow}$ (-)		$\log C_w^{sat}$ (mol m <sup>-3</sup> )		$\log K_{ow} * \log C_w^{sat}$ (mol m <sup>-3</sup> )		$\log C_w^{sat} * \log K_{ow}^{-1}$ (mol m <sup>-3</sup> )		$\log K_{ow} * \log C_w^{sat-1}$ (m <sup>3</sup> mol <sup>-1</sup> )		$(\log K_{ow} * \log C_w^{sat})^{-1}$ (m <sup>3</sup> mol <sup>-1</sup> )	
		$R_v^2$	$R_h^2$	$R_v^2$	$R_h^2$	$R_v^2$	$R_h^2$	$R_v^2$	$R_h^2$	$R_v^2$	$R_h^2$		
$X_c$ (%) * $d_{50}$ ( $\mu m$ )	T <sub>m</sub> (K)	0.77	0.93	0.82	0.92	0.82	0.94	0.81	0.90	0.05	0.81	0.04	0.81
	T <sub>m</sub> <sup>-1</sup> (K <sup>-1</sup> )	0.88	0.95	0.92	0.94	0.93	0.96	0.92	0.92	0.06	0.82	0.05	0.82
	T <sub>g</sub> (K)	0.63	0.87	0.65	0.87	0.65	0.88	0.65	0.85	0.05	0.76	0.04	0.76
	T <sub>g</sub> <sup>-1</sup> (K <sup>-1</sup> )	0.77	0.95	0.84	0.94	0.84	0.96	0.83	0.92	0.04	0.82	0.04	0.82
	SA (m <sup>2</sup> g <sup>-1</sup> )	0.04	0.54	0.04	0.54	0.04	0.54	0.04	0.53	0.00	0.49	0.00	0.49
	SA <sup>-1</sup> (g m <sup>-2</sup> )	0.76	0.87	0.79	0.86	0.80	0.88	0.79	0.84	0.05	0.74	0.05	0.74
	V <sub>p</sub> (cm <sup>3</sup> g <sup>-1</sup> )	0.04	0.54	0.05	0.54	0.05	0.54	0.05	0.53	0.00	0.49	0.00	0.49
	V <sub>p</sub> <sup>-1</sup> (g cm <sup>-3</sup> )	0.76	0.87	0.80	0.87	0.80	0.88	0.79	0.85	0.05	0.74	0.05	0.74
	Σ SFE (mN m <sup>-1</sup> )	0.69	0.81	0.70	0.81	0.70	0.82	0.69	0.79	0.06	0.69	0.06	0.69
	Σ SFE <sup>-1</sup> (m Nm <sup>-1</sup> )	0.30	0.82	0.34	0.82	0.34	0.83	0.34	0.81	0.01	0.73	0.01	0.73

Table A7.49: Calculation of  $R_h^2$  and  $R_v^2$  with the matrix of two PAH properties (MW,  $\log K_{\text{hdw}}$ ) multiplied with three plastic properties ( $X_c * d_{50}$  as fixed parameters) and the  $\log K_{\text{p-w}}$  matrix

1 <sup>st</sup> * 2 <sup>nd</sup> fixed parameter	3 <sup>rd</sup> variable parameter	PAH properties											
		MW (g mol <sup>-1</sup> )		$\log K_{\text{hdw}}$ (-)		MW * $\log K_{\text{hdw}}$ (g mol <sup>-1</sup> )		MW * $\log K_{\text{hdw}}^{-1}$ (g mol <sup>-1</sup> )		$\log K_{\text{hdw}} * MW^{-1}$ (mol g <sup>-1</sup> )		$(MW * \log K_{\text{hdw}})^{-1}$ (mol g <sup>-1</sup> )	
		$R_v^2$	$R_h^2$	$R_v^2$	$R_h^2$	$R_v^2$	$R_h^2$	$R_v^2$	$R_h^2$	$R_v^2$	$R_h^2$		
$X_c$ (%) * $d_{50}$ ( $\mu\text{m}$ )	T <sub>m</sub> (K)	0.78	0.92	0.77	0.93	0.30	0.22	0.70	0.78	0.71	0.78	0.49	0.90
	T <sub>m</sub> <sup>-1</sup> (K <sup>-1</sup> )	0.89	0.94	0.88	0.95	0.33	0.24	0.80	0.79	0.81	0.79	0.57	0.91
	T <sub>g</sub> (K)	0.64	0.87	0.63	0.87	0.24	0.22	0.57	0.73	0.58	0.73	0.41	0.84
	T <sub>g</sub> <sup>-1</sup> (K <sup>-1</sup> )	0.78	0.94	0.78	0.95	0.29	0.23	0.70	0.80	0.71	0.80	0.49	0.91
	SA (m <sup>2</sup> g <sup>-1</sup> )	0.04	0.54	0.04	0.54	0.02	0.10	0.04	0.47	0.04	0.47	0.02	0.53
	SA <sup>-1</sup> (g m <sup>-2</sup> )	0.77	0.86	0.76	0.87	0.27	0.25	0.69	0.71	0.70	0.71	0.50	0.83
	V <sub>p</sub> (cm <sup>3</sup> g <sup>-1</sup> )	0.04	0.54	0.04	0.54	0.02	0.10	0.04	0.48	0.04	0.48	0.03	0.53
	V <sub>p</sub> <sup>-1</sup> (g cm <sup>-3</sup> )	0.77	0.87	0.77	0.87	0.27	0.25	0.69	0.71	0.70	0.71	0.50	0.84
	$\sum SFE$ (mN m <sup>-1</sup> )	0.70	0.81	0.69	0.81	0.24	0.24	0.63	0.66	0.64	0.66	0.46	0.78
	$\sum SFE^{-1}$ (m Nm <sup>-1</sup> )	0.30	0.82	0.30	0.82	0.13	0.17	0.26	0.71	0.27	0.71	0.18	0.80

Table A7.50: Calculation of  $R_h^2$  and  $R_v^2$  with the matrix of two PAH properties (MW,  $\log C_w^{\text{sat}}$ ) multiplied with three plastic properties ( $X_c * d_{50}$  as fixed parameters) and the  $\log K_{\text{p-w}}$  matrix

1 <sup>st</sup> * 2 <sup>nd</sup> fixed parameter	3 <sup>rd</sup> variable parameter	PAH properties											
		MW (g mol <sup>-1</sup> )		$\log C_w^{\text{sat}}$ (mol m <sup>-3</sup> )		MW * $\log C_w^{\text{sat}}$ (g m <sup>-3</sup> )		$\log C_w^{\text{sat}} * MW^{-1}$ (mol <sup>2</sup> m <sup>-3</sup> g <sup>-1</sup> )		MW * $\log C_w^{\text{sat}-1}$ (g m <sup>3</sup> mol <sup>-2</sup> )		$(\log K_{\text{ow}} * \log C_w^{\text{sat}})^{-1}$ (m <sup>3</sup> g <sup>-1</sup> )	
		$R_v^2$	$R_h^2$	$R_v^2$	$R_h^2$	$R_v^2$	$R_h^2$	$R_v^2$	$R_h^2$	$R_v^2$	$R_h^2$		
$X_c$ (%) * $d_{50}$ ( $\mu\text{m}$ )	T <sub>m</sub> (K)	0.78	0.92	0.82	0.92	0.27	0.02	0.81	0.90	0.05	0.81	0.04	0.81
	T <sub>m</sub> <sup>-1</sup> (K <sup>-1</sup> )	0.89	0.94	0.92	0.94	0.29	0.02	0.92	0.92	0.06	0.82	0.05	0.82
	T <sub>g</sub> (K)	0.64	0.87	0.65	0.87	0.21	0.02	0.65	0.85	0.05	0.76	0.04	0.76
	T <sub>g</sub> <sup>-1</sup> (K <sup>-1</sup> )	0.78	0.94	0.84	0.94	0.27	0.02	0.83	0.92	0.04	0.82	0.04	0.82
	SA (m <sup>2</sup> g <sup>-1</sup> )	0.04	0.54	0.04	0.54	0.03	0.03	0.04	0.53	0.00	0.49	0.00	0.49
	SA <sup>-1</sup> (g m <sup>-2</sup> )	0.77	0.86	0.79	0.86	0.23	0.01	0.79	0.84	0.05	0.74	0.05	0.74
	V <sub>p</sub> (cm <sup>3</sup> g <sup>-1</sup> )	0.04	0.54	0.05	0.54	0.03	0.03	0.05	0.53	0.00	0.49	0.00	0.49
	V <sub>p</sub> <sup>-1</sup> (g cm <sup>-3</sup> )	0.77	0.87	0.80	0.87	0.23	0.01	0.79	0.84	0.05	0.74	0.05	0.74
	$\sum SFE$ (mN m <sup>-1</sup> )	0.70	0.81	0.70	0.81	0.20	0.01	0.69	0.78	0.06	0.69	0.06	0.69
	$\sum SFE^{-1}$ (m Nm <sup>-1</sup> )	0.30	0.82	0.34	0.82	0.14	0.03	0.34	0.80	0.01	0.73	0.01	0.73

Table A7.51: Calculation of  $R_h^2$  and  $R_v^2$  with the matrix of two PAH properties ( $\log K_{\text{hdw}}$ ,  $\log C_w^{\text{sat}}$ ) multiplied with three plastic properties ( $X_c * d_{50}$  as fixed parameters) and the  $\log K_{\text{p-w}}$  matrix

1 <sup>st</sup> * 2 <sup>nd</sup> fixed parameter	3 <sup>rd</sup> variable parameter	PAH properties											
		$\log K_{\text{hdw}}$ (-)		$\log C_w^{\text{sat}}$ (mol m <sup>-3</sup> )		$\log K_{\text{hdw}} * \log C_w^{\text{sat}}$ (mol m <sup>-3</sup> )		$\log C_w^{\text{sat}} * \log K_{\text{hdw}}^{-1}$ (mol m <sup>-3</sup> )		$\log K_{\text{hdw}} * \log C_w^{\text{sat}-1}$ (m <sup>3</sup> mol <sup>-1</sup> )		$(\log K_{\text{hdw}} * \log C_w^{\text{sat}})^{-1}$ (m <sup>3</sup> mol <sup>-1</sup> )	
		$R_v^2$	$R_h^2$	$R_v^2$	$R_h^2$	$R_v^2$	$R_h^2$	$R_v^2$	$R_h^2$	$R_v^2$	$R_h^2$		
$X_c$ (%) * $d_{50}$ ( $\mu\text{m}$ )	T <sub>m</sub> (K)	0.77	0.93	0.82	0.92	0.82	0.94	0.81	0.90	0.05	0.81	0.04	0.81
	T <sub>m</sub> <sup>-1</sup> (K <sup>-1</sup> )	0.88	0.95	0.92	0.94	0.93	0.96	0.92	0.92	0.06	0.82	0.05	0.82
	T <sub>g</sub> (K)	0.63	0.87	0.65	0.87	0.65	0.88	0.65	0.85	0.05	0.76	0.04	0.76
	T <sub>g</sub> <sup>-1</sup> (K <sup>-1</sup> )	0.78	0.95	0.84	0.94	0.84	0.96	0.83	0.92	0.04	0.82	0.04	0.82
	SA (m <sup>2</sup> g <sup>-1</sup> )	0.04	0.54	0.04	0.54	0.04	0.54	0.04	0.53	0.00	0.49	0.00	0.49
	SA <sup>-1</sup> (g m <sup>-2</sup> )	0.76	0.87	0.79	0.86	0.80	0.88	0.79	0.84	0.05	0.74	0.05	0.74
	V <sub>p</sub> (cm <sup>3</sup> g <sup>-1</sup> )	0.04	0.54	0.05	0.54	0.05	0.54	0.05	0.53	0.00	0.49	0.00	0.49
	V <sub>p</sub> <sup>-1</sup> (g cm <sup>-3</sup> )	0.77	0.87	0.80	0.87	0.80	0.89	0.79	0.84	0.05	0.74	0.05	0.74
	$\sum SFE$ (mN m <sup>-1</sup> )	0.69	0.81	0.70	0.81	0.71	0.83	0.69	0.78	0.06	0.69	0.06	0.69
	$\sum SFE^{-1}$ (m Nm <sup>-1</sup> )	0.30	0.82	0.34	0.82	0.34	0.83	0.34	0.80	0.01	0.73	0.01	0.73

Table A7.52: Calculation of  $R_h^2$  and  $R_v^2$  with the matrix of two PAH properties ( $\log K_{ow}$ , MW,) multiplied with three plastic properties ( $X_c * d_{50}^{-1}$  as fixed parameters) and the  $\log K_{p-w}$  matrix

plastic property product		PAH properties											
1 <sup>st</sup> * 2 <sup>nd</sup> fixed parameter	3 <sup>rd</sup> variable parameter	log $K_{ow}$ (-)		MW (g mol <sup>-1</sup> )		$\log K_{ow} * MW$ (g mol <sup>-1</sup> )		MW * $\log K_{ow}^{-1}$ (g mol <sup>-1</sup> )		$\log K_{ow} * MW^{-1}$ (mol g <sup>-1</sup> )		$(\log K_{ow} * MW)^{-1}$ (mol g <sup>-1</sup> )	
		$R_v^2$	$R_h^2$	$R_v^2$	$R_h^2$	$R_v^2$	$R_h^2$	$R_v^2$	$R_h^2$	$R_v^2$	$R_h^2$	$R_v^2$	$R_h^2$
$X_c$ (%) * $d_{50}^{-1}$ ( $\mu m^{-1}$ )	T <sub>m</sub> (K)	0.73	0.94	0.74	0.94	0.78	0.95	0.68	0.88	0.65	0.87	0.47	0.91
	T <sub>m</sub> <sup>-1</sup> (K <sup>-1</sup> )	0.83	0.96	0.84	0.95	0.88	0.96	0.77	0.89	0.74	0.88	0.54	0.92
	T <sub>g</sub> (K)	0.75	0.92	0.76	0.92	0.80	0.93	0.70	0.86	0.68	0.85	0.50	0.89
	T <sub>g</sub> <sup>-1</sup> (K <sup>-1</sup> )	0.56	0.89	0.57	0.89	0.61	0.90	0.52	0.83	0.50	0.83	0.35	0.86
	SA (m <sup>2</sup> g <sup>-1</sup> )	0.06	0.59	0.06	0.58	0.07	0.59	0.06	0.56	0.05	0.56	0.04	0.57
	SA <sup>-1</sup> (g m <sup>-2</sup> )	0.72	0.88	0.73	0.87	0.77	0.88	0.67	0.81	0.65	0.80	0.47	0.84
	V <sub>p</sub> (cm <sup>3</sup> g <sup>-1</sup> )	0.06	0.59	0.07	0.59	0.07	0.59	0.06	0.56	0.06	0.56	0.04	0.58
	V <sub>p</sub> <sup>-1</sup> (g cm <sup>-3</sup> )	0.71	0.88	0.72	0.87	0.76	0.88	0.66	0.81	0.64	0.80	0.46	0.84
	Σ SFE (mN m <sup>-1</sup> )	0.78	0.87	0.79	0.86	0.83	0.87	0.73	0.79	0.71	0.79	0.53	0.83
	Σ SFE <sup>-1</sup> (m Nm <sup>-1</sup> )	0.25	0.79	0.25	0.79	0.27	0.80	0.23	0.75	0.22	0.75	0.15	0.77

Table A7.53: Calculation of  $R_h^2$  and  $R_v^2$  with the matrix of two PAH properties ( $\log K_{ow}$ ,  $\log K_{hdw}$ ) multiplied with three plastic properties ( $X_c * d_{50}^{-1}$  as fixed parameters) and the  $\log K_{p-w}$  matrix

plastic property product		PAH properties											
1 <sup>st</sup> * 2 <sup>nd</sup> fixed parameter	3 <sup>rd</sup> variable parameter	log $K_{ow}$ (-)		log $K_{hdw}$ (-)		$\log K_{ow} * \log K_{hdw}$ (-)		$\log K_{hdw} * \log K_{ow}^{-1}$ (-)		$\log K_{ow} * \log K_{hdw}^{-1}$ (-)		$(\log K_{ow} * \log K_{hdw})^{-1}$ (-)	
		$R_v^2$	$R_h^2$	$R_v^2$	$R_h^2$	$R_v^2$	$R_h^2$	$R_v^2$	$R_h^2$	$R_v^2$	$R_h^2$	$R_v^2$	$R_h^2$
$X_c$ (%) * $d_{50}^{-1}$ ( $\mu m^{-1}$ )	T <sub>m</sub> (K)	0.73	0.94	0.74	0.94	0.78	0.95	0.68	0.88	0.65	0.87	0.47	0.91
	T <sub>m</sub> <sup>-1</sup> (K <sup>-1</sup> )	0.83	0.96	0.84	0.95	0.88	0.96	0.77	0.89	0.74	0.88	0.54	0.92
	T <sub>g</sub> (K)	0.75	0.92	0.76	0.92	0.80	0.93	0.70	0.86	0.68	0.85	0.50	0.89
	T <sub>g</sub> <sup>-1</sup> (K <sup>-1</sup> )	0.56	0.89	0.57	0.89	0.61	0.90	0.52	0.83	0.50	0.83	0.35	0.86
	SA (m <sup>2</sup> g <sup>-1</sup> )	0.06	0.59	0.06	0.58	0.07	0.59	0.06	0.56	0.05	0.56	0.04	0.57
	SA <sup>-1</sup> (g m <sup>-2</sup> )	0.72	0.88	0.73	0.87	0.77	0.88	0.67	0.81	0.65	0.80	0.47	0.84
	V <sub>p</sub> (cm <sup>3</sup> g <sup>-1</sup> )	0.06	0.59	0.07	0.59	0.07	0.59	0.06	0.56	0.06	0.56	0.04	0.58
	V <sub>p</sub> <sup>-1</sup> (g cm <sup>-3</sup> )	0.71	0.88	0.72	0.87	0.76	0.88	0.66	0.81	0.64	0.80	0.46	0.84
	Σ SFE (mN m <sup>-1</sup> )	0.78	0.87	0.79	0.86	0.83	0.87	0.73	0.79	0.71	0.79	0.53	0.83
	Σ SFE <sup>-1</sup> (m Nm <sup>-1</sup> )	0.25	0.79	0.25	0.79	0.27	0.80	0.23	0.75	0.22	0.75	0.15	0.77

Table A7.54: Calculation of  $R_h^2$  and  $R_v^2$  with the matrix of two PAH properties ( $\log K_{ow}$ ,  $\log C_w^{sat}$ ) multiplied with three plastic properties ( $X_c * d_{50}^{-1}$  as fixed parameters) and the  $\log K_{p-w}$  matrix

plastic property product		PAH properties											
1 <sup>st</sup> * 2 <sup>nd</sup> fixed parameter	3 <sup>rd</sup> variable parameter	log $K_{ow}$ (-)		log $C_w^{sat}$ (mol m <sup>-3</sup> )		$\log K_{ow} * \log C_w^{sat}$ (mol m <sup>-3</sup> )		$\log C_w^{sat} * \log K_{ow}^{-1}$ (mol m <sup>-3</sup> )		$\log K_{ow} * \log C_w^{sat-1}$ (m <sup>3</sup> mol <sup>-1</sup> )		$(\log K_{ow} * \log C_w^{sat})^{-1}$ (m <sup>3</sup> mol <sup>-1</sup> )	
		$R_v^2$	$R_h^2$	$R_v^2$	$R_h^2$	$R_v^2$	$R_h^2$	$R_v^2$	$R_h^2$	$R_v^2$	$R_h^2$	$R_v^2$	$R_h^2$
$X_c$ (%) * $d_{50}^{-1}$ ( $\mu m^{-1}$ )	T <sub>m</sub> (K)	0.73	0.94	0.79	0.94	0.80	0.95	0.79	0.92	0.04	0.82	0.03	0.82
	T <sub>m</sub> <sup>-1</sup> (K <sup>-1</sup> )	0.83	0.96	0.89	0.95	0.89	0.96	0.88	0.93	0.05	0.83	0.04	0.83
	T <sub>g</sub> (K)	0.75	0.92	0.80	0.92	0.80	0.93	0.79	0.90	0.05	0.80	0.04	0.80
	T <sub>g</sub> <sup>-1</sup> (K <sup>-1</sup> )	0.56	0.89	0.63	0.89	0.63	0.90	0.62	0.87	0.02	0.78	0.02	0.78
	SA (m <sup>2</sup> g <sup>-1</sup> )	0.06	0.59	0.07	0.58	0.07	0.59	0.07	0.58	0.00	0.53	0.00	0.53
	SA <sup>-1</sup> (g m <sup>-2</sup> )	0.72	0.88	0.77	0.87	0.77	0.89	0.76	0.85	0.04	0.75	0.04	0.75
	V <sub>p</sub> (cm <sup>3</sup> g <sup>-1</sup> )	0.06	0.59	0.07	0.59	0.07	0.59	0.07	0.58	0.00	0.53	0.00	0.53
	V <sub>p</sub> <sup>-1</sup> (g cm <sup>-3</sup> )	0.71	0.88	0.76	0.87	0.76	0.89	0.75	0.85	0.04	0.75	0.04	0.75
	Σ SFE (mN m <sup>-1</sup> )	0.78	0.87	0.80	0.86	0.81	0.88	0.80	0.84	0.06	0.73	0.06	0.73
	Σ SFE <sup>-1</sup> (m Nm <sup>-1</sup> )	0.25	0.79	0.29	0.79	0.29	0.80	0.29	0.78	0.00	0.71	0.00	0.71

Table A7.55: Calculation of  $R_h^2$  and  $R_v^2$  with the matrix of two PAH properties (MW,  $\log K_{hdw}$ ) multiplied with three plastic properties ( $X_c * d_{50}^{-1}$  as fixed parameters) and the  $\log K_{p-w}$  matrix

plastic property product		PAH properties											
1 <sup>st</sup> * 2 <sup>nd</sup> fixed parameter	3 <sup>rd</sup> variable parameter	MW (g mol <sup>-1</sup> )		$\log K_{hdw}$ (-)		MW * $\log K_{hdw}$ (g mol <sup>-1</sup> )		MW * $\log K_{hdw}^{-1}$ (g mol <sup>-1</sup> )		$\log K_{hdw} * MW^1$ (mol g <sup>-1</sup> )		$(MW * \log K_{hdw})^{-1}$ (mol g <sup>-1</sup> )	
		$R_v^2$	$R_h^2$	$R_v^2$	$R_h^2$	$R_v^2$	$R_h^2$	$R_v^2$	$R_h^2$	$R_v^2$	$R_h^2$	$R_v^2$	$R_h^2$
$X_c (\%) * d_{50}^{-1} (\mu\text{m}^{-1})$	T <sub>m</sub> (K)	0.74	0.94	0.74	0.94	0.28	0.22	0.66	0.80	0.67	0.80	0.46	0.91
	T <sub>m</sub> <sup>-1</sup> (K <sup>-1</sup> )	0.84	0.95	0.83	0.96	0.31	0.24	0.75	0.80	0.76	0.80	0.52	0.92
	T <sub>g</sub> (K)	0.76	0.92	0.76	0.92	0.29	0.22	0.68	0.77	0.70	0.77	0.49	0.89
	T <sub>g</sub> <sup>-1</sup> (K <sup>-1</sup> )	0.57	0.89	0.57	0.89	0.21	0.21	0.51	0.75	0.52	0.75	0.35	0.86
	SA (m <sup>2</sup> g <sup>-1</sup> )	0.06	0.58	0.06	0.59	0.03	0.11	0.05	0.52	0.05	0.52	0.04	0.57
	SA <sup>-1</sup> (g m <sup>-2</sup> )	0.73	0.87	0.73	0.88	0.26	0.24	0.65	0.72	0.66	0.72	0.46	0.84
	V <sub>p</sub> (cm <sup>3</sup> g <sup>-1</sup> )	0.07	0.59	0.06	0.59	0.03	0.11	0.06	0.52	0.06	0.52	0.04	0.58
	V <sub>p</sub> <sup>-1</sup> (g cm <sup>-3</sup> )	0.72	0.87	0.72	0.88	0.25	0.24	0.65	0.72	0.66	0.72	0.46	0.84
	Σ SFE (mN m <sup>-1</sup> )	0.79	0.86	0.79	0.87	0.28	0.25	0.71	0.71	0.72	0.71	0.52	0.83
	Σ SFE <sup>-1</sup> (m Nm <sup>-1</sup> )	0.25	0.79	0.25	0.79	0.10	0.16	0.22	0.69	0.22	0.69	0.14	0.77

Table A7.56: Calculation of  $R_h^2$  and  $R_v^2$  with the matrix of two PAH properties (MW,  $\log C_w^{\text{sat}}$ ) multiplied with three plastic properties ( $X_c * d_{50}^{-1}$  as fixed parameters) and the  $\log K_{p-w}$  matrix

plastic property product		PAH properties											
1 <sup>st</sup> * 2 <sup>nd</sup> fixed parameter	3 <sup>rd</sup> variable parameter	MW (g mol <sup>-1</sup> )		$\log C_w^{\text{sat}}$ (mol m <sup>-3</sup> )		MW * $\log C_w^{\text{sat}}$ (g m <sup>-3</sup> )		$\log C_w^{\text{sat}} * MW^1$ (mol <sup>2</sup> m <sup>-3</sup> g <sup>-1</sup> )		$MW * \log C_w^{\text{sat}-1}$ (g m <sup>3</sup> mol <sup>-2</sup> )		$(\log K_{ow} * \log C_w^{\text{sat}})^{-1}$ (m <sup>3</sup> g <sup>-1</sup> )	
		$R_v^2$	$R_h^2$	$R_v^2$	$R_h^2$	$R_v^2$	$R_h^2$	$R_v^2$	$R_h^2$	$R_v^2$	$R_h^2$	$R_v^2$	$R_h^2$
$X_c (\%) * d_{50}^{-1} (\mu\text{m}^{-1})$	T <sub>m</sub> (K)	0.74	0.94	0.79	0.94	0.27	0.02	0.79	0.92	0.04	0.82	0.03	0.82
	T <sub>m</sub> <sup>-1</sup> (K <sup>-1</sup> )	0.84	0.95	0.89	0.95	0.29	0.02	0.88	0.93	0.05	0.83	0.04	0.83
	T <sub>g</sub> (K)	0.76	0.92	0.80	0.92	0.26	0.02	0.79	0.89	0.05	0.80	0.04	0.80
	T <sub>g</sub> <sup>-1</sup> (K <sup>-1</sup> )	0.57	0.89	0.63	0.89	0.21	0.02	0.62	0.87	0.02	0.78	0.02	0.78
	SA (m <sup>2</sup> g <sup>-1</sup> )	0.06	0.58	0.07	0.58	0.04	0.03	0.07	0.58	0.00	0.53	0.00	0.53
	SA <sup>-1</sup> (g m <sup>-2</sup> )	0.73	0.87	0.77	0.87	0.23	0.01	0.76	0.85	0.05	0.75	0.04	0.75
	V <sub>p</sub> (cm <sup>3</sup> g <sup>-1</sup> )	0.07	0.59	0.07	0.59	0.04	0.03	0.07	0.58	0.00	0.53	0.00	0.53
	V <sub>p</sub> <sup>-1</sup> (g cm <sup>-3</sup> )	0.72	0.87	0.76	0.87	0.23	0.01	0.75	0.85	0.04	0.75	0.04	0.75
	Σ SFE (mN m <sup>-1</sup> )	0.79	0.86	0.80	0.86	0.23	0.01	0.80	0.84	0.06	0.73	0.06	0.73
	Σ SFE <sup>-1</sup> (m Nm <sup>-1</sup> )	0.25	0.79	0.29	0.79	0.12	0.03	0.29	0.78	0.00	0.71	0.00	0.71

Table A7.57: Calculation of  $R_h^2$  and  $R_v^2$  with the matrix of two PAH properties ( $\log K_{hdw}$ ,  $\log C_w^{\text{sat}}$ ) multiplied with three plastic properties ( $X_c * d_{50}^{-1}$  as fixed parameters) and the  $\log K_{p-w}$  matrix

plastic property product		PAH properties											
1 <sup>st</sup> * 2 <sup>nd</sup> fixed parameter	3 <sup>rd</sup> variable parameter	$\log K_{hdw}$ (-)		$\log C_w^{\text{sat}}$ (mol m <sup>-3</sup> )		$\log K_{hdw} * \log C_w^{\text{sat}}$ (mol m <sup>-3</sup> )		$\log C_w^{\text{sat}} * \log K_{hdw}^{-1}$ (mol m <sup>-3</sup> )		$\log K_{hdw} * \log C_w^{\text{sat}-1}$ (m <sup>3</sup> mol <sup>-1</sup> )		$(\log K_{hdw} * \log C_w^{\text{sat}})^{-1}$ (m <sup>3</sup> mol <sup>-1</sup> )	
		$R_v^2$	$R_h^2$	$R_v^2$	$R_h^2$	$R_v^2$	$R_h^2$	$R_v^2$	$R_h^2$	$R_v^2$	$R_h^2$	$R_v^2$	$R_h^2$
$X_c (\%) * d_{50}^{-1} (\mu\text{m}^{-1})$	T <sub>m</sub> (K)	0.74	0.94	0.79	0.94	0.80	0.95	0.79	0.92	0.04	0.82	0.03	0.82
	T <sub>m</sub> <sup>-1</sup> (K <sup>-1</sup> )	0.83	0.96	0.89	0.95	0.89	0.97	0.88	0.93	0.05	0.83	0.04	0.83
	T <sub>g</sub> (K)	0.76	0.92	0.80	0.92	0.80	0.93	0.79	0.89	0.05	0.80	0.04	0.80
	T <sub>g</sub> <sup>-1</sup> (K <sup>-1</sup> )	0.57	0.89	0.63	0.89	0.63	0.90	0.62	0.87	0.02	0.78	0.02	0.78
	SA (m <sup>2</sup> g <sup>-1</sup> )	0.06	0.59	0.07	0.58	0.07	0.59	0.07	0.58	0.00	0.53	0.00	0.53
	SA <sup>-1</sup> (g m <sup>-2</sup> )	0.73	0.88	0.77	0.87	0.77	0.89	0.76	0.85	0.04	0.75	0.04	0.75
	V <sub>p</sub> (cm <sup>3</sup> g <sup>-1</sup> )	0.06	0.59	0.07	0.59	0.07	0.59	0.07	0.58	0.00	0.53	0.00	0.53
	V <sub>p</sub> <sup>-1</sup> (g cm <sup>-3</sup> )	0.72	0.88	0.76	0.87	0.76	0.89	0.75	0.85	0.04	0.75	0.04	0.75
	Σ SFE (mN m <sup>-1</sup> )	0.79	0.87	0.80	0.86	0.81	0.88	0.80	0.83	0.06	0.73	0.06	0.73
	Σ SFE <sup>-1</sup> (m Nm <sup>-1</sup> )	0.25	0.79	0.29	0.79	0.29	0.80	0.29	0.78	0.00	0.71	0.00	0.71

Table A7.58: Calculation of  $R_h^2$  and  $R_v^2$  with the matrix of two PAH properties ( $\log K_{ow}$ , MW<sub>w</sub>) multiplied with three plastic properties ( $X_c * T_m$  as fixed parameters) and the  $\log K_{p-w}$  matrix

plastic property product		PAH properties											
1 <sup>st</sup> * 2 <sup>nd</sup> fixed parameter	3 <sup>rd</sup> variable parameter	$\log K_{ow}$ (-)		MW (g mol <sup>-1</sup> )		$\log K_{ow} * MW$ (g mol <sup>-1</sup> )		$MW * \log K_{ow}^{-1}$ (g mol <sup>-1</sup> )		$\log K_{ow} * MW^{-1}$ (mol g <sup>-1</sup> )		$(\log K_{ow} * MW)^{-1}$ (mol g <sup>-1</sup> )	
		$R_v^2$	$R_h^2$	$R_v^2$	$R_h^2$	$R_v^2$	$R_h^2$	$R_v^2$	$R_h^2$	$R_v^2$	$R_h^2$		
$X_c$ (%)	T <sub>g</sub> (K)	0.56	0.87	0.56	0.86	0.59	0.87	0.52	0.81	0.50	0.81	0.37	0.84
	T <sub>g</sub> <sup>-1</sup> (K <sup>-1</sup> )	0.63	0.92	0.64	0.92	0.68	0.93	0.59	0.86	0.56	0.86	0.40	0.89
	SA (m <sup>2</sup> g <sup>-1</sup> )	0.02	0.50	0.02	0.50	0.02	0.50	0.02	0.48	0.02	0.48	0.01	0.49
	SA <sup>-1</sup> (g m <sup>-2</sup> )	0.75	0.89	0.76	0.89	0.80	0.90	0.70	0.82	0.67	0.82	0.49	0.86
	T <sub>m</sub> (K)	0.02	0.51	0.02	0.51	0.03	0.51	0.02	0.49	0.02	0.48	0.01	0.50
	V <sub>p</sub> (cm <sup>3</sup> g <sup>-1</sup> )	0.75	0.90	0.76	0.89	0.80	0.90	0.70	0.82	0.67	0.82	0.49	0.86
$\Sigma SFE$ (mN m <sup>-1</sup> )	Σ SFE (mN m <sup>-1</sup> )	0.74	0.86	0.75	0.86	0.78	0.87	0.69	0.79	0.67	0.79	0.50	0.83
	Σ SFE <sup>-1</sup> (m Nm <sup>-1</sup> )	0.20	0.78	0.20	0.77	0.22	0.78	0.18	0.73	0.17	0.73	0.12	0.76

Table A7.59: Calculation of  $R_h^2$  and  $R_v^2$  with the matrix of two PAH properties ( $\log K_{ow}$ ,  $\log K_{hdw}$ ) multiplied with three plastic properties ( $X_c * T_m$  as fixed parameters) and the  $\log K_{p-w}$  matrix

plastic property product		PAH properties											
1 <sup>st</sup> * 2 <sup>nd</sup> fixed parameter	3 <sup>rd</sup> variable parameter	$\log K_{ow}$ (-)		$\log K_{hdw}$ (-)		$\log K_{ow} * \log K_{hdw}$ (-)		$\log K_{hdw} * \log K_{ow}^{-1}$ (-)		$\log K_{ow} * \log K_{hdw}^{-1}$ (-)		$(\log K_{ow} * \log K_{hdw})^{-1}$ (-)	
		$R_v^2$	$R_h^2$	$R_v^2$	$R_h^2$	$R_v^2$	$R_h^2$	$R_v^2$	$R_h^2$	$R_v^2$	$R_h^2$		
$X_c$ (%)	T <sub>g</sub> (K)	0.56	0.87	0.56	0.86	0.59	0.87	0.52	0.81	0.50	0.81	0.37	0.84
	T <sub>g</sub> <sup>-1</sup> (K <sup>-1</sup> )	0.63	0.92	0.64	0.92	0.68	0.93	0.59	0.86	0.56	0.86	0.40	0.89
	SA (m <sup>2</sup> g <sup>-1</sup> )	0.02	0.50	0.02	0.50	0.02	0.50	0.02	0.48	0.02	0.48	0.01	0.49
	SA <sup>-1</sup> (g m <sup>-2</sup> )	0.75	0.89	0.76	0.89	0.80	0.90	0.70	0.82	0.67	0.82	0.49	0.86
	T <sub>m</sub> (K)	0.02	0.51	0.02	0.51	0.03	0.51	0.02	0.49	0.02	0.48	0.01	0.50
	V <sub>p</sub> (cm <sup>3</sup> g <sup>-1</sup> )	0.75	0.90	0.76	0.89	0.80	0.90	0.70	0.82	0.67	0.82	0.49	0.86
$\Sigma SFE$ (mN m <sup>-1</sup> )	Σ SFE (mN m <sup>-1</sup> )	0.74	0.86	0.75	0.86	0.78	0.87	0.69	0.79	0.67	0.79	0.50	0.83
	Σ SFE <sup>-1</sup> (m Nm <sup>-1</sup> )	0.20	0.78	0.20	0.77	0.22	0.78	0.18	0.73	0.17	0.73	0.12	0.76

Table A7.60: Calculation of  $R_h^2$  and  $R_v^2$  with the matrix of two PAH properties ( $\log K_{ow}$ ,  $\log C_w^{sat}$ ) multiplied with three plastic properties ( $X_c * T_m$  as fixed parameters) and the  $\log K_{p-w}$  matrix

plastic property product		PAH properties											
1 <sup>st</sup> * 2 <sup>nd</sup> fixed parameter	3 <sup>rd</sup> variable parameter	$\log K_{ow}$ (-)		$\log C_w^{sat}$ (mol m <sup>-3</sup> )		$\log K_{ow} * \log C_w^{sat}$ (mol m <sup>-3</sup> )		$\log C_w^{sat} * \log K_{ow}^{-1}$ (mol m <sup>-3</sup> )		$\log K_{ow} * \log C_w^{sat-1}$ (m <sup>3</sup> mol <sup>-1</sup> )		$(\log K_{ow} * \log C_w^{sat})^{-1}$ (m <sup>3</sup> mol <sup>-1</sup> )	
		$R_v^2$	$R_h^2$	$R_v^2$	$R_h^2$	$R_v^2$	$R_h^2$	$R_v^2$	$R_h^2$	$R_v^2$	$R_h^2$		
$X_c$ (%)	T <sub>g</sub> (K)	0.56	0.87	0.59	0.86	0.59	0.87	0.58	0.84	0.04	0.76	0.03	0.76
	T <sub>g</sub> <sup>-1</sup> (K <sup>-1</sup> )	0.63	0.92	0.70	0.92	0.70	0.93	0.69	0.90	0.03	0.81	0.03	0.81
	SA (m <sup>2</sup> g <sup>-1</sup> )	0.02	0.50	0.03	0.50	0.02	0.50	0.03	0.50	0.00	0.46	0.00	0.46
	SA <sup>-1</sup> (g m <sup>-2</sup> )	0.75	0.89	0.79	0.89	0.80	0.90	0.79	0.87	0.05	0.76	0.05	0.76
	T <sub>m</sub> (K)	0.02	0.51	0.03	0.51	0.03	0.51	0.03	0.50	0.00	0.46	0.00	0.46
	V <sub>p</sub> (cm <sup>3</sup> g <sup>-1</sup> )	0.75	0.90	0.79	0.89	0.80	0.91	0.79	0.87	0.05	0.76	0.05	0.76
$\Sigma SFE$ (mN m <sup>-1</sup> )	Σ SFE (mN m <sup>-1</sup> )	0.74	0.86	0.76	0.86	0.76	0.87	0.75	0.83	0.06	0.73	0.06	0.73
	Σ SFE <sup>-1</sup> (m Nm <sup>-1</sup> )	0.20	0.78	0.24	0.77	0.24	0.78	0.24	0.76	0.00	0.70	0.00	0.70

Table A7.61: Calculation of  $R_h^2$  and  $R_v^2$  with the matrix of two PAH properties (MW,  $\log K_{\text{hdw}}$ ) multiplied with three plastic properties ( $X_c * T_m$  as fixed parameters) and the  $\log K_{\text{p-w}}$  matrix

plastic property product		PAH properties											
1 <sup>st</sup> * 2 <sup>nd</sup> fixed parameter	3 <sup>rd</sup> variable parameter	MW (g mol <sup>-1</sup> )		$\log K_{\text{hdw}}$ (-)		MW * $\log K_{\text{hdw}}$ (g mol <sup>-1</sup> )		MW * $\log K_{\text{hdw}}^{-1}$ (g mol <sup>-1</sup> )		$\log K_{\text{hdw}} * MW^{-1}$ (mol g <sup>-1</sup> )		$(MW * \log K_{\text{hdw}})^{-1}$ (mol g <sup>-1</sup> )	
		$R_v^2$	$R_h^2$	$R_v^2$	$R_h^2$	$R_v^2$	$R_h^2$	$R_v^2$	$R_h^2$	$R_v^2$	$R_h^2$		
$X_c$ (%)	T <sub>g</sub> (K)	0.56	0.86	0.56	0.87	0.22	0.20	0.51	0.73	0.52	0.73	0.36	0.84
	T <sub>g</sub> <sup>-1</sup> (K <sup>-1</sup> )	0.64	0.92	0.64	0.92	0.24	0.22	0.57	0.78	0.58	0.78	0.39	0.89
	SA (m <sup>2</sup> g <sup>-1</sup> )	0.02	0.50	0.02	0.50	0.01	0.09	0.02	0.45	0.02	0.45	0.01	0.49
	SA <sup>-1</sup> (g m <sup>-2</sup> )	0.76	0.89	0.76	0.89	0.27	0.25	0.68	0.73	0.69	0.73	0.48	0.86
	T <sub>m</sub> (K)	0.02	0.51	0.02	0.51	0.02	0.09	0.02	0.45	0.02	0.45	0.01	0.50
	V <sub>p</sub> (cm <sup>3</sup> g <sup>-1</sup> )	0.76	0.89	0.75	0.90	0.27	0.25	0.68	0.74	0.69	0.74	0.48	0.86
$\Sigma$ SFE (mN m <sup>-1</sup> )	SFE (mN m <sup>-1</sup> )	0.75	0.86	0.75	0.86	0.27	0.25	0.68	0.71	0.69	0.70	0.49	0.82
	SFE <sup>-1</sup> (m Nm <sup>-1</sup> )	0.20	0.77	0.20	0.78	0.09	0.15	0.18	0.68	0.18	0.68	0.11	0.76

Table A7.62: Calculation of  $R_h^2$  and  $R_v^2$  with the matrix of two PAH properties (MW,  $\log C_w^{\text{sat}}$ ) multiplied with three plastic properties ( $X_c * T_m$  as fixed parameters) and the  $\log K_{\text{p-w}}$  matrix

plastic property product		PAH properties											
1 <sup>st</sup> * 2 <sup>nd</sup> fixed parameter	3 <sup>rd</sup> variable parameter	MW (g mol <sup>-1</sup> )		$\log C_w^{\text{sat}}$ (mol m <sup>-3</sup> )		MW * $\log C_w^{\text{sat}}$ (g m <sup>-3</sup> )		$\log C_w^{\text{sat}} * MW^{-1}$ (mol <sup>2</sup> m <sup>-3</sup> g <sup>-1</sup> )		$MW * \log C_w^{\text{sat}} * MW^{-1}$ (g m <sup>3</sup> mol <sup>-2</sup> )		$(\log K_{\text{ow}} * \log C_w^{\text{sat}})^{-1}$ (m <sup>3</sup> g <sup>-1</sup> )	
		$R_v^2$	$R_h^2$	$R_v^2$	$R_h^2$	$R_v^2$	$R_h^2$	$R_v^2$	$R_h^2$	$R_v^2$	$R_h^2$		
$X_c$ (%)	T <sub>g</sub> (K)	0.56	0.86	0.59	0.86	0.20	0.02	0.58	0.84	0.04	0.76	0.03	0.76
	T <sub>g</sub> <sup>-1</sup> (K <sup>-1</sup> )	0.64	0.92	0.70	0.92	0.24	0.02	0.69	0.90	0.03	0.81	0.03	0.81
	SA (m <sup>2</sup> g <sup>-1</sup> )	0.02	0.50	0.03	0.50	0.02	0.03	0.03	0.50	0.00	0.46	0.00	0.46
	SA <sup>-1</sup> (g m <sup>-2</sup> )	0.76	0.89	0.79	0.89	0.23	0.01	0.79	0.86	0.05	0.76	0.05	0.76
	T <sub>m</sub> (K)	0.02	0.51	0.03	0.51	0.02	0.03	0.03	0.50	0.00	0.46	0.00	0.46
	V <sub>p</sub> (cm <sup>3</sup> g <sup>-1</sup> )	0.76	0.89	0.79	0.89	0.23	0.01	0.78	0.87	0.05	0.76	0.05	0.76
$\Sigma$ SFE (mN m <sup>-1</sup> )	SFE (mN m <sup>-1</sup> )	0.75	0.86	0.76	0.86	0.22	0.01	0.75	0.83	0.06	0.73	0.06	0.73
	SFE <sup>-1</sup> (m Nm <sup>-1</sup> )	0.20	0.77	0.24	0.77	0.10	0.03	0.24	0.76	0.00	0.70	0.00	0.70

Table A7.63: Calculation of  $R_h^2$  and  $R_v^2$  with the matrix of two PAH properties ( $\log K_{\text{hdw}}$ ,  $\log C_w^{\text{sat}}$ ) multiplied with three plastic properties ( $X_c * T_m$  as fixed parameters) and the  $\log K_{\text{p-w}}$  matrix

plastic property product		PAH properties											
1 <sup>st</sup> * 2 <sup>nd</sup> fixed parameter	3 <sup>rd</sup> variable parameter	$\log K_{\text{hdw}}$ (-)		$\log C_w^{\text{sat}}$ (mol m <sup>-3</sup> )		$\log K_{\text{hdw}} * \log C_w^{\text{sat}}$ (mol m <sup>-3</sup> )		$\log C_w^{\text{sat}} * \log K_{\text{hdw}}^{-1}$ (mol m <sup>-3</sup> )		$\log K_{\text{hdw}} * \log C_w^{\text{sat}} * \log K_{\text{hdw}}^{-1}$ (m <sup>3</sup> mol <sup>-1</sup> )		$(\log K_{\text{hdw}} * \log C_w^{\text{sat}})^{-1}$ (m <sup>3</sup> mol <sup>-1</sup> )	
		$R_v^2$	$R_h^2$	$R_v^2$	$R_h^2$	$R_v^2$	$R_h^2$	$R_v^2$	$R_h^2$	$R_v^2$	$R_h^2$	$R_v^2$	$R_h^2$
$X_c$ (%)	T <sub>g</sub> (K)	0.56	0.87	0.59	0.86	0.59	0.87	0.58	0.84	0.04	0.76	0.03	0.76
	T <sub>g</sub> <sup>-1</sup> (K <sup>-1</sup> )	0.64	0.92	0.70	0.92	0.70	0.93	0.69	0.90	0.03	0.81	0.03	0.81
	SA (m <sup>2</sup> g <sup>-1</sup> )	0.02	0.50	0.03	0.50	0.02	0.50	0.03	0.50	0.00	0.46	0.00	0.46
	SA <sup>-1</sup> (g m <sup>-2</sup> )	0.76	0.89	0.79	0.89	0.80	0.90	0.79	0.86	0.05	0.76	0.05	0.76
	T <sub>m</sub> (K)	0.02	0.51	0.03	0.51	0.03	0.51	0.03	0.50	0.00	0.46	0.00	0.46
	V <sub>p</sub> (cm <sup>3</sup> g <sup>-1</sup> )	0.75	0.90	0.79	0.89	0.80	0.91	0.78	0.87	0.05	0.76	0.05	0.76
$\Sigma$ SFE (mN m <sup>-1</sup> )	SFE (mN m <sup>-1</sup> )	0.75	0.86	0.76	0.86	0.76	0.87	0.75	0.83	0.06	0.73	0.06	0.73
	SFE <sup>-1</sup> (m Nm <sup>-1</sup> )	0.20	0.78	0.24	0.77	0.24	0.78	0.24	0.76	0.00	0.70	0.00	0.70

Table A7.64: Calculation of  $R_h^2$  and  $R_v^2$  with the matrix of two PAH properties ( $\log K_{ow}$ , MW<sub>w</sub>) multiplied with three plastic properties ( $X_c * T_m^{-1}$  as fixed parameters) and the  $\log K_{p-w}$  matrix

plastic property product		PAH properties											
1 <sup>st</sup> * 2 <sup>nd</sup> fixed parameter	3 <sup>rd</sup> variable parameter	$\log K_{ow}$ (-)		MW (g mol <sup>-1</sup> )		$\log K_{ow} * MW$ (g mol <sup>-1</sup> )		$MW * \log K_{ow}^{-1}$ (g mol <sup>-1</sup> )		$\log K_{ow} * MW^{-1}$ (mol g <sup>-1</sup> )		$(\log K_{ow} * MW)^{-1}$ (mol g <sup>-1</sup> )	
		$R_v^2$	$R_h^2$	$R_v^2$	$R_h^2$	$R_v^2$	$R_h^2$	$R_v^2$	$R_h^2$	$R_v^2$	$R_h^2$	$R_v^2$	$R_h^2$
$X_c$ (%) * $T_m^{-1}$ (K <sup>-1</sup> )	T <sub>g</sub> (K)	0.78	0.91	0.79	0.91	0.83	0.92	0.73	0.85	0.71	0.84	0.52	0.88
	T <sub>g</sub> <sup>-1</sup> (K <sup>-1</sup> )	0.70	0.92	0.71	0.92	0.75	0.93	0.65	0.86	0.62	0.86	0.45	0.89
	SA (m <sup>2</sup> g <sup>-1</sup> )	0.10	0.62	0.10	0.62	0.10	0.63	0.09	0.59	0.08	0.59	0.06	0.61
	SA <sup>-1</sup> (g m <sup>-2</sup> )	0.75	0.86	0.76	0.86	0.80	0.87	0.70	0.79	0.68	0.79	0.50	0.83
	V <sub>p</sub> (cm <sup>3</sup> g <sup>-1</sup> )	0.10	0.63	0.10	0.63	0.11	0.63	0.09	0.60	0.09	0.60	0.06	0.62
	V <sub>p</sub> <sup>-1</sup> (g cm <sup>-3</sup> )	0.75	0.87	0.76	0.86	0.80	0.87	0.70	0.79	0.67	0.79	0.50	0.83
	Σ SFE (mN m <sup>-1</sup> )	0.73	0.82	0.74	0.81	0.77	0.82	0.68	0.74	0.66	0.74	0.49	0.78
	Σ SFE <sup>-1</sup> (m Nm <sup>-1</sup> )	0.36	0.84	0.36	0.84	0.39	0.85	0.33	0.79	0.31	0.79	0.22	0.82

Table A7.65: Calculation of  $R_h^2$  and  $R_v^2$  with the matrix of two PAH properties ( $\log K_{ow}$ ,  $\log K_{hdw}$ ) multiplied with three plastic properties ( $X_c * T_m^{-1}$  as fixed parameters) and the  $\log K_{p-w}$  matrix

plastic property product		PAH properties											
1 <sup>st</sup> * 2 <sup>nd</sup> fixed parameter	3 <sup>rd</sup> variable parameter	$\log K_{ow}$ (-)		$\log K_{hdw}$ (-)		$\log K_{ow} * \log K_{hdw}$ (-)		$\log K_{hdw} * \log K_{ow}^{-1}$ (-)		$\log K_{ow} * \log K_{hdw}^{-1}$ (-)		$(\log K_{ow} * \log K_{hdw})^{-1}$ (-)	
		$R_v^2$	$R_h^2$	$R_v^2$	$R_h^2$	$R_v^2$	$R_h^2$	$R_v^2$	$R_h^2$	$R_v^2$	$R_h^2$	$R_v^2$	$R_h^2$
$X_c$ (%) * $T_m^{-1}$ (K <sup>-1</sup> )	T <sub>g</sub> (K)	0.78	0.91	0.79	0.91	0.83	0.92	0.73	0.85	0.71	0.84	0.52	0.88
	T <sub>g</sub> <sup>-1</sup> (K <sup>-1</sup> )	0.70	0.92	0.71	0.92	0.75	0.93	0.65	0.86	0.62	0.86	0.45	0.89
	SA (m <sup>2</sup> g <sup>-1</sup> )	0.10	0.62	0.10	0.62	0.10	0.63	0.09	0.59	0.08	0.59	0.06	0.61
	SA <sup>-1</sup> (g m <sup>-2</sup> )	0.75	0.86	0.76	0.86	0.80	0.87	0.70	0.79	0.68	0.79	0.50	0.83
	V <sub>p</sub> (cm <sup>3</sup> g <sup>-1</sup> )	0.10	0.63	0.10	0.63	0.11	0.63	0.09	0.60	0.09	0.60	0.06	0.62
	V <sub>p</sub> <sup>-1</sup> (g cm <sup>-3</sup> )	0.75	0.87	0.76	0.86	0.80	0.87	0.70	0.79	0.67	0.79	0.50	0.83
	Σ SFE (mN m <sup>-1</sup> )	0.73	0.82	0.74	0.81	0.77	0.82	0.68	0.74	0.66	0.74	0.49	0.78
	Σ SFE <sup>-1</sup> (m Nm <sup>-1</sup> )	0.36	0.84	0.36	0.84	0.39	0.85	0.33	0.79	0.31	0.79	0.22	0.82

Table A7.66: Calculation of  $R_h^2$  and  $R_v^2$  with the matrix of two PAH properties ( $\log K_{ow}$ ,  $\log C_w^{sat}$ ) multiplied with three plastic properties ( $X_c * T_m^{-1}$  as fixed parameters) and the  $\log K_{p-w}$  matrix

plastic property product		PAH properties											
1 <sup>st</sup> * 2 <sup>nd</sup> fixed parameter	3 <sup>rd</sup> variable parameter	$\log K_{ow}$ (-)		$\log C_w^{sat}$ (mol m <sup>-3</sup> )		$\log K_{ow} * \log C_w^{sat}$ (mol m <sup>-3</sup> )		$\log C_w^{sat} * \log K_{ow}^{-1}$ (mol m <sup>-3</sup> )		$\log K_{ow} * \log C_w^{sat-1}$ (m <sup>3</sup> mol <sup>-1</sup> )		$(\log K_{ow} * \log C_w^{sat})^{-1}$ (m <sup>3</sup> mol <sup>-1</sup> )	
		$R_v^2$	$R_h^2$	$R_v^2$	$R_h^2$	$R_v^2$	$R_h^2$	$R_v^2$	$R_h^2$	$R_v^2$	$R_h^2$	$R_v^2$	$R_h^2$
$X_c$ (%) * $T_m^{-1}$ (K <sup>-1</sup> )	T <sub>g</sub> (K)	0.78	0.91	0.82	0.91	0.82	0.92	0.81	0.89	0.05	0.79	0.05	0.79
	T <sub>g</sub> <sup>-1</sup> (K <sup>-1</sup> )	0.70	0.92	0.76	0.92	0.77	0.93	0.76	0.90	0.03	0.80	0.03	0.80
	SA (m <sup>2</sup> g <sup>-1</sup> )	0.10	0.62	0.11	0.62	0.11	0.63	0.11	0.61	0.00	0.56	0.00	0.56
	SA <sup>-1</sup> (g m <sup>-2</sup> )	0.75	0.86	0.79	0.86	0.79	0.87	0.78	0.83	0.05	0.73	0.05	0.73
	V <sub>p</sub> (cm <sup>3</sup> g <sup>-1</sup> )	0.10	0.63	0.11	0.63	0.11	0.63	0.11	0.62	0.00	0.57	0.00	0.57
	V <sub>p</sub> <sup>-1</sup> (g cm <sup>-3</sup> )	0.75	0.87	0.79	0.86	0.79	0.88	0.78	0.84	0.05	0.74	0.05	0.74
	Σ SFE (mN m <sup>-1</sup> )	0.73	0.82	0.74	0.81	0.75	0.83	0.74	0.79	0.06	0.69	0.06	0.69
	Σ SFE <sup>-1</sup> (m Nm <sup>-1</sup> )	0.36	0.84	0.41	0.84	0.41	0.85	0.41	0.82	0.01	0.75	0.01	0.75

Table A7.67: Calculation of  $R_h^2$  and  $R_v^2$  with the matrix of two PAH properties (MW,  $\log K_{\text{hdw}}$ ) multiplied with three plastic properties ( $X_c * T_m^{-1}$  as fixed parameters) and the  $\log K_{\text{p-w}}$  matrix

plastic property product		PAH properties											
1 <sup>st</sup> * 2 <sup>nd</sup> fixed parameter	3 <sup>rd</sup> variable parameter	MW (g mol <sup>-1</sup> )		$\log K_{\text{hdw}}$ (-)		MW * $\log K_{\text{hdw}}$ (g mol <sup>-1</sup> )		MW * $\log K_{\text{hdw}}^{-1}$ (g mol <sup>-1</sup> )		$\log K_{\text{hdw}} * MW^{-1}$ (mol g <sup>-1</sup> )		$(MW * \log K_{\text{hdw}})^{-1}$ (mol g <sup>-1</sup> )	
		$R_v^2$	$R_h^2$	$R_v^2$	$R_h^2$	$R_v^2$	$R_h^2$	$R_v^2$	$R_h^2$	$R_v^2$	$R_h^2$		
$X_c$ (%) * $T_m^{-1}$ (K <sup>-1</sup> )	T <sub>g</sub> (K)	0.79	0.91	0.79	0.91	0.30	0.23	0.71	0.76	0.73	0.76	0.51	0.88
	T <sub>g</sub> <sup>-1</sup> (K <sup>-1</sup> )	0.71	0.92	0.71	0.92	0.26	0.23	0.63	0.78	0.64	0.78	0.44	0.89
	SA (m <sup>2</sup> g <sup>-1</sup> )	0.10	0.62	0.10	0.62	0.05	0.12	0.09	0.55	0.09	0.55	0.06	0.61
	SA <sup>-1</sup> (g m <sup>-2</sup> )	0.76	0.86	0.76	0.86	0.27	0.25	0.68	0.71	0.69	0.70	0.49	0.83
	V <sub>p</sub> (cm <sup>3</sup> g <sup>-1</sup> )	0.10	0.63	0.10	0.63	0.05	0.12	0.09	0.55	0.09	0.55	0.06	0.61
	V <sub>p</sub> <sup>-1</sup> (g cm <sup>-3</sup> )	0.76	0.86	0.76	0.87	0.26	0.25	0.68	0.71	0.69	0.71	0.49	0.83
	$\sum SFE$ (mN m <sup>-1</sup> )	0.74	0.81	0.73	0.82	0.26	0.25	0.67	0.66	0.68	0.66	0.49	0.78
$\Sigma SFE^{-1}$ (m Nm <sup>-1</sup> )		0.36	0.84	0.36	0.84	0.14	0.18	0.32	0.73	0.32	0.73	0.21	0.82

Table A7.68: Calculation of  $R_h^2$  and  $R_v^2$  with the matrix of two PAH properties (MW,  $\log C_w^{\text{sat}}$ ) multiplied with three plastic properties ( $X_c * T_m^{-1}$  as fixed parameters) and the  $\log K_{\text{p-w}}$  matrix

plastic property product		PAH properties											
1 <sup>st</sup> * 2 <sup>nd</sup> fixed parameter	3 <sup>rd</sup> variable parameter	MW (g mol <sup>-1</sup> )		$\log C_w^{\text{sat}}$ (mol m <sup>-3</sup> )		MW * $\log C_w^{\text{sat}}$ (g m <sup>-3</sup> )		$\log C_w^{\text{sat}} * MW^{-1}$ (mol <sup>2</sup> m <sup>-3</sup> g <sup>-1</sup> )		$MW * \log C_w^{\text{sat}-1}$ (g m <sup>3</sup> mol <sup>-2</sup> )		$(\log K_{\text{ow}} * \log C_w^{\text{sat}})^{-1}$ (m <sup>3</sup> g <sup>-1</sup> )	
		$R_v^2$	$R_h^2$	$R_v^2$	$R_h^2$	$R_v^2$	$R_h^2$	$R_v^2$	$R_h^2$	$R_v^2$	$R_h^2$		
$X_c$ (%) * $T_m^{-1}$ (K <sup>-1</sup> )	T <sub>g</sub> (K)	0.79	0.91	0.82	0.91	0.26	0.02	0.81	0.89	0.05	0.79	0.05	0.79
	T <sub>g</sub> <sup>-1</sup> (K <sup>-1</sup> )	0.71	0.92	0.76	0.92	0.25	0.02	0.76	0.90	0.03	0.80	0.03	0.80
	SA (m <sup>2</sup> g <sup>-1</sup> )	0.10	0.62	0.11	0.62	0.05	0.03	0.11	0.61	0.00	0.56	0.00	0.56
	SA <sup>-1</sup> (g m <sup>-2</sup> )	0.76	0.86	0.79	0.86	0.23	0.01	0.78	0.83	0.05	0.73	0.05	0.73
	V <sub>p</sub> (cm <sup>3</sup> g <sup>-1</sup> )	0.10	0.63	0.11	0.63	0.05	0.03	0.11	0.62	0.00	0.57	0.00	0.57
	V <sub>p</sub> <sup>-1</sup> (g cm <sup>-3</sup> )	0.76	0.86	0.79	0.86	0.23	0.01	0.78	0.84	0.05	0.74	0.05	0.74
	$\sum SFE$ (mN m <sup>-1</sup> )	0.74	0.81	0.74	0.81	0.21	0.01	0.74	0.79	0.06	0.69	0.06	0.69
$\Sigma SFE^{-1}$ (m Nm <sup>-1</sup> )		0.36	0.84	0.41	0.84	0.16	0.03	0.41	0.82	0.01	0.75	0.01	0.75

Table A7.69: Calculation of  $R_h^2$  and  $R_v^2$  with the matrix of two PAH properties ( $\log K_{\text{hdw}}$ ,  $\log C_w^{\text{sat}}$ ) multiplied with three plastic properties ( $X_c * T_m^{-1}$  as fixed parameters) and the  $\log K_{\text{p-w}}$  matrix

plastic property product		PAH properties											
1 <sup>st</sup> * 2 <sup>nd</sup> fixed parameter	3 <sup>rd</sup> variable parameter	$\log K_{\text{hdw}}$ (-)		$\log C_w^{\text{sat}}$ (mol m <sup>-3</sup> )		$\log K_{\text{hdw}} * \log C_w^{\text{sat}}$ (mol m <sup>-3</sup> )		$\log C_w^{\text{sat}} * \log K_{\text{hdw}}^{-1}$ (mol m <sup>-3</sup> )		$\log K_{\text{hdw}} * \log C_w^{\text{sat}-1}$ (m <sup>3</sup> mol <sup>-1</sup> )		$(\log K_{\text{hdw}} * \log C_w^{\text{sat}})^{-1}$ (m <sup>3</sup> mol <sup>-1</sup> )	
		$R_v^2$	$R_h^2$	$R_v^2$	$R_h^2$	$R_v^2$	$R_h^2$	$R_v^2$	$R_h^2$	$R_v^2$	$R_h^2$		
$X_c$ (%) * $T_m^{-1}$ (K <sup>-1</sup> )	T <sub>g</sub> (K)	0.79	0.91	0.82	0.91	0.82	0.92	0.81	0.89	0.05	0.79	0.05	0.79
	T <sub>g</sub> <sup>-1</sup> (K <sup>-1</sup> )	0.71	0.92	0.76	0.92	0.77	0.93	0.76	0.90	0.03	0.80	0.03	0.80
	SA (m <sup>2</sup> g <sup>-1</sup> )	0.10	0.62	0.11	0.62	0.11	0.63	0.11	0.61	0.00	0.56	0.00	0.56
	SA <sup>-1</sup> (g m <sup>-2</sup> )	0.76	0.86	0.79	0.86	0.79	0.87	0.78	0.83	0.05	0.73	0.05	0.73
	V <sub>p</sub> (cm <sup>3</sup> g <sup>-1</sup> )	0.10	0.63	0.11	0.63	0.11	0.63	0.11	0.62	0.00	0.57	0.00	0.57
	V <sub>p</sub> <sup>-1</sup> (g cm <sup>-3</sup> )	0.76	0.87	0.79	0.86	0.79	0.88	0.78	0.84	0.05	0.74	0.05	0.74
	$\sum SFE$ (mN m <sup>-1</sup> )	0.73	0.82	0.74	0.81	0.75	0.83	0.74	0.79	0.06	0.69	0.06	0.69
$\Sigma SFE^{-1}$ (m Nm <sup>-1</sup> )		0.36	0.84	0.41	0.84	0.41	0.85	0.41	0.82	0.01	0.75	0.01	0.75

Table A7.70: Calculation of  $R_h^2$  and  $R_v^2$  with the matrix of two PAH properties ( $\log K_{ow}$ , MW<sub>w</sub>) multiplied with three plastic properties ( $X_c * T_g$  as fixed parameters) and the  $\log K_{p-w}$  matrix

plastic property product		PAH properties											
1 <sup>st</sup> * 2 <sup>nd</sup> fixed parameter	3 <sup>rd</sup> variable parameter	log $K_{ow}$ (-)		MW (g mol <sup>-1</sup> )		$\log K_{ow} * MW$ (g mol <sup>-1</sup> )		$MW * \log K_{ow}^{-1}$ (g mol <sup>-1</sup> )		$\log K_{ow} * MW^{-1}$ (mol g <sup>-1</sup> )		$(\log K_{ow} * MW)^{-1}$ (mol g <sup>-1</sup> )	
		$R_v^2$	$R_h^2$	$R_v^2$	$R_h^2$	$R_v^2$	$R_h^2$	$R_v^2$	$R_h^2$	$R_v^2$	$R_h^2$		
$X_c$ (%)	SA (m <sup>2</sup> g <sup>-1</sup> )	0.01	0.45	0.01	0.45	0.02	0.45	0.01	0.43	0.01	0.43		
	SA <sup>-1</sup> (g m <sup>-2</sup> )	0.75	0.86	0.76	0.85	0.80	0.86	0.70	0.78	0.68	0.78		
	Vp (cm <sup>3</sup> g <sup>-1</sup> )	0.02	0.46	0.02	0.46	0.02	0.46	0.01	0.44	0.01	0.44		
	Vp <sup>-1</sup> (g cm <sup>-3</sup> )	0.76	0.86	0.77	0.86	0.81	0.87	0.71	0.79	0.69	0.79		
$T_g$ (K)	$\sum SFE$ (mN m <sup>-1</sup> )	0.63	0.79	0.63	0.78	0.66	0.80	0.59	0.72	0.57	0.72		
	$\sum SFE^{-1}$ (m Nm <sup>-1</sup> )	0.20	0.76	0.21	0.76	0.22	0.77	0.19	0.72	0.18	0.72		

Table A7.71: Calculation of  $R_h^2$  and  $R_v^2$  with the matrix of two PAH properties ( $\log K_{ow}$ ,  $\log K_{hdw}$ ) multiplied with three plastic properties ( $X_c * T_g$  as fixed parameters) and the  $\log K_{p-w}$  matrix

plastic property product		PAH properties											
1 <sup>st</sup> * 2 <sup>nd</sup> fixed parameter	3 <sup>rd</sup> variable parameter	log $K_{ow}$ (-)		log $K_{hdw}$ (-)		$\log K_{ow} * \log K_{hdw}$ (-)		$\log K_{hdw} * \log K_{ow}^{-1}$ (-)		$\log K_{ow} * \log K_{hdw}^{-1}$ (-)		$(\log K_{ow} * \log K_{hdw})^{-1}$ (-)	
		$R_v^2$	$R_h^2$	$R_v^2$	$R_h^2$	$R_v^2$	$R_h^2$	$R_v^2$	$R_h^2$	$R_v^2$	$R_h^2$		
$X_c$ (%)	SA (m <sup>2</sup> g <sup>-1</sup> )	0.01	0.45	0.01	0.45	0.02	0.45	0.01	0.43	0.01	0.43		
	SA <sup>-1</sup> (g m <sup>-2</sup> )	0.75	0.86	0.76	0.85	0.80	0.86	0.70	0.78	0.68	0.78		
	Vp (cm <sup>3</sup> g <sup>-1</sup> )	0.02	0.46	0.02	0.46	0.02	0.46	0.01	0.44	0.01	0.44		
	Vp <sup>-1</sup> (g cm <sup>-3</sup> )	0.76	0.86	0.77	0.86	0.81	0.87	0.71	0.79	0.69	0.79		
$T_g$ (K)	$\sum SFE$ (mN m <sup>-1</sup> )	0.63	0.79	0.63	0.78	0.66	0.80	0.59	0.72	0.57	0.72		
	$\sum SFE^{-1}$ (m Nm <sup>-1</sup> )	0.20	0.76	0.21	0.76	0.22	0.77	0.19	0.72	0.18	0.72		

Table A7.72: Calculation of  $R_h^2$  and  $R_v^2$  with the matrix of two PAH properties ( $\log K_{ow}$ ,  $\log C_w^{sat}$ ) multiplied with three plastic properties ( $X_c * T_g$  as fixed parameters) and the  $\log K_{p-w}$  matrix

plastic property product		PAH properties											
1 <sup>st</sup> * 2 <sup>nd</sup> fixed parameter	3 <sup>rd</sup> variable parameter	log $K_{ow}$ (-)		log $C_w^{sat}$ (mol m <sup>-3</sup> )		$\log K_{ow} * \log C_w^{sat}$ (mol m <sup>-3</sup> )		$\log C_w^{sat} * \log K_{ow}^{-1}$ (mol m <sup>-3</sup> )		$\log K_{ow} * \log C_w^{sat-1}$ (m <sup>3</sup> mol <sup>-1</sup> )		$(\log K_{ow} * \log C_w^{sat})^{-1}$ (m <sup>3</sup> mol <sup>-1</sup> )	
		$R_v^2$	$R_h^2$	$R_v^2$	$R_h^2$	$R_v^2$	$R_h^2$	$R_v^2$	$R_h^2$	$R_v^2$	$R_h^2$	$R_v^2$	$R_h^2$
$X_c$ (%)	SA (m <sup>2</sup> g <sup>-1</sup> )	0.01	0.45	0.02	0.45	0.02	0.46	0.02	0.45	0.00	0.41	0.00	0.41
	SA <sup>-1</sup> (g m <sup>-2</sup> )	0.75	0.86	0.78	0.85	0.78	0.87	0.77	0.83	0.06	0.72	0.06	0.72
	Vp (cm <sup>3</sup> g <sup>-1</sup> )	0.02	0.46	0.02	0.46	0.02	0.46	0.02	0.45	0.00	0.42	0.00	0.42
	Vp <sup>-1</sup> (g cm <sup>-3</sup> )	0.76	0.86	0.79	0.86	0.79	0.87	0.78	0.83	0.06	0.73	0.06	0.73
$T_g$ (K)	$\sum SFE$ (mN m <sup>-1</sup> )	0.63	0.79	0.63	0.78	0.64	0.80	0.63	0.76	0.06	0.67	0.05	0.67
	$\sum SFE^{-1}$ (m Nm <sup>-1</sup> )	0.20	0.76	0.23	0.76	0.23	0.77	0.23	0.75	0.01	0.68	0.00	0.68

Table A7.73: Calculation of  $R_h^2$  and  $R_v^2$  with the matrix of two PAH properties (MW,  $\log K_{hdw}$ ) multiplied with three plastic properties ( $X_c * T_g$  as fixed parameters) and the  $\log K_{p-w}$  matrix

plastic property product		PAH properties											
1 <sup>st</sup> * 2 <sup>nd</sup> fixed parameter	3 <sup>rd</sup> variable parameter	MW (g mol <sup>-1</sup> )		log $K_{hdw}$ (-)		$MW * \log K_{hdw}$ (g mol <sup>-1</sup> )		$MW * \log K_{hdw}^{-1}$ (g mol <sup>-1</sup> )		$\log K_{hdw} * MW^{-1}$ (mol g <sup>-1</sup> )		$(MW * \log K_{hdw})^{-1}$ (mol g <sup>-1</sup> )	
		$R_v^2$	$R_h^2$	$R_v^2$	$R_h^2$	$R_v^2$	$R_h^2$	$R_v^2$	$R_h^2$	$R_v^2$	$R_h^2$	$R_v^2$	$R_h^2$
$X_c$ (%)	SA (m <sup>2</sup> g <sup>-1</sup> )	0.01	0.45	0.01	0.45	0.01	0.08	0.01	0.40	0.01	0.40	0.01	0.44
	SA <sup>-1</sup> (g m <sup>-2</sup> )	0.76	0.85	0.76	0.86	0.27	0.25	0.69	0.70	0.70	0.70	0.50	0.82
	Vp (cm <sup>3</sup> g <sup>-1</sup> )	0.02	0.46	0.02	0.46	0.01	0.08	0.01	0.41	0.01	0.41	0.01	0.45
	Vp <sup>-1</sup> (g cm <sup>-3</sup> )	0.77	0.86	0.77	0.86	0.27	0.25	0.69	0.70	0.70	0.70	0.50	0.82
$T_g$ (K)	$\sum SFE$ (mN m <sup>-1</sup> )	0.63	0.78	0.63	0.79	0.22	0.23	0.58	0.64	0.58	0.64	0.42	0.76
	$\sum SFE^{-1}$ (m Nm <sup>-1</sup> )	0.21	0.76	0.21	0.76	0.09	0.15	0.18	0.66	0.19	0.66	0.12	0.74

Table A7.74: Calculation of  $R_h^2$  and  $R_v^2$  with the matrix of two PAH properties (MW,  $\log C_w^{\text{sat}}$ ) multiplied with three plastic properties ( $X_c * T_g$  as fixed parameters) and the  $\log K_{\text{p-w}}$  matrix

plastic property product		PAH properties											
1 <sup>st</sup> * 2 <sup>nd</sup> fixed parameter	3 <sup>rd</sup> variable parameter	MW (g mol <sup>-1</sup> )		$\log C_w^{\text{sat}}$ (mol m <sup>-3</sup> )		MW * $\log C_w^{\text{sat}}$ (g m <sup>-3</sup> )		$\log C_w^{\text{sat}} * \text{MW}^{-1}$ (mol <sup>2</sup> m <sup>-3</sup> g <sup>-1</sup> )		MW * $\log C_w^{\text{sat}-1}$ (g m <sup>3</sup> mol <sup>-2</sup> )		$(\log K_{\text{ow}} * \log C_w^{\text{sat}})^{-1}$ (m <sup>3</sup> g <sup>-1</sup> )	
		$R_v^2$	$R_h^2$	$R_v^2$	$R_h^2$	$R_v^2$	$R_h^2$	$R_v^2$	$R_h^2$	$R_v^2$	$R_h^2$		
$X_c$ (%)	SA (m <sup>2</sup> g <sup>-1</sup> )	0.01	0.45	0.02	0.45	0.01	0.02	0.02	0.45	0.00	0.41		
	SA <sup>-1</sup> (g m <sup>-2</sup> )	0.76	0.85	0.78	0.85	0.22	0.01	0.77	0.83	0.06	0.72		
	Vp (cm <sup>3</sup> g <sup>-1</sup> )	0.02	0.46	0.02	0.46	0.01	0.02	0.02	0.45	0.00	0.42		
	Vp <sup>-1</sup> (g cm <sup>-3</sup> )	0.77	0.86	0.79	0.86	0.22	0.01	0.78	0.83	0.06	0.73		
	$\sum \text{SFE}$ (mN m <sup>-1</sup> )	0.63	0.78	0.63	0.78	0.18	0.01	0.63	0.76	0.06	0.67		
	$\sum \text{SFE}^{-1}$ (m Nm <sup>-1</sup> )	0.21	0.76	0.23	0.76	0.10	0.03	0.23	0.75	0.01	0.68		

Table A7.75: Calculation of  $R_h^2$  and  $R_v^2$  with the matrix of two PAH properties ( $\log K_{\text{hdw}}$ ,  $\log C_w^{\text{sat}}$ ) multiplied with three plastic properties ( $X_c * T_g$  as fixed parameters) and the  $\log K_{\text{p-w}}$  matrix

plastic property product		PAH properties											
1 <sup>st</sup> * 2 <sup>nd</sup> fixed parameter	3 <sup>rd</sup> variable parameter	$\log K_{\text{hdw}}$ (-)		$\log C_w^{\text{sat}}$ (mol m <sup>-3</sup> )		$\log K_{\text{hdw}} * \log C_w^{\text{sat}}$ (mol m <sup>-3</sup> )		$\log C_w^{\text{sat}} * \log K_{\text{hdw}}^{-1}$ (mol m <sup>-3</sup> )		$\log K_{\text{hdw}} * \log C_w^{\text{sat}-1}$ (m <sup>3</sup> mol <sup>-1</sup> )		$(\log K_{\text{hdw}} * \log C_w^{\text{sat}})^{-1}$ (m <sup>3</sup> mol <sup>-1</sup> )	
		$R_v^2$	$R_h^2$	$R_v^2$	$R_h^2$	$R_v^2$	$R_h^2$	$R_v^2$	$R_h^2$	$R_v^2$	$R_h^2$		
$X_c$ (%)	SA (m <sup>2</sup> g <sup>-1</sup> )	0.01	0.45	0.02	0.45	0.02	0.46	0.02	0.45	0.00	0.41		
	SA <sup>-1</sup> (g m <sup>-2</sup> )	0.76	0.86	0.78	0.85	0.78	0.87	0.77	0.82	0.06	0.72		
	Vp (cm <sup>3</sup> g <sup>-1</sup> )	0.02	0.46	0.02	0.46	0.02	0.46	0.02	0.45	0.00	0.42		
	Vp <sup>-1</sup> (g cm <sup>-3</sup> )	0.77	0.86	0.79	0.86	0.79	0.87	0.78	0.83	0.06	0.73		
	$\sum \text{SFE}$ (mN m <sup>-1</sup> )	0.63	0.79	0.63	0.78	0.64	0.80	0.63	0.76	0.06	0.67		
	$\sum \text{SFE}^{-1}$ (m Nm <sup>-1</sup> )	0.21	0.76	0.23	0.76	0.23	0.77	0.23	0.75	0.01	0.68		

Table A7.76: Calculation of  $R_h^2$  and  $R_v^2$  with the matrix of two PAH properties ( $\log K_{\text{ow}}$ , MW<sub>w</sub>) multiplied with three plastic properties ( $X_c * T_g^{-1}$  as fixed parameters) and the  $\log K_{\text{p-w}}$  matrix

plastic property product		PAH properties											
1 <sup>st</sup> * 2 <sup>nd</sup> fixed parameter	3 <sup>rd</sup> variable parameter	$\log K_{\text{ow}}$ (-)		MW (g mol <sup>-1</sup> )		$\log K_{\text{ow}} * \text{MW}$ (g mol <sup>-1</sup> )		$\text{MW} * \log K_{\text{ow}}^{-1}$ (g mol <sup>-1</sup> )		$\log K_{\text{ow}} * \text{MW}^{-1}$ (mol g <sup>-1</sup> )		$(\log K_{\text{ow}} * \text{MW})^{-1}$ (mol g <sup>-1</sup> )	
		$R_v^2$	$R_h^2$	$R_v^2$	$R_h^2$	$R_v^2$	$R_h^2$	$R_v^2$	$R_h^2$	$R_v^2$	$R_h^2$		
$X_c$ (%)	SA (m <sup>2</sup> g <sup>-1</sup> )	0.12	0.69	0.13	0.68	0.13	0.69	0.11	0.65	0.11	0.65		
	SA <sup>-1</sup> (g m <sup>-2</sup> )	0.63	0.85	0.63	0.84	0.67	0.85	0.58	0.78	0.56	0.78		
	Vp (cm <sup>3</sup> g <sup>-1</sup> )	0.13	0.69	0.13	0.69	0.14	0.69	0.12	0.66	0.11	0.65		
	Vp <sup>-1</sup> (g cm <sup>-3</sup> )	0.61	0.85	0.62	0.84	0.66	0.85	0.57	0.78	0.55	0.78		
	$\sum \text{SFE}$ (mN m <sup>-1</sup> )	0.81	0.88	0.82	0.88	0.86	0.89	0.75	0.81	0.73	0.81		
	$\sum \text{SFE}^{-1}$ (m Nm <sup>-1</sup> )	0.22	0.75	0.22	0.74	0.24	0.75	0.20	0.71	0.19	0.70		

Table A7.77: Calculation of  $R_h^2$  and  $R_v^2$  with the matrix of two PAH properties ( $\log K_{\text{ow}}$ ,  $K_{\text{hdw}}$ ) multiplied with three plastic properties ( $X_c * T_g^{-1}$  as fixed parameters) and the  $\log K_{\text{p-w}}$  matrix

plastic property product		PAH properties											
1 <sup>st</sup> * 2 <sup>nd</sup> fixed parameter	3 <sup>rd</sup> variable parameter	$\log K_{\text{ow}}$ (-)		$\log K_{\text{hdw}}$ (-)		$\log K_{\text{ow}} * \log K_{\text{hdw}}$ (-)		$\log K_{\text{hdw}} * \log K_{\text{ow}}^{-1}$ (-)		$\log K_{\text{ow}} * \log K_{\text{hdw}}^{-1}$ (-)		$(\log K_{\text{ow}} * \log K_{\text{hdw}})^{-1}$ (-)	
		$R_v^2$	$R_h^2$	$R_v^2$	$R_h^2$	$R_v^2$	$R_h^2$	$R_v^2$	$R_h^2$	$R_v^2$	$R_h^2$		
$X_c$ (%)	SA (m <sup>2</sup> g <sup>-1</sup> )	0.12	0.69	0.13	0.68	0.13	0.69	0.11	0.65	0.11	0.65		
	SA <sup>-1</sup> (g m <sup>-2</sup> )	0.63	0.85	0.63	0.84	0.67	0.85	0.58	0.78	0.56	0.78		
	Vp (cm <sup>3</sup> g <sup>-1</sup> )	0.13	0.69	0.13	0.69	0.14	0.69	0.12	0.66	0.11	0.65		
	Vp <sup>-1</sup> (g cm <sup>-3</sup> )	0.61	0.85	0.62	0.84	0.66	0.85	0.57	0.78	0.55	0.78		
	$\sum \text{SFE}$ (mN m <sup>-1</sup> )	0.81	0.88	0.82	0.88	0.86	0.89	0.75	0.81	0.73	0.81		
	$\sum \text{SFE}^{-1}$ (m Nm <sup>-1</sup> )	0.22	0.75	0.22	0.74	0.24	0.75	0.20	0.71	0.19	0.70		

Table A7.78: Calculation of  $R_h^2$  and  $R_v^2$  with the matrix of two PAH properties ( $\log K_{ow}$ ,  $\log C_w^{sat}$ ) multiplied with three plastic properties ( $X_c * T_g^{-1}$  as fixed parameters) and the  $\log K_{p-w}$  matrix

plastic property product		PAH properties								
1 <sup>st</sup> * 2 <sup>nd</sup> fixed parameter	3 <sup>rd</sup> variable parameter	log $K_{ow}$ (-)	log $C_w^{sat}$ (mol m <sup>-3</sup> )	log $K_{ow} * \log C_w^{sat}$ (mol m <sup>-3</sup> )	log $C_w^{sat} * \log K_{ow}^{-1}$ (mol m <sup>-3</sup> )	log $K_{ow} * \log C_w^{sat-1}$ (m <sup>3</sup> mol <sup>-1</sup> )	(log $K_{ow} * \log C_w^{sat})^{-1}$ (m <sup>3</sup> mol <sup>-1</sup> )			
		$R_v^2$	$R_h^2$	$R_v^2$	$R_h^2$	$R_v^2$	$R_h^2$	$R_v^2$	$R_h^2$	
	SA (m <sup>2</sup> g <sup>-1</sup> )	0.12	0.69	0.14	0.68	0.14	0.67	0.00	0.62	
	SA <sup>-1</sup> (g m <sup>-2</sup> )	0.63	0.85	0.67	0.84	0.68	0.82	0.03	0.73	
$X_c$ (%)	*	Vp (cm <sup>3</sup> g <sup>-1</sup> )	0.13	0.69	0.15	0.69	0.15	0.68	0.00	0.62
$T_g^{-1}$ (K <sup>-1</sup> )	*	Vp <sup>-1</sup> (g cm <sup>-3</sup> )	0.61	0.85	0.66	0.84	0.66	0.82	0.03	0.73
		$\sum SFE$ (mN m <sup>-1</sup> )	0.81	0.88	0.84	0.88	0.83	0.85	0.06	0.75
		$\sum SFE^{-1}$ (m Nm <sup>-1</sup> )	0.22	0.75	0.26	0.74	0.26	0.73	0.00	0.67

Table A7.79: Calculation of  $R_h^2$  and  $R_v^2$  with the matrix of two PAH properties (MW,  $\log K_{hdw}$ ) multiplied with three plastic properties ( $X_c * T_g^{-1}$  as fixed parameters) and the  $\log K_{p-w}$  matrix

plastic property product		PAH properties								
1 <sup>st</sup> * 2 <sup>nd</sup> fixed parameter	3 <sup>rd</sup> variable parameter	MW (g mol <sup>-1</sup> )	log $K_{hdw}$ (-)	MW * log $K_{hdw}$ (g mol <sup>-1</sup> )	MW * log $K_{hdw}^{-1}$ (g mol <sup>-1</sup> )	log $K_{hdw} * MW^1$ (mol g <sup>-1</sup> )	(MW * log $K_{hdw})^{-1}$ (mol g <sup>-1</sup> )			
		$R_v^2$	$R_h^2$	$R_v^2$	$R_h^2$	$R_v^2$	$R_h^2$	$R_v^2$	$R_h^2$	
	SA (m <sup>2</sup> g <sup>-1</sup> )	0.13	0.68	0.12	0.69	0.06	0.13	0.11	0.60	
	SA <sup>-1</sup> (g m <sup>-2</sup> )	0.63	0.84	0.63	0.85	0.22	0.23	0.57	0.70	
$X_c$ (%)	*	Vp (cm <sup>3</sup> g <sup>-1</sup> )	0.13	0.69	0.13	0.69	0.06	0.13	0.12	0.60
$T_g^{-1}$ (K <sup>-1</sup> )	*	Vp <sup>-1</sup> (g cm <sup>-3</sup> )	0.62	0.84	0.62	0.85	0.22	0.23	0.55	0.70
		$\sum SFE$ (mN m <sup>-1</sup> )	0.82	0.88	0.81	0.88	0.29	0.26	0.74	0.72
		$\sum SFE^{-1}$ (m Nm <sup>-1</sup> )	0.22	0.74	0.22	0.75	0.09	0.15	0.19	0.65

Table A7.80: Calculation of  $R_h^2$  and  $R_v^2$  with the matrix of two PAH properties (MW,  $\log C_w^{sat}$ ) multiplied with three plastic properties ( $X_c * T_g^{-1}$  as fixed parameters) and the  $\log K_{p-w}$  matrix

plastic property product		PAH properties								
1 <sup>st</sup> * 2 <sup>nd</sup> fixed parameter	3 <sup>rd</sup> variable parameter	MW (g mol <sup>-1</sup> )	log $C_w^{sat}$ (mol m <sup>-3</sup> )	MW * log $C_w^{sat}$ (g m <sup>-3</sup> )	log $C_w^{sat} * MW^1$ (mol <sup>2</sup> m <sup>-3</sup> g <sup>-1</sup> )	MW * log $C_w^{sat-1}$ (g m <sup>3</sup> mol <sup>-2</sup> )	(log $K_{ow} * \log C_w^{sat})^{-1}$ (m <sup>3</sup> g <sup>-1</sup> )			
		$R_v^2$	$R_h^2$	$R_v^2$	$R_h^2$	$R_v^2$	$R_h^2$	$R_v^2$	$R_h^2$	
	SA (m <sup>2</sup> g <sup>-1</sup> )	0.13	0.68	0.14	0.68	0.07	0.03	0.14	0.67	
	SA <sup>-1</sup> (g m <sup>-2</sup> )	0.63	0.84	0.67	0.84	0.20	0.01	0.67	0.82	
$X_c$ (%)	*	Vp (cm <sup>3</sup> g <sup>-1</sup> )	0.13	0.69	0.15	0.69	0.07	0.03	0.15	0.68
$T_g^{-1}$ (K <sup>-1</sup> )	*	Vp <sup>-1</sup> (g cm <sup>-3</sup> )	0.62	0.84	0.66	0.84	0.20	0.01	0.66	0.82
		$\sum SFE$ (mN m <sup>-1</sup> )	0.82	0.88	0.84	0.88	0.24	0.01	0.83	0.85
		$\sum SFE^{-1}$ (m Nm <sup>-1</sup> )	0.22	0.74	0.26	0.74	0.10	0.03	0.26	0.73

Table A7.81: Calculation of  $R_h^2$  and  $R_v^2$  with the matrix of two PAH properties ( $\log K_{hdw}$ ,  $\log C_w^{sat}$ ) multiplied with three plastic properties ( $X_c * T_g^{-1}$  as fixed parameters) and the  $\log K_{p-w}$  matrix

plastic property product		PAH properties								
1 <sup>st</sup> * 2 <sup>nd</sup> fixed parameter	3 <sup>rd</sup> variable parameter	log $K_{hdw}$ (-)	log $C_w^{sat}$ (mol m <sup>-3</sup> )	log $K_{hdw} * \log C_w^{sat}$ (mol m <sup>-3</sup> )	log $C_w^{sat} * \log K_{hdw}^{-1}$ (mol m <sup>-3</sup> )	log $K_{hdw} * \log C_w^{sat-1}$ (m <sup>3</sup> mol <sup>-1</sup> )	(log $K_{hdw} * \log C_w^{sat})^{-1}$ (m <sup>3</sup> mol <sup>-1</sup> )			
		$R_v^2$	$R_h^2$	$R_v^2$	$R_h^2$	$R_v^2$	$R_h^2$	$R_v^2$	$R_h^2$	
	SA (m <sup>2</sup> g <sup>-1</sup> )	0.12	0.69	0.14	0.68	0.14	0.69	0.14	0.67	
	SA <sup>-1</sup> (g m <sup>-2</sup> )	0.63	0.85	0.67	0.84	0.68	0.86	0.67	0.82	
$X_c$ (%)	*	Vp (cm <sup>3</sup> g <sup>-1</sup> )	0.13	0.69	0.15	0.69	0.15	0.68	0.00	0.62
$T_g^{-1}$ (K <sup>-1</sup> )	*	Vp <sup>-1</sup> (g cm <sup>-3</sup> )	0.62	0.85	0.66	0.84	0.66	0.86	0.03	0.73
		$\sum SFE$ (mN m <sup>-1</sup> )	0.81	0.88	0.84	0.88	0.84	0.90	0.83	0.85
		$\sum SFE^{-1}$ (m Nm <sup>-1</sup> )	0.22	0.75	0.26	0.74	0.26	0.75	0.00	0.67

Table A7.82: Calculation of  $R_h^2$  and  $R_v^2$  with the matrix of two PAH properties ( $\log K_{ow}$ , MW,) multiplied with three plastic properties ( $X_c * SA$  as fixed parameters) and the  $\log K_{p-w}$  matrix

plastic property product		PAH properties											
1 <sup>st</sup> * 2 <sup>nd</sup> fixed parameter	3 <sup>rd</sup> variable parameter	$\log K_{ow}$ (-)		MW (g mol <sup>-1</sup> )		$\log K_{ow} * MW$ (g mol <sup>-1</sup> )		$MW * \log K_{ow}^{-1}$ (g mol <sup>-1</sup> )		$\log K_{ow} * MW^{-1}$ (mol g <sup>-1</sup> )		$(\log K_{ow} * MW)^{-1}$ (mol g <sup>-1</sup> )	
		$R_v^2$	$R_h^2$	$R_v^2$	$R_h^2$	$R_v^2$	$R_h^2$	$R_v^2$	$R_h^2$	$R_v^2$	$R_h^2$		
$X_c$ (%)	$Vp$ (cm <sup>3</sup> g <sup>-1</sup> )	0.00	0.26	0.00	0.26	0.00	0.26	0.00	0.25	0.00	0.25		
*	$Vp^{-1}$ (g cm <sup>-3</sup> )	0.83	0.95	0.84	0.95	0.88	0.96	0.77	0.89	0.74	0.88		
SA (m <sup>2</sup> g <sup>-1</sup> )	$\sum SFE$ (mN m <sup>-1</sup> )	0.31	0.75	0.32	0.74	0.33	0.75	0.29	0.70	0.28	0.70		
	$\sum SFE^{-1}$ (m Nm <sup>-1</sup> )	0.00	0.42	0.00	0.42	0.00	0.42	0.00	0.41	0.00	0.41		

Table A7.83: Calculation of  $R_h^2$  and  $R_v^2$  with the matrix of two PAH properties ( $\log K_{ow}$ ,  $\log K_{hdw}$ ) multiplied with three plastic properties ( $X_c * SA$  as fixed parameters) and the  $\log K_{p-w}$  matrix

plastic property product		PAH properties											
1 <sup>st</sup> * 2 <sup>nd</sup> fixed parameter	3 <sup>rd</sup> variable parameter	$\log K_{ow}$ (-)		$\log K_{hdw}$ (-)		$\log K_{ow} * \log K_{hdw}$ (-)		$\log K_{hdw} * \log K_{ow}^{-1}$ (-)		$\log K_{ow} * \log K_{hdw}^{-1}$ (-)		$(\log K_{ow} * \log K_{hdw})^{-1}$ (-)	
		$R_v^2$	$R_h^2$	$R_v^2$	$R_h^2$	$R_v^2$	$R_h^2$	$R_v^2$	$R_h^2$	$R_v^2$	$R_h^2$		
$X_c$ (%)	$Vp$ (cm <sup>3</sup> g <sup>-1</sup> )	0.00	0.26	0.00	0.26	0.00	0.26	0.00	0.25	0.00	0.25	0.00	0.25
*	$Vp^{-1}$ (g cm <sup>-3</sup> )	0.83	0.95	0.84	0.95	0.88	0.96	0.77	0.89	0.74	0.88	0.54	0.92
SA (m <sup>2</sup> g <sup>-1</sup> )	$\sum SFE$ (mN m <sup>-1</sup> )	0.31	0.75	0.32	0.74	0.33	0.75	0.29	0.70	0.28	0.70	0.21	0.73
	$\sum SFE^{-1}$ (m Nm <sup>-1</sup> )	0.00	0.42	0.00	0.42	0.00	0.42	0.00	0.41	0.00	0.41	0.00	0.42

Table A7.84: Calculation of  $R_h^2$  and  $R_v^2$  with the matrix of two PAH properties ( $\log K_{ow}$ ,  $\log C_w^{sat}$ ) multiplied with three plastic properties ( $X_c * SA$  as fixed parameters) and the  $\log K_{p-w}$  matrix

plastic property product		PAH properties											
1 <sup>st</sup> * 2 <sup>nd</sup> fixed parameter	3 <sup>rd</sup> variable parameter	$\log K_{ow}$ (-)		$\log C_w^{sat}$ (mol m <sup>-3</sup> )		$\log K_{ow} * \log C_w^{sat}$ (mol m <sup>-3</sup> )		$\log C_w^{sat} * \log K_{ow}^{-1}$ (mol m <sup>-3</sup> )		$\log K_{ow} * \log C_w^{sat-1}$ (m <sup>3</sup> mol <sup>-1</sup> )		$(\log K_{ow} * \log C_w^{sat})^{-1}$ (m <sup>3</sup> mol <sup>-1</sup> )	
		$R_v^2$	$R_h^2$	$R_v^2$	$R_h^2$	$R_v^2$	$R_h^2$	$R_v^2$	$R_h^2$	$R_v^2$	$R_h^2$		
$X_c$ (%)	$Vp$ (cm <sup>3</sup> g <sup>-1</sup> )	0.00	0.26	0.00	0.26	0.00	0.26	0.00	0.26	0.00	0.24	0.00	0.24
*	$Vp^{-1}$ (g cm <sup>-3</sup> )	0.83	0.95	0.89	0.95	0.89	0.96	0.88	0.93	0.05	0.83	0.04	0.83
SA (m <sup>2</sup> g <sup>-1</sup> )	$\sum SFE$ (mN m <sup>-1</sup> )	0.31	0.75	0.33	0.74	0.33	0.75	0.33	0.73	0.02	0.66	0.02	0.66
	$\sum SFE^{-1}$ (m Nm <sup>-1</sup> )	0.00	0.42	0.01	0.42	0.01	0.42	0.01	0.42	0.00	0.39	0.00	0.39

Table A7.85: Calculation of  $R_h^2$  and  $R_v^2$  with the matrix of two PAH properties (MW,  $\log K_{hdw}$ ) multiplied with three plastic properties ( $X_c * SA$  as fixed parameters) and the  $\log K_{p-w}$  matrix

plastic property product		PAH properties											
1 <sup>st</sup> * 2 <sup>nd</sup> fixed parameter	3 <sup>rd</sup> variable parameter	MW (g mol <sup>-1</sup> )		$\log K_{hdw}$ (-)		$MW * \log K_{hdw}$ (g mol <sup>-1</sup> )		$MW * \log K_{hdw}^{-1}$ (g mol <sup>-1</sup> )		$\log K_{hdw} * MW^{-1}$ (mol g <sup>-1</sup> )		$(MW * \log K_{hdw})^{-1}$ (mol g <sup>-1</sup> )	
		$R_v^2$	$R_h^2$	$R_v^2$	$R_h^2$	$R_v^2$	$R_h^2$	$R_v^2$	$R_h^2$	$R_v^2$	$R_h^2$		
$X_c$ (%)	$Vp$ (cm <sup>3</sup> g <sup>-1</sup> )	0.00	0.26	0.00	0.26	0.00	0.03	0.00	0.24	0.00	0.24	0.00	0.25
*	$Vp^{-1}$ (g cm <sup>-3</sup> )	0.84	0.95	0.83	0.95	0.31	0.23	0.75	0.80	0.76	0.80	0.53	0.92
SA (m <sup>2</sup> g <sup>-1</sup> )	$\sum SFE$ (mN m <sup>-1</sup> )	0.32	0.74	0.32	0.75	0.13	0.17	0.29	0.64	0.29	0.64	0.21	0.72
	$\sum SFE^{-1}$ (m Nm <sup>-1</sup> )	0.00	0.42	0.00	0.42	0.00	0.06	0.00	0.38	0.00	0.38	0.00	0.42

Table A7.86: Calculation of  $R_h^2$  and  $R_v^2$  with the matrix of two PAH properties (MW,  $\log C_w^{\text{sat}}$ ) multiplied with three plastic properties ( $X_c * \text{SA}$  as fixed parameters) and the  $\log K_{\text{p-w}}$  matrix

plastic property product		PAH properties											
1 <sup>st</sup> * 2 <sup>nd</sup> fixed parameter	3 <sup>rd</sup> variable parameter	MW (g mol <sup>-1</sup> )		$\log C_w^{\text{sat}}$ (mol m <sup>-3</sup> )		MW * $\log C_w^{\text{sat}}$ (g m <sup>-3</sup> )		$\log C_w^{\text{sat}} * MW^{-1}$ (mol <sup>2</sup> m <sup>-3</sup> g <sup>-1</sup> )		MW * $\log C_w^{\text{sat}-1}$ (g m <sup>3</sup> mol <sup>-2</sup> )		$(\log K_{\text{ow}} * \log C_w^{\text{sat}})^{-1}$ (m <sup>3</sup> g <sup>-1</sup> )	
		$R_v^2$	$R_h^2$	$R_v^2$	$R_h^2$	$R_v^2$	$R_h^2$	$R_v^2$	$R_h^2$	$R_v^2$	$R_h^2$		
$X_c$ (%)	Vp (cm <sup>3</sup> g <sup>-1</sup> )	0.00	0.26	0.00	0.26	0.00	0.02	0.00	0.26	0.00	0.24		
	Vp <sup>-1</sup> (g cm <sup>-3</sup> )	0.84	0.95	0.89	0.95	0.29	0.02	0.88	0.93	0.05	0.83		
	$\sum \text{SFE}$ (mN m <sup>-1</sup> )	0.32	0.74	0.33	0.74	0.12	0.02	0.33	0.73	0.02	0.66		
SA (m <sup>2</sup> g <sup>-1</sup> )	$\sum \text{SFE}^{-1}$ (m Nm <sup>-1</sup> )	0.00	0.42	0.01	0.42	0.01	0.03	0.01	0.42	0.00	0.39		

Table A7.87: Calculation of  $R_h^2$  and  $R_v^2$  with the matrix of two PAH properties ( $\log K_{\text{hdw}}$ ,  $\log C_w^{\text{sat}}$ ) multiplied with three plastic properties ( $X_c * \text{SA}$  as fixed parameters) and the  $\log K_{\text{p-w}}$  matrix

plastic property product		PAH properties											
1 <sup>st</sup> * 2 <sup>nd</sup> fixed parameter	3 <sup>rd</sup> variable parameter	$\log K_{\text{hdw}}$ (-)		$\log C_w^{\text{sat}}$ (mol m <sup>-3</sup> )		$\log K_{\text{hdw}} * \log C_w^{\text{sat}}$ (mol m <sup>-3</sup> )		$\log C_w^{\text{sat}} * \log K_{\text{hdw}}^{-1}$ (mol m <sup>-3</sup> )		$\log K_{\text{hdw}} * \log C_w^{\text{sat}-1}$ (m <sup>3</sup> mol <sup>-1</sup> )		$(\log K_{\text{hdw}} * \log C_w^{\text{sat}})^{-1}$ (m <sup>3</sup> mol <sup>-1</sup> )	
		$R_v^2$	$R_h^2$	$R_v^2$	$R_h^2$	$R_v^2$	$R_h^2$	$R_v^2$	$R_h^2$	$R_v^2$	$R_h^2$		
$X_c$ (%)	Vp (cm <sup>3</sup> g <sup>-1</sup> )	0.00	0.26	0.00	0.26	0.00	0.26	0.00	0.26	0.00	0.24		
	Vp <sup>-1</sup> (g cm <sup>-3</sup> )	0.83	0.95	0.89	0.95	0.89	0.96	0.88	0.93	0.05	0.83		
	$\sum \text{SFE}$ (mN m <sup>-1</sup> )	0.32	0.75	0.33	0.74	0.33	0.76	0.33	0.73	0.02	0.66		
SA (m <sup>2</sup> g <sup>-1</sup> )	$\sum \text{SFE}^{-1}$ (m Nm <sup>-1</sup> )	0.00	0.42	0.01	0.42	0.01	0.42	0.01	0.42	0.00	0.39		

Table A7.88: Calculation of  $R_h^2$  and  $R_v^2$  with the matrix of two PAH properties ( $\log K_{\text{ow}}$ , MW,) multiplied with three plastic properties ( $X_c * \text{SA}^{-1}$  as fixed parameters) and the  $\log K_{\text{p-w}}$  matrix

plastic property product		PAH properties											
1 <sup>st</sup> * 2 <sup>nd</sup> fixed parameter	3 <sup>rd</sup> variable parameter	$\log K_{\text{ow}}$ (-)		MW (g mol <sup>-1</sup> )		$\log K_{\text{ow}} * MW$ (g mol <sup>-1</sup> )		$MW * \log K_{\text{ow}}^{-1}$ (g mol <sup>-1</sup> )		$\log K_{\text{ow}} * MW^{-1}$ (mol g <sup>-1</sup> )		$(\log K_{\text{ow}} * MW)^{-1}$ (mol g <sup>-1</sup> )	
		$R_v^2$	$R_h^2$	$R_v^2$	$R_h^2$	$R_v^2$	$R_h^2$	$R_v^2$	$R_h^2$	$R_v^2$	$R_h^2$		
$X_c$ (%)	Vp (cm <sup>3</sup> g <sup>-1</sup> )	0.85	0.95	0.86	0.95	0.91	0.96	0.79	0.89	0.76	0.88	0.55	0.92
	Vp <sup>-1</sup> (g cm <sup>-3</sup> )	0.70	0.81	0.71	0.81	0.74	0.82	0.65	0.74	0.63	0.74	0.46	0.78
	$\sum \text{SFE}$ (mN m <sup>-1</sup> )	0.65	0.73	0.66	0.72	0.69	0.74	0.61	0.66	0.59	0.66	0.45	0.69
SA <sup>-1</sup> (g m <sup>-2</sup> )	$\sum \text{SFE}^{-1}$ (m Nm <sup>-1</sup> )	0.44	0.82	0.44	0.82	0.47	0.83	0.40	0.76	0.39	0.76	0.27	0.79

Table A7.89: Calculation of  $R_h^2$  and  $R_v^2$  with the matrix of two PAH properties ( $\log K_{\text{ow}}$ ,  $\log K_{\text{hdw}}$ ) multiplied with three plastic properties ( $X_c * \text{SA}^{-1}$  as fixed parameters) and the  $\log K_{\text{p-w}}$  matrix

plastic property product		PAH properties											
1 <sup>st</sup> * 2 <sup>nd</sup> fixed parameter	3 <sup>rd</sup> variable parameter	$\log K_{\text{ow}}$ (-)		$\log K_{\text{hdw}}$ (-)		$\log K_{\text{ow}} * \log K_{\text{hdw}}$ (-)		$\log K_{\text{hdw}} * \log K_{\text{ow}}^{-1}$ (-)		$\log K_{\text{ow}} * \log K_{\text{hdw}}^{-1}$ (-)		$(\log K_{\text{ow}} * \log K_{\text{hdw}})^{-1}$ (-)	
		$R_v^2$	$R_h^2$	$R_v^2$	$R_h^2$	$R_v^2$	$R_h^2$	$R_v^2$	$R_h^2$	$R_v^2$	$R_h^2$		
$X_c$ (%)	Vp (cm <sup>3</sup> g <sup>-1</sup> )	0.85	0.95	0.86	0.95	0.91	0.96	0.79	0.89	0.76	0.88	0.55	0.92
	Vp <sup>-1</sup> (g cm <sup>-3</sup> )	0.70	0.81	0.71	0.81	0.74	0.82	0.65	0.74	0.63	0.74	0.46	0.78
	$\sum \text{SFE}$ (mN m <sup>-1</sup> )	0.65	0.73	0.66	0.72	0.69	0.74	0.61	0.66	0.59	0.66	0.45	0.69
SA <sup>-1</sup> (g m <sup>-2</sup> )	$\sum \text{SFE}^{-1}$ (m Nm <sup>-1</sup> )	0.44	0.82	0.44	0.82	0.47	0.83	0.40	0.76	0.39	0.76	0.27	0.79

Table A7.90: Calculation of  $R_h^2$  and  $R_v^2$  with the matrix of two PAH properties ( $\log K_{ow}$ ,  $\log C_w^{sat}$ ) multiplied with three plastic properties ( $X_c * SA^{-1}$  as fixed parameters) and the  $\log K_{p-w}$  matrix

plastic property product 1 <sup>st</sup> * 2 <sup>nd</sup> fixed * variable parameter	$\log K_{ow}$ (-)	PAH properties						
		$R_v^2$	$R_h^2$	$R_v^2$	$R_h^2$	$R_v^2$	$R_h^2$	$R_v^2$
$X_c (\%)$	$Vp (\text{cm}^3 \text{g}^{-1})$	0.85	0.95	0.91	0.95	0.91	0.96	0.90
*	$Vp^{-1} (\text{g cm}^{-3})$	0.70	0.81	0.73	0.81	0.74	0.82	0.72
$SA^{-1} (\text{g m}^{-2})$	$\sum SFE (\text{mN m}^{-1})$	0.65	0.73	0.67	0.72	0.67	0.74	0.66
	$\sum SFE^{-1} (\text{m Nm}^{-1})$	0.44	0.82	0.49	0.82	0.49	0.83	0.49

Table A7.91: Calculation of  $R_h^2$  and  $R_v^2$  with the matrix of two PAH properties (MW,  $\log K_{hdw}$ ) multiplied with three plastic properties ( $X_c * SA^{-1}$  as fixed parameters) and the  $\log K_{p-w}$  matrix

plastic property product 1 <sup>st</sup> * 2 <sup>nd</sup> fixed * variable parameter	MW (g mol <sup>-1</sup> )	PAH properties						
		$R_v^2$	$R_h^2$	$R_v^2$	$R_h^2$	$R_v^2$	$R_h^2$	$R_v^2$
$X_c (\%)$	$Vp (\text{cm}^3 \text{g}^{-1})$	0.86	0.95	0.86	0.95	0.32	0.24	0.77
*	$Vp^{-1} (\text{g cm}^{-3})$	0.71	0.81	0.70	0.81	0.24	0.24	0.63
$SA^{-1} (\text{g m}^{-2})$	$\sum SFE (\text{mN m}^{-1})$	0.66	0.72	0.66	0.73	0.23	0.24	0.60
	$\sum SFE^{-1} (\text{m Nm}^{-1})$	0.44	0.82	0.44	0.82	0.16	0.20	0.39

Table A7.92: Calculation of  $R_h^2$  and  $R_v^2$  with the matrix of two PAH properties (MW,  $\log C_w^{sat}$ ) multiplied with three plastic properties ( $X_c * SA^{-1}$  as fixed parameters) and the  $\log K_{p-w}$  matrix

plastic property product 1 <sup>st</sup> * 2 <sup>nd</sup> fixed * variable parameter	MW (g mol <sup>-1</sup> )	PAH properties						
		$R_v^2$	$R_h^2$	$R_v^2$	$R_h^2$	$R_v^2$	$R_h^2$	$R_v^2$
$X_c (\%)$	$Vp (\text{cm}^3 \text{g}^{-1})$	0.86	0.95	0.91	0.95	0.29	0.02	0.90
*	$Vp^{-1} (\text{g cm}^{-3})$	0.71	0.81	0.73	0.81	0.21	0.01	0.72
$SA^{-1} (\text{g m}^{-2})$	$\sum SFE (\text{mN m}^{-1})$	0.66	0.72	0.67	0.72	0.18	0.00	0.66
	$\sum SFE^{-1} (\text{m Nm}^{-1})$	0.44	0.82	0.49	0.82	0.16	0.02	0.49

Table A7.93: Calculation of  $R_h^2$  and  $R_v^2$  with the matrix of two PAH properties ( $\log K_{hdw}$ ,  $\log C_w^{sat}$ ) multiplied with three plastic properties ( $X_c * SA^{-1}$  as fixed parameters) and the  $\log K_{p-w}$  matrix

plastic property product 1 <sup>st</sup> * 2 <sup>nd</sup> fixed * variable parameter	$\log K_{hdw}$ (-)	PAH properties						
		$R_v^2$	$R_h^2$	$R_v^2$	$R_h^2$	$R_v^2$	$R_h^2$	$R_v^2$
$X_c (\%)$	$Vp (\text{cm}^3 \text{g}^{-1})$	0.86	0.95	0.91	0.95	0.91	0.96	0.90
*	$Vp^{-1} (\text{g cm}^{-3})$	0.70	0.81	0.73	0.81	0.74	0.82	0.72
$SA^{-1} (\text{g m}^{-2})$	$\sum SFE (\text{mN m}^{-1})$	0.66	0.73	0.67	0.72	0.67	0.74	0.66
	$\sum SFE^{-1} (\text{m Nm}^{-1})$	0.44	0.82	0.49	0.82	0.49	0.83	0.49

Table A7.94: Calculation of  $R_h^2$  and  $R_v^2$  with the matrix of two PAH properties ( $\log K_{ow}$ , MW,) multiplied with three plastic properties ( $X_c * Vp$  as fixed parameters) and the  $\log K_{p-w}$  matrix

plastic property product		PAH properties											
1 <sup>st</sup> * 2 <sup>nd</sup> fixed parameter	3 <sup>rd</sup> variable parameter	$\log K_{ow}$ (-)		MW (g mol <sup>-1</sup> )		$\log K_{ow} * MW$ (g mol <sup>-1</sup> )		$MW * \log K_{ow}^{-1}$ (g mol <sup>-1</sup> )		$\log K_{ow} * MW^{-1}$ (mol g <sup>-1</sup> )		$(\log K_{ow} * MW)^{-1}$ (mol g <sup>-1</sup> )	
		$R_v^2$	$R_h^2$	$R_v^2$	$R_h^2$	$R_v^2$	$R_h^2$	$R_v^2$	$R_h^2$	$R_v^2$	$R_h^2$	$R_v^2$	$R_h^2$
$X_c (\%) * \sum SFE (\text{mN m}^{-1})$		0.33	0.75	0.33	0.75	0.35	0.76	0.31	0.70	0.30	0.70	0.22	0.73
$Vp (\text{cm}^3 \text{g}^{-1}) * \sum SFE^{-1} (\text{m Nm}^{-1})$		0.00	0.42	0.00	0.42	0.00	0.42	0.00	0.41	0.00	0.41	0.00	0.42

Table A7.95: Calculation of  $R_h^2$  and  $R_v^2$  with the matrix of two PAH properties ( $\log K_{ow}$ ,  $\log K_{hdw}$ ) multiplied with three plastic properties ( $X_c * Vp$  as fixed parameters) and the  $\log K_{p-w}$  matrix

plastic property product		PAH properties											
1 <sup>st</sup> * 2 <sup>nd</sup> fixed parameter	3 <sup>rd</sup> variable parameter	$\log K_{ow}$ (-)		$\log K_{hdw}$ (-)		$\log K_{ow} * \log K_{hdw}$ (-)		$\log K_{hdw} * \log K_{ow}^{-1}$ (-)		$\log K_{ow} * \log K_{hdw}^{-1}$ (-)		$(\log K_{ow} * \log K_{hdw})^{-1}$ (-)	
		$R_v^2$	$R_h^2$	$R_v^2$	$R_h^2$	$R_v^2$	$R_h^2$	$R_v^2$	$R_h^2$	$R_v^2$	$R_h^2$	$R_v^2$	$R_h^2$
$X_c (\%) * \sum SFE (\text{mN m}^{-1})$		0.33	0.75	0.33	0.75	0.35	0.76	0.31	0.70	0.30	0.70	0.22	0.73
$Vp (\text{cm}^3 \text{g}^{-1}) * \sum SFE^{-1} (\text{m Nm}^{-1})$		0.00	0.42	0.00	0.42	0.00	0.42	0.00	0.41	0.00	0.41	0.00	0.42

Table A7.96: Calculation of  $R_h^2$  and  $R_v^2$  with the matrix of two PAH properties ( $\log K_{ow}$ ,  $\log C_w^{sat}$ ) multiplied with three plastic properties ( $X_c * Vp$  as fixed parameters) and the  $\log K_{p-w}$  matrix

plastic property product		PAH properties											
1 <sup>st</sup> * 2 <sup>nd</sup> fixed parameter	3 <sup>rd</sup> variable parameter	$\log K_{ow}$ (-)		$\log C_w^{sat}$ (mol m <sup>-3</sup> )		$\log K_{ow} * \log C_w^{sat}$ (mol m <sup>-3</sup> )		$\log C_w^{sat} * \log K_{ow}^{-1}$ (mol m <sup>-3</sup> )		$\log K_{ow} * \log C_w^{sat-1}$ (m <sup>3</sup> mol <sup>-1</sup> )		$(\log K_{ow} * \log C_w^{sat})^{-1}$ (m <sup>3</sup> mol <sup>-1</sup> )	
		$R_v^2$	$R_h^2$	$R_v^2$	$R_h^2$	$R_v^2$	$R_h^2$	$R_v^2$	$R_h^2$	$R_v^2$	$R_h^2$	$R_v^2$	$R_h^2$
$X_c (\%) * \sum SFE (\text{mN m}^{-1})$		0.33	0.75	0.34	0.75	0.34	0.76	0.34	0.73	0.02	0.66	0.02	0.66
$Vp (\text{cm}^3 \text{g}^{-1}) * \sum SFE^{-1} (\text{m Nm}^{-1})$		0.00	0.42	0.01	0.42	0.01	0.42	0.01	0.42	0.00	0.39	0.00	0.39

Table A7.97: Calculation of  $R_h^2$  and  $R_v^2$  with the matrix of two PAH properties (MW,  $\log K_{hdw}$ ) multiplied with three plastic properties ( $X_c * Vp$  as fixed parameters) and the  $\log K_{p-w}$  matrix

plastic property product		PAH properties											
1 <sup>st</sup> * 2 <sup>nd</sup> fixed parameter	3 <sup>rd</sup> variable parameter	MW (g mol <sup>-1</sup> )		$\log K_{hdw}$ (-)		$MW * \log K_{hdw}$ (g mol <sup>-1</sup> )		$MW * \log K_{hdw}^{-1}$ (g mol <sup>-1</sup> )		$\log K_{hdw} * MW^{-1}$ (mol g <sup>-1</sup> )		$(MW * \log K_{hdw})^{-1}$ (mol g <sup>-1</sup> )	
		$R_v^2$	$R_h^2$	$R_v^2$	$R_h^2$	$R_v^2$	$R_h^2$	$R_v^2$	$R_h^2$	$R_v^2$	$R_h^2$	$R_v^2$	$R_h^2$
$X_c (\%) * \sum SFE (\text{mN m}^{-1})$		0.33	0.75	0.33	0.75	0.13	0.17	0.30	0.64	0.30	0.64	0.21	0.73
$Vp (\text{cm}^3 \text{g}^{-1}) * \sum SFE^{-1} (\text{m Nm}^{-1})$		0.00	0.42	0.00	0.42	0.01	0.06	0.00	0.38	0.00	0.38	0.00	0.42

Table A7.98: Calculation of  $R_h^2$  and  $R_v^2$  with the matrix of two PAH properties (MW,  $\log C_w^{sat}$ ) multiplied with three plastic properties ( $X_c * Vp$  as fixed parameters) and the  $\log K_{p-w}$  matrix

plastic property product		PAH properties											
1 <sup>st</sup> * 2 <sup>nd</sup> fixed parameter	3 <sup>rd</sup> variable parameter	MW (g mol <sup>-1</sup> )		$\log C_w^{sat}$ (mol m <sup>-3</sup> )		$MW * \log C_w^{sat}$ (g m <sup>-3</sup> )		$\log C_w^{sat} * MW^{-1}$ (mol <sup>2</sup> m <sup>-3</sup> g <sup>-1</sup> )		$MW * \log C_w^{sat-1}$ (g m <sup>3</sup> mol <sup>-2</sup> )		$(\log K_{ow} * \log C_w^{sat})^{-1}$ (m <sup>3</sup> g <sup>-1</sup> )	
		$R_v^2$	$R_h^2$	$R_v^2$	$R_h^2$	$R_v^2$	$R_h^2$	$R_v^2$	$R_h^2$	$R_v^2$	$R_h^2$	$R_v^2$	$R_h^2$
$X_c (\%) * \sum SFE (\text{mN m}^{-1})$		0.33	0.75	0.34	0.75	0.12	0.02	0.34	0.73	0.02	0.66	0.02	0.66
$Vp (\text{cm}^3 \text{g}^{-1}) * \sum SFE^{-1} (\text{m Nm}^{-1})$		0.00	0.42	0.01	0.42	0.01	0.03	0.01	0.42	0.00	0.39	0.00	0.39

Table A7.99: Calculation of  $R_h^2$  and  $R_v^2$  with the matrix of two PAH properties ( $\log K_{hdw}$ ,  $\log C_w^{sat}$ ) multiplied with three plastic properties ( $X_c * Vp$  as fixed parameters) and the  $\log K_{p-w}$  matrix

plastic property product		PAH properties							
1 <sup>st</sup> * 2 <sup>nd</sup> fixed parameter	3 <sup>rd</sup> variable parameter	$\log K_{hdw}$	$\log C_w^{sat}$ (mol m <sup>-3</sup> )	$\log K_{hdw} * \log C_w^{sat}$ (mol m <sup>-3</sup> )	$\log C_w^{sat} * \log K_{hdw}^{-1}$ (mol m <sup>-3</sup> )	$\log K_{hdw} * \log C_w^{sat-1}$ (m <sup>3</sup> mol <sup>-1</sup> )	$(\log K_{hdw} * \log C_w^{sat})^{-1}$ (m <sup>3</sup> mol <sup>-1</sup> )		
		$R_v^2$	$R_h^2$	$R_v^2$	$R_h^2$	$R_v^2$	$R_h^2$	$R_v^2$	$R_h^2$
$X_c (\%) * \sum SFE (mN m^{-1})$		0.33	0.75	0.34	0.75	0.34	0.76	0.34	0.73
$Vp (cm^3 g^{-1})$	$\sum SFE^{-1} (m Nm^{-1})$	0.00	0.42	0.01	0.42	0.01	0.42	0.01	0.42

Table A7.100: Calculation of  $R_h^2$  and  $R_v^2$  with the matrix of two PAH properties ( $\log K_{ow}$ , MW<sub>w</sub>) multiplied with three plastic properties ( $X_c * Vp^{-1}$  as fixed parameters) and the  $\log K_{p-w}$  matrix

plastic property product		PAH properties							
1 <sup>st</sup> * 2 <sup>nd</sup> fixed parameter	3 <sup>rd</sup> variable parameter	$\log K_{ow}$ (-)	MW <sub>w</sub> (g mol <sup>-1</sup> )	$\log K_{ow} * MW$ (g mol <sup>-1</sup> )	$MW * \log K_{ow}^{-1}$ (g mol <sup>-1</sup> )	$\log K_{ow} * MW^{-1}$ (mol g <sup>-1</sup> )	$(\log K_{ow} * MW)^{-1}$ (mol g <sup>-1</sup> )		
		$R_v^2$	$R_h^2$	$R_v^2$	$R_h^2$	$R_v^2$	$R_h^2$	$R_v^2$	$R_h^2$
$X_c (\%) * \sum SFE (mN m^{-1})$		0.66	0.74	0.67	0.73	0.70	0.74	0.62	0.67
$Vp^{-1} (g cm^{-3})$	$\sum SFE^{-1} (m Nm^{-1})$	0.42	0.81	0.43	0.81	0.45	0.82	0.39	0.76

Table A7.101: Calculation of  $R_h^2$  and  $R_v^2$  with the matrix of two PAH properties ( $\log K_{ow}$ ,  $\log K_{hdw}$ ) multiplied with three plastic properties ( $X_c * Vp^{-1}$  as fixed parameters) and the  $\log K_{p-w}$  matrix

plastic property product		PAH properties							
1 <sup>st</sup> * 2 <sup>nd</sup> fixed parameter	3 <sup>rd</sup> variable parameter	$\log K_{ow}$	$\log K_{hdw}$	$\log K_{ow} * \log K_{hdw}$	$\log K_{hdw} * \log K_{ow}^{-1}$	$\log K_{ow} * \log K_{hdw}^{-1}$	$(\log K_{ow} * \log K_{hdw})^{-1}$		
		$R_v^2$	$R_h^2$	$R_v^2$	$R_h^2$	$R_v^2$	$R_h^2$	$R_v^2$	$R_h^2$
$X_c (\%) * \sum SFE (mN m^{-1})$		0.66	0.74	0.67	0.73	0.70	0.74	0.62	0.67
$Vp^{-1} (g cm^{-3})$	$\sum SFE^{-1} (m Nm^{-1})$	0.42	0.81	0.43	0.81	0.45	0.82	0.39	0.76

Table A7.102: Calculation of  $R_h^2$  and  $R_v^2$  with the matrix of two PAH properties ( $\log K_{ow}$ ,  $\log C_w^{sat}$ ) multiplied with three plastic properties ( $X_c * Vp^{-1}$  as fixed parameters) and the  $\log K_{p-w}$  matrix

plastic property product		PAH properties							
1 <sup>st</sup> * 2 <sup>nd</sup> fixed parameter	3 <sup>rd</sup> variable parameter	$\log K_{ow}$ (-)	$\log C_w^{sat}$ (mol m <sup>-3</sup> )	$\log K_{ow} * \log C_w^{sat}$ (mol m <sup>-3</sup> )	$\log C_w^{sat} * \log K_{ow}^{-1}$ (mol m <sup>-3</sup> )	$\log K_{ow} * \log C_w^{sat-1}$ (m <sup>3</sup> mol <sup>-1</sup> )	$(\log K_{ow} * \log C_w^{sat})^{-1}$ (m <sup>3</sup> mol <sup>-1</sup> )		
		$R_v^2$	$R_h^2$	$R_v^2$	$R_h^2$	$R_v^2$	$R_h^2$	$R_v^2$	$R_h^2$
$X_c (\%) * \sum SFE (mN m^{-1})$		0.66	0.74	0.67	0.73	0.68	0.75	0.67	0.71
$Vp^{-1} (g cm^{-3})$	$\sum SFE^{-1} (m Nm^{-1})$	0.42	0.81	0.47	0.81	0.47	0.82	0.47	0.79

Table A7.103: Calculation of  $R_h^2$  and  $R_v^2$  with the matrix of two PAH properties (MW,  $\log K_{hdw}$ ) multiplied with three plastic properties ( $X_c * Vp^{-1}$  as fixed parameters) and the  $\log K_{p-w}$  matrix

plastic property product		PAH properties							
1 <sup>st</sup> * 2 <sup>nd</sup> fixed parameter	3 <sup>rd</sup> variable parameter	MW	$\log K_{hdw}$	MW * $\log K_{hdw}$	$MW * \log K_{hdw}^{-1}$	$\log K_{hdw} * MW^{-1}$	$(MW * \log K_{hdw})^{-1}$		
		(g mol <sup>-1</sup> )	(-) (-)	(g mol <sup>-1</sup> )	(g mol <sup>-1</sup> )	(mol g <sup>-1</sup> )	(mol g <sup>-1</sup> )	$R_v^2$	$R_h^2$
$X_c (\%) * \sum SFE (mN m^{-1})$		0.67	0.73	0.66	0.74	0.23	0.24	0.60	0.59
$Vp^{-1} (g cm^{-3})$	$\sum SFE^{-1} (m Nm^{-1})$	0.43	0.81	0.42	0.81	0.15	0.19	0.38	0.69

Table A7.104: Calculation of  $R_h^2$  and  $R_v^2$  with the matrix of two PAH properties (MW,  $\log C_w^{\text{sat}}$ ) multiplied with three plastic properties ( $X_c * Vp^{-1}$  as fixed parameters) and the  $\log K_{p-w}$  matrix

plastic property product		PAH properties							
1 <sup>st</sup> * 2 <sup>nd</sup> fixed parameter	3 <sup>rd</sup> variable parameter	MW (g mol <sup>-1</sup> )	$\log C_w^{\text{sat}}$ (mol m <sup>-3</sup> )	MW * $\log C_w^{\text{sat}}$ (g m <sup>-3</sup> )	$\log C_w^{\text{sat}} * MW^{-1}$ (mol <sup>2</sup> m <sup>-3</sup> g <sup>-1</sup> )	MW * $\log C_w^{\text{sat}-1}$ (g m <sup>3</sup> mol <sup>-2</sup> )	$(\log K_{p-w} * \log C_w^{\text{sat}})^{-1}$ (m <sup>3</sup> g <sup>-1</sup> )		
$X_c (\%) * Vp^{-1} (g cm^{-3})$	$\sum SFE (m N m^{-1})$	$R_v^2$	$R_h^2$	$R_v^2$	$R_h^2$	$R_v^2$	$R_h^2$	$R_v^2$	$R_h^2$
		0.67	0.73	0.67	0.73	0.18	0.00	0.67	0.71
		0.43	0.81	0.47	0.81	0.15	0.02	0.47	0.79

Table A7.105: Calculation of  $R_h^2$  and  $R_v^2$  with the matrix of two PAH properties ( $\log K_{hdw}$ ,  $\log C_w^{\text{sat}}$ ) multiplied with three plastic properties ( $X_c * Vp^{-1}$  as fixed parameters) and the  $\log K_{p-w}$  matrix

plastic property product		PAH properties							
1 <sup>st</sup> * 2 <sup>nd</sup> fixed parameter	3 <sup>rd</sup> variable parameter	$\log K_{hdw}$ (-)	$\log C_w^{\text{sat}}$ (mol m <sup>-3</sup> )	$\log K_{hdw} * \log C_w^{\text{sat}}$ (mol m <sup>-3</sup> )	$\log C_w^{\text{sat}} * \log K_{hdw}^{-1}$ (mol m <sup>-3</sup> )	$\log K_{hdw} * \log C_w^{\text{sat}-1}$ (m <sup>3</sup> mol <sup>-1</sup> )	$(\log K_{hdw} * \log C_w^{\text{sat}})^{-1}$ (m <sup>3</sup> mol <sup>-1</sup> )		
$X_c (\%) * Vp^{-1} (g cm^{-3})$	$\sum SFE (m N m^{-1})$	$R_v^2$	$R_h^2$	$R_v^2$	$R_h^2$	$R_v^2$	$R_h^2$	$R_v^2$	$R_h^2$
		0.66	0.74	0.67	0.73	0.68	0.75	0.67	0.71
		0.42	0.81	0.47	0.81	0.47	0.82	0.47	0.79

Table A7.106: n = 100 published  $\log K_{LDPE-W/PE-W}$  (L kg<sup>-1</sup>), which are the basis for the calculation of the RMSE

PAHs	$\log C_w^{\text{sat}}$ (mol m <sup>-3</sup> )	26 $\mu$ m thick PE      51 $\mu$ m thick PE									
		Booji et al. (2003) <sup>a</sup>	Adams et al. (2007)	Cornelissen et al. (2008)	Smedes et al. (2009)	Fernandez et al. (2009)	Hale et al. (2010)	Bao et al. (2012)	Choi et al. (2013) <sup>b</sup>	Zhu et al. (2015)	Wang et al. (2019)
naphthalene	-0.01			3.04	2.81				3.23	2.94	2.84
acenaphthylene	-0.78				3.16					3.85	
acenaphthene	-0.84	3.67			3.62					3.94	
fluorene	-1.23			3.78	3.77				4.51	3.67	4.14
phenanthrene	-1.61	4.27	4.30	4.14	4.22	4.3	4.17	4.13	4.78	4.04	4.22
anthracene	-1.61	4.90		4.37	4.33	4.3	4.33	4.26		4.15	4.50
floranthene	-2.38		4.90	4.85	4.93	4.9	5.01	4.96	4.93	4.75	5.05
pyrene	-2.38	5.05	5.00		5.1	4.7			5.07	4.89	5.50
benzo(a)anthracene	-3.22	5.51	5.70	5.62	5.73	5.5			5.79	5.43	6.35
chrysene	-3.22	5.57	5.70	5.56	5.78	5.5			5.7	5.51	5.99
benzo(b)fluoranthene	-3.98			6.06	6.66	6.3			6.33	6.06	6.46
benzo(k)fluoranthene	-3.98			6.07	6.66	6.3			6.56	6.16	6.44
benzo(a)pyrene	-3.98	5.90		6.22	6.75	6.4			6.14	6.39	
dibenz(a,h)anthracene	-4.82				7.32				7.2	6.3	7.39
benzo(g,h,i)perylene	-4.75			5.81	7.27				7.36	6.23	7.20
indeno(1,2,3-cd)pyrene	-4.75			6.01	7.4				7.04	6.5	7.19

<sup>a</sup> average  $\log K_{LDPE-W}$  value of 13 °C and 30 °C has been used

<sup>b</sup> 15 EPA PAHs has been used

Table A7.107: Calculation of RMSE for selected equations from method 1 and n = 100 published data listed in Table A7.106

No.	Equations of methode 1	RMSE
equation 26	$\log K_{p-w} = -1.90 * \log C_w^{sat}_{PAH} * X_{cp} * \rho_p + 2.90$	0.3026
equation 27	$\log K_{p-w} = -685.00 * \log C_w^{sat}_{PAH} * X_{cp} * T_{mp}^{-1} + 2.93$	0.2964
equation 28	$\log K_{p-w} = 6.37E-3 * \log K_{ow PAH} * MW_{PAH} * X_{cp} * \rho_p + 1.98$	0.3248
equation 29	$\log K_{p-w} = 2.26 * \log K_{ow PAH} * MW_{PAH} * X_{cp} * T_{mp}^{-1} + 1.98$	0.3248
equation 30	$\log K_{p-w} = 0.18 * \log K_{ow PAH} * \log K_{hdw PAH} * X_{cp} * \rho_p + 2.28$	0.5567
equation 31	$\log K_{p-w} = 68.90 * \log K_{ow PAH} * \log K_{hdw PAH} * X_{cp} * T_{mp}^{-1} + 2.36$	0.3981
equation 32	$\log K_{p-w} = -0.26 * \log K_{ow PAH} * \log C_w^{sat}_{PAH} * X_{cp} * \rho_p + 2.90$	0.6548
equation 33	$\log K_{p-w} = -11.50 * \log C_w^{sat}_{PAH} * \log K_{ow PAH}^{-1} * X_{cp} * \rho_p + 2.90$	0.3984
equation 34	$\log K_{p-w} = -93.37 * \log C_w^{sat}_{PAH} * \log K_{ow PAH} * X_{cp} * T_{mp}^{-1} + 2.90$	0.6311
equation 35	$\log K_{p-w} = -4562.02 * \log C_w^{sat}_{PAH} * \log K_{ow PAH}^{-1} * X_{cp} * T_{mp}^{-1} + 2.90$	0.5357
equation 36	$\log K_{p-w} = -523.44 * \log C_w^{sat}_{PAH} * MW_{PAH}^{-1} * X_{cp} * \rho_p + 2.90$	0.5575
equation 37	$\log K_{p-w} = -1.98E+5 * \log C_w^{sat}_{PAH} * MW_{PAH}^{-1} * X_{cp} * T_{mp}^{-1} + 2.90$	0.6936
equation 38	$\log K_{p-w} = -0.25 * \log C_w^{sat}_{PAH} * \log K_{hdw PAH} * X_{cp} * \rho_p + 2.90$	0.5331
equation 39	$\log K_{p-w} = -15.20 * \log C_w^{sat}_{PAH} * \log K_{hdw PAH}^{-1} * X_{cp} * \rho_p + 2.90$	0.6332
equation 40	$\log K_{p-w} = -89.50 * \log C_w^{sat}_{PAH} * \log K_{hdw PAH} * X_{cp} * T_{mp}^{-1} + 2.90$	0.5201
equation 41	$\log K_{p-w} = -5521.82 * \log C_w^{sat}_{PAH} * \log K_{hdw PAH}^{-1} * X_{cp} * T_{mp}^{-1} + 2.90$	0.6946
equation 42	$\log K_{p-w} = 2.90E-3 * \log K_{ow PAH} * MW_{PAH} * X_{cp} * \rho_p * d_{50p}^{-1} + 1.98$	0.3248
equation 43	$\log K_{p-w} = 0.11 * \log K_{ow PAH} * \log K_{hdw PAH} * X_{cp} * \rho_p * d_{50p}^{-1} + 1.88$	0.3459
equation 44	$\log K_{p-w} = -0.87 * \log C_w^{sat}_{PAH} * X_{cp} * \rho_p * d_{50p}^{-1} + 2.95$	0.2952
equation 45	$\log K_{p-w} = -0.15 * \log K_{ow PAH} * \log C_w^{sat}_{PAH} * X_{cp} * \rho_p * d_{50p}^{-1} + 2.95$	0.4197
equation 46	$\log K_{p-w} = 8.89E-3 * \log K_{ow PAH} * \log C_w^{sat}_{PAH}^{-1} * X_{cp} * \rho_p * d_{50p}^{-1} + 5.37$	1.0479
equation 47	$\log K_{p-w} = 1.00E+6 * MW_{PAH} * \log C_w^{sat}_{PAH}^{-1} * X_{cp} * \rho_p * d_{50p}^{-1} + 5.25$	1.1740
equation 48	$\log K_{p-w} = -0.12 * \log K_{hdw PAH} * \log C_w^{sat}_{PAH} * X_{cp} * \rho_p * d_{50p}^{-1} + 3.14$	0.3800
equation 49	$\log K_{p-w} = 4.96 * \log K_{hdw PAH} * \log C_w^{sat}_{PAH} * X_{cp} * d_{50p} * T_{mp} + 1.98$	0.3248
equation 50	$\log K_{p-w} = 183.99 * \log K_{ow PAH} * \log K_{hdw PAH} * X_{cp} * d_{50p} * T_{mp}^{-1} + 1.88$	0.3459
equation 51	$\log K_{p-w} = -1510.00 * \log C_w^{sat}_{PAH} * X_{cp} * d_{50p} * T_{mp}^{-1} + 2.92$	0.2968
equation 52	$\log K_{p-w} = -235.00 * \log K_{ow PAH} * \log C_w^{sat}_{PAH} * X_{cp} * d_{50p} * T_{mp}^{-1} + 2.99$	0.4141
equation 53	$\log K_{p-w} = 0.50E-5 * MW_{PAH} * \log C_w^{sat}_{PAH}^{-1} * X_{cp} * \rho_p * d_{50p}^{-1} + 5.43$	1.0480
equation 54	$\log K_{p-w} = 1.67E-5 * \log K_{ow PAH} * MW_{PAH} * X_{cp} * \rho_p * T_{mp} + 1.98$	0.3248
equation 55	$\log K_{p-w} = 6.14E-4 * \log K_{ow PAH} * \log K_{hdw PAH} * X_{cp} * \rho_p * T_{mp} + 1.88$	0.3459
equation 56	$\log K_{p-w} = 0.50E-2 * \log C_w^{sat}_{PAH} * X_{cp} * \rho_p * T_{mp} + 2.93$	0.2964
equation 57	$\log K_{p-w} = -7.54E-4 * \log K_{ow PAH} * \log C_w^{sat}_{PAH} * X_{cp} * \rho_p * T_{mp} + 2.92$	0.4881
equation 58	$\log K_{p-w} = -0.70E-3 * \log K_{hdw PAH} * \log C_w^{sat}_{PAH} * X_{cp} * \rho_p * T_{mp} + 2.90$	0.4616
equation 59	$\log K_{p-w} = 1.26E-4 * \log K_{ow PAH} * MW_{PAH} * X_{cp} * \rho_p * T_{mp}^{-1} + 9.56$	4.4827
equation 60	$\log K_{p-w} = 91.00 * \log K_{ow PAH} * \log K_{hdw PAH} * X_{cp} * \rho_p * T_{mp}^{-1} + 1.88$	0.3459
equation 61	$\log K_{p-w} = 106.42 * \log K_{ow PAH} * \log C_w^{sat}_{PAH} * X_{cp} * \rho_p * T_{mp}^{-1} + 3.32$	0.3419
equation 62	$\log K_{p-w} = 0.50E-5 * \log K_{ow PAH} * \log C_w^{sat}_{PAH}^{-1} * X_{cp} * \rho_p * T_{mp}^{-1} + 5.23$	1.1523
equation 63	$\log K_{p-w} = -89.00 * \log K_{hdw PAH} * \log C_w^{sat}_{PAH} * X_{cp} * \rho_p * T_{mp}^{-1} + 3.43$	0.3417
equation 64	$\log K_{p-w} = 0.82E-2 * \log K_{hdw PAH} * \log C_w^{sat}_{PAH}^{-1} * X_{cp} * \rho_p * d_{50p}^{-1} + 5.38$	1.0479
equation 65	$\log K_{p-w} = 15.19 * \log K_{ow PAH} * \log C_w^{sat}_{PAH}^{-1} * X_{cp} * d_{50p} * T_{mp}^{-1} + 5.37$	1.0479
equation 66	$\log K_{p-w} = 0.40 * MW_{PAH} * \log C_w^{sat}_{PAH}^{-1} * X_{cp} * d_{50p} * T_{mp}^{-1} + 5.38$	1.0480
equation 67	$\log K_{p-w} = 0.11 * \log K_{hdw PAH} * \log C_w^{sat}_{PAH}^{-1} * X_{cp} * d_{50p} * T_{mp}^{-1} + 3.43$	0.3417
equation 68	$\log K_{p-w} = 71.41 * \log K_{ow PAH} * MW_{PAH} * X_{cp} * Vp_p * \sum SFE_p^{-1} + 2.10$	0.3220
equation 69	$\log K_{p-w} = 2641.17 * \log K_{ow PAH} * \log K_{hdw PAH} * X_{cp} * Vp_p * \sum SFE_p^{-1} + 2.01$	0.3434
equation 70	$\log K_{p-w} = 2.35E+4 * \log C_w^{sat}_{PAH} * X_{cp} * Vp_p * \sum SFE_p^{-1} + 2.93$	0.3241
equation 71	$\log K_{p-w} = 3500.00 * \log K_{ow PAH} * \log C_w^{sat}_{PAH} * X_{cp} * Vp_p * SFE_p^{-1} + 2.93$	0.4465
equation 72	$\log K_{p-w} = -1.57E+5 * \log K_{ow PAH} * \log C_w^{sat}_{PAH}^{-1} * X_{cp} * Vp_p * \sum SFE_p^{-1} + 2.93$	0.6642
equation 73	$\log K_{p-w} = -3045.00 * \log K_{hdw PAH} * \log C_w^{sat}_{PAH} * X_{cp} * Vp_p * \sum SFE_p^{-1} + 2.94$	0.4588

Table A7.108: plastic-water partition coefficient of selected PAHs for PP, PBS and PET

PAHs	$\log C_w^{\text{sat}}$ (mol m <sup>-3</sup> )	Lee et al. (2014) <sup>a</sup>	Lončarski et al. (2021) <sup>b</sup>	Zhao et al. (2020)	Lončarski et al. (2021) <sup>b</sup>
naphthalene	-0.01		4.18		4.39
acenaphthylene	-0.78				
acenaphthene	-0.84				
fluorene	-1.23		4.16		4.55
phenanthrene	-1.61	3.73		4.92	
anthracene	-1.61	4.05			
fluoranthene	-2.38	4.54	4.29		4.43
pyrene	-2.38	4.55	4.27	5.04	4.95
benzo(a)anthracene	-3.22				
chrysene	-3.22				
benzo(b)fluoranthene	-3.98				
benzo(k)fluoranthene	-3.98				
benzo(a)pyrene	-3.98	5.85			
dibenz(a,h)anthracene	-4.82	6.76			
benzo(g,h,i)perylene	-4.75	6.49			
indeno(1,2,3-cd)pyrene	-4.75				

<sup>a</sup> converted to  $\log K_{\text{PP-W}}$  in fresh water based on the Setschenow constant from Jonker and Muijs (2010); <sup>b</sup> converted to  $\log K_{\text{PP-W}}$  in fresh water based on the Setschenow constant from Burant et al. (2016) and Jonker and Muijs (2010)

## References of Appendix:

- Adams, R. G., Lohmann, R., Fernandez, L. A., MacFarlane, J. K., Gschwend, P. M. (2007). Polyethylene Devices: Passive Samplers for Measuring Dissolved Hydrophobic Organic Compounds in Aquatic Environments. *Environmental Science Technology*. Vol. 41, 1317-1323.
- Badia, J.D., Srömberg, E., Karlsson, S., Ribes-Greus, A. (2012). The role of crystalline, mobile amorphous and rigid amorphous fractions in the performance of recycled poly (ethylene terephthalate) (PET). *Polymer Degradation and Stability*. Vol. 97, 98-107.
- Bao, L. J., Xu, S. P., Liang, Y., Zang, E. Y. (2012). Development of a low-density polyethylene-containing passive sampler for measuring dissolved hydrophobic organic compounds in open waters. *Environmental Toxicology and Chemistry*. Vol. 31, (5), 1012–1018.
- Booij, K., Hofmans, H. E., Fischer C. V., Van Weerlee, E. M. (2003). Temperature-dependent uptake rates of nonpolar organic compounds by semipermeable membrane devices and low-density polyethylene membranes. *Environmental Science and Technology*. Vol. 37, 361-366.
- Burant, A., Lowry, G.V., Karamalidis, A.K. (2016). Measurement of Setschenow constants for six hydrophobic compounds in simulated brines and use in predictive modeling for oil and gas systems. *Chemosphere*. Vol. 144, 2247–2256.
- Choi, Y., Cho, Y. M., Luthy R. G. (2013). Polyethylen-Water Partitioning Coefficients for Parent- and Alkylated-Polycyclic Aromatic Hydrocarbons and Polychlorinated Biphenyls. *Environmental Science & Technology*. Vol. 47, 6943-6950.
- Cornelissen, G., Pettersen, A., Broman, D., Mayer, P., Breedveld, G. D. (2008). Field testing equilibrium passive samplers to determine freely dissolved native polycyclic aromatic hydrocarbon concentrations. *Environmental Toxicology Chemistry*. Vol. 27 (3), 499-508.
- Fernandez, L. A., MacFarlane, J. K., Tcaciuc, A. P., Gschwend, P. M. (2009). Measurement of freely dissolved PAH concentrations in sediment beds using passive sampling with low-density polyethylene strips. *Environmental Science and Technology*. Vol. 43, 1430 – 1436.
- Gahleitner, M., Bachner, C., Ratajski, E., Rohazcek, G., Neißl, W. (1999). Effects of the Catalyst System on the Crystallization of Polypropylene. *Journal of Applied Polymer Science*. Vol. 73, 2507-2515.
- Hale, S. E., Martin, T. J., Goss, K. U., Arp, H. P. H., Werner, D. (2010). Partitioning of organochlorine pesticides from water to polyethylene passive samplers. *Environmental Pollution*. Vol. 158 (7), 2511-2517.
- Jonker, M. T. O., Muijs, B. (2010). Using solid phase micro extraction to determine salting-out (Setschenow) constants for hydrophobic organic chemicals. *Chemosphere*. Vol. 80 (3), 223-227.
- Karapanagioti, H. K., Klontza, I. (2008). Testing phenanthrene distribution properties of virgin plastic pellets and plastic eroded pellets found on Lesvos island beaches (Greece). *Marine Environmental Research*. Vol. 65, 283–290.
- Khonakdar, H.A., Jafari, S.H., Hässler, R. (2007). Glass-Transition-Temperature Depression in Chemically Crosslinked Low-Density Polyethylene and High-Density Polyethylene and their Blends with Ethylene Vinyl Acetate Copolymer. *Journal of Applied Polymer Science*. Vol. 104, 1654-1660.
- Lee, H., Shim, W.J., Kwon, J. H. (2014). Sorption capacity of plastic debris for hydrophobic organic chemicals. *Science of the total environment*. Vol. 470-471, 1545-1552.
- Lončarski, M., Gvoić, V., Prica, M., Cveticanin, L., Agbaba, J., Tubić, A. (2021). Sorption behavior of polycyclic aromatic hydrocarbons on biodegradable polylactic acid and various nondegradable microplastics: Model fitting and mechanism analysis. *Science of the Total Environment*. Vol. 785, 147289.

- Mackay, D., Shiu, W. Y., Ma, K. C. (1992). Illustrated Handbook of Physical-Chemical Properties and Environmental Fate for Organic Chemicals. Volume II: Polynuclear Aromatic Hydrocarbons, Polychlorinated Dioxins, and Dibenzofurans. Lewis Publishers, Boca Raton, FL.
- Smedes, F., Geertsma, R. W., van der Zande, T., Booij, K. (2009). Polymer-water partition coefficients of hydrophobic compounds for passive sampling: Application of cosolvent models for validation. *Environmental Science & Technology*. Vol. 43 (18), 7047-7054.
- Teuten, E. L., Rowland, S. J., Galloway, T. S., Thompson, R. C. (2007). Potential for plastics to transport hydrophobic contaminants. *Environmental Science & Technology*. Vol. 41 (22), 7759-7764.
- Wang, J., Liu, X., Liu, G. (2019). Sorption behaviors of phenanthrene, nitrobenzene, and naphthalene on mesoplastics and microplastics. *Environmental Science and Pollution Research*. Vol. 26, 12563–12573.
- Xu, Y., Xu, J., Liu, D., Guo, B., Xie, X. (2008). Synthesis and Characterization of Biodegradable Poly(butylene succinate-co-propylene succinate)s. *Journal of Applied Polymer Science*. Vol. 109, 1881-1889.
- Zhao, L., Rong, L., Xu, J., Lian, J., Wang, L., Sun, H. (2020). Sorption of five organic compounds by polar and nonpolar microplastics. *Chemosphere*. Vol. 257, 127206.
- Zhu, T., Jafvert, C. T., Fu, D., Hu, Y. (2015). A novel method for measuring polymer-water partition coefficients. *Chemosphere*. Vol. 138, 973-979.